477

THE PHYSICAL REVIEW

VOLUME 47 Second Series NUMBER 12

JUNE 15, 1935

Published for the

AMERICAN PHYSICAL SOCIETY

by the

AMERICAN INSTITUTE OF PHYSICS

Incorporated

LANCASTER, PA., AND NEW YORK, N. Y.

THE
PHYSICAL REVIEW
A Journal of Experimental and Theoretical Physics
VOL. 47, NO. 12 JUNE 15, 1935 SECOND SERIES

The Absorption of Cosmic-Ray Electrons*

J. C. STREET, R. H. WOODWARD AND E. C. STEVENSON, *Research Laboratory of Physics, Harvard University*

(Received April 5, 1935)

The interpretation that the coincident discharge of three or more G-M counters in line represents the passage of a single ionizing particle through the counters and any intervening material has been checked by two methods: (1) A vertical cloud chamber between the central and lower counters of a triple-counter telescope controlling the chamber has shown in 90 percent of the coincidences a single electron directed through the counters even when lead up to 45 cm in thickness is placed between the central and upper counters. Soft or hard rays associated with the single particle are rare. (2) Four counters so spaced that 90 cm of material could be introduced between them controlled additional counters which were placed adjacent to the telescope elements and connected as in a hodoscope circuit for the detection of rays associated with those producing the quadruple counts. In only 10 percent of the coincidences were any of the side counters discharged. Absorption data obtained with the latter arrangement for lead, iron and marble ($CaCO_3$) indicate that the absorption as a function of the thickness of absorber on a scale of extranuclear electrons per cm² is approximately the same for all three materials. The lead values have been compared with Anderson's electron energy distribution (for the counter controlled data) to determine what specific energy loss values for electrons in lead must be assumed to satisfy both sets of data. The results are:

Average energy loss (MEV) per cm Pb	45	31	25	20
Energy range MEV	0–680	680–1150	1150–1900	1900–2500

INTRODUCTION

IN 1933 Rossi[1] presented in the form of a summary a description of a series of important counter studies of the cosmic radiation at sea level. As a result of these and more recent investigations[2] Rossi has concluded that two-thirds of the penetrating radiation at sea level consists of high energy (sufficient to penetrate at least 10 cm of lead) ionizing corpuscles, and that this corpuscular component is reduced to about half-value in traversing a meter of lead. In 1934 Anderson, Millikan, *et al.*[3] in a report of cloud-chamber observations of cosmic-ray phenomena presented two objections to Rossi's conclusions which may be stated as follows:

(1) Shower processes may account for a large fraction of the coincident counts of a set of Geiger-Müller counters when thick lead absorbers are placed between the units.

(2) It is impossible to reconcile the absorption curve obtained by Rossi with their energy distribution and specific energy loss observations. Recently, however, Anderson has presented a very different energy distribution curve[4] and a higher average specific energy loss for electrons in the range below 300 mev.

Further studies by Rossi,[2] Street and Johnson[5] and others[6] support the original interpretation of single ionizing corpuscles. In view of the need for a definite decision concerning the significance of the counter absorption experiments we have

* Presented at the New York meeting of the American Physical Society, February, 1935. See abstracts Nos. 31 and 32.

[1] B. Rossi, Zeits. f. Physik **82**, 151 (1933).

[2] B. Rossi, Internat. Conf. Phys., London, October, 1934.

[3] Anderson, Millikan, Neddermeyer and Pickering, Phys. Rev. **45**, 352 (1934).

[4] Anderson and Neddermeyer, Internat. Conf. Phys., London, October, 1934.

[5] Street and Johnson, Phys. Rev. **42**, 142 (1932).

[6] D. S. Hsiung, Phys. Rev. **46**, 653 (1934).

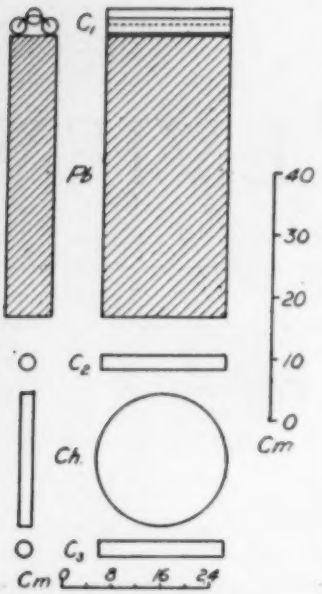

FIG. 1. Geometrical arrangement of counters (C_1, C_2, C_3) absorbing material (Pb), and cloud chamber (Ch).

investigated in detail the phenomena associated with the coincidences of a set of counters when thick absorbers are placed between them. We present in this paper the results of this investigation together with some new observations on the absorption of the fast corpuscles in lead and other materials.

Study of the Coincidence Mechanism with the Cloud Chamber

Three counters were placed one above the other in a vertical plane with their axes horizontal. The absorbing material was introduced between the central and upper counters and a vertical cloud chamber was between the central and lower counters. Fig. 1 is a scale drawing of the arrangement. (The upper counter actually consists of three tubes in parallel to increase the solid angle.) In order to reduce secondary effects to a minimum the apparatus was unshielded from above except for a light wooden roof and care was taken to remove dense material from the immediate neighborhood of the counters. The arrangement is therefore well designed to examine the discharge mechanism of the usual coincident counter telescope adapted for absorption measurements. On the basis of Rossi's interpretation the counter-controlled cloud photographs should show single tracks directed in some line through the counters and the absorbing material, whereas if the objections cited above are valid, such single tracks should be absent from most of the photographs.

We have taken photographs with both a 45-cm and a 15-cm lead absorber, 112 in the first case and 107 in the second. With the 45-cm block, 101, or 90 percent, show single rays directed through the counters; with the 15-cm block there are 101, or 94 percent such cases.

These direct observations with thick absorbers show that the first objection of Anderson, Millikan, *et al.* is not valid. Our results are not contradictory to their actual observation that the relative importance of shower produced coincidences is increased by placing one cm of lead between a pair of counters. However, their assumption that showers become increasingly important with thicker absorbers is definitely in error. Auger and Ehrenfest[7] have recently reached the same conclusion from a similar experiment.

It is of some interest to determine the frequency of occurrence of secondary radiation associated with the penetrating corpuscles. This is a difficult problem with a cloud chamber because of the poor time resolving power of the method, but the photographs do give some qualitative information. Many of them show, in addition to the straight track directed through the counters, other tracks of the same apparent sharpness. However, 58 photographs taken at

TABLE I. *Summary of data on photographs.*

	Counter Controlled 45 cm Lead	15 cm Lead	Random under 15 cm Lead
Total Photographs	112	107	58
Photographs with a straight track through the lead and counters	101	101	1
Photographs with 1 inclined* ray contemporary with the expansion	24	24	12
Photographs with 2 inclined rays contemporary with the expansion	6	14	6
Photographs with more than 2 inclined rays contemporary with the expansion	3	4	0
Total inclined rays contemporary with the expansions	36	51	24

* By "inclined" rays we mean those directed at such angles that they would not pass through the counters and absorbing material. β-rays which are obviously soft have not been classified as they are probably due to the normal radioactivity of the air and matter surrounding the chamber.

[7] Auger and Ehrenfest, Comptes rendus **199**, 1609 (1934).

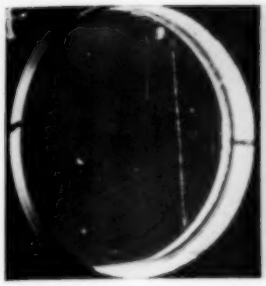

FIG. 2. Single electron track.

FIG. 3. Single electron track.

random show about the same percentages of soft beta-rays and sharply inclined straight rays apparently contemporary with the expansion. Thus we conclude that, with a thick absorber, complex phenomena actually associated with the single rays through the counters are infrequent.

The complete data are classified and described in Table I. Figs. 2 and 3 are typical examples of straight rays unaccompanied by any other contemporary phenomenon. Fig. 4 shows a straight track and soft electron tracks in addition. Fig. 5 shows a complex shower, the only one observed in 219 photographs.

STUDY OF THE EFFECT OF SHOWERS WITH A HODOSCOPE CIRCUIT

A set of counters, designed for the investigation of the abundance of associated rays, has been constructed as shown in Fig. 6. There are four groups of counters so spaced that six blocks of absorbing material with a total thickness of 91.5 cm can be placed between them. The two central counters in each group are connected in parallel so that they act as a single counter. Quadruple coincidences between the four pairs of central counters are recorded for various thicknesses of absorbing material. The eight outside counters and eight corresponding neon lamps are connected in the same way as the hodoscope unit designed by Johnson and Stevenson[8] and are controlled by the coincidence set. A discharge of an outside counter causes its corresponding neon lamp to flash, provided a quadruple coincidence occurs simultaneously. The lamp flashes are photographed by an automatic camera, each quadruple count advancing the film one frame. The number and positions of the flashes recorded on the film indicate the number and positions of the outside counters which are discharged by rays associated (coincident in time) with the ray or rays which caused the quadruple coincidence. Examination of a total of a thousand frames shows that the flashes are distributed statistically at random among the eight counters—no positions seeming to be preferred. Of 355 frames taken with no absorber between counters 9.5 percent show at least one flash, and 3.6 percent

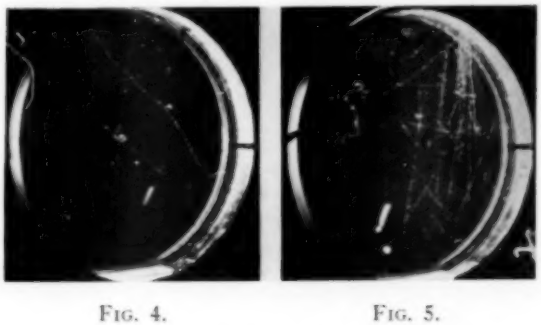

FIG. 4.

FIG. 5.

FIG. 4. Single electron track with 3 beta-tracks contemporary with the expansion.
FIG. 5. A shower. The heavy tracks are almost certainly old.

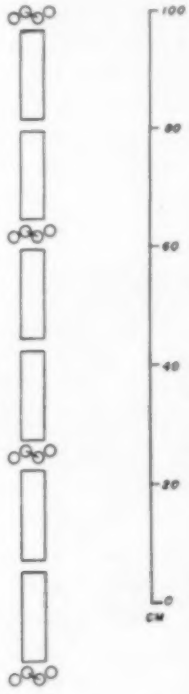

FIG. 6. Arrangement of counters for the measurement of the absorption of cosmic-ray electrons.

[8] Johnson and Stevenson, J. Frank. Inst. **216**, 329 (1933).

show more than one. Of 343 frames taken with 91.5 cm of lead between counters 10.2 percent show at least one flash, and 4.5 percent show several. In an effort to obtain the greatest possible number of associated rays, we placed 1.4 cm of lead (the thickness[1] giving maximum shower production) above the top counters, and observed that 16.8 percent of 326 frames show at least one flash and 9.3 percent show more than one. The probabilities of accidental flashes (0.3 percent and of lamp failures (6 percent entirely due to the inefficiency of the corresponding counters) have been measured in the usual way[9] and corrections have been made. The results indicate that groups of rays coming from the atmosphere and from the absorbing material are comparatively rare, and thus the chance of four counters being discharged simultaneously by associated rays is too small to account for an appreciable part of the observed counting rate. The counting rate is reduced to 3 percent of the original value by displacing the central counters just out of line. Moreover, the relative abundance of associated rays remains approximately constant with various thicknesses of absorbing material, and, therefore, such associated rays cause no appreciable error in the relative counting rates.

Errors due to associated rays at thicknesses near the optimum scattering value may be avoided by building the absorbing material up from the bottom of the unit. Although Fünfer[10] has found some upward scattering, it is small compared to the downward intensity. In fact the introduction of 1.4 cm of lead below the bottom counter was found to produce no observable increase in the quadruple counting rate.

TABLE II. *Absorption of electrons in lead, iron and marble*

	Thickness of Absorber (cm)	Electrons per cm² ($\times 10^{-28}$)	Time (min.)	Quadruple Counts	Counts per min.	Probable Error	Corrected Counting Rate
Lead	0.00	0.000	10528	3052	0.289	0.0048	0.289
	1.43	.038	7535	1860	.247	.0056	.245
	15.2	.411	6146	1308	.213	.0038	.209
	30.5	.822	4565	832	.178	.0033	.167
	61.0	1.64	4149	573	.138	.0042	.128
	91.5	2.47	7111	832	.117	.0029	.107
Iron	.00	.00	4071	1140	.280	.0062	.280
	15.2	.337	4534	1058	.234	.0053	.229
	30.5	.674	4391	848	.193	.0041	.181
	61.0	1.35	4053	652	.161	.0044	.149
	91.5	2.02	4448	591	.133	.0066	.122
Marble	.00	.00	4234	1202	.284	.0059	.284
	30.5	.250	7071	1587	.223	.0049	.223
	61.0	.500	4402	911	.207	.0026	.206
	91.5	.750	14536	2938	.202	.0027	.197

[9] Street and Woodward, Phys. Rev. **46**, 1029 (1934).
[10] Von E. Fünfer, Zeits. f. Physik **83**, 92 (1933).

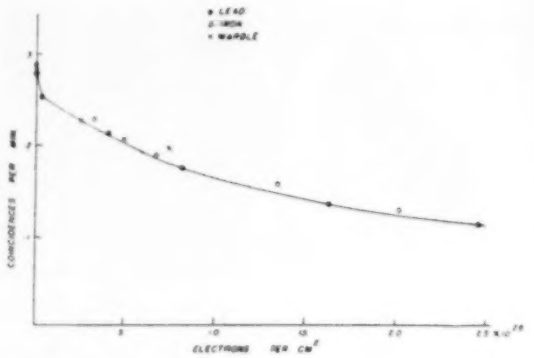

FIG. 7. The absorption of cosmic rays in lead, iron and marble.

As a result of these experiments we conclude in agreement with Rossi[2] that the use of efficient counters in carefully designed quadruple or triple coincidence telescopes will result in data which may be interpreted on the basis of the passage of charged particles through the counters.

New Absorption Results Obtained with the Coincidence Unit

In view of this conclusion we have made a more extensive study of the absorption of the fast electrons in three materials. The results for lead iron and marble are tabulated in Table II. The counting rates have been corrected for barometric fluctuation[11] and the probable errors have been estimated from the residuals. The accidental counting rate has been found to be too small 0.00011 per min.) to cause any error, but the change in efficiency[9] of the counters with thickness of absorber (and consequent change of individual rates) has been found to be appreciable. The corrected rates are given in the final column. In Fig. 7 the quadruple counting rates have been plotted against the thickness of absorber expressed in extranuclear electrons per cm². The iron points lie within the probable error of the lead curve, but there is an indication that the absorption per electron of iron is less than that of lead, and that the marble is less absorbing than the iron. If these apparent differences are

[11] Stevenson and Johnson, Phys. Rev. **47**, 578 (1935).

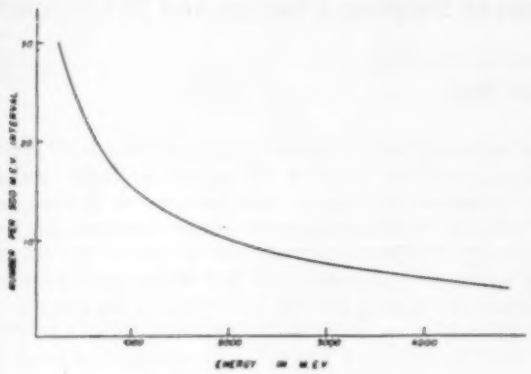

FIG. 8. Anderson's energy distribution of cosmic-ray electrons.

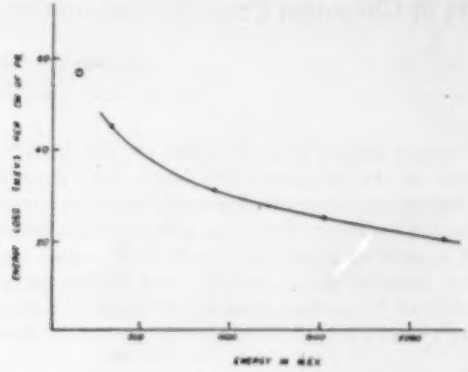

FIG. 9. Specific energy loss for lead as obtained from comparison of the lead absorption curve with Anderson's energy distribution curve.

due to nuclear absorption, the absorption per nucleus increases somewhat more rapidly than linearly with the atomic number.

COMPARISON OF THE LEAD ABSORPTION CURVE WITH THE ENERGY DISTRIBUTION CURVE

Since we are confident that the lead absorption curve is reliable, it is instructive to compare it with Anderson's energy distribution curve.[4] These two curves are related by the energy loss per cm of lead, and, as Anderson has pointed out, are in disagreement, if, as he assumes, the specific energy loss is independent of the energy of the rays. At the International Conference in London, Anderson reported a list of 104 cosmic-ray energy measurements obtained with a counter-controlled cloud chamber. No measurements of energies less than 300 millions of electron volts (MEV) are included, so we have added a reasonable number (30) of low energy rays to the list (this choice of 30 will be justified to a certain extent below) and have plotted the number of rays per 500 MEV interval against the energy of the rays to obtain the smoothed curve given in Fig. 8. Assuming that the penetration of the rays depends on their energies, i.e., that rays of a given energy have approximately the same range and that that range is greater for rays of greater energy, it is possible to determine the specific energy loss as a function of the energy by comparing the lead absorption and energy distribution curves. The first block (15.2 cm) of lead absorbs a definite fraction of the cosmic-ray electrons, and that fraction on the energy distribution curve corresponds to an energy range (0–680 MEV). The second block absorbs a further fraction corresponding to a higher range of energy (680–1150 MEV). Then the average specific energy loss per cm of lead is obtained by dividing the energy loss in the lead block by the thickness. The results are plotted in Fig. 9. The large open circle is an average of Anderson's direct measurements. The choice of 30 low energy electrons to complete Anderson's energy distribution curve below 300 MEV gave the best fit between the initial part of this plot and Anderson's value of 57 MEV per cm. The value 45 MEV on our curve of Fig. 9 is questionable since it depends on the choice of the number of low energy electrons, but the other values are only slightly influenced by that number. All of Anderson's nine measurements of the specific energy loss reported at London were obtained from observations of rays of energy less than 300 MEV. They fluctuate from 18 (less than our lowest value) to 120 MEV per cm. Thus we may consider our results as an extension of the average specific energy loss to higher energies. Consideration of the curve and Anderson's fluctuating values leads to the speculation that fast electrons may lose energy by two processes: (1) Encounters with extranuclear electrons resulting in a nonfluctuating energy loss, probably independent of the energy, and which has a value of about 18 MEV per cm; and (2) nuclear or possibly close electron encounters with large energy losses (due to radiation or pair production), the probability of these encounters decreasing with increasing energy.

Effect of Chemical Combination on the $K\beta_1$ Lines of Sulphur, Chlorine and Potassium*

JOSEPH VALASEK, *University of Minnesota*

(Received April 20, 1935)

By using a special form of target, the $K\beta_1$ lines in the spectrum of the secondary x-radiation from a series of alkali halides and some alkaline earth sulphides have been measured. Combining the results with Stelling's values for the K absorption edges one readily finds values for the electron affinities of Cl^- and S^{--} and for the ionization potentials of K^+ as they exist in the respective crystals. Pauling's theory is used to reduce these values to those for the free ions. Good agreement with other data is obtained in the case of the chlorides, fair agreement in the case of the potassium compounds, and poor results in the case of sulphur. Possible causes for these discrepancies are suggested. The general method used in this work to obtain the spectra of compounds may find useful application in methods of chemical analysis by means of x-ray spectra.

THE change in wavelength of an x-ray emission line as a result of the state of chemical combination is usually very small even when the line involves the "optical" energy levels. The effect is best observed in the $K\beta$ lines of light elements such as sulphur, chlorine and potassium. However, practically all but the most recent data on this point are unreliable. This results from the use of the powdered substance rubbed into fine scratches on the surface of the target as the source of the radiation. Under the intense heat in the focal spot, the material reacts with the target metal and one thus observes the spectra of the products of the reaction. This difficulty can be overcome to a large extent by using a fluorescence method and by changing the substance frequently since even the x-rays dissociate the material in many cases. However, most of the recent investigations[1, 2, 3] employing a strict fluorescence method have been necessarily restricted to the strong $K\alpha$ lines. These do not show much displacement as a result of chemical combination and are not fundamentally as interesting as the $K\beta$ lines which are radiated when the most loosely bound electrons in the compound fall into a vacancy in the K shell.

The writer has been experimenting with a method which excites the spectra with sufficient intensity so that the $K\beta$ lines can be studied without much difficulty. As first developed and described,[4] the target was simply provided with a clamp which held the substance to be studied within a millimeter or two of the focal spot. The substances used at first were pieces of single crystal or mineral. Because of the difficulty in obtaining the materials and the purity desired, the compounds have lately been obtained as pure chemicals or prepared by precipitation from solution. The slightly damp powder is pressed into a semi-cylindrical "pill" and dried in vacuum. The compound is then placed under the clamp with its flat side toward the focal spot. With the form of target described, there is a troublesome background of direct radiation from the target which, in spite of care, becomes more or less contaminated with the material being studied. Consequently there is always at least a weak spectrum of the products of reaction with the target metal superposed on the spectrum it is desired to observe. To overcome this difficulty, the target was remodeled as shown in Fig. 1. The shield, a, attached to the side facing the spectrograph effectively prevents any radiation

TABLE I. *Wavelengths of reference lines.*

Line	Reference	Wavelength	Order
S $K\beta$	Ni $K\alpha_1$	1654.50	3
	Ni $K\alpha_2$	1658.35	3
Cl $K\beta$	W $L\alpha_1$	1473.36	3
K $K\beta$	Ni $K\alpha_1$	1654.50	2
	Ni $K\alpha_2$	1658.35	2
	Co $K\alpha_1$	1785.29	2
	Co $K\alpha_2$	1789.19	2

* A preliminary report was made at the Pittsburgh Meeting of the American Physical Society, December 28–29, 1934.

[1] Faessler, Zeits. f. Physik **72**, 734 (1931).

[2] Lundquist, Zeits. f. Physik **77**, 778 (1932); **83**, 85 (1933); **89**, 273 (1934).

[3] Yoshida, Inst. Phys. Chem. Research Tokyo, Sci. Rep. **421**, 298 (1933).

[4] Valasek, Phys. Rev. **43**, 612 (1933).

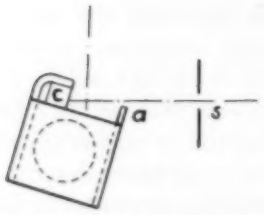

FIG. 1. X-ray target. c is a pressed block of the compound; a is a metal shield which screens the spectrograph slit s from the direct radiation from the face of the target.

except that from the compound, c, from entering the spectrograph, s. The spectrograph was of the Siegbahn vacuum type with a calcite crystal. The wavelengths were determined by measuring their distances from certain selected standard lines. These lines and their assumed wavelengths are given in Table I.

The results of measurements of the principal beta-lines are given in column four of Table II. In several cases weak satellites were observed and measured, but the data are as yet incomplete and not very accurate because of the faintness of these lines. It is planned to use a concave crystal spectrometer to finish the study of these weak lines. The compounds listed are all of the rare gas electron shell type and, except for CsCl, they all form crystals of the familiar NaCl type with the interionic distances given under R. The column headed K_∞ gives the wavelengths of the principal K absorption edges as measured by Stelling.[5] The fifth column gives the difference between K_∞ and $K\beta_1$ in X. U. (10^{-11} cm), while the last column gives this difference expressed in electron volts.

These results give information in regard to the energy levels and photoionization frequencies of solids. If we let ν_K represent the K absorption frequency, and ν_β the frequency of the beta-line, then the difference

$$h\nu_K - h\nu_\beta = eV_M = h\nu_M$$

represents the energy required to remove an M electron from the ion in the crystal. These M electrons, it might be noted, constitute the outermost or rare gas shell of the ion. Thus one obtains a measure of the ionization potential or electron affinity of the ion in the crystal. Furthermore, the most easily removed electron which will belong to the negative ion, should determine

[5] Stelling, Zeits. f. Physik **50**, 506 (1928).

TABLE II. *Interionic distances and x-ray wavelengths.*

Compound	R	K_∞	$K\beta_1$	Diff. X. U.	Diff. volts
		Sulphides			
MgS	2.595	5005.3	5018.40	13.1	6.5
CaS	2.84	5006.6	5019.00	12.4	6.2
SrS	2.935		5019.39		
BaS	3.175	5007.5	5019.74	12.2	6.1
		Chlorides			
LiCl	2.57	4383.8	4394.57	10.8	6.9
NaCl	2.814	4384.1	4395.36	11.3	7.2
KCl	3.14	4385.0	4395.44	10.4	6.6
RbCl	3.285	4385.3	4395.24	9.9	6.3
CsCl	3.55	4387.4	4394.77	7.4	4.7
		Potassium halides			
KF	2.665	3427.7	3447.16	19.5	20.3
KCl	3.14	3427.9	3446.98	19.1	19.9
KBr	3.289	3427.9	3447.34	19.4	20.3
KI	3.526	3427.7	3447.43	19.7	20.5

the photoelectric threshold of the crystal. There are presumably no free electrons in these crystals.

The values listed in the last column of Table II are these ionization potentials for the ions in the crystals. In most cases it is possible to reduce these values to those pertaining to the free ions and to compare the results with those obtained by independent methods. In order to make this reduction we will use Pauling's theory[6] on the effects of chemical combination on x-ray absorption edges and on photoelectric thresholds. According to Pauling, if the energy required to remove an electron from a free ion is represented by $h\nu_0$, then the energy required to remove the same electron when the ion is in a crystal lattice is

$$h\nu = h\nu_0 + e\phi - E_c.$$

Here $e\phi$ is the increase in binding energy of an electron due to the external screening effect of the surrounding ions and is approximately equal to the lattice energy. E_c is the electron affinity of the crystal and is proportional to the magnetic susceptibility of the crystal. It is closely related to the inner field in the Sommerfeld theory of electrical properties of metals. The sign and magnitude of E_c is the same for both ions in the crystal, while $e\phi$ is positive for a negative ion and negative in the case of the positive ion. Pauling[6] finds that the photoelectric threshold of the crystal, which is the energy required to remove an electron from the negative ion, is

[6] Pauling, Phys. Rev. **34**, 954 (1929).

affected by chemical combination to exactly the same extent as the K absorption edge of the negative ion. Thus there is no appreciable ionic deformation even in the ion in which it would most likely occur. However, most of the data on the wavelengths of the x-ray emission lines, Table II, show that there is some differential shift in the various energy levels but that this is small compared to the shift in the levels themselves.

As a specific example of the relation of Pauling's theory to the data given here, consider the Cl^- ion in KCl. The value of $e\phi$ is 7.98 electron volts and E_c is 5.2 volts. Thus the x-ray energy levels are shifted upward by +2.8 volts with respect to their locations for the free Cl^- ion. The emission of a $K\beta$ line by the K shell ionized Cl^- ion brings it to within 6.6 volts of its ground state, that is, to its M level. (Table II, last column.) This is the energy required to remove an electron from the outer rare gas shell of the Cl^- ion when it is in the crystal. If this state is also 2.8 volts higher than it would be in the case of free Cl^-, the electron affinity of free Cl is 6.6−2.8 or 3.8 electron volts which is in good agreement with the accepted value of 3.7 volts. The other chlorides give equally good agreement as is shown in the last column of Table III where results of similar calculations are given.

In the case of the K^+ ion in KCl, the energy levels are all displaced by $-e\phi-E_c$ according to Pauling, or by 13.2 electron volts. This is a downward displacement of the levels for the ions in the crystal with respect to their positions for free ions. Now the x-ray data give 19.9 volts as the ionization potential for the K^+ in KCl; consequently the ionization potential of free K^+ ions turns out to be 33.1 volts. This is farther from the accepted value of 31.7 for the second ionization potential of potassium than one may account for by experimental error in the x-ray data. It seems significant that all the values obtained in this way are quite uniformly high by about 1.5 volts.

TABLE III. *Electron affinities and ionization potential of ions.*

Substance	$e\phi-E_c$	$h\nu_K-h\nu_\beta$	El. Aff. (calc.)
Chlorine ion. Electron affinity = 3.7 volts			
LiCl	+3.5 v	6.9 v	3.4 v
NaCl	3.3	7.2	3.9
KCl	2.8	6.6	3.8
RbCl	2.6	6.3	3.7
CsCl	1.2	4.7	3.5
Potassium ion. Ionization potential = 31.7 volts			
KF	−13.0	20.3	33.3
KCl	13.2	19.9	33.1
KBr	12.9	20.4	33.3
KI	12.7	20.5	33.2
Sulphur ion. Electron affinity = 2.06 volts			
BaS	+0.9	6.1	5.2 *

In the case of the only sulphide for which the magnetic susceptibility could be found, namely BaS, the electron affinity of S^{--} comes out much too high, as is shown in Table III.

Several causes for these discrepancies may be suggested. In the first place, a point lattice of positive and negative charges is assumed in the derivation of the formula for the crystal potential $e\phi$ which contributes to the energy level shifts. A formula based on a distribution of electrons throughout space, which is more in accord with that existing, may give better results. Secondly, the M levels are not single levels and the use of only the strongest $K\beta_1$ line may lead to a calculated M level which is consistently higher than the lowest level. The multiplicity or fine structure of the M level may be partly due to the fields of the neighboring ions and thus be different for the different types of compounds. Previous study of the sulphur $K\beta$ lines[4] demonstrates the existence of such an effect. A more complete study of the entire pattern of the beta-lines of the compounds reported on here will be made with a focusing spectrograph.

The method described here for obtaining the x-radiation from compounds may find useful application in problems of chemical analysis along lines given by von Hevesy.[7] It seems to be an advantage to work with a pressed block of the material instead of a thin layer of the powder in intimate contact with a metallic background. The spectra obtained are more intense when the block is used, and one avoids the risk of chemical reaction with the metallic surface.

The writer is indebted to the Graduate School of the University of Minnesota for financial support of this research, and to Mr. Richard Carlson for his able assistance with the laboratory work.

[7] v. Hevesy, *Chemical Analysis by X-Rays and its Applications*, McGraw-Hill Book Company.

X-Ray Extinction in Piezoelectrically Oscillating Crystals

GERALD W. FOX AND WALTER A. FRASER, *Physics Department, Iowa State College*

(Received March 30, 1935)

The original work of Fox and Carr on the effect of piezoelectric vibrations of quartz crystals on the Laue patterns has been continued and extended to include tourmaline and Rochelle salt. The effect of different surface conditions on the Laue patterns has also been studied. The results obtained for all three types of crystals were similar, though the effects were most pronounced in quartz. Quartz is undoubtedly the best material for the study of x-ray extinction in piezoelectric crystals. The increased blackening of the spots in a Laue pattern resulting from piezoelectric oscillation is explained as a consequence of decreased extinction brought about by the warping of the lattice planes during the vibration.

INTRODUCTION

IN 1931,[1] it was observed that the intensity of the Laue diffraction patterns of quartz was greatly increased when the crystal slip was oscillating piezoelectrically. Since that time, a number of investigators[2–11] have studied various phases of the general problem of the reflection of x-rays from crystals subjected to mechanical or piezoelectric strain. The results reported here further contribute to an understanding of the relations between x-ray reflection, surface conditions, and piezoelectric oscillation in crystals.

EXPERIMENTAL

(1) The law of blackening

The law of photographic blackening for the x-rays used in this experiment was determined in the usual way. The opacity of the spots was measured by the microphotometer and the density of each was calculated and plotted against the logarithm of the corresponding time. The blackening proved to be linear above a density of 0.3.

(2) The effect of piezoelectric oscillation on Laue patterns

The increased blackening of the spots in a Laue pattern which results from piezoelectric oscillation of a quartz specimen is very striking, but, for tourmaline and Rochelle salt, it is barely noticeable. The examination of a large number of corresponding pictures involving specimens of quartz, tourmaline and Rochelle salt, oscillating and nonoscillating, leads to the following observations.

(a) The pattern of the oscillating specimen is in every case uniformly increased in intensity over that of the nonoscillating specimen.

(b) Where the crystal slip is thick enough to show double spots, each spot of a pair appears to have the same intensity. Fig. 1 shows typical microphotometer traces of symmetrically located pairs of spots in the pattern produced by a Y-cut quartz plate.

(c) In every instance, individual spots in the Laue patterns are better resolved and sharper for the nonoscillating case. This applies to all

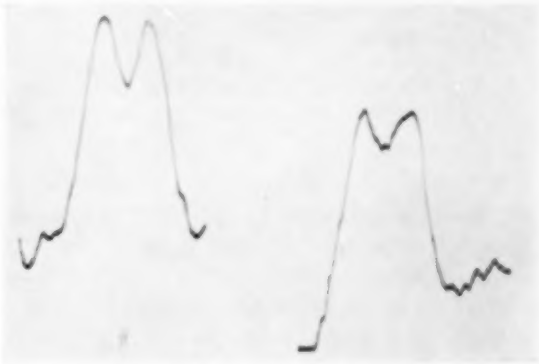

FIG. 1. Microphotometer traces of double spots.

[1] G. W. Fox, and P. H. Carr, Phys. Rev. **37**, 1622 (1931).
[2] C. S. Barrett, and C. E. Howe, Phys. Rev. **39**, 889 (1932).
[3] M. Y. Colby, and S. Harris, Phys. Rev. **42**, 733 (1932).
[4] M. Y. Colby, and S. Harris, Phys. Rev. **43**, 562 (1933).
[5] J. M. Cork, Phys. Rev. **42**, 749 (1932).
[6] G. W. Fox, and J. M. Cork, Phys. Rev. **38**, 1420 (1931).
[7] S. Nishikawa, Y. Sakisaka and I. Sumoto, Phys. Rev. **43**, 363 (1933).
[8] S. Nishikawa, Y. Sakisaka and I. Sumoto, Sci. Pap Inst. Phys. and Chem. Res. **25**, 20 (1934).
[9] Y. Sakisaka, Jap. J. Phys. **4**, 171 (1927).
[10] Y. Sakisaka, Proc. Phys.-Math. Soc. Japan **12**, 189 (1930).
[11] Y. Sakisaka, and I. Sumoto, Proc. Phys.-Math. Soc. Japan **13**, 211 (1931).

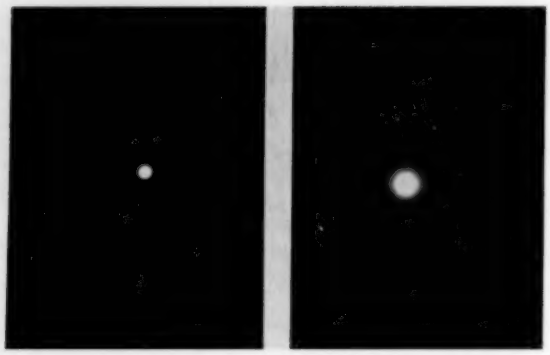

FIG. 2. Laue photographs of quartz, nonoscillating (A), oscillating (B).

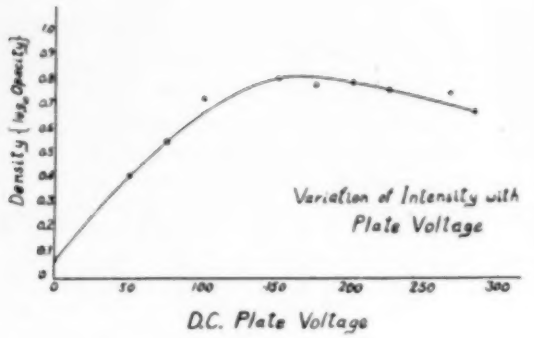

FIG. 3. Density of Laue spots *vs.* voltage on crystal plate.

crystals studied: quartz, Rochelle salt, tourmaline. The boundaries of the spots appear fuzzy and somewhat indistinct when the crystal is oscillating, and, for thick quartz specimens in which complete resolution of the double spots occurs when the plate is not oscillating, a slight additional darkening appears between the spots of a pair under conditions of oscillation.[12]

(d) A more complete pattern results when the crystal is oscillating. This does not mean that any additional spots appear for the oscillating case but that spots representing high orders which ordinarily require long exposures, come out in a shorter time.

(e) A curious observation is that, when a specimen is oscillating, the central spot caused by the undeviated primary beam appears to be more intense. At least the image covers a larger area on the film than in cases where the specimen is not oscillating (Fig. 2). This has been observed for all the crystals studied.

(3) The effect of amplitude of vibration on the pattern of the oscillating crystal

In the preliminary investigation of Fox and Carr,[1] a change in the intensity of the Laue pattern was observed when the piezoelectric amplitude of oscillation of the diffracting crystal was altered. This was investigated more thoroughly through a series of exposures in which the input to the x-ray tube (75 kv, 13 mils) and the time of exposure were constant but the d.c. voltage on the plate of the pliotron was changed.

To insure uniform treatment, the exposures were all developed, and likewise fixed, simultaneously. The opacities of certain corresponding spots in the patterns were determined by the microphotometer and the densities were plotted against the corresponding plate voltages. Fig. 3 shows the data from a series of such exposures. It may be observed that in all cases a maximum exists. Beyond the maximum, the amplitude of crystal oscillation decreases, probably because of partial short circuiting resulting from the high potentials developed across the crystal.

(4) The effect of etching the crystals

For this problem, a plate of quartz and a plate of Rochelle salt were ground with No. 400 carborundum and Laue pictures were taken for each specimen under oscillating and nonoscillating conditions. The quartz plate was then etched for 48 hours in a three percent solution of hydrofluoric acid and the Rochelle salt plate was placed for a short time in water. Laue pictures were then taken of the etched crystals oscillating and nonoscillating. The quartz plate was again etched for the same period and pictures taken. This process of etching and picture taking was repeated for the quartz until the total period of etching reached two weeks. Photomicrographs of the surface of the plate were made at intervals so that the smoothing process could be observed. The results of the study are as follows:

(a) Etching does not change any of the relationships previously observed for the unetched quartz crystal.

[12] C. C. Murdock, Phys. Rev. **45**, 117 (1934).

(b) In the case of Rochelle salt, the Laue photographs of the etched crystal oscillating show slightly increased intensity and a more complete pattern with better spot resolution than do those for the unetched crystal oscillating. For the nonoscillating Rochelle salt crystal, the intensity of the pattern for the unetched crystal is greater than for the etched crystal. There is, however, better resolution of individual spots and the pattern is more complete for the etched crystal.

(c) The effect of etching is more evident with quartz than with Rochelle salt. After the first period of etching, a great increase in intensity of the Laue pattern of the oscillating crystal is evident, and the pattern is more complete than that of the unetched oscillating crystal. Additional etching, however, results in no further increase but actually in a decrease of both the intensity and completeness of the patterns. The surfaces eventually become passive to further action of the acid. For nonoscillating quartz crystals, etching appears to bring about decreased intensity of the Laue pattern and to cause first an increase and then a decrease in the completeness of the pattern. The resolution of the individual spots is better for the etched surfaces, though the first period of etching produces most of the effect.

(d) Rochelle salt plates are so active that the effect of etching on their oscillating properties is not very apparent. The effect on quartz plates, however, is to increase considerably the strength of oscillation. Perhaps this treatment may find commercial application.

Discussion

The unusual diffraction of x-rays by oscillating piezoelectric crystals seems to be intimately tied up with the phenomenon of x-ray extinction and a plausible explanation of the results herein stated may be given on this basis.

By extinction is meant the unusually great absorption of particular frequencies in an x-ray beam of white radiation, the wavelengths and glancing angles of which are such that multiple reflections occur within each nearly perfect crystal fragment. The extent to which extinction occurs is dependent upon the size of the individual fragments.

An ideally perfect crystal is one in which the atoms throughout its entire extent are accurately placed in accordance with the requirements of an undistorted lattice. In such a perfect crystal, there should be no reflection of a particular x-ray wavelength from a set of planes until the grazing angle approaches the particular value given by the Bragg law ($n\lambda = 2d \sin \theta$), at which the reflection should be complete over an angular interval $\Delta\theta$, after which it again falls abruptly to zero. Quartz appears to approximate the conditions representing a perfect crystal.

The inner parts of any crystal, provided it is homogeneous throughout, must be more regular than the surfaces where unbalanced forces between the atoms of the lattice will produce distortion. Just how much crystal should be included in the term "surface" is not entirely clear, but it seems reasonable to include all the outside region where unbalanced atomic forces are evident. If a crystal is roughened with an abrasive, its surface is rendered more imperfect by virtue of the additional strains introduced. Under such conditions, the "surface" must extend deeper into the body of the crystal. If extinction occurs in quartz, one would expect little or no contribution to the spots in the Laue pattern except from the surface region. The formation of double spots is in agreement with this point of view. As a beam of white radiation strikes the first surface of the crystal, it encounters a mosaic of small crystallites and in these occur the diffraction characteristic of the lattice. Because of the strains present in this region, small variations of the lattice constants and tilt of the atomic planes will exist so that the various $d\lambda$'s selected from the incident beam are wider than would be the case under unstrained conditions. Proceeding into the crystal, the lattice becomes more regular, until at a depth of a few thousand layers at the most, the "perfection" characteristic of the unstrained lattice is reached. The resolving power of the lattice depends on the degree of this "perfection." In the ideal case, the width of the $d\lambda$'s selected by this region would be extremely narrow, though finite, and, for those fulfilling the Bragg conditions, complete reflections should occur. Thus, the higher the degree of the lattice perfection, the less x-ray energy will it be able to contribute to the Laue diffraction images. Even if the reflection should be complete for

certain wavelengths, the spectral intervals are so narrow that the actual energy contributions would be quite negligible.

Under piezoelectric oscillation, a number of mechanical pressure waves travel through the crystal simultaneously and a standing wave pattern occurs. As a result, the effective spacing throughout the crystal will vary somewhat and the central part of the crystal which, under non-oscillating conditions, can reflect only a number of very narrow wavelength intervals, now is able to reflect wider ones and so can contribute considerably to the reflection. It seems evident that, because no additional spots appear on the patterns of oscillating crystals, the variation in grating constants must be small. The increased intensity of each spot in the Laue pattern thus results from a slight increase in the width of the $d\lambda$ representing that spot. The fact that the spots are always sharper in the patterns for the non-oscillating crystal bears out this idea.

It is not at all evident why the area covered by the undeviated beam should be so much larger and apparently more intense for the oscillating cases. Perhaps increased scattering power results from the oscillation, though this is only conjecture.

On the basis of the foregoing, one would naturally expect increased amplitude of piezoelectric oscillation to bring about increased blackening. As the amplitude increases, the regularity of the lattice is further distorted and this results in reduced extinction so that each spot in the diffraction pattern represents an increasingly wider $d\lambda$ selected from the incident continuous x-ray spectrum. The fact that, in neither tourmaline nor Rochelle salt is there any great increase in spot blackening with increased amplitude of oscillation, indicates that, in these crystals, extinction does not play as important a role as in quartz. One might conclude that these crystals are not as "perfect" as quartz.

Etching, by removing to some extent the irregularities existing on the surfaces of crystals, tends to increase the extinction effects and so has an opposite effect from that of piezoelectric oscillation. The great increase in spot blackening observed after the first period of etching of the quartz specimen can be attributed to the unusual increase in amplitude of oscillation resulting from such treatment. Since subsequent periods of etching produce no further increase in blackening but actually a decrease, one can say that, after a certain time of etching, further treatment produces no further increased amplitude of oscillation but does have an important effect in decreasing the random orientation of the surface, thereby increasing the effects of extinction and hence decreasing the intensity of the spots in the pattern.

The writers are indebted to Professor J. V. Atanasoff of this department for a number of stimulating discussions of this paper.

The Interaction Between a Neutron and a Proton and the Structure of H^3

L. H. THOMAS, *Mendenhall Laboratory, Ohio State University*

(Received April 17, 1935)

Suppose that the interaction between a neutron and a proton depends on their distance apart so as to be negligible above a certain small distance a, and yet is responsible for the mass defect of H^3. Suppose further that the interaction between two neutrons and a proton may be compounded in the usual way from that between a neutron and a proton, the interaction between two neutrons being neglected, while there is no prohibition of a wave function symmetrical in the positions of two neutrons. Then it is shown that the mass defect of H^3 is made arbitrarily large by taking a small enough. The observed mass defect of H^3 thus provides, on the above assumptions, a lower limit for a; and in particular rules out the possibility that the interaction may be regarded as arising from a singularity in configuration space. We conclude, in effect, that: either two neutrons repel one another by an amount not negligible compared with the attraction between a neutron and a proton; or that the wave function cannot be symmetrical in their positions; or else that the interaction between a neutron and a proton is not confined within a relative distance very small compared with 10^{-13} cm[1].

THE EQUATION ASSUMED FOR A NEUTRON AND A PROTON

SUPPOSE that the positional part $\psi(\mathbf{r}_1, \mathbf{r}_2)$ of a wave function for a neutron (at $\mathbf{r}_2$) and a proton (at $\mathbf{r}_1$) satisfies the equation

$$-(h^2/8\pi^2 m)\{\nabla_1^2\psi+\nabla_2^2\psi\}+V(r_{12})\psi-E\psi=0, \tag{1}$$

where the effective potential energy $V(r_{12})$, depending only on the distance apart, r_{12}, of the two particles, is such that

$$V(r)<0, \quad r<a; \qquad V(r)=0, \quad r\geq a. \tag{2}$$

Suppose that Eq. (1) has a solution of the form

$$\psi=\varphi(r_{12}), \qquad E=E_0<0, \tag{3}$$

such that (a)
$$4\pi\int_0^\infty \varphi(r)^2 r^2 dr=1, \tag{4}$$

so that
$$\varphi(r)=Ae^{-\lambda r}/r, \tag{5}$$

where
$$(h^2/4\pi^2 m)\lambda^2=-E_0, \tag{6}$$

and
$$4\pi A^2 e^{-2\lambda a}/2\lambda<1; \tag{7}$$

and (b)
$$4\pi\int_0^a (d\varphi/dr)^2 r^2 dr<K/a. \tag{8}$$

In the above, h is to be taken to be the usual Planck's constant, m the proton mass or the neutron mass, and E_0 the energy of the normal state of a deuteron.

Assumption (b) is probably not necessary for the result that will be obtained, but is necessary for the proof that will be given. It is true if $V(r)$ and $\varphi(r)$ are everywhere finite, and remains true, K approaching a limit, if we suppose that, E_0 remaining unaltered, a tends to zero while $V(r)$ approaches a definite form,

i.e.,
$$V(r)\sim a^{-2}f(r/a). \tag{9}$$

The modifications required in the proof when the potential energy $V(r)$ is replaced by a singularity of ψ in the configuration space as $r\to 0$ will be considered later.

[1] Such a lower limit to a cannot be deduced from the observations of neutron-proton scattering until these are known more accurately. (See E. Wigner, Zeits. f. Physik **83**, 253 (1933).)

The Equation Assumed for Two Neutrons and a Proton

Suppose that the positional part $\psi(\mathbf{r}_1, \mathbf{r}_2, \mathbf{r}_3)$ of a wave function for two neutrons (at $\mathbf{r}_1$ and $\mathbf{r}_2$) and a proton (at $\mathbf{r}_3$), symmetrical in the positions of the two neutrons, satisfies the equation

$$-(h^2/8\pi^2 m)\{\nabla_1^2\psi+\nabla_2^2\psi+\nabla_3^2\psi\}+V(r_{13})\psi+V(r_{23})\psi-E\psi=0, \tag{10}$$

where $V(r_{13})$ and $V(r_{23})$ represent the effective potential energies of interaction of the neutrons and the proton, depending only on their distances apart r_{13} and r_{23}, and are of the form 2 above: the interaction between two neutrons is neglected, but it cannot affect the result that will be obtained unless it gives rise to a repulsion of the same order of magnitude as the attraction between a neutron and a proton.

If $\psi=\psi(\mathbf{s}_1, \mathbf{s}_2)$, where $\mathbf{s}_1=\mathbf{r}_1-\mathbf{r}_3$, $\mathbf{s}_2=\mathbf{r}_2-\mathbf{r}_3$ (11)

(10) becomes

$$-(h^2/4\pi^2 m)\{\nabla_1^2\psi+(\nabla_1\cdot\nabla_2)\psi+\nabla_2^2\psi\}+V(s_1)\psi+V(s_2)\psi-E\psi=0 \tag{12}$$

and the algebraically least value E_1 of E, if it exists, for which a continuous differentiable function $\psi(\mathbf{s}_1, \mathbf{s}_2)$ can be found to satisfy (12), must obey the inequality

$$E_1<\frac{\int\int[(h^2/4\pi^2 m)\{(\nabla_1\psi)^2+(\nabla_1\psi\cdot\nabla_2\psi)+(\nabla_2\psi)^2\}+V(s_1)\psi^2+V(s_2)\psi^2]dv_1dv_2}{\int\int\psi^2 dv_1dv_2}, \tag{13}$$

where ψ is any continuous function of $\mathbf{s}_1$ and $\mathbf{s}_2$, differentiable almost everywhere, for which the integrals exist, dv_1 and dv_2 being volume elements in $\mathbf{s}_1$ and $\mathbf{s}_2$ space.

The Choice of a Function

Put $s^2=(4/3)(\mathbf{s}_1^2-(\mathbf{s}_1\cdot\mathbf{s}_2)+\mathbf{s}_2^2)$,

$$\tan\theta_1=3^{\frac{1}{2}}s_1/|\mathbf{s}_1-2\mathbf{s}_2|, \qquad \tan\theta_2=3^{\frac{1}{2}}s_2/|\mathbf{s}_2-2\mathbf{s}_1|. \tag{14}$$

Then
$$\psi=\frac{1}{s^2}K_0(\mu s)\left[\frac{\pi/2-\theta_1}{\sin\theta_1\cos\theta_1}+\frac{\pi/2-\theta_2}{\sin\theta_2\cos\theta_2}\right] \tag{15}$$

satisfies the equation

$$\nabla_1^2\psi+(\nabla_1\cdot\nabla_2)\psi+\nabla_2^2\psi=\mu^2\psi, \tag{16}$$

where K_0 is Macdonald's Bessel function of order zero.[2]

For if
$$\mathbf{s}_1=\mathbf{u}, \qquad \mathbf{s}_1+2\mathbf{s}_2=3^{\frac{1}{2}}\mathbf{v}, \tag{17}$$

then
$$\nabla_1^2\psi+(\nabla_1\cdot\nabla_2)\psi+\nabla_2^2\psi\equiv\nabla_u^2\psi+\nabla_v^2\psi,$$

and if
$$u=s\sin\theta_1, \qquad v=s\cos\theta_1$$

then
$$\frac{\partial^2\psi}{\partial u^2}+\frac{2}{u}\frac{\partial\psi}{\partial u}+\frac{\partial^2\psi}{\partial v^2}+\frac{2}{v}\frac{\partial\psi}{\partial v}\equiv\frac{\partial^2\psi}{\partial s^2}+\frac{5}{s}\frac{\partial\psi}{\partial s}+2\frac{(\cot\theta_1-\tan\theta_1)}{s^2}\frac{\partial\psi}{\partial\theta_1}+\frac{1}{s^2}\frac{\partial^2\psi}{\partial\theta_1^2},$$

while
$$2(\cot\theta-\tan\theta)\frac{d}{d\theta}\left[\frac{A+B\theta}{\sin\theta\cos\theta}\right]+\frac{d^2}{d\theta^2}\left[\frac{A+B\theta}{\sin\theta\cos\theta}\right]=\frac{4(A+B\theta)}{\sin\theta\cos\theta},$$

and
$$\frac{d^2}{ds^2}\left[\frac{K_0(\mu s)}{s^2}\right]+\frac{5}{s}\frac{d}{ds}\left[\frac{K_0(\mu s)}{s^2}\right]+\frac{4}{s^2}\left[\frac{K_0(\mu s)}{s^2}\right]=\mu^2\left[\frac{K_0(\mu s)}{s^2}\right].$$

[2] Watson, *Theory of Bessel Functions*, p. 78.

From the function given by (15) we build up one continuous, and differentiable almost everywhere, as follows: Let $l \gg a$.

In region (i), $s>l$, $s \sin\theta_1>a$, $s\sin\theta_2>a$, let

$$\psi(\mathbf{s}_1,\mathbf{s}_2)=\frac{1}{s^2}K_0(\mu s)\left[\frac{\pi/2-\theta_1}{\sin\theta_1\cos\theta_1}+\frac{\pi/2-\theta_2}{\sin\theta_2\cos\theta_2}\right]; \tag{18}$$

in region (ii) $s>l$, $s\sin\theta_1<a$, $s\sin\theta_2>a$, let

$$\psi(\mathbf{s}_1,\mathbf{s}_2)=\frac{1}{s^2}K_0(\mu s)\left[C(s)\varphi(s\sin\theta_1)+\frac{\pi/2-\theta_2}{\sin\theta_2\cos\theta_2}-\frac{2\pi}{3^{\frac{1}{2}}}\right]; \tag{19}$$

in region (iii), $s>l$, $s\sin\theta_1>a$, $s\sin\theta_2<a$, let

$$\psi(\mathbf{s}_1,\mathbf{s}_2)=\frac{1}{s^2}K_0(\mu s)\left[\frac{\pi/2-\theta_1}{\sin\theta_1\cos\theta_1}-\frac{2\pi}{3^{\frac{1}{2}}}+C(s)\varphi(s\sin\theta_2)\right]; \tag{20}$$

where
$$C(s)A\frac{e^{-\lambda a}}{a}=\frac{\pi/2-\sin^{-1}(a/s)}{a/s(1-a^2/s^2)^{\frac{1}{2}}}+\frac{2\pi}{3^{\frac{1}{2}}}=\frac{\pi s}{2a}+\frac{2\pi}{3^{\frac{1}{2}}}-1+0(a/s),\quad a\ll s, \tag{21}$$

and φ is given by (3); in region (iv), $s<l$, let

$$\psi(\mathbf{s}_1,\mathbf{s}_2)=\frac{s}{l}\psi\left(\frac{l}{s}\mathbf{s}_1,\frac{l}{s}\mathbf{s}_2\right). \tag{22}$$

In the sequel ψ will stand for the function given by (18), (19), (20) and (22).

The Bound for the Energy

As $a/l\to 0$ and $\mu l\to 0$,

$$\int\int\psi^2 dv_1dv_2\to\int\int\left\{\frac{1}{s^2}K_0(\mu s)\left[\frac{\pi/2-\theta_1}{\sin\theta_1\cos\theta_1}+\frac{\pi/2-\theta_2}{\sin\theta_2\cos\theta_2}\right]\right\}^2 dv_1dv_2=G,\quad \text{say,} \tag{23}$$

a convergent integral of which the value lies between twice and four times

$$\int\int\left\{\frac{1}{s^2}K_0(\mu s)\frac{\pi/2-\theta_1}{\sin\theta_1\cos\theta_1}\right\}^2 dv_1dv_2=\frac{3^{\frac{1}{2}}}{2^3}16\pi^2\int_0^\infty s\{K_0(\mu s)\}^2 ds\int_0^{\pi/2}\left(\frac{\pi}{2}-\theta\right)^2 d\theta=\frac{3^{\frac{1}{2}}}{2^3}16\pi^2\frac{1}{2\mu^2}\frac{\pi^2}{24}, \tag{24}$$

i.e., between $3^{\frac{1}{2}}\pi^4/4\mu^2$ and $3^{\frac{1}{2}}\pi^4/2\mu^2$. Let

$$I=\int\int\left[\{(\nabla_1\psi)^2+(\nabla_1\psi\cdot\nabla_2\psi)+(\nabla_2\psi)^2\}+\frac{4\pi^2 m}{h^2}\{V(s_1)\psi^2+V(s_2)\psi^2\}\right]dv_1dv_2$$
$$=I_{(i)}+I_{(ii)}+I_{(iii)}+I_{(iv)}, \tag{25}$$

where the integration is extended through region (i) in $I_{(i)}$, and so on.

In region (i), $V(s_1)=0$ and $V(s_2)=0$ by (2), and, in virtue of (16),

$$\begin{aligned} I_{(i)}&=\int\{(\mathbf{l}_1\cdot\{\nabla_1\psi+\tfrac{1}{2}\nabla_2\psi\})+(\mathbf{l}_2\cdot\{\tfrac{1}{2}\nabla_1\psi+\nabla_2\psi\})\}dS-\mu^2{}_{(i)}\int\int\psi^2 dv_1dv_2\\ &=J_{(ii)}+J_{(iii)}+J_{(iv)}-\mu^2{}_{(i)}\int\int\psi^2 dv_1dv_2, \end{aligned} \tag{26}$$

where the surface integral is extended over the boundary between (i) and (ii) in $J_{(ii)}$, between (i) and (iii) in $J_{(iii)}$, and between (i) and (iv) in $J_{(iv)}$. $\mathbf{l}_1$ and $\mathbf{l}_2$ are the direction cosines in the directions $\mathbf{s}_1$ and $\mathbf{s}_2$ of the normal to the five-dimensional boundary region outward from (i).

The volume integral in (26) gives in the limit the term $-\mu^2 G$.

The surface integral $J_{(ii)}$ reduces to

$$-\int\int s_1(\mathbf{s}_1\cdot\psi\{\nabla_1\psi+\tfrac{1}{2}\nabla_2\psi\})d\omega_1 dv_2',$$

where the inner integral is taken over all solid angle in $\mathbf{s}_1$ space for $s_1=a$ and $\mathbf{s}_2=\mathbf{s}_2'+\frac{1}{2}\mathbf{s}_1$, and then the outer integration over $\mathbf{s}_2'$ space for $s_2'^2>\frac{3}{4}(l^2-a^2)$. Now as $s_1/s_2\to 0$, so that $s_1\sim s\theta_1$,

$$\psi=(1/s^2)K_0(\mu s)[\pi/2\theta_1-1+2\pi/3^{\frac{1}{2}}+0(\theta_1)] \text{ and } (\mathbf{s}_1\cdot\{\nabla_1\psi+\tfrac{1}{2}\nabla_2\psi\})=-(1/s^2)K_0(ms)[\pi/2\theta_1+0(\theta_1)],$$

so that the inner integral becomes

$$4\pi K_0^2(\mu s)[\pi^2/4s^2a+\pi/2\{2\pi/3^{\frac{1}{2}}-1\}1/s^3+0(a/s^4)]$$

(terms of order $1/s^3$ in the parenthesis arising from the difference between $\mathbf{s}_2$ and $\mathbf{s}_2'$ vanishing on integration) and

$$J_{(ii)}=-\int 4\pi K_0^2(\mu s)[\pi^2/4s^2a+\pi/2\{2\pi/3^{\frac{1}{2}}-1\}1/s^3+0(a/s^4)]dv_2, \tag{27}$$

integrated over $\mathbf{s}_2$ space for $s=2s_2/3^{\frac{1}{2}}>l$.

The volume-integral $I_{(ii)}$ reduces, in like manner, first to

$$\int\int[(\nabla_1\varphi(s_1))^2+(4\pi^2m/h^2)V(s_1)\varphi^2(s_1)]dv_1\{(1/s^2)K_0(\mu s)C(s)\}^2[1+0(a^2/s^2)]dv_2,$$

where the inner integral is over $\mathbf{s}_1$ space for $s_1<a$, and the outer over $\mathbf{s}_2$ space for $s=2s_2/3^{\frac{1}{2}}>l$; ($V(s_2)$ vanishing in this region, and terms arising from $(\nabla_1\psi\cdot\nabla_2\psi)$ and $\nabla_2^2\psi$, as well as from the term $(\pi/2-\theta_2)/\sin\theta_2\cos\theta_2-(2\pi/3^{\frac{1}{2}})(\to 0)$ in the expression for ψ, of order a/s compared with terms retained, vanishing on integration over $\mathbf{s}_1$ space, leaving only terms of order a^2/s^2). Now, from (1), (3) and (5),

$$\int_{s_1<a}[(\nabla_1\varphi(s_1))^2+(4\pi^2m/h^2)\{V(s_1)-E_0\}\varphi(s_1)^2]dv_1=\int_{s_1=a}(\mathbf{s}_1\cdot\nabla_1\varphi(s_1))\varphi(s_1)s_1d\omega_1$$
$$=-4\pi A^2\{1/a+\lambda\}e^{-2\lambda a}.$$

The term involving E_0, $\lambda^2\int_{s_1<a}\varphi(s_1)^2dv_1$, tends to zero by (4) and (6), and, with the expression for $C(s)$, (21),

$$I_{(ii)}=\int 4\pi K_0^2(\mu s)[\pi^2/4s^2a+(\pi^2/4s^2)\lambda+2(\pi/2)(2\pi/3^{\frac{1}{2}}-1)+0(a/s^4)]dv_2, \tag{28}$$

integrated over $\mathbf{s}_2$ space for $s=2s_2/3^{\frac{1}{2}}>l$.

From (27) and (28),

$$I_{(ii)}+J_{(ii)}=-\int_{s>l}4\pi K_0^2(\mu s)\{(\pi^2/4s^2)\lambda+\pi/2(2\pi/3^{\frac{1}{2}}-1)(1/s^3)+0(a/s^4)\}dv_2$$
$$=-16\pi^2(3^{\frac{1}{2}}/2^3)\int_l^\infty K_0^2(\mu s)\{\pi^2\lambda+\pi/2s(2\pi/3^{\frac{1}{2}}-1)+0(a/s^4)\}ds$$
$$=-16\pi^2(3^{\frac{1}{2}}/2^3)(\pi/2)(2\pi/3^{\frac{1}{2}}-1)|\log\mu l|^3\{1+0(1/|\log\mu l|)+0(a/l)\} \tag{29}$$

as $a/l\to 0$ and $\mu l\to 0$, since

$$K_0(\mu s)=-\{\log\tfrac{1}{2}\mu s+\gamma\}\{1+0(\mu s)\} \quad \text{as} \quad \mu s\to 0. \tag{30}$$

$$I_{(iii)}+J_{(iii)}=I_{(ii)}+J_{(ii)}. \tag{31}$$

The surface integral $J_{(iv)}$ over part of the five-dimensional surface $s=l$ gives in the limit a similar integral to that for G (23), $-s^5(1/s^2)K_0(\mu s)(\partial/\partial s)(1/s^2)K_0(\mu s)$ replacing $\int_0^\infty sK_0(\mu s)ds$, so that

$$J_{(iv)}=0(|\log \mu l|^2) \quad \text{as} \quad \mu l\to 0. \tag{32}$$

The volume integral $I_{(iv)}$ consists of terms in $V(s_1)$ and $V(s_2)$ that are always negative and the volume integral throughout the six-dimensional region inside the surface $s=l$ of (in terms of the coordinates $\mathbf{u}$ and $\mathbf{v}$ of 17), $(\nabla_u(s/l)\psi_{(s=l)})^2+(\nabla_v(s/l)\psi_{(s=l)})^2$, which reduces to the surface integral over $s=l$ of

$$l/6\{\psi^2/l^2+(\nabla_u\psi)^2+(\nabla_v\psi)^2-(\partial\psi/\partial s)^2\},$$

which, in virtue of (8) and (30), is of order $K(l/a)|\log \mu l|^2$. Thus

$$I_{(iv)}<0(K(l/a)|\log \mu l|^2). \tag{33}$$

Thus, combining (25), (26), (29), (31), (32) and (33),

$$I=I_{(i)}+I_{(ii)}+I_{(iii)}+I_{(iv)}<(J_{(ii)}+I_{(ii)})+(J_{(iii)}+I_{(iii)})+J_{(iv)}+I_{(iv)}$$
$$<-32\pi^2(3^{\frac{1}{2}}\pi/2^32)(2\pi/3^{\frac{1}{2}}-1)|\log \mu l|^3\{1+0(K/(a/l)|\log \mu l|)+0(a/l)\} \tag{34}$$

and from (34), (13), (6) and (24),

$$\frac{E_1}{E_0}>\frac{24(2\pi/3^{\frac{1}{2}}-1)}{\pi}\frac{\mu^2}{\lambda^2}|\log \mu l|^3\left\{1+0\left(\frac{K}{(a/l)|\log \mu l|}\right)+0(a/l)\right\}. \tag{35}$$

Now put $l=a/\epsilon$, $\mu=(1/a)\epsilon e^{-1/K\epsilon^2}$, where ϵ is chosen so that ϵ and $K\epsilon^2$ are small, and we obtain

$$E_1/E_0>(1\cdot 6/a^2\lambda^2)e^{-2/K\epsilon^2}/K^3\epsilon^4\{1+0(\epsilon)\}. \tag{36}$$

In order to obtain a numerical result from this it would be necessary first to take a value for K. If $V(r)$ is of the form given by (9) and (2), this can be done. Secondly it would be necessary to know how small ϵ must be taken, which would involve estimates of a number of complicated integrals. For the observed ratio $E_1/E_0\approx 4$, a lower bound of a as a definite fraction of $1/\lambda$, $=h/2\pi(mE_0)^{\frac{1}{2}}$ $\approx 6\cdot 10^{-13}$ cm would be obtained. The value so obtained would be a rather poor one, for there is no reason why the function ψ chosen should (if $a\lambda$ is not very small) be at all a good approximation to the solution of (12); moreover the introduction of K into (36) came from $I_{(iv)}$ in which negative terms in $V(r_{13})$ and $V(r_{23})$ were left out; if these could be taken into account, and if ψ were chosen suitably in region (iv), this could probably be avoided.

However, it is seen that a cannot be very small compared with 10^{-13} cm. A closer limit could perhaps best be obtained by numerical approximation to E_1 for particular forms of $V(r)$.

The Assumptions When the Potential Energy is Replaced by a Singularity[2]

Suppose that the positional part $\psi(\mathbf{r}_1, \mathbf{r}_2)$ of a wave function for a neutron (at $\mathbf{r}_2$) and a proton (at $\mathbf{r}_1$) satisfies the equation

$$-(h^2/8\pi^2m)\{\nabla_1^2\psi+\nabla_2^2\psi\}-E\psi=0 \tag{37}$$

but is not continuous at $r_{12}=0$, satisfying, however, the boundary condition

$$\psi(\mathbf{r}_1, \mathbf{r}_2)-A(1/r_{12}-\lambda)\to 0 \quad \text{as} \quad r_{12}\to 0. \tag{38}$$

(37) has a solution of the form

$$\psi=\varphi(r_{12}), \qquad E=E_0<0, \tag{39}$$

[2] I owe to Professor E. Wigner the remark that this case does not immediately follow from the above, as the integral I does not converge.

such that $$4\pi\int_0^\infty \varphi(r)^2 r^2 dr = 1, \tag{40}$$

viz. $$\varphi(r) = Ae^{-\lambda r}/r, \tag{41}$$

where $$(h^2/4\pi^2 m)\lambda^2 = -E_0 \tag{42}$$

and $$4\pi A^2 = 2\lambda. \tag{43}$$

Suppose that the positional part $\psi(\mathbf{r}_1, \mathbf{r}_2, \mathbf{r}_3)$ of a wave function for two neutrons (at $\mathbf{r}_1$ and $\mathbf{r}_2$) and a proton at ($\mathbf{r}_3$), symmetrical in the positions of the two neutrons, satisfies the equation

$$-(h^2/8\pi^2 m)\{\nabla_1^2\psi + \nabla_2^2\psi + \nabla_3^2\psi\} - E\psi = 0 \tag{44}$$

but is not continuous as $r_{12} \to 0$ or $r_{23} \to 0$, although functions $f(\mathbf{r}_1, \mathbf{r}_3)$ and $f(\mathbf{r}_2, \mathbf{r}_3)$ exist such that

$$\left.\begin{aligned} &\psi(\mathbf{r}_1, \mathbf{r}_2, \mathbf{r}_3) - f(\mathbf{r}_1, \mathbf{r}_3)\{1/r_{23} - \lambda\} \to 0 \quad \text{as} \quad r_{23} \to 0 \quad \text{for fixed } \mathbf{r}_1 \\ \text{and} \quad &\psi(\mathbf{r}_1, \mathbf{r}_2, \mathbf{r}_3) - f(\mathbf{r}_2, \mathbf{r}_3)\{1/r_{13} - \lambda\} \to 0 \quad \text{as} \quad r_{13} \to 0 \quad \text{for fixed } \mathbf{r}_2 \end{aligned}\right\} \tag{45}$$

(while if $A(\mathbf{r}_3)$ exists such that

$$\psi(\mathbf{r}_1, \mathbf{r}_2, \mathbf{r}_3) - A(\mathbf{r}_3)(1/r_{23} - \lambda)(1/r_{13} - \lambda) \to 0 \quad \text{as} \quad (r_{13}, r_{23}) \to (0, 0), \tag{46}$$

no boundary condition at $(r_{13}, r_{23}) = (0, 0)$ would be violated: another requirement at $(r_{13}, r_{23}) = (0, 0)$ would correspond to the limit of an equation of type (10) with potential energy $V(\mathbf{r}_1, \mathbf{r}_2, \mathbf{r}_3)$ not of the form $V(r_{12}) + V(r_{13})$); as before, interaction between the two neutrons is neglected.

If $\psi = \psi(\mathbf{s}_1, \mathbf{s}_2)$, where $$\mathbf{s}_1 = \mathbf{r}_1 - \mathbf{r}_3, \qquad \mathbf{s}_2 = \mathbf{r}_2 - \mathbf{r}_3 \tag{47}$$

(44) becomes $$-(h^2/4\pi^2 m)\{\nabla_1^2\psi + (\nabla_1 \cdot \nabla_2)\psi + \nabla_2^2\psi\} - E\psi = 0, \tag{48}$$

subject to the condition that $f(\mathbf{s}_1)$ exists such that

$$\left.\begin{aligned} &\psi(\mathbf{s}_1, \mathbf{s}_2) - f(\mathbf{s}_1)(1/s_2 - \lambda) \to 0 \quad \text{as} \quad s_2 \to 0, \\ &\psi(\mathbf{s}_1, \mathbf{s}_2) - f(\mathbf{s}_2)(1/s_1 - \lambda) \to 0 \quad \text{as} \quad s_1 \to 0 \end{aligned}\right\} \tag{49}$$

(while if A exists such that

$$\psi(\mathbf{s}_1, \mathbf{s}_2) - A(1/s_2 - \lambda)(1/s_1 - \lambda) \to 0 \quad \text{as} \quad (s_1, s_2) \to (0, 0),$$

no boundary condition at $(s_1, s_2) = (0, 0)$ would be violated).

The algebraically least value E_1 of E, if it exists, for which a continuous twice differentiable function $\psi(\mathbf{s}_1, \mathbf{s}_2)$ can be found to satisfy (48) and (49) must obey the inequality

$$E_1 < (h^2/4\pi^2 m)\int\int\{\nabla_1^2\psi + (\nabla_1 \cdot \nabla_2)\psi + \nabla_2^2\psi\}\psi dv_1 dv_2 / \int\int\psi^2 dv_1 dv_2 \tag{50}$$

where ψ is any continuous differentiable function of $\mathbf{s}_1$ and $\mathbf{s}_2$, twice differentiable almost everywhere, except as $s_1 \to 0$ and $s_2 \to 0$, where it must satisfy (49). A form like (13) cannot be used here because the integral does not converge.

Under the Singularity Assumption There is No Algebraically Least Energy

As we wish to use the same function $\psi(\mathbf{s}_1, \mathbf{s}_2)$ as above, except that $\varphi(r)$ is now to be given by (41) everywhere, which is not differentiable at $s = l$, $r_1 = a$, and $r_2 = a$, (50) must be modified to take account of this: to the volume integral in the numerator must be added the difference of surface integrals

$$\tfrac{2}{1}\left|\int\{(\mathbf{l}_1 \cdot \{\nabla_1\psi + \tfrac{1}{2}\nabla_2\psi\}) + (\mathbf{l}_2 \cdot \{\tfrac{1}{2}\nabla_1\psi + \nabla_2\psi\})\}\psi dS\right| \tag{51}$$

over all five-dimensional surfaces of discontinuity of the first derivatives of ψ, $\mathbf{l}_1$ and $\mathbf{l}_2$ being the direction cosines in the directions $\mathbf{s}_1$ and $\mathbf{s}_2$ of the normal to the five-dimensional boundary region from region 1 to region 2. A function with continuous first derivatives and near ψ will have a value for (50) nearly equal to that for ψ with this addition.

We can now write (50) in the form

$$E_1<(h^2/4\pi^2m)\{I_{(i)}+I_{(ii)}+I_{(iii)}+I_{(iv)}+J_{(ii)}+J_{(iii)}+J_{(iv)}\}/\int\int\psi^2 dv_1 dv_2 \tag{52}$$

where $I_{(i)}$, $I_{(ii)}$, $I_{(iii)}$, and $I_{(iv)}$, are the values of the volume integral extended over the regions (i), (ii), (iii) and (iv), and $J_{(ii)}$, $J_{(iii)}$ and $J_{(iv)}$, are the values of the surface integral (51) over the regions $s_1=a$, $s_2=a$, and $s=l$.

By (16), $$I_{(i)}=0. \tag{53}$$

$I_{(ii)}$ can be expressed as in (28) as an integration over $\mathbf{s}_1$ space followed by one over $\mathbf{s}_2$ space. Terms of order $1/s_1^3$ and $1/s_1^4$ which would make the inner integral diverge do not occur, on account of (41), and the terms that remain give rise to terms of order a/l in the result compared to the principal terms from $J_{(ii)}$.

The two integrals in $J_{(ii)}$ now combine like (27) and (28) to give (as before)

$$I_{(ii)}+J_{(ii)}=-16\pi^2(3^1\pi/2^32)(2\pi/3^1-1)|\log\mu l|^3\{1+0(1/|\log\mu l|)+0(a/l)\}, \tag{54}$$

while $$I_{(iii)}+J_{(iii)}=I_{(ii)}+J_{(ii)}. \tag{55}$$

The integral over the side $s>l$ of $s=l$ in $J_{(iv)}$ is as before, (32). The integral over the side $s<l$ of $s=l$ reduces to the integral of ψ^2/l over $s=l$, and so gives a result of order $|\log\mu l|^2$.

The volume integral $I_{(iv)}$ reduces (in terms of $\mathbf{u}$ and $\mathbf{v}$ of (17)) to the surface integral over $s=l$ of

$$\psi l\{\tfrac{3}{8}(\psi/l^2-\partial\psi/l\partial s)+\tfrac{1}{8}(\partial\psi/l\partial s+\{\nabla_u{}^2\psi+\nabla_v{}^2\psi-\partial^2\psi/\partial s^2\})\}. \tag{56}$$

The terms in (33) which required (8) now do not occur, terms in $\nabla_u{}^2\psi+\nabla_v{}^2\psi$ that would make the integral diverge not occurring on account of (41), and no term gives a result larger than of order $|\log\mu l|^2$: i.e.,

$$I_{(iv)}+J_{(iv)}=0(|\log\mu l|^2). \tag{57}$$

Thus, combining (53), (54), (55) and (57), with (50), (42) and (24),

$$\frac{E_1}{E_0}>\frac{24(2\pi/3^1-1)}{\pi}\frac{\mu^2}{\lambda^2}|\log\mu l|^3\left\{1+0\left(\frac{1}{|\log\mu l|}\right)+0\left(\frac{a}{l}\right)\right\} \tag{58}$$

where we may let μ have any value, $\mu l\to 0$, and $a/l\to 0$, so that E_1 cannot exist.

My thanks are due to Professor Uhlenbeck for suggesting this problem to me and to Professor Wigner for helpful discussion.[4]

Note added in proof: No change is made in the above argument if the force assumed between a neutron and a proton is of Majorana[5] type, for the wave function used is symmetrical in their positions wherever the potential energy differs from zero.

---

[4] Some remarks on the H^3 problem may be found in E. Wigner, Phys. Rev. **43**, 252 (1933).
[5] Majorana, Zeits. f. Physik **82**, 137 (1932).

The Energy Spectrum of the Neutrons from the Disintegration of Beryllium by Deuterons*

T. W. BONNER** AND W. M. BRUBAKER, *Kellogg Radiation Laboratory, California Institute of Technology*

(Received April 1, 1935)

The energy distribution of the neutrons from the disintegration of beryllium by high speed deuterons has been investigated by the method of recoil-protons in a high pressure cloud chamber. The maximum neutron energies which were observed correspond to an energy of disintegration of 4.14 MEV. The mass of Be^9 calculated from these data, assuming the reaction $_4Be^9 + _1H^2 \rightarrow _5B^{10} + _0n^1$, is 9.0123 ± 0.0008. Several other neutron groups of lower energies were observed which indicate that the B^{10} nucleus is left in one of several possible excited states. The excited B^{10} nucleus presumably falls to the normal state by the emission of a γ-ray.

THE copious emission of neutrons from the bombardment of beryllium by high speed deuterons was first reported by Crane, Lauritsen and Soltan.[1] Indications of the energies of the neutrons produced in this disintegration have been obtained by Kurie,[2] Oliphant,[3] and Bjerge and Westcott.[4] From the disintegrations produced in nitrogen by the neutrons from beryllium which was bombarded with 2 M.E.V. deuterons, Kurie has inferred that their maximum energy is about 10 M.E.V. On the other hand, the results of Oliphant,[3] who used a helium-filled counting chamber and linear amplifier, suggest that there are not many neutrons with energies over 3 M.E.V. The energy of the bombarding deuterons in the latter experiment was only 0.3 M.E.V., but there still remains a considerable discrepancy in the two results. Bjerge and Westcott[4] have found that the deuteron-beryllium neutrons do not induce radioactivity in fluorine and silicon as do the high energy neutrons from lithium + deuterons and beryllium + alpha-particles. This suggests that the deuteron-beryllium neutrons are of low energy.

The purpose of the present experiment was to determine accurately the maximum energy of the deuteron-beryllium neutrons, and to study their energy distribution. This was done by measuring the ranges of the recoil-protons ejected from CH_4 in a high pressure cloud chamber, a method which has been described and used by Bonner and Mott-Smith.[5] In a high pressure cloud chamber, it is possible to stop a recoil-proton of high energy in a comparatively short distance, so that the entire track lies within the chamber.

The maximum energy of the neutrons cannot be determined definitely unless the velocity and mass of the recoil nucleus are known. Range-velocity curves are accurately known only for protons and α-particles. At present it is impossible without the aid of a very strong magnetic field to distinguish unambiguously between the tracks left in a cloud chamber by these two particles. Because of the water or alcohol vapor used in an expansion chamber, there are always hydrogen atoms present. Thus we cannot determine the maximum energy of neutrons with a helium-filled chamber as the recoil H-particles have a longer range for the same energy. The above reasons force one to the use of recoil-protons for the cloud-chamber determinations of neutron energies. The presence of carbon or other atoms heavier than hydrogen does not interfere with this work, since such atoms have very much shorter ranges than recoil-protons of the same energy.

APPARATUS

The automatic high pressure cloud chamber which was used in this experiment has been described previously.[6] It is 9 cm in diameter, and 3 cm deep. In use, its center was placed 20 cm from the center of the beryllium target which had a radius of 2.5 cm. The arrangement was such that the neutrons which entered the chamber

* A preliminary report of this work was given at the meeting of the American Physical Society, Los Angeles, December 1934. Phys. Rev. **47**, 254 (1935).

** National Research Fellow.

[1] Crane, Lauritsen and Soltan, Phys. Rev. **44**, 692 (1933).

[2] F. N. D. Kurie, Phys. Rev. **47**, 97, 253A (1935).

[3] Oliphant, Int. Conf. of Physics, London, October, 1934.

[4] Bjerge and Westcott, Nature **134**, 177 (1934).

[5] Bonner and Mott-Smith, Phys. Rev. **46**, 258 (1934).

[6] Brubaker and Bonner, Rev. Sci. Inst. **6**, 143 (1935).

made an angle of approximately 90° with the incident beam of deuterons on the target. The deuterons were accelerated by the Crane and Lauritsen apparatus, which was operated in such a manner that the deuterons struck the target for only a fraction of a second following the expansion. Thus no neutrons entered the chamber until it was expanded. The cloud chamber was filled with gas from a cylinder which contained 85.1 percent CH_4, 13.5 percent C_2H_6, and 1.4 percent N_2. The pressure of the gas in the chamber before and after expansion was read from an ordinary pressure gauge which had been calibrated hydraulically. The stopping power of the gas relative to air was computed from the known pressure and the relative amounts of the gases contained in the chamber. The stopping powers used there were those determined by Bragg, and were 0.86 for CH_4, 1.52 for C_2H_6, and 0.99 for N_2. The stopping power of the alcohol vapor contained in the chamber was computed from data given by Phillipp.[7]

Results

Approximately 3000 sets of stereoscopic photographs were taken when beryllium was bombarded by 0.9 M.E.V. deuterons. On the photographs, numerous recoil-protons were observed and the ranges of approximately 900 were measured. Test runs were made in which the beryllium target was replaced by a brass one; less than 1/1000 as many recoil-protons were observed. The effect of the small amount of proton contamination in the deuterons was examined by making a control run in which the bombarding ions were protons. The results indicated that the proton impurity in the deuteron gas could not have been responsible for more than 1/2000 of the observed neutrons.

Three series of runs were made in this experiment, in which the expanded pressures in the chamber were 10.5, 7.20 and 5.85 atmospheres. The ranges of the protons were measured by reprojecting the photographs through the camera lens system in the usual manner. These lengths were converted into cm of air-equivalent range from the calculated stopping-power of the gas. The energies of the protons were then computed from the range-velocity curve of Duncanson.[8]

In an elastic head-on collision, a neutron gives all of its energy to a proton. If, however, the neutron-proton collision is not head-on, only a portion of the kinetic energy of the neutron will be transferred to the proton. In general, the energy given to the proton will be $E_p = E_n \cos^2 \theta$ where E_p is the energy of the proton, E_n the energy of the neutron and θ the angle between the direction of motion of the incident neutron and the recoil-proton. Thus, to get the energy of the neutron from that of the proton, one must know the direction of the incident neutron. To assume that the neutron came directly from the source and to apply this equation would introduce serious error, because some neutrons are scattered into the chamber. These produce a small number of high energy recoil-proton tracks, which are sometimes at large angles to a line drawn to the source. Obviously the application of the above equation to these tracks would give neutron energies which are too high. In this experiment, we have eliminated this difficulty by measuring only those tracks which made angles less than 8° with the lines drawn from the points of collision to the center of the target. A proton projected at 8° gets 98.1 percent of the neutron's energy. However, because of the size of the source, some protons were measured which were projected at angles as large as 16° and so received only 92.4 percent of the neutron's energy. Thus we should expect that a large proportion of the measured recoil-protons received between 98.1 and 100 percent of the neutron energies, and that a rapidly diminishing number received from 98.1 down to 92.4 percent. Of course, a small number of protons which appeared to be in this angular range (0–8°) were actually protons which had been projected at large angles by scattered neutrons. This number is probably quite small and is effective only in giving a low energy background or tail to the energy distribution curve.

The curves given in Fig. 1 represent the energy distribution of the recoil-protons which have been measured in this manner. The three curves *A*, *B* and *C* refer to tracks obtained when the chamber was operated at expanded pressures of

[7] K. Phillipp, Zeits. f. Physik **17**, 23 (1923).

[8] W. E. Duncanson, Proc. Camb. Phil. Soc. **30**, 102 (1934).

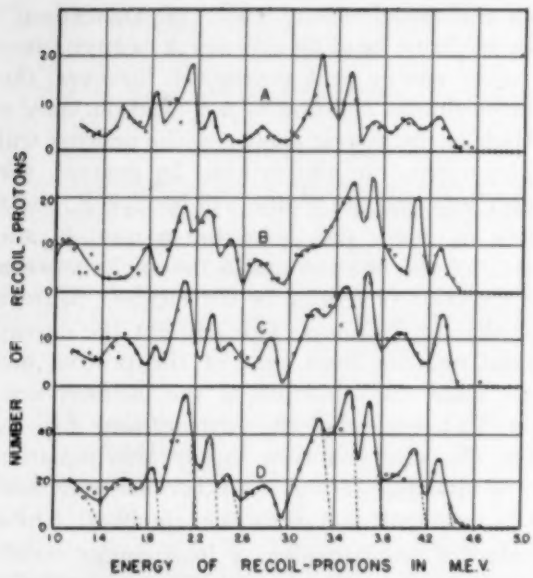

FIG. 1. Energy-distribution curves of recoil-protons projected in the forward direction. Curves *A*, *B*, *C* include proton tracks which were obtained at expanded pressures of 10.5, 5.85 and 7.20 atmospheres, respectively. The ordinates of points on curve *D* are equal to the sum of the ordinates of curves *A*, *B* and *C*.

10.5, 5.85 and 7.20 atmospheres, respectively. Curve *D* is the sum of these three curves. The four curves all give approximately the same maximum energy of the recoil-protons, and consequently the same maximum energy of 4.42 $\pm$0.27 M.E.V. for the neutrons. Recoil-protons of higher energy would have been observed, if present, since the length of the highest energy group of tracks photographed was less than a third of the diameter of the chamber.

The energy distribution curves show distinct maxima and minima which indicate that there are several energy groups. Essentially the same groups are indicated by the separate curves, although the heights of the peaks vary. Such variations are probably caused by statistical fluctuations. The agreement of the positions of the maxima and minima on the curves obtained at different pressures leads us to believe that most of the groups indicated are real, and are not due to statistical fluctuations.

THEORY OF RESULTS

The neutrons in this experiment are attributed to the reaction

$$_4Be^9 + {}_1H^2 \rightarrow {}_5B^{10} + {}_0n^1.$$

The energy of the disintegration can be computed from the well-known relation,

$$Q = \tfrac{1}{2}MV^2 - \tfrac{1}{2}M_hV_h^2 + (1/2M_n)(M^2V^2 - 2MM_hVV_h\cos\phi + M_h^2V_h^2) \quad (1)$$

where Q is the energy of the disintegration, M the mass of the neutron, V the velocity of the neutron, M_h the mass of the deuteron, V_h the velocity of the deuteron, ϕ the angle between the incident deuteron and the neutron, and M_n the mass of the resulting nucleus (B^{10} in the present case). In this experiment ϕ was 90°, so the relation becomes

$$Q = 11E/10 - 4E_h/5,$$

where E and E_h are the energies of the neutron and deuteron.

With 4.42 M.E.V. as the energy of the neutrons, the above formula gives 4.14 M.E.V. as the energy of disintegration. Corresponding to this value of Q, a neutron ejected in the forward direction has an energy of 4.93 M.E.V. If a few of the neutrons which were ejected at angles less than 90° were scattered into the chamber by the brass beneath the beryllium target, we should find a few recoil-protons which had energies between 4.4 and 4.9 M.E.V. We attribute the small number of observed energies above 4.42 M.E.V. to such neutrons.

For a given energy of disintegration, all the neutrons emitted at a 90° angle do not have exactly the same energy. This is due to the fact that deuterons of all energies up to 0.9 M.E.V. produce disintegrations. However, the excitation curve of Crane, Lauritsen and Soltan[1] shows that the efficiency of disintegration increases very rapidly with deuteron energy, so that the number of neutrons produced by 0.8 M.E.V. deuterons is only about half that produced by 0.9 M.E.V. deuterons. Since at 90° $E_n = 10Q/11 + 8E_h/11$, we see that the change in energy of the neutron is only 8/11 that of the deuteron. Thus, we should expect to get a neutron line with a half-width of about 0.07 M.E.V.

The other neutron groups indicated by the curves of Fig. 1 probably correspond to cases where the entire energy of the reaction does not go into the kinetic energy of the neutron and recoil nucleus. The B^{10} nucleus may be left in an excited state and then fall to the normal state with the emission of a γ-ray. The energies of dis-

integration (in M.E.V.) calculated from the various neutron groups are $Q_0=4.14$, $Q_1=3.89$, $Q_2=3.48$, $Q_3=3.25$, $Q_4=3.00$, $Q_5=2.51$, $Q_6=2.14$, $Q_7=1.93$, $Q_8=1.73$, $Q_9=1.39$, $Q_{10}=1.19$ and $Q_{11}=0.82$. The maximum difference in the Q's might be expected to correspond to the highest energy γ-ray emitted by the excited B^{10} nucleus. This value of 3.32 M.E.V. is in good agreement with the maximum energy of the γ-rays found in cloud chamber experiments by Crane, Delsasso, Fowler and Lauritsen.[9] We might also expect two intense γ-ray lines with energies equal to $Q_0-Q_2=0.66$, and $Q_0-Q_3=0.89$, which together probably correspond to the 0.8 M.E.V. γ-ray line they have reported. Another intense γ-ray line $Q_0-Q_8=2.41$ seems to correspond to their γ-ray line of 2.50 M.E.V.

It is seen that the neutron energy spectrum is considerably more complex than the γ-ray spectrum which supposedly arises from the same reaction. This is probably due to a difference in the resolving power of the two methods, more than one line being included in a single hump in the γ-ray spectrum. Exact correlation between the two spectra is therefore not possible.

The energy of the disintegration calculated from the masses of the isotopes $_4Be^9=9.0155$, $H^2=2.0136$, $B^{10}=10.0135$, and $n^1=1.0080$ is 7.1 M.E.V. which differs by 3 M.E.V. from our experimental value of 4.14 M.E.V. The limit of error in this experiment is much smaller than this difference. Assuming a maximum uncertainty in the stopping power of the gas in the cloud chamber of as much as 10 percent, the uncertainty in the maximum energy of the neutrons is only 0.27 M.E.V. The possibility that this 3 M.E.V. of energy is always given off as a γ-ray seems very unlikely on the basis of the known γ-ray spectrum. If this were the case, we should expect to find an intense γ-ray with an energy of 3 M.E.V. and also γ-rays with energies up to 6.32 M.E.V. On the basis of the neutron energy spectrum there should be at least 11 possible transitions giving γ-ray energies between 3 and 6.32 M.E.V. It would be strange if none of these were permitted. Crane, Delsasso, Fowler and Lauritsen find only a γ-ray with an energy of 3.3 and possibly a weak one at 4.0 M.E.V. and no γ-rays with an energy greater than this.

Thus it seems as if at least one of the masses listed above is in error. It appears most likely that this error is in the mass of Be^9, as there is considerable evidence from other disintegrations that its mass should be lower by approximately 3.0 M.E.V. A number of the disintegrations which give a lower mass for Be^9 have been pointed out by Kirchner and Neuert,[10] Ridenour, Shinohara and Yost,[11] and Crane and Lauritsen.[12]

A summary of the disintegrations and the computed mass of Be^9 is given below.

$$_4Be^9+{}_1H^1\rightarrow{}_3Li^6+{}_2He^4 \text{ (Kirchner and Neuert—}Be^9=9.0110\pm0.0006), \quad (2)$$
$$_4Be^9+h\nu\rightarrow2{}_2He^4+{}_0n^1 \text{ (Ridenour, Shinohara and Yost—}Be^9=9.0114\pm0.0011), \quad (3)$$
$$_3Li^6+{}_2He^4\rightarrow{}_5B^9+{}_0n^1\rightarrow{}_4Be^9+e^++{}_0n^1 \text{ (Meitner—}Be^9=9.0110\pm0.0006), \quad (4)$$
$$_4Be^9+{}_1H^1\rightarrow2{}_2He^4+{}_1H^2 \text{ (Oliphant—}Be^9=9.0110), \quad (5)$$
$$_4Be^9+{}_1H^2\rightarrow{}_4Be^{10}+H^1 \text{ (Crane and Lauritsen—}Be^9=9.0125), \quad (6)$$
$$_4Be^9+{}_1H^2\rightarrow{}_5B^{10}+{}_0n^1 \text{ (Bonner and Brubaker—}Be^9=9.0123\pm0.0008). \quad (7)$$

There seems to be a considerable body of evidence which indicates that the mass of beryllium should be between three and four million volts lower than Bainbridge's value of 9.0155. This would just make Be^9 stable against disintegration into two α-particles and a neutron.[13]

We wish to thank Dr. C. C. Lauritsen and Dr. H. R. Crane for the use of the high potential apparatus, and for valuable suggestions made during the course of this experiment. We are indebted to the Seeley W. Mudd fund for the financial support of this work.

[9] Crane, Delsasso, Fowler and Lauritsen, Phys. Rev. **47**, 782 (1935).

[10] Kirchner and Neuert, Physik. Zeits. **36**, 54 (1935).

[11] Ridenour, Shinohara and Yost, Phys. Rev. **47**, 318 (1935).

[12] Crane and Lauritsen, Phys. Rev. **47**, 420 (1935).

[13] *Note added in proof:* If we use a revised set of isotopic masses as recently suggested by Oliphant and Rutherford, Bethe and Aston, we get a different computed mass of beryllium. If we use the masses given by Bethe we get the following consistent set of masses for $_4Be^9$ from the above reactions (2) 9.0139, (3) 9.0143, (4) 9.0133, (5) 9.0137, (6) 9.0133, (7) 9.0133. Beryllium then will be stable by 1.5 M.E.V. against disintegration into two alpha-particles and a neutron.

On the Absorption of Acetylene and Di-Deutero-Acetylene in the Photographic Infrared

CHARLES A. BRADLEY, JR.* AND ANDREW MCKELLAR,* *George Eastman Research Laboratory of Physics, Massachusetts Institute of Technology*

(Received May 2, 1935)

Using an absorbing column 9 meters long of over 90 percent pure C_2D_2 at a pressure of 85 cm, we observed no absorption bands in the region 7000 to 11,500A. This lack of absorption is discussed. A new absorption band of C_2H_2 is found with origin at 7859A when an absorbing column 7.5 meters long at 90 cm pressure is used. The possible vibrational transitions giving rise to this band are discussed.

ALTHOUGH the absorption spectrum of acetylene[1] in the photographic infrared has been studied extensively, its interpretation is still in doubt. A careful study of the absorption spectrum of the "heavy" acetylenes, C_2HD and C_2D_2, in conjunction with the results for C_2H_2 should result in the correct interpretation of the spectra and also yield unique values for C−C and C−H and C−D distances.

The absorption of "heavy" acetylene has been examined by Randall and Barker[2] in the far infrared and by Herzberg, Patat and Spinks[3] and by the authors[4] in the photographic infrared. In the two latter cases only bands due to the mono-deutero-acetylene, C_2HD, were observed.[5] Since no quantitative analyses of the relative abundance of C_2HD and C_2D_2 were made in these cases, the effective lengths of the absorbing columns of the gases are not accurately known.

On the basis of the dependence of vibrational frequency upon mass as enunciated in the theory of the effect of isotopy on the structure of band spectra, the vibrational frequencies for C_2D_2 were calculated. The expressions derived by Mecke[1] and Olson and Kramers[6] were used in the computation. From the frequencies so obtained, it was found that the bands $\nu_3+2\nu_2+\nu_1$, $3\nu_3+\nu_1$ and $\nu_3+3\nu_2$ using the notation and assignments given by Sutherland[1] (we obtain sensibly the same results from the assignments of Herzberg and Spinks) should occur at the wavelengths 11,100, 11,200 and 10,250A, respectively. In these calculations the anharmonic terms were considered equal to those found for C_2H_2. In all likelihood these terms are smaller in absolute value for the heavier molecule. Therefore since for C_2H_2 the anharmonic constants are negative, the above given wavelengths are to be considered as the longest at which the respective bands would be expected to occur. These calculations are in close agreement with the recent work of Colby[7] who has calculated the vibrational frequencies for the heavy acetylenes.

EXPERIMENTAL

Through the kindness of Professors H. C. Urey and J. E. Zanetti, of Columbia University, we were able to obtain 9 grams of 100 percent pure D_2O and some special CaC_2 for the preparation of the C_2D_2. The CaC_2 was prepared with a slight excess of carbon to eliminate the possibility of containing free line. Extreme precautions were taken in the handling of the carbide to eliminate any contamination by reaction with atmospheric water. The carbide was received in a sealed

* National Research Fellow.

[1] Levin and Meyer, J. Opt. Soc. Am. **16**, 137 (1928); Hedfeld and Mecke, Zeits. f. Physik **64**, 151 (1930); Childs and Mecke, Zeits. f. Physik **64**, 162 (1930); Mecke, Zeits. f. Physik **64**, 173 (1930); Hedfeld and Lueg, Zeits. f. Physik **77**, 446 (1932); Lochte-Holtgreven and Eastwood, Zeits. f. Physik **79**, 450 (1932); Mecke, Zeits. f. physik. Chemie **B17**, 1 (1932); Sutherland, Phys. Rev. **43**, 883 (1933); Herzberg and Spinks, Zeits. f. Physik **91**, 386 (1934).

[2] Randall and Barker, Phys. Rev. **45**, 124 (1934).

[3] Herzberg, Patat and Spinks, Zeits. f. Physik **92**, 87 (1934); Nature **133**, 951 (1934).

[4] McKellar and Bradley, Phys. Rev. **46**, 236, 664 (1934).

[5] It should be pointed out that the two bands ascribed to C_2D_2 in the recent paper *Hydrogen Isotope of Atomic Weight Two* by H. C. Urey and G. K. Teal (Rev. Mod. Phys. **7**, 87 (1935)) are the 10,370A and 10,167A bands of C_2H_2. This error is undoubtedly due to a misinterpretation of a table in the article of Herzberg, Patat and Spinks (Nature **133**, 951 (1934)).

[6] Olson and Kramers, J. Am. Chem. Soc. **54**, 136 (1932).

[7] Colby, Phys. Rev. **47**, 388 (1935).

bottle and only exposed to the air while being transferred to the reaction flask. The D_2O was opened in vacuum and distilled into the dropping funnel of the acetylene generating apparatus. The C_2D_2 was prepared by allowing the D_2O to drop slowly upon the CaC_2. The gas was dried by passing through a trap cooled with solid CO_2; from there it passed directly into the absorption cells. Previous to the generation of the C_2D_2 the whole generating apparatus and the absorption cells were evacuated thoroughly (to a pressure of 10^{-4} mm) and flamed.

The absorption cells were two lengths of Pyrex tubing, one 7.5 meters long, the other 1.5 meters long, and 20 mm in diameter. The tubes were mounted in the shape of an L.

The positive crater of the carbon arc served as a light source. The beam was collimated by a quartz lens, passed through the long cell, was reflected by an aluminum mirror through the short cell and a red filter which cut off light of wavelength less than 6300A, and was focused upon the slit of a 21-foot, 15,000 lines per inch concave grating.

First, by using a glass prism spectrograph, plates were taken from the visible region up to about 10,500A. No absorption bands appeared on these photographs. Then through this 9-meter path of C_2D_2 exposures were taken on the grating from 8900A to 11,500A. No bands whatsoever were observed. The exposure times were up to 18 hours. Eastman 1P and 1Q plates and also those with the new 1Z type emulsion were used. These last-mentioned plates possess a maximum sensitivity at 10,900A and a sensitivity range from 7500A to 11,800A. All the plates were supersensitized with ammonia. With only the 1.5-meter cell of C_2D_2 as the absorbing column, exposures of four hours gave good blackening up to 12,500A. Under these conditions again no bands were observed.

Inasmuch as the absorbing column we used was more than twice as long as we considered necessary to observe the bands we have mentioned above, and in particular the C_2D_2 analog of the 7887A band of C_2H_2, this lack of absorption was somewhat surprising. Observation of the fundamental bands in the far infrared offers a means of testing the purity of the gas, for in the region of the ν_4 fundamental band (18μ) the "heavy" acetylenes absorb very strongly. Accordingly a small sample of our gas was taken from the cells and sent to Professor E. F. Barker who had very kindly offered to test it for us. He has informed us that the gas was well over 90 percent C_2D_2. Besides the C_2D_2 fundamental he observed much more faintly the one due to C_2HD. Additional proof of the scarcity of C_2HD and C_2H_2 in our tube is given by our failure to detect any trace of the very strong absorption bands due to these molecules at 10,302A and 10,370A, respectively. Further evidence as to the purity of our gas was obtained when some of the heavy acetylene was taken from the cells and excited in a hollow cathode discharge tube at a pressure of about one millimeter. The spectrum of the discharge was photographed in the first order of the Institute's 10-meter 30,000 lines per inch concave grating. The atomic lines of deuterium and also the bands due to the CD molecule with heads at 4307A and 3867A were observed without any trace whatsoever of the atomic lines of hydrogen or the CH bands at 4315A and 3872A. The analysis of the CD bands as well as intensity measurements in the 4315A CH band are now in progress.

It was decided to rephotograph the bands in the absorption spectrum of C_2H_2 at 7887, 10,167 and 10,370A in order to test our experimental arrangement. The 7.5-meter cell was filled with C_2H_2 at 90 cm pressure. The above-mentioned bands were easily observed.

This lack of absorption indicates a considerable difference in behavior between C_2D_2 compared to C_2H_2 and C_2HD. In a previous experiment[4] we observed at 10,302A a band due to C_2HD. It could be photographed with a 1.5-meter tube which contained also some C_2H_2 and considerable C_2D_2 so the path length required was only of the order of one meter or less of C_2HD. Herzberg, Patat and Spinks[3] observed no bands due to C_2D_2 in this region of the spectrum and four due to C_2HD. It is to be noted that in the Raman spectrum[5] of C_2D_2 while lines corresponding both to ν_1 and ν_2 have been observed, the latter one only appears on prolonged exposure.

The frequency of a band origin may be expressed to a first approximation by the formula

[4] Glockler and Davis, Phys. Rev. **46**, 535 (1934); Glockler and Morrell, Phys. Rev. **47**, 569 (1935).

$$\nu=\omega_1 V_1+X_{11}V_1^2+\omega_2 V_2+X_{22}V_2^2+\omega_3 V_3+X_{33}V_3^2+\omega_4 V_4+X_{44}V_4^2+\omega_5 V_5+X_{55}V_5^2+X_{12}V_1V_2+X_{13}V_1V_3+\cdots+X_{45}V_4V_5$$

where the ω's are the normal frequencies of vibration, the V's the vibrational quantum numbers, and the X's the anharmonic constants. The interpretations of the C_2H_2 spectrum by Sutherland[1] and by Herzberg and Spinks[1] indicate that the combination bands which appear most strongly are those which involve the largest anharmonic constants. This has also been found to be the case in the interpretation of the CO_2 vibration-rotation spectrum.[9]

Let us compare the frequencies of vibration for C_2H_2 and C_2D_2.

	C_2H_2 (obs)	C_2H_2 (Calc. by Colby)
ν_1	1974	1750
ν_2	3372	2690
ν_3	3288	2414
ν_4	730	535
ν_5	605	505

In the case of C_2H_2 the anharmonic constants (X's) are the following (Herzberg and Spinks' values):

$X_{22}=+13.6$; $X_{33}=-28.1$; $Y_{333}=-2.3$; $X_{55}=-26.3$;
$X_{12}=-4.9$; $X_{13}=-4.9$; $X_{23}=-112.1$; $X_{14}=-1.3$;
$X_{15}=-0.2$; $X_{24}=-9.3$; $X_{25}=-1.2$; $X_{45}=-18.8$.

It has been observed[10] in the case of isotopic molecules that the potential energy functions are the same to a high degree of approximation for corresponding electronic states. One can conclude therefore that for a state represented by certain vibrational quantum numbers the energy of that state will be less for C_2D_2 than for C_2H_2 and that the vibrations for C_2D_2 will be for any state more nearly harmonic than for the corresponding one of C_2H_2. This would indicate that for C_2D_2 the anharmonic terms would be smaller than the analogous ones for C_2H_2. Thus it might be expected that vibration-rotation bands of C_2D_2 would be less intense than the corresponding bands of C_2H_2. It may further be pointed out that in the case of C_2H_2 the coefficient, X_{23}, coupling the two largest frequencies is larger than their difference. This will in all likelihood not be so for C_2D_2.

[9] Adel and Dennison, Phys. Rev. **43**, 716; **44**, 99 (1933).
[10] Beutler and Mie, Naturwiss. **22**, 419 (1934); Mie, Zeits. f. Physik **91**, 475 (1934).

Both experimental and theoretical work on the intensities of vibration-rotation bands is very meager[11] and no work has been done on polyatomic molecules. For diatomic molecules Dunham[11] has shown that the electric moment, μ, can be expressed as a power series expansion in terms of ξ, where $\xi=(r-r_e)/r_e$ and the observed intensities agree fairly well with those he has calculated. Mulliken[11] has indicated the probable behavior of μ as function of r for the hydrogen halides and has drawn some interesting conclusions regarding the intensities of the observed bands for H_2O. He points out that while H_2O has a large permanent electric moment, i.e., $\mu_z\neq 0$, $\mu_y=0$ for the nonvibrating molecule where z is the symmetry axis, bands associated with a varying μ_z ($\Delta V_3=$even) are weak, while those associated with a changing μ_y ($\Delta V_3=$odd) are strong. Thus probably μ_z is near its maximum for the nonvibrating molecule, and in the first case terms analogous to the coefficients of ξ for diatomic molecules are small, while in the latter case the terms are large.

In the comparison of C_2H_2 and C_2D_2, the ν_4 band is probably of comparable intensity for both as it has been found to appear quite strongly. This is a $\perp$ type band and one may suppose that while of course for the nonvibrating molecule $\mu_z=\mu_y=0$, the terms analogous to the coefficients of ξ for diatomic molecules are large and of comparable magnitude. Since the ν_3 fundamental has not yet been observed for C_2D_2, and the present results indicate combination bands involving ν_3 to be several times weaker for C_2D_2 than for C_2H_2, the coefficients are probably many times smaller for C_2D_2 than for C_2H_2.

A New C_2H_2 Band at 7859A

A very careful study of our photograph of the C_2H_2 band at 7887A taken with the 7.5 meters absorbing column at 90 cm pressure revealed the presence of a heretofore unreported band. It was made manifest by the appearance of a series of weak lines extending outwards from the end of the R branch of the 7887A band towards

[11] Dunham, Phys. Rev. **35**, 1347 (1930); **34**, 438 (1929); Bourgin, Phys. Rev. **29**, 794 (1927); Matheson, Phys. Rev. **40**, 813 (1932); Bartholome, Zeits. f. physik. Chemie **B23**, 131 (1933); Mulliken, J. Chem. Phys. **2**, 400, 712 (1934).

shorter wavelengths. The series obviously corresponded to the R branch of a new band, the P branch of which was obscured by the strong R branch of the band at 7887A. The faint R branch showed alternating intensities and six of the stronger lines (odd J values) were measured and two of the weaker ones (even J values). These lines are quite apparent on the reproduction given by Hedfeld and Lueg[1] of the 7887A band but are designated by them as higher members of the R branch of that band. That their assignment is erroneous may be seen by taking first differences in the list of frequencies for the R branch lines given by these authors. Upon doing so one finds that the differences decrease, reaching a minimum at $R(26)$, and then *increase*.[12] The frequencies of the lines of the new band at 7859A measured with reference to the lines of the 7887A band are given, along with their assignments, in Table I. Because of the faintness of the lines, we do not consider the frequencies accurate to more than ± 0.2 cm^{-1}.

TABLE I. *Frequencies of the lines of the band at 7859A.*

J	0	1	2	3	5	7	9	11
$R(J)$	12,722.0 cm^{-1}	24.2	26.4	28.7	32.9	36.8	40.8	44.6

In order to determine the allotment of rotational quantum numbers to the lines of the new band, it was assumed that the structure of the band, in particular the spacing of the lines, is the same as for the strong band at 7887A. This is quite probably justifiable. We calculate that the origin of the faint band is at 12,720 cm^{-1}. This is considered accurate to ± 4 cm^{-1} (corresponding to the numbering of the lines being correct to within $\Delta J = 2$).

According to Sutherland's arrangement of the C_2H_2 bands the combination band occurring closest to our band at 12,720 cm^{-1} would be $\nu_1+2\nu_2+\nu_3+2\nu_5$ which, with his constants, should lie at 12,766 cm^{-1}. Closer agreement is found if one uses Herzberg and Spinks' constants and assignment. With these it is found that the combination band $\nu_1+3\nu_3+2\nu_5$ should lie at 12,708 cm^{-1}. Although Herzberg and Spinks assign the band at 7956A to this combination, in view of the data concerning this band given in footnote 12, we consider the assignment of the combination $\nu_1+3\nu_2+2\nu_5$ to the new band at 12,720 cm^{-1} more trustworthy than the former assignment of this transition. Additional weight is added by the definite alternation of intensities evident in the observed band which would classify it as a $\parallel$ type vibration.

It is a pleasure to express our appreciation to Professors H. C. Urey and J. E. Zanetti of Columbia University and Professor E. F. Barker of the University of Michigan for their kind cooperation, and to Professor G. R. Harrison of the Massachusetts Institute of Technology for the privilege of working in his laboratory.

[12] Hedfeld and Mecke[1] in the original photographic work on acetylene absorption reported a band at 7956A. We used twice their path length but found no trace of this band in which the above authors measured over 30 lines. It is odd that the 7956A band is not reported by Hedfeld and Lueg[1] who used a path length of 24 meters. However, several lines designated by them as members of the P branch of the 7887A band coincide with lines reported by Hedfeld and Mecke as members of the R branch of the band at 7956A. Herzberg and Spinks[1] give two possible vibrational transitions to which this band may be ascribed but the agreement between observed and calculated frequencies is poor in both cases, observed minus calculated values being 70 cm^{-1} and 144 cm^{-1}.

The Far Infrared Spectrum of H_2O

R. Bowling Barnes, W. S. Benedict* and C. M. Lewis,* *Palmer Physical Laboratory, Princeton*

(Received April 18, 1935)

The absorption of atmospheric water vapor is mapped between 38μ and 170μ. The results are shown to be in good agreement with Mecke's analysis of the vibration-rotation bands, and permit an extension of his results.

IN all investigations in the far infrared (>20μ), the energy spectrum shows great irregularities. These, it is well known, are due to the absorption of the atmospheric water vapor. In fact, in order to obtain sufficient energy to work satisfactorily in this region, it is necessary to remove most of the water vapor by drying the interior of the spectrometer with trays of P_2O_5. The H_2O molecule possesses a large permanent dipole moment, is an asymmetric rotator, and hence shows this very strong and irregular absorption, due to "pure rotation." In the course of various investigations in this region, with the apparatus already described[1] we have obtained detailed energy curves throughout the region 38–170μ. In this paper we will present these, and discuss them in the light of our present knowledge of the H_2O molecule.

The very excellent work of Mecke and his collaborators[2] has solved the fundamental problems concerning the term-structure of H_2O. From the vibration-rotation bands in the near and photographic infrared, they have obtained the energy term values of 32 of the lowest rotational levels of the ground vibrational state, and correlated these with the predicted levels for an asymmetric top with moments of inertia $A=0.996$, $B=1.908$, $C=2.981$. This corresponds to an H−O distance of 0.97A and an H−O−H angle of 105°. To apply these results to the interpretation of the pure rotation spectrum, it is necessary only to take the differences between these terms, using the correct selection rules. There are two limitations to this, however. In the first place, Mecke's levels, although they account for most of the strong lines, are far from complete. Secondly, even with the good resolving power obtained with our instrument or the somewhat better resolving power applied in a more limited frequency range by Wright and Randall,[3] there is often an overlapping of lines. This latter fact makes an exact agreement with the calculated spectrum impossible, until the technique in this region is still further improved. Approximate agreement has however been achieved, as Fig. 1 and Tables I and II demonstrate.

TABLE I. *Term values for the H_2O molecule.* Values marked *a* and *b* are taken from Mecke's measurements in the photographic infrared. Values marked *c* are assumed in order to explain the experimental results of this paper.

J_τ	cm^{-1}	Class	J_τ	cm^{-1}	Class	J_τ	cm^{-1}	Class	J_τ	cm^{-1}	Class
0_0	0	a	3_3	286.93	a	5_{-1}	446.59	b	7_{-6}	586.6	a
1_{-1}	23.78	a	4_{-4}	222.07	a	5_0	505.54	b	7_{-5}	699.6	c
1_0	37.09	a	4_{-3}	224.81	a	5_1	510.33	b	7_{-4}	705.0	c
1_1	42.31	a	4_{-2}	275.50	a	5_2	611.8	c	7_{-3}	780.5	c
2_{-2}	70.09	a	4_{-1}	300.44	a	5_3	612.1	c	7_{-2}	813.0	c
2_{-1}	79.43	a	4_0	315.83	a	6_{-6}	446.7	a	7_{-1}	840.0	c
2_0	95.15	a	4_1	384.03	a	6_{-5}	447.2	a	8_{-8}	744.1	a
2_1	134.98	a	4_2	385.44	a	6_{-4}	540.5	c	8_{-7}	744.2	a
2_2	136.24	a	4_3	490.64	b	6_{-3}	548.7	b	8_{-6}	871.5	c
3_{-3}	136.76	a	4_4	490.79	b	6_{-2}	601.5	c	8_{-5}	876.8	c
3_{-2}	142.23	a	5_{-5}	325.37	a	6_{-1}	648.0	c	9_{-8}	920.8	b
3_{-1}	173.31	a	5_{-4}	326.56	a	6_0	665.0	c	9_{-9}	920.8	b
3_0	206.35	a	5_{-3}	399.42	a	6_1	761.1	c	10_{-10}	1116.0	b
3_1	212.24	a	5_{-2}	416.21	b	6_2	762.5	c	10_{-9}	1116.0	b
3_2	286.80	a				7_{-7}	586.3	a	11_{-11}	1329.7	c

Fig. 1 shows the energy curves obtained. The curve is a smoothed idealization of all the points measured. The accuracy varies from region to region, as most of the points were taken with absorption measurements as the primary aim, the energy spectrum being of secondary importance at the time. In some regions, for example, the energy curve has been gone over 7 or 8 times with the narrowest possible slits; in others, only two or three times. The concentration of water vapor in the optical path also varied from time to time. In smoothing the curve for publication, however, no hump that can be construed as an absorption line has been included unless its presence is definitely indicated by two

* National Research Fellows.

[1] R. Bowling Barnes, Rev. Sci. Inst. **5**, 237 (1934).

[2] Mecke, Baumann and Freudenberg, Zeits. f. Physik **81**, 313, 445, 465 (1933).

[3] Wright and Randall, Phys. Rev. **44**, 391 (1933).

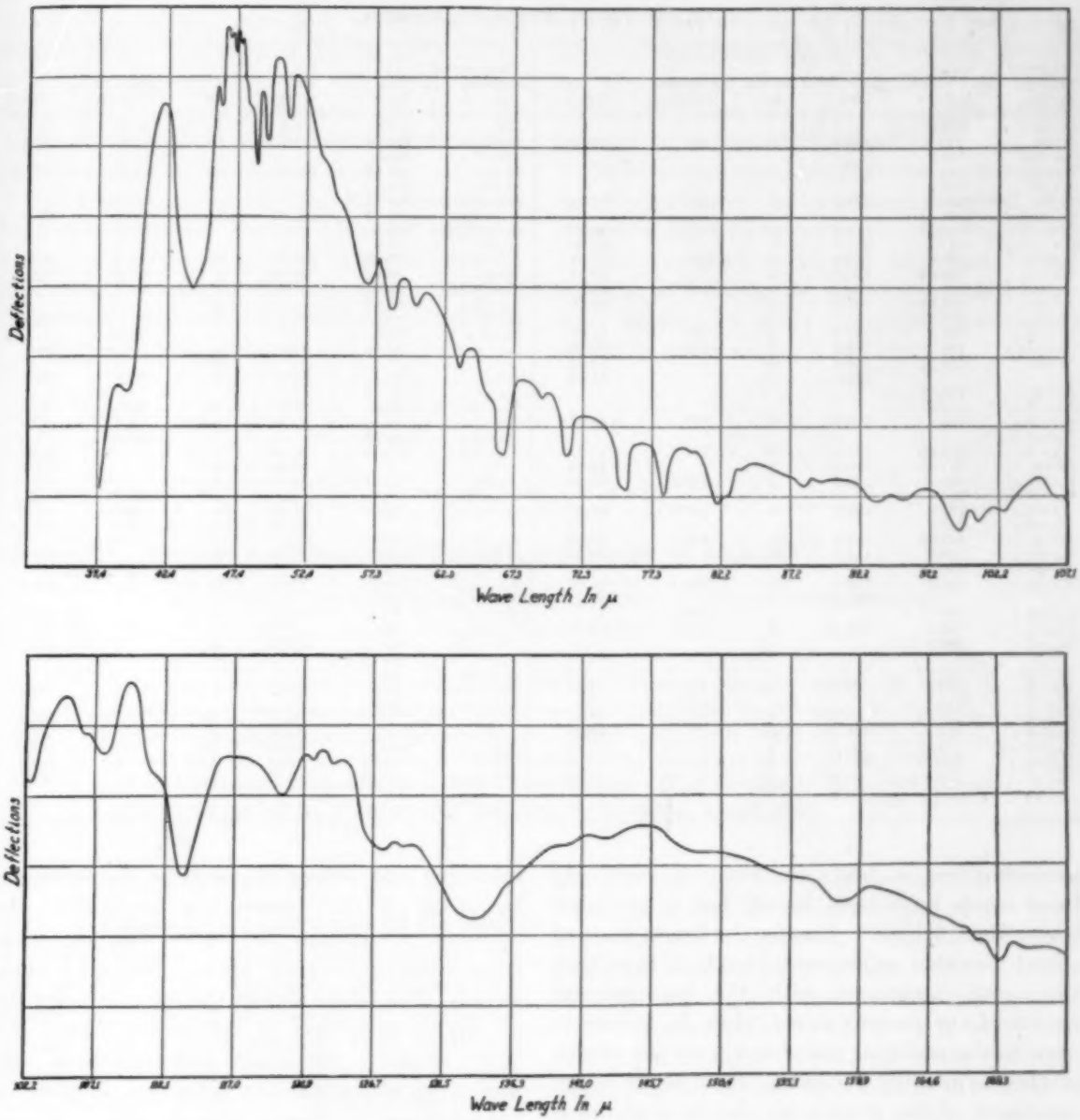

FIG. 1. Far infrared spectrum of water vapor, as obtained by using about 3 meters of vapor which had been dried with P_2O_5. The slit-widths used varied considerably in the various parts of the spectrum.

or more separate groups of points. The agreement with the results of Wright and Randall, in the region reported by them (65–130μ), is satisfactory, as reference to their curves will show. The wavelengths of the various minima in the curve are calculated by the method described in an earlier paper on the absorption spectrum of ammonia,[4] and are tabulated, together with the approximate relative intensity, in Table II.

Table I gives the term values used in correlating the observed results. Most of the lower levels are taken from Mecke's tables. These are marked *a*, and should be accurate to 0.02 cm^{-1}. The levels marked *b* have been obtained by extending Mecke's methods to the same body of photographic infrared data. The details will be published later by one of us. The accuracy is

[4] R. Bowling Barnes, Phys. Rev. **47**, 658 (1935).

TABLE II. *The far infrared of water vapor.*

ALLOWED TRANS. $J_\tau - J_\tau$	CALC. ν	OBS. ν	INTEN-SITY	OBS. BY OTHERS	OBS. μ
5_0-6_2	257.0				
5_1-6_1	250.8	250.8	4	247	39.87
$5_{-2}-6_0$	248.8				
$3_{-3}-4_1$	247.27				
4_1-5_3	228.1				
4_2-5_2	226.4	227.6	7	228	43.94
$4_{-2}-5_{-1}$	221.78				
$2_{-3}-3_2$	216.71	216.4	3		46.22
$10_{-9}-11_{-11}$	213.7	213.7	0		46.80
$6_{-2}-7_{-2}$	211.5	211.5	2	211	47.28
$4_{-1}-5_1$	209.89	210.2	0		47.57
		206.7	0		48.17
3_2-4_4	202.99	205.0	5		48.79
3_3-4_3	202.71				
$5_{-1}-6_{-1}$	201.4	201.3	4	201	49.68
$9_{-9}-10_{-9}$	195.2	195.3	3	192	51.20
4_0-5_0	189.71	186.9	0?		53.51
		182.7	0?		54.73
3_0-4_2	179.09				
$7_{-8}-8_{-5}$	177.2				
$8_{-7}-9_{-9}$	176.7	176.9	5	177	56.53
$8_{-8}-9_{-8}$					
$3_{-2}-4_0$	173.60	174.4	0?	172	57.53
3_1-4_1	171.79	170.8	5		58.53
$6_{-4}-7_{-4}$	166.5	166.4	3	166.6	60.09
$7_{-4}-8_{-6}$	166.3				
$7_{-7}-8_{-7}$	157.8	157.8	4	157.9	63.38
$7_{-6}-8_{-6}$	157.5				
2_1-3_1	151.95	152.7	2	153.5	65.49
$6_{-3}-7_{-3}$	150.9	151.2	6		66.13
2_2-3_2	150.56				
$5_{-3}-6_{-3}$	149.3	150.2	6	150.1	66.58
		143.99	1		69.45
$4_{-2}-5_{-2}$	140.71			140.9	
$6_{-5}-7_{-5}$	139.9	139.74	6	139.3	71.56
$6_{-5}-7_{-7}$	139.1				
					73.1
$2_{-1}-3_1$	132.81				
$8_{-7}-8_{-5}$	132.6	132.62	7w	132.8	75.41
$6_{-1}-7_{-3}$	132.5			128.8	
$3_{-1}-4_{-1}$	127.13	127.32	6	127.2	78.55
$5_{-2}-6_{-4}$	124.3	124.25	0?		80.49
$5_{-5}-6_{-5}$	121.95	121.87	6	12.197	82.06
$5_{-4}-6_{-6}$	120.11	120.3	2	120.20	83.16
$7_{-6}-7_{-4}$	118.4	119.0	1?	118.08	84.04
		114.9	0?	116.74	87.0

ALLOWED TRANS. $J_\tau - J_\tau$	CALC. ν	OBS. ν	INTEN-SITY	OBS. BY OTHERS	OBS. μ
$7_{-7}-7_{-5}$	113.3	113.3	2	112.97	88.26
2_0-3_0	111.20	111.9	1	111.21	89.4
$7_{-4}-7_{-2}$	107.8			107.92	
4_3-4_5	106.61	107.0	3w	107.30	93.43
5_0-5_2	106.3				
4_2-4_4	105.35			105.78	
$4_{-4}-5_{-4}$	104.49	104.52	2	104.59	95.7
$6_{-5}-6_{-3}$	101.4			101.46	
5_1-5_3	100.7				
$4_{-2}-5_{-5}$	100.56	100.78	8w	100.59	99.23
1_0-2_2	99.15	99.20	5	99.04	100.80
$6_{-3}-6_{-1}$	99.0				
$4_{-1}-5_{-3}$	98.98				
6_0-6_2	97.5	97.4	2		102.7
5_0-6_{-3}	96.0			96.12	
$6_{-6}-6_{-4}$	93.8	93.8	1		106.6
1_1-2_1	92.67	92.9	2	92.51	108.1
$5_{-3}-4_{-3}$	91.22				
$5_{-4}-5_{-2}$	89.65	90.3	0?	89.53	110.7
$5_{-3}-5_0$	89.33	88.41	6w	88.42	113.1
$3_{-3}-4_{-3}$	88.05			87.44	
$4_{-1}-4_1$	83.59	83.20	2		120.1
		81.83	0		122.2
3_0-3_2	80.45	80.94	1		123.5
$3_{-2}-4_{-4}$	79.84			79.59	
$6_{-2}-7_{-1}$	78.9	78.78	4	79.02	126.9
		77.50	1?	78.26	129.0
$4_{-2}-4_{-1}$	75.63			75.59	
3_1-3_3	74.69	75.10	6w		133.2
$3_{-2}-3_0$	74.12			74.22	
$5_{-5}-5_{-3}$	74.05	73.47	0?		136.1
$2_{-2}-3_{-2}$	72.14				
3_0-4_{-2}	71.15	71.37	1		140.1
4_0-4_2	69.61	70.00	1		142.9
201.3/3=	67.1	67.41	1		148.4
$5_{-1}-5_1$	63.74				
$6_{-3}-6_0$	63.5				
$6_{-4}-6_{-2}$	63.0	63.02	3		158.7
4_1-5_{-1}	62.56				
		60.76	0?		164.5
		60.08	0?		166.4
$7_{-3}-7_{-1}$	59.5	59.69	1?		167.5
176.91/3=	58.97	58.57	3		169.6
174.44/3=	58.14	58.47	0		171.0

somewhat less, as fewer combinations involving these levels have been found, but is probably better than 0.2 cm^{-1}. Finally the levels marked *c* have no other experimental backing than that they give agreement with the experimental results of the present paper; they lie, however, close to the positions calculated from the theory of the asymmetrical rotator. Pending an exact treatment of the corrections due to centrifugal stretching of such a rotator, it has not seemed worth while to give the calculated values of these terms. The accuracy of levels *c* may not exceed ± 1 cm^{-1}.

Table II gives the correlation between experiment and theory. The first column gives all the combinations allowed between the terms of Table I, that would lie in the observed region. The "allowed" combinations comprise the strong lines of the types $J_\tau \rightarrow J_{\tau+2}$, $J_\tau \rightarrow (J+1)_\tau$ (J and τ both odd or both even) or $J_\tau \rightarrow (J+1)_{\tau\pm 2}$ (J odd, τ even and *vice versa*). Of these, the lines involving odd values of τ will be the stronger, by virtue of the "alternating intensities." In addition, transitions to states differing from these levels by $\tau = 4$ will appear, but much more weakly. The tables should therefore account for all the possible lines in this region except the very weakest. An exact calculation of the intensities is possible but laborious; in view of the wholesale overlappings of the observed lines it was not attempted.

The second column of Table II gives the frequency of these transitions, calculated from the term values of Table I. The next column gives the frequencies, and the next the intensities, of the nearest observed line. It is seen that the correlation with column 2 is good throughout, considering the overlappings. The next column shows the agreement between our results and those of previous workers in the field. The comparison for frequencies above 167 is with

the results, of low accuracy, of Kühne,[5] and from 167 to 74 with those of Wright and Randall. The latter agree with the calculated values somewhat more closely than do our measurements, showing that as resolving power increases, still closer agreement may be expected.

Our results extend to 170μ. However, in the longest wave region, beyond 138μ, our energy is not pure, but contains some of the third order radiation. Accordingly, lines appear in the spectrum which are really third order lines, not lines of H_2O. That at least 40 percent of the energy detected remains first order is, however, certain; and the absence of any strong H_2O lines in this region other than at 63 cm^{-1}, in agreement with calculation, is proved experimentally.

We may thus conclude that the pure rotation spectrum of water, as at present observed, is in complete agreement with the results of the rotation-vibration spectrum; and that further progress in locating the higher rotational levels must depend on more complete experimental results in either region.

[5] Kühne, Zeits. f. Physik **84**, 722 (1933).

JUNE 15, 1935 PHYSICAL REVIEW VOLUME 47

Vibrational Raman Scattering in Liquids

S. Bhagavantam and A. Veerabhadra Rao, *Department of Physics, Andhra University*

(Received April 10, 1935)

A quantitative investigation reveals that the distribution of intensity within the wings accompanying the vibrational Raman line 656 cm^{-1} in liquid carbon disulphide is very similar to that obtained in the wings accompanying the Rayleigh lines. The intensity starts from being a maximum at or very near the center, rapidly falls off till a distance of 20 cm^{-1} is reached after which it gradually diminishes till it fades away altogether. These features are in marked contrast to the predictions of the existing theories of the rotational Raman effect.

Introduction

It is well known that practically all the vibrational Raman lines in liquids exhibit the phenomenon of depolarization. It follows as a natural consequence that, as in the case of depolarized Rayleigh scattering, they should in general be accompanied by unresolved wings arising from the rotation of the molecules. Recent investigations by Weiler,[1] Trumpy,[2] Ranganadham[3] and more extensively by the authors[4–7] have shown that in liquids the so-called rotation wings accompanying the Rayleigh scattering are characterized by a very large concentration of intensity in the close neighborhood of the Rayleigh line and a relatively feeble but a definite extension of the wing to an unexpected distance from the center. The authors have pointed out that such complex patterns are not wholly explicable in terms of the simple theory of rotational Raman scattering by gaseous molecules but are to be attributed partly to internal oscillations in liquids similar to those that exist in a solid. Such conclusions have also been drawn by Gross and Vuks[8] from their investigations on diphenyl ether. These results obviously give rise to the important question whether the wings accompaning the depolarized vibrational Raman lines in liquids behave in a similar manner. This paper describes the experimental results obtained by us in this direction by using liquid carbon disulphide.

[1] J. Weiler, Zeits. f. Physik **68**, 782 (1931).
[2] B. Trumpy, D. Kgl. Norske Viskens-Selsk. Forh. **5**, Nos. 16 and 47 (1932).
[3] S. P. Ranganadham, Ind. J. Phys. **7**, 353 (1932).
[4] S. Bhagavantam, Ind. J. Phys. **8**, 197 (1933).
[5] S. Bhagavantam and A. Veerabhadra Rao, Ind. J. Phys. **8**, 437 (1933).
[6] A. Veerabhadra Rao, Proc. Ind. Acad. Sci. **1**, 274 (1934).
[7] S. Bhagavantam and A. Veerabhadra Rao, Proc. Ind. Acad. Sci. **1**, 419 (1935).
[8] E. Gross and M. Vuks, Nature **135**, 100 (1935).

Experimental Arrangement

The liquid, purified by distillation, is contained in a wide glass tube and illuminated by focusing the light from a 6-inch mercury arc onto the tube by means of a large aperture glass condenser. The usual precautions of painting the tube black and drawing the end opposite to the observation window into the shape of a horn have been taken so as to eliminate all parasitic light. The spectrum of the scattered light is photographed by means of a glass spectrograph consisting of 2 large prisms. A fine slit (3/200 mm) is used with a view to obtaining the maximum possible resolution. The liquid gets slightly colored on exposure and in order to avoid the resulting loss of light, it is renewed frequently during the exposure. Two different plates showing the Raman line 656 cm^{-1} and its accompanying wings excited by λ4046 have been obtained. With a standard tungsten ribbon lamp running at about 16 amp. from a 220-volt battery as the source, a scale of intensity marks is furnished alongside the scattered spectrum by the method of varying slit widths. The density-log intensity curve is drawn with the help of a Moll microphotometer at the wavelength corresponding to 656 cm^{-1} Raman line excited by λ4046 and the intensities at various points on either side of this line are read off from this curve. This line in carbon disulphide is chosen for the investigation as it is particularly intense and at the same time exhibits an appreciable depolarization. It is also accompanied by a satellite ($\Delta\nu = 648$) separated from the main line only by about 8 wave numbers which, if resolved, provides a measure of the resolution employed.

Results

Fig. 1 is a microphotometric record of the 656 cm^{-1} line excited by λ4046. The arrow indicates the position of the satellite ($\Delta\nu 648$) which is seen as a separate peak, on the shorter wavelength side although it is only at a distance of about 8 cm^{-1} from the main line. It is to be noted that no such discontinuity in intensity is present on the longer wavelength side of the main line. This result at once permits us to draw the important conclusion *that the intensity of the wing accompanying the vibration line goes on continuously increasing as we approach the center or the Q branch, no discontinuity being perceptible even at a distance as close as 8 cm^{-1} from the center.* That the instrument would undoubtedly have shown up such a discontinuity if it were present is evidenced by the fact that the satellite 648 cm^{-1} is seen as a separate peak on the record and as a distinctly separated line in the negative.

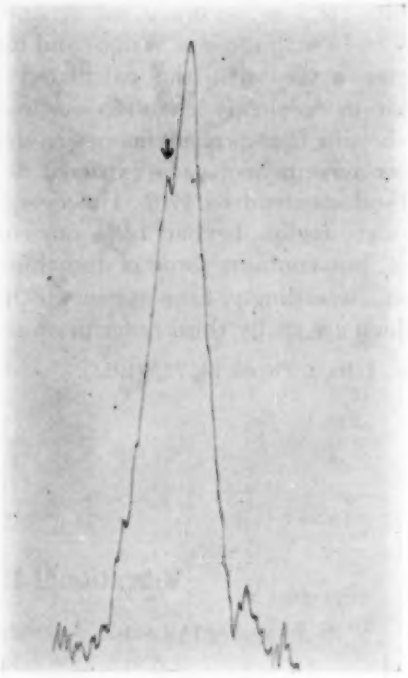

Fig. 1. Microphotometer record of 656 cm^{-1} line.

In the second row of Table I the results of a photometric study of the intensity distribution in the wing on the longer wavelength side of the line are given. The numbers are the averages of those obtained on two different plates and represent the intensities at the respective points on an arbitrary scale.

Table I.

$\Delta\nu$ (cm^{-1})	0	2.85	5.7	8.55	11.4	14.25	17.1	19.95	22.8	25.65	28.5	34.2	39.9	45.6
Intensity	360	215	112.9	80	63	47	38	30	25.7	22.4	20.4	19	16.4	12.6

As there are no satellites on the longer wavelength side of the line, these results may be regarded as giving a true picture of the intensity distribution in the *RR* branch of the 656 cm^{-1} Raman line. These are represented graphically in

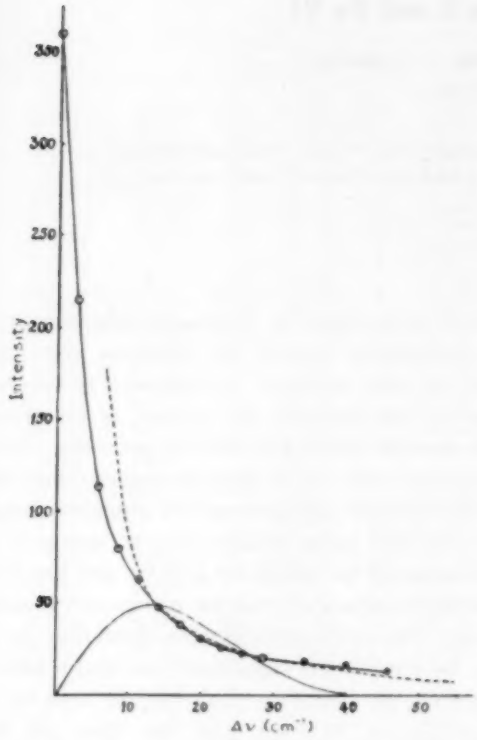

FIG. 2. Intensity distribution in Raman line. Unbroken line, theory; dotted line, Rayleigh scattering; lines with encircled points, vibrational Raman scattering.

Fig. 2 by the curve joining the encircled points. The intensity distribution (unbroken curve) to be expected on the basis of the theory of rotational Raman scattering applicable to gaseous molecules, by taking the moment of inertia of CS_2 as 264×10^{-40}, and the experimentally-observed intensity distribution (broken curve) within the wing accompanying the Q branch of the Rayleigh scattering,[8] are also represented graphically on the same scale in Fig. 2 for comparison.

Discussion of Results

The following outstanding features in Fig. 2 may be noted. The intensity distribution observed in the wing accompanying the 656 cm^{-1} vibration line differs in one respect from that observed in the wing accompanying the Rayleigh scattering in as much as the Q branch in the latter appears to be relatively stronger as may be seen from the courses of the curves in the region 0 to 10 cm^{-1}. Otherwise the courses of the two curves are in good general agreement with each other. The intensity distribution in the wing accompanying 656 cm^{-1} line is practically identical with that observed for the wing accompanying the Rayleigh line at all distances larger than about 10 wave numbers from the center whereas in closer regions (from 0 to 10 cm^{-1}) the experimental curves maintain in common the general characteristics such as a continuous and rapid increase in the intensity as the center is approached. In these respects both the curves agree amongst themselves and differ very markedly from the theoretical curve. According to the theory we should expect the wing to start from zero intensity at the center, gradually increase in intensity till it reaches a maximum at about 14 cm^{-1}, and then fall off and nearly completely vanish by the time a distance of 45 cm^{-1} is reached.

Experimental results show on the contrary that the wing has a maximum intensity at or very near the center, its intensity rapidly diminishing till about 20 wave numbers and thereafter falling off only gradually with the result that it persists long after the distance of 45 cm^{-1} is reached. Such close similarity between the structure of the Rayleigh scattering and the vibrational Raman scattering unmistakably suggests that the wing in both cases is of the same origin and cannot in either case be explained on the basis of a simple theory that it all arises from the rotation of molecules.

It must also be pointed out here that a recognition of the existence of such an unresolved wing in the vibrational scattering which cannot be separated from the Q branch proper is of utmost importance in the investigations relating to the intensity and polarization characters of these lines. This point has not, however, been realized by the earlier investigators[9] and its full significance will be dealt with by one of us in a separate communication relating to the intensity and polarization characters of the vibrational Raman lines in carbon disulphide.

---

[9] S. Bhagavantam, Ind. J. Phys. **5**, 35 (1930); J. Cabannes and A. Rousset, Ann. d. Physik **19**, 229 (1933); and A. Langseth, J. U. Sørensen and J. R. Nielsen, J. Chem. Phys. **2**, 402 (1934).

The Low Terms in Mn V and Fe VI

I. S. BOWEN, *California Institute of Technology*

(Received April 29, 1935)

Most of the strong lines arising from transitions between the d^3 and d^24p configurations in Mn V and Fe VI have been classified. The presence of forbidden lines of these ions in nebulae and novae is discussed.

WHITE[1] has made a study of the isoelectronic sequence VIII, Cr IV and Mn V. In Mn V he identified transitions to the ^2G, ^2H and ^4F terms of the d^3 configuration but, since no intercombination lines were found, he was unable to fix the relative positions of the doublets and quartets. In the present analysis about 50 additional lines have been classified in Mn V and about 100 lines in Fe VI. In both cases these include intercombination lines. The classified lines are listed in Tables I and II and the terms deduced from them in Table III.

As practically nothing has been known about the relative positions of the low metastable states in the stages of ionization of these atoms between Mn II and Mn VI and Fe II and Fe VII it is of importance to determine whether any of the forbidden transitions between the terms, fixed in this analysis, correspond to observed lines in the nebulae or novae. A comparison with various spectra of these objects has yielded, in general, only an occasional chance coincidence due to the wide tolerance which is made necessary both by the large uncertainty of many of the astronomical wavelengths and by the low wave-number accuracy of extreme ultraviolet measurements. The only coincidences that may in any way be considered significant are those between $^4F_{3\frac{1}{2}}-{}^2G_{4\frac{1}{2}}$ at 4968.8A, $^4F_{3\frac{1}{2}}-{}^2G_{3\frac{1}{2}}$ at 5146.8A and $^4F_{4\frac{1}{2}}-{}^2G_{4\frac{1}{2}}$ at 5177.0A and the lines of Nova Pictoris[2] in 1931–1932 at 4968.1A, 5148.5A and 5176.3A.

TABLE I. *Classified lines of Mn V.*

INT.	λ	ν	CLASSIFICATION d^3	CLASSIFICATION d^24p	INT.	λ	ν	CLASSIFICATION d^3	CLASSIFICATION d^24p	INT.	λ	ν	CLASSIFICATION d^3	CLASSIFICATION d^24p
1	382.061	261738	$^4F_{3\frac{1}{2}}$	$-(^3P)\,^4D_{3\frac{1}{2}}$	7	406.417	246053	$^4F_{3\frac{1}{2}}$	$-(^3F)\,^4D_{3\frac{1}{2}}$	8	415.980	240396	$^4P_{2\frac{1}{2}}$	$-(^3P)\,^4S$
6	382.907	261160	$^4F_{4\frac{1}{2}}$	$-(^3P)\,^4D_{3\frac{1}{2}}$	6	406.845	245794	$^4F_{3\frac{1}{2}}$	$-(^3F)\,^4D_{1\frac{1}{2}}$				$^2H_{5\frac{1}{2}}$	$-(^1G)\,^2G_{4\frac{1}{2}}$
1	382.980	261110	$^4F_{2\frac{1}{2}}$	$-(^3P)\,^4D_{2\frac{1}{2}}$	2	407.301	245519	$^4P_{2\frac{1}{2}}$	$-(^3P)\,^4D_{3\frac{1}{2}}$	1	422.228	236839	A	$-(^3P)\,^4D_{2\frac{1}{2}}$
2	383.422	260809	$^4F_{1\frac{1}{2}}$	$-(^3P)\,^4D_{1\frac{1}{2}}$	6	408.322	244905	$^4F_{4\frac{1}{2}}$	$-(^3F)\,^2F_{3\frac{1}{2}}$	5	428.600*	233318	$^2G_{4\frac{1}{2}}$	$-(^3F)\,^2G_{4\frac{1}{2}}$
4	383.681	260633	$^4F_{3\frac{1}{2}}$	$-(^3P)\,^4D_{2\frac{1}{2}}$	1	408.390	244864	$^4P_{1\frac{1}{2}}$	$-(^3P)\,^4D_{2\frac{1}{2}}$	5	429.054*	233071	$^2G_{3\frac{1}{2}}$	$-(^3F)\,^2G_{3\frac{1}{2}}$
5	383.939	260458	$^4F_{2\frac{1}{2}}$	$-(^3P)\,^4D_{1\frac{1}{2}}$	4	408.733	244658	$^4F_{3\frac{1}{2}}$	$-(^3F)\,^2F_{2\frac{1}{2}}$	1	429.984	232567	$^2G_{4\frac{1}{2}}$	$-(^3F)\,^2G_{3\frac{1}{2}}$
3	393.324	254243	$^2G_{4\frac{1}{2}}$	$-(^1G)\,^2H_{5\frac{1}{2}}$	1	409.217	244369	$^4P_{\frac{1}{2}}$	$-(^3P)\,^4D_{1\frac{1}{2}}$	0	431.973	231496	$^4P_{1\frac{1}{2}}$	$-(^3F)\,^2D_{2\frac{1}{2}}$
1	394.322	253600	$^2G_{3\frac{1}{2}}$	$-(^1G)\,^2H_{4\frac{1}{2}}$	2	409.335*	244299	$^4F_{3\frac{1}{2}}$	$-(^3F)\,^4F_{4\frac{1}{2}}$	7	433.558	230650	$^4P_{2\frac{1}{2}}$	$-(^3F)\,^4D_{3\frac{1}{2}}$
2	398.604	250876	$^4F_{3\frac{1}{2}}$	$-(^3F)\,^2G_{4\frac{1}{2}}$	3	409.546	244173	$^2G_{4\frac{1}{2}}$	$-(^3P)\,^4D_{2\frac{1}{2}}$	3	434.210	230303	$^4P_{1\frac{1}{2}}$	$-(^3F)\,^4D_{2\frac{1}{2}}$
4	399.538	250289	$^4F_{4\frac{1}{2}}$	$-(^3F)\,^2G_{4\frac{1}{2}}$	4	409.795*	244024	$^4F_{3\frac{1}{2}}$	$-(^3F)\,^4F_{3\frac{1}{2}}$	0	434.403	230201	$^2G_{3\frac{1}{2}}$	$-(^3F)\,^2D_{2\frac{1}{2}}$
3	401.787	248888	$^4P_{1\frac{1}{2}}$	$-(^3P)\,^4P_{2\frac{1}{2}}$	8	410.311*	243718	$^4F_{4\frac{1}{2}}$	$-(^3F)\,^4F_{4\frac{1}{2}}$	2	434.575	230110	$^4P_{\frac{1}{2}}$	$-(^3F)\,^4D_{\frac{1}{2}}$
4	402.525	248432	$^4P_{2\frac{1}{2}}$	$-(^3P)\,^4P_{2\frac{1}{2}}$	5	410.459*	243630	$^4F_{4\frac{1}{2}}$	$-(^3F)\,^4G_{5\frac{1}{2}}$	2	435.069	229849	$^4P_{2\frac{1}{2}}$	$-(^3F)\,^4D_{2\frac{1}{2}}$
3	402.754	248291	$^4P_{\frac{1}{2}}$	$-(^3P)\,^4P_{1\frac{1}{2}}$				$^4F_{1\frac{1}{2}}$	$-(^3F)\,^4F_{2\frac{1}{2}}$	1	435.291	229731	$^4P_{\frac{1}{2}}$	$-(^3F)\,^4D_{1\frac{1}{2}}$
0	403.007	248135	$^4P_{1\frac{1}{2}}$	$-(^3P)\,^4P_{1\frac{1}{2}}$	8	410.611*	243540	$^4F_{3\frac{1}{2}}$	$-(^3F)\,^4F_{3\frac{1}{2}}$	1	435.594	229572	$^4P_{1\frac{1}{2}}$	$-(^3F)\,^4D_{1\frac{1}{2}}$
0	403.281	247966	$^4P_{\frac{1}{2}}$	$-(^3P)\,^4P_{\frac{1}{2}}$	8	410.990*	243315	$^4F_{3\frac{1}{2}}$	$-(^3F)\,^4F_{2\frac{1}{2}}$	2	436.093	229309	$^2G_{4\frac{1}{2}}$	$-(^3F)\,^4D_{3\frac{1}{2}}$
3	403.552	247800	$^4P_{1\frac{1}{2}}$	$-(^3P)\,^4P_{\frac{1}{2}}$	7	411.329*	243114	$^4F_{1\frac{1}{2}}$	$-(^3F)\,^4F_{1\frac{1}{2}}$	8	436.174	229266	$^4P_{2\frac{1}{2}}$	$-(^3F)\,^2F_{3\frac{1}{2}}$
1	403.680	247721	$^4F_{3\frac{1}{2}}$	$-(^3F)\,^2D_{2\frac{1}{2}}$	7	411.585*	242963	$^4F_{4\frac{1}{2}}$	$-(^3F)\,^4F_{3\frac{1}{2}}$	1	436.660	229011	$^2G_{3\frac{1}{2}}$	$-(^3F)\,^4D_{2\frac{1}{2}}$
4	403.754	247676	$^4P_{2\frac{1}{2}}$	$-(^3P)\,^4P_{1\frac{1}{2}}$				$^4F_{3\frac{1}{2}}$	$-(^3F)\,^4G_{4\frac{1}{2}}$	1	436.857	228908	$^4P_{1\frac{1}{2}}$	$-(^3F)\,^2F_{2\frac{1}{2}}$
			$^2G_{4\frac{1}{2}}$	$-(^1G)\,^2G_{4\frac{1}{2}}$	3	411.789*	242843	$^4F_{3\frac{1}{2}}$	$-(^3F)\,^4F_{2\frac{1}{2}}$	5	438.735*	227928	$^2G_{4\frac{1}{2}}$	$-(^3F)\,^2F_{3\frac{1}{2}}$
8	404.358	247306	$^2G_{4\frac{1}{2}}$	$-(^1G)\,^2G_{4\frac{1}{2}}$	3	411.920*	242766	$^4F_{2\frac{1}{2}}$	$-(^3F)\,^4F_{1\frac{1}{2}}$	5	439.352*	227608	$^2G_{4\frac{1}{2}}$	$-(^3F)\,^2F_{2\frac{1}{2}}$
			$^2H_{5\frac{1}{2}}$	$-(^1G)\,^2H_{5\frac{1}{2}}$	5	412.534*	242404	$^4F_{3\frac{1}{2}}$	$-(^3F)\,^4G_{3\frac{1}{2}}$	1	441.008	226753	$^2H_{4\frac{1}{2}}$	$-(^3F)\,^2G_{4\frac{1}{2}}$
4	404.455	247246	$^4F_{3\frac{1}{2}}$	$-(^3F)\,^2D_{2\frac{1}{2}}$	4	413.384*	241906	$^4F_{1\frac{1}{2}}$	$-(^3F)\,^4G_{2\frac{1}{2}}$	7	441.725*	226385	$^2H_{5\frac{1}{2}}$	$-(^3F)\,^2G_{4\frac{1}{2}}$
5	405.094*	246856	$^4F_{3\frac{1}{2}}$	$-(^3F)\,^4D_{3\frac{1}{2}}$	3	414.933	241003	$^4P_{\frac{1}{2}}$	$-(^3P)\,^4S$	7	442.495*	225991	$^2H_{4\frac{1}{2}}$	$-(^3F)\,^2G_{3\frac{1}{2}}$
8	405.654	246516	$^4F_{1\frac{1}{2}}$	$-(^3F)\,^4D_{\frac{1}{2}}$	5	415.207	240844	$^4P_{1\frac{1}{2}}$	$-(^3P)\,^4S$	4	447.498	223465	A	$-(^3F)\,^2D_{2\frac{1}{2}}$
			$^2H_{4\frac{1}{2}}$	$-(^1G)\,^2H_{4\frac{1}{2}}$	0	415.336	240769	$^2H_{4\frac{1}{2}}$	$-(^1G)\,^2G_{4\frac{1}{2}}$	3	448.262	223084	A	$-(^3F)\,^4D_{3\frac{1}{2}}$
7	406.037*	246283	$^4F_{4\frac{1}{2}}$	$-(^3F)\,^4D_{3\frac{1}{2}}$	7	415.622	240603	$^4H_{4\frac{1}{2}}$	$-(^1G)\,^2G_{3\frac{1}{2}}$	3	451.065	221698	A	$-(^3F)\,^2F_{3\frac{1}{2}}$
1	406.240	246160	$^4F_{1\frac{1}{2}}$	$-(^3F)\,^4D_{1\frac{1}{2}}$						2	452.758	220869	A	$-(^3F)\,^2F_{2\frac{1}{2}}$

* Classified by White, (reference 1).

[1] H. E. White, Phys. Rev. **33**, 672 (1929).

[2] H. Spencer Jones, M. N. R. A. S. **92**, 728 (1932).

TABLE II. *Classified lines in Fe VI.*

INT.	λ	ν	CLASSIFICATION d^3	$d^2 4p$
3	276.947	361080	$^4F_{3\frac{1}{2}}$	$-(^3P)^4D_{3\frac{1}{2}}$
6	277.569	360271	$^4F_{4\frac{1}{2}}$	$-(^3P)^4D_{3\frac{1}{2}}$
2	277.610	360218	$^4F_{3\frac{1}{2}}$	$-(^3P)^4D_{2\frac{1}{2}}$
3	277.951	359776	$^4F_{1\frac{1}{2}}$	$-(^3P)^4D_{1\frac{1}{2}}$
5	278.149	359520	$^4F_{2\frac{1}{2}}$	$-(^3P)^4D_{2\frac{1}{2}}$
5	278.339	359274	$^4F_{2\frac{1}{2}}$	$-(^3P)^4D_{1\frac{1}{2}}$
3	278.471	359104	$^4F_{1\frac{1}{2}}$	$-(^3P)^4D_{\frac{1}{2}}$
5	283.770	352398	$^2G_{4\frac{1}{2}}$	$-(^1G)^2H_{5\frac{1}{2}}$
4	284.504	351489	$^2G_{3\frac{1}{2}}$	$-(^1G)^2H_{4\frac{1}{2}}$
1	287.333	348028	$^4F_{4\frac{1}{2}}$	$-(^3F)^2G_{4\frac{1}{2}}$
4	288.551	346559	$^4P_{1\frac{1}{2}}$	$-(^3P)^4P_{2\frac{1}{2}}$
5	289.112	345887	$^4P_{3\frac{1}{2}}$	$-(^3P)^4P_{2\frac{1}{2}}$
4	289.302	345660	$^4P_{\frac{1}{2}}$	$-(^3P)^4P_{1\frac{1}{2}}$
3	289.468	345462	$^4P_{1\frac{1}{2}}$	$-(^3P)^4P_{1\frac{1}{2}}$
4	289.520	345400	$^4F_{3\frac{1}{2}}$	$-(^3F)^2D_{3\frac{1}{2}}$
2	289.672	345218	$^4P_{\frac{1}{2}}$	$-(^3P)^4P_{\frac{1}{2}}$
4	289.851	345005	$^4P_{1\frac{1}{2}}$	$-(^3P)^4P_{1\frac{1}{2}}$
4	290.038	344782	$^4P_{2\frac{1}{2}}$	$-(^3P)^4P_{1\frac{1}{2}}$
4	290.089	344722	$^4F_{3\frac{1}{2}}$	$-(^3F)^2D_{2\frac{1}{2}}$
4	290.146	344654	$^4F_{1\frac{1}{2}}$	$-(^3F)^2D_{1\frac{1}{2}}$
6	290.271	344506	$^2H_{5\frac{1}{2}}$	$-(^1G)^2H_{5\frac{1}{2}}$
5	290.302	344469	$^2G_{5\frac{1}{2}}$	$-(^1G)^2G_{5\frac{1}{2}}$
2	290.499	344235	$^4F_{4\frac{1}{2}}$	$-(^3F)^4D_{3\frac{1}{2}}$
4	290.577	344143	$^4F_{3\frac{1}{2}}$	$-(^3F)^2D_{1\frac{1}{2}}$
4	290.737	343953	$^2G_{4\frac{1}{2}}$	$-(^1G)^2G_{4\frac{1}{2}}$
2	290.890	343773	$^4F_{3\frac{1}{2}}$	$-(^3F)^4D_{2\frac{1}{2}}$
			$^2G_{4\frac{1}{2}}$	$-(^1G)^2G_{3\frac{1}{2}}$
5	291.020	343619	$^4F_{1\frac{1}{2}}$	$-(^3F)^4D_{\frac{1}{2}}$
6	291.184	343425	^4F	$-(^3F)^4D_{2\frac{1}{2}}$
6	291.229	343372	$^2H_{4\frac{1}{2}}$	$-(^1G)^2H_{4\frac{1}{2}}$
5	291.473	343085	$^4F_{2\frac{1}{2}}$	$-(^3F)^4D_{2\frac{1}{2}}$
2	291.632	342898	$^2H_{5\frac{1}{2}}$	$-(^1G)^2H_{4\frac{1}{2}}$
5	291.800	342700	$^4F_{2\frac{1}{2}}$	$-(^3F)^4D_{1\frac{1}{2}}$
5	291.829	342666	$^4F_{3\frac{1}{2}}$	$-(^3P)^4D_{3\frac{1}{2}}$
0	291.931	342547	$^4F_{1\frac{1}{2}}$	$-(^3F)^2F_{2\frac{1}{2}}$
2	292.038	342421	$^4F_{3\frac{1}{2}}$	$-(^3F)^2F_{3\frac{1}{2}}$
1	292.343	342064	$^4F_{2\frac{1}{2}}$	$-(^3F)^2F_{2\frac{1}{2}}$
4	292.597	341767	$^4F_{1\frac{1}{2}}$	$-(^3P)^4D_{2\frac{1}{2}}$
7	292.736	341605	$^4F_{4\frac{1}{2}}$	$-(^3F)^2F_{3\frac{1}{2}}$
5	292.925	341384	$^4F_{3\frac{1}{2}}$	$-(^3F)^2F_{2\frac{1}{2}}$
2	293.046	341244	$^4F_{3\frac{1}{2}}$	$-(^3F)^4F_{4\frac{1}{2}}$
1	293.214	341048	$^4P_{\frac{1}{2}}$	$-(^3P)^4D_{1\frac{1}{2}}$
4	293.292	340957	$^2G_{4\frac{1}{2}}$	$-(^3P)^4D_{2\frac{1}{2}}$
4	293.384	340850	$^4F_{2\frac{1}{2}}$	$-(^3F)^4F_{3\frac{1}{2}}$
4	293.488	340729	$^4F_{4\frac{1}{2}}$	$-(^3F)^4G_{5\frac{1}{2}}$
8	293.745	340431	$^4F_{4\frac{1}{2}}$	$-(^3F)^4F_{4\frac{1}{2}}$
1	293.820	340345	$^4F_{1\frac{1}{2}}$	$-(^3F)^4F_{2\frac{1}{2}}$
8	293.966	340175	$^4F_{2\frac{1}{2}}$	$-(^3F)^4F_{2\frac{1}{2}}$
0	294.040	340090	$^2G_{3\frac{1}{2}}$	$-(^3P)^4D_{2\frac{1}{2}}$
7	294.265	339830	$^4F_{3\frac{1}{2}}$	$-(^3F)^4F_{3\frac{1}{2}}$
5	294.339	339744	$^4F_{3\frac{1}{2}}$	$-(^3F)^4G_{4\frac{1}{2}}$
7	294.520	339536	$^4F_{1\frac{1}{2}}$	$-(^3F)^4F_{1\frac{1}{2}}$
4	294.665	339368	$^4F_{4\frac{1}{2}}$	$-(^3F)^4F_{3\frac{1}{2}}$
4	294.850	339155	$^4F_{3\frac{1}{2}}$	$-(^3F)^4F_{2\frac{1}{2}}$
4	294.960	339029	$^4F_{2\frac{1}{2}}$	$-(^3F)^4F_{1\frac{1}{2}}$
4	295.014	338967	$^4F_{3\frac{1}{2}}$	$-(^3F)^4G_{3\frac{1}{2}}$
2	295.042	338935	$^4F_{4\frac{1}{2}}$	$-(^3F)^4G_{4\frac{1}{2}}$
4	295.634	338256	$^4F_{1\frac{1}{2}}$	$-(^3F)^4G_{2\frac{1}{2}}$
			$^4F_{2\frac{1}{2}}$	$-(^3F)^4G_{3\frac{1}{2}}$
1	296.317	337477	$^4F_{4\frac{1}{2}}$	$-(^3F)^4G_{5\frac{1}{2}}$
3	296.723	337015	A	$-(^3P)^4P_{2\frac{1}{2}}$
5	296.808	336918	$^4P_{\frac{1}{2}}$	$-(^3P)^4S$
6	296.988	336714	$^4P_{1\frac{1}{2}}$	$-(^3P)^4S$
2	297.131	336552	$^2H_{4\frac{1}{2}}$	$-(^1G)^2G_{4\frac{1}{2}}$
7	297.308	336352	$^2H_{4\frac{1}{2}}$	$-(^1G)^2G_{3\frac{1}{2}}$
8d	297.568	336058	$^2H_{5\frac{1}{2}}$	$-(^1G)^2G_{4\frac{1}{2}}$
			$^4P_{2\frac{1}{2}}$	$-(^3P)^4S$
1	299.579	333802	A	$-(^3P)^4D_{2\frac{1}{2}}$
1	299.803	333552	$^2H_{4\frac{1}{2}}$	$-(^1P)^4D_{2\frac{1}{2}}$
2	300.997	332229	A	$-(^3P)^4D_{3\frac{1}{2}}$
4	303.558	329426	$^2G_{3\frac{1}{2}}$	$-(^3F)^2G_{4\frac{1}{2}}$
7	304.221	328708	$^2G_{4\frac{1}{2}}$	$-(^3F)^2G_{4\frac{1}{2}}$
7	304.551	328352	$^2G_{4\frac{1}{2}}$	$-(^3F)^2G_{3\frac{1}{2}}$
4	305.200	327654	$^2G_{4\frac{1}{2}}$	$-(^3F)^2G_{4\frac{1}{2}}$
1	305.837	326972	$^4P_{1\frac{1}{2}}$	$-(^3F)^2D_{2\frac{1}{2}}$
1	306.460	326307	$^4P_{2\frac{1}{2}}$	$-(^3F)^2D_{2\frac{1}{2}}$
2	306.823	325921	$^4P_{\frac{1}{2}}$	$-(^3F)^2D_{1\frac{1}{2}}$
5	306.922	325816	$^4P_{2\frac{1}{2}}$	$-(^3F)^4D_{2\frac{1}{2}}$
2	307.013	325719	$^4P_{1\frac{1}{2}}$	$-(^3F)^2D_{1\frac{1}{2}}$
4	307.375	325336	$^4P_{1\frac{1}{2}}$	$-(^3F)^4D_{2\frac{1}{2}}$
3	307.404	325305	$^2G_{3\frac{1}{2}}$	$-(^3F)^2D_{2\frac{1}{2}}$
3	307.800	324886	$^4P_{\frac{1}{2}}$	$-(^3F)^4D_{\frac{1}{2}}$
0	307.884	324798	$^2G_{4\frac{1}{2}}$	$-(^3F)^4D_{2\frac{1}{2}}$
3	308.007	324668	$^4P_{1\frac{1}{2}}$	$-(^3F)^4D_{\frac{1}{2}}$
			$^4P_{2\frac{1}{2}}$	$-(^3F)^4D_{2\frac{1}{2}}$
2	308.187	324478	$^4P_{\frac{1}{2}}$	$-(^3F)^4D_{1\frac{1}{2}}$
2	308.383	324272	$^4P_{1\frac{1}{2}}$	$-(^3F)^4D_{1\frac{1}{2}}$
4	308.534	324113	$^2G_{4\frac{1}{2}}$	$-(^3F)^4D_{3\frac{1}{2}}$
5	308.644	323998	$^4P_{2\frac{1}{2}}$	$-(^3F)^2F_{2\frac{1}{2}}$
3	308.960	323666	$^2G_{4\frac{1}{2}}$	$-(^3F)^4D_{2\frac{1}{2}}$
3	308.993	323632	$^4P_{1\frac{1}{2}}$	$-(^3F)^2F_{2\frac{1}{2}}$
1	309.627	322969	$^4P_{2\frac{1}{2}}$	$-(^3F)^2F_{2\frac{1}{2}}$
			$^2G_{4\frac{1}{2}}$	$-(^3F)^2F_{3\frac{1}{2}}$
5	310.274	322296	$^2G_{4\frac{1}{2}}$	$-(^3F)^2F_{3\frac{1}{2}}$
4	310.601	321956	$^2G_{4\frac{1}{2}}$	$-(^3F)^2F_{2\frac{1}{2}}$
0	310.807	321743	$^4P_{2\frac{1}{2}}$	$-(^3F)^4F_{2\frac{1}{2}}$
1	311.138	321401	$^4P_{1\frac{1}{2}}$	$-(^3F)^4F_{3\frac{1}{2}}$
2	311.236	321300	$^2H_{4\frac{1}{2}}$	$-(^3F)^2G_{4\frac{1}{2}}$
7	311.702	320819	$^2H_{4\frac{1}{2}}$	$-(^3F)^2G_{4\frac{1}{2}}$
7	312.263	320243	$^2H_{4\frac{1}{2}}$	$-(^3F)^2G_{3\frac{1}{2}}$
3	314.299	318168	$^2G_{4\frac{1}{2}}$	$-(^3F)^4G_{4\frac{1}{2}}$
1	314.814	317648	$^2G_{3\frac{1}{2}}$	$-(^3F)^4G_{3\frac{1}{2}}$
4	315.027	317433	A	$-(^3F)^2D_{2\frac{1}{2}}$
3	315.506	316951	A	$-(^3F)^4D_{3\frac{1}{2}}$
3	317.319	315140	A	$-(^3F)^2F_{3\frac{1}{2}}$
3	318.364	314106	A	$-(^3F)^2F_{2\frac{1}{2}}$

TABLE III. *Term values of Mn V and Fe VI.*

d^3	Mn V	Fe VI	$d^2 4p$	Mn V	Fe VI	$d^2 4p$	Mn V	Fe VI
$^4F_{1\frac{1}{2}}$	000	000	$(^2F)^4G_{5\frac{1}{2}}$	241906	338256	$(^2F)^2D_{2\frac{1}{2}}$	248074	345908
$^4F_{2\frac{1}{2}}$	349	510	$(^2F)^4G_{2\frac{1}{2}}$	242753	339477	$(^2F)^2G_{4\frac{1}{2}}$	250949	348962
$^4F_{3\frac{1}{2}}$	827	1185	$(^2F)^4F_{1\frac{1}{2}}$	243115	339538	$(^2F)^2G_{4\frac{1}{2}}$	251700	350016
$^4F_{4\frac{1}{2}}$	1406	1994	$(^2F)^4F_{2\frac{1}{2}}$	243667	340341	$(^2P)^4S$	257424	355652
$^4P_{\frac{1}{2}}$	16420	18734	$(^2F)^4G_{4\frac{1}{2}}$	243790	340929	$(^2P)^4D_{\frac{1}{2}}$		359104
$^4P_{1\frac{1}{2}}$	16580	18937	$(^2F)^4F_{2\frac{1}{2}}$	244370	341361	$(^2P)^4D_{1\frac{1}{2}}$	260808	359784
$^4P_{2\frac{1}{2}}$	17036	19601	$(^2F)^4G_{3\frac{1}{2}}$	245036	342723	$(^2P)^4D_{2\frac{1}{2}}$	261460	360705
$^2G_{4\frac{1}{2}}$	17878	20609	$(^2F)^4F_{4\frac{1}{2}}$	245125	342426	$(^2P)^4D_{3\frac{1}{2}}$	262566	362265
$^2G_{4\frac{1}{2}}$	18382	21305	$(^2F)^2F_{2\frac{1}{2}}$	245486	342570	$(^2P)^4P_{\frac{1}{2}}$	264382	363944
A	24610	28469	$(^2F)^4D_{1\frac{1}{2}}$	246143	343210	$(^2P)^4P_{1\frac{1}{2}}$	264712	364390
$^2H_{4\frac{1}{2}}$	24953	28723	$(^2F)^2F_{2\frac{1}{2}}$	246307	343600	$(^2P)^4P_{2\frac{1}{2}}$	265468	365492
$^2H_{5\frac{1}{2}}$	25315	29196	$(^2F)^4D_{\frac{1}{2}}$	246530	343619	$(^1G)^2G_{4\frac{1}{2}}$	265555	365077
			$(^2F)^4D_{2\frac{1}{2}}$	246880	344270	$(^1G)^2G_{4\frac{1}{2}}$	265715	365262
			$(^2F)^2D_{1\frac{1}{2}}$		344656	$(^1G)^2H_{4\frac{1}{2}}$	271475	372096
			$(^2F)^4D_{3\frac{1}{2}}$	247686	345419	$(^1G)^2H_{5\frac{1}{2}}$	272624	373702

Intensity Relations in Chromium Spectra

J. S. V. ALLEN AND C. E. HESTHAL, *Mendenhall Laboratory of Physics, Ohio State University*

(Received April 26, 1935)

The relative intensities of lines in four multiplets in the spectrum of Cr I, and eight multiplets in the spectrum of Cr II, have been measured with a concave-grating spectrograph and photographic photometry. The intensities in many cases deviate from those calculated for Russell-Saunders coupling, the deviations being in accord with observations of others on intensities in the spectra of elements of the iron group. Perturbing energy levels offer a possible explanation of many of the deviations. Two multiplets in the septet system of Cr II have been corrected for excitation. The temperature of the chromium arc source consistent with this correction was found to be 4060°K.

I. INTRODUCTION

INTENSITY measurements in the complex spectra of the elements composing the iron group are particularly interesting because of the increasing divergence from intensity rules for Russell-Saunders coupling as the atomic number increases. The elements at the beginning of the group show fairly good agreement with these intensity rules, but there is an increase in the proportion of anomalous line intensities as one passes through this group to nickel. This is shown by the intensity studies of titanium (22),[1] vanadium (23),[2] chromium (24),[3] manganese (25),[4] iron (26),[5] cobalt (27)[6] and nickel (28).[7] This investigation was undertaken to determine some of the intensity relations in chromium.

II. EXPERIMENTAL

The method of photographic photometry as described by G. R. Harrison was used for the determination of relative intensities of spectral lines.

Excitation of spectrum

Two pieces of purified chromium metal were clamped in water-cooled holders in a glass bulb, 19 cm in diameter, where the pressure was maintained at 7 to 15 cm of mercury. The arc was excited by approximately 2.4 amperes, furnished by a 110-volt storage battery with a large reactance in series. The glass bulb was provided with a quartz window which transmitted the desired wavelengths.

Spectrograph

A concave grating with a radius of curvature of 6.4 meters, having 6000 lines per cm for a length of 11.6 cm, was used in the second order with a dispersion of 1.25A/mm, on a Paschen-type mounting. The intensity of the light was varied by absorbing screens made of screen wire of different mesh placed between the lens and the slit. The intensity could be varied from 100 to 3 percent. The plateholders were held in position and manipulated by means of cassettes, making it possible to expose any portion of the plate. The cassettes, taking 4×10-inch plates, were placed on two concentric rails on a rigid circular table. The plate was raised 4 mm between each exposure, making it possible to take 22 exposures on one plate. These exposures were accurately timed by an automatic timing device consisting of a pendulum, vacuum-tube relay, and magnetic shutter. The two central exposures were of the chromium arc. Above and below these were three exposures of the mercury arc for calibration purposes. Exposures were made simultaneously on both sides of the normal in such a way that there was a 40-Angstrom overlap, thus giving a continuous exposure to the chromium or other sources. Eastman 36 plates were used.

Determination of intensities of spectral lines

The photographic plates were calibrated, as described by Harrison, with a series of exposures

[1] G. R. Harrison, J. O. S. A. **17**, 389 (1928).
[2] G. R. Harrison, unpublished material.
[3] C. E. Hesthal, unpublished material.
[4] R. S. Seward, Phys. Rev. **37**, 344 (1931).
[5] J. B. van Milaan, Zeits. f. Physik **34**, 921 (1925); R. Frerichs, Ann. d. Physik **81**, 807 (1926).
[6] L. S. Ornstein and T. Bouma, Phys. Rev. **36**, 679 (1930).
[7] H. N. Russell, Astrophys. J. **66**, 335 (1927); but modified later, see J. O. S. A. **18**, 296 (1929).

to a mercury arc operated on a 110-volt storage battery. To get the intensity of a given chromium line the percentage transmissions were measured by means of a densitometer employing a photoelectric cell and a Wynn-Williams[8] Wheatstone-bridge amplifier as described by C. E. Hesthal and G. R. Harrison.[9] The transmissions as given by the densitometer were then converted to the corresponding intensities by means of a calibration curve. To correct for variations in the arc, 48 exposures were made of each chromium line.

Corrections and errors

1. The intensity of the background upon which the spectrum was superimposed was determined separately and subtracted from the intensity of the line.

2. A correction for self-reversal was made by adding to the intensity that fraction of the light which was absorbed as the radiation passed through the cooler layers of chromium vapor surrounding the arc, in the manner described by Harrison.

3. The transmissions of the most intense lines could not be read accurately in the stronger exposures, and very weak lines could be measured only in the more intense exposures, while other lines could be obtained in all exposures. To correct for this experimental limitation, weighted averages were used, the proper weight for each exposure (or group of exposures) being determined from the intensity readings of four lines that appeared in all exposures on all photographic plates. In this way all exposures were converted to the same arbitrary scale.

4. Since the rate of radiation of an oscillator is proportional to the fourth power of the frequency, it is necessary to divide each intensity by the fourth power of its frequency in order to compare theoretically intensities of different frequencies.

5. The variation in sensitivity of the spectrograph with wavelength was determined in a separate experiment, and the results were used to correct all intensities for this variation.

6. All measured intensities have been checked for superimposed lines of aluminum and iron, the two most abundant impurities in the chromium arc.

7. In a few cases the superposition of ghosts upon spectral lines has augmented the measured intensities. These cases have been indicated in the results.

8. In varying the intensity of the calibrating source of light, it was necessary to move the screens with an irregular motion to average out the effect of moire patterns. This gives rise to three kinds of errors. (a) Intermittency effect of the photographic plate introduces an error because of the small variations in the intensity due to the motion of the absorbing screens. This variation is under 10 percent and results in an intermittency error of less than 1 percent.[10] (b) The error due to the diffraction of light in passing through the screens was reduced to a minimum by removing the slit, flooding the grating with light. (c) The error due to lack of achromatism is negligible. Landsberg[11] has found wire screens to be neutral in their absorption to within 1 or 2 percent over the wavelength region from 2000A to 5000A.

III. Results

In Table I and Table II observed intensities of the lines of each multiplet have been compared with the theoretical relative intensities[12] calculated for Russell-Saunders coupling. The notation here used is that given by Bacher and Goudsmit.[13]

Chromium I

Multiplet $a^5D - y^5D^0$ $(3d^4\,4s^2 - 3d^4\,4s(^4D)\,4p)$. Some of the abnormally high intensities may be attributed to overlapping ghosts. Other anomalies may arise from perturbations between the terms of y^5D^0 and y^5F^0 which overlap.

Multiplet $a^5D - x^5D^0$ $(3d^4\,4s^2 - ?)$. Line 2889.3A of this multiplet is coincident with 2889.2A of $a^4D - z^4D^0$ of Cr II. The observed intensity was arbitrarily divided so that the latter line would be approximately normal. The results show both lines to be normal. The self-reversal curves of $a^5D - w^5P^0$, $a^5D - x^5D^0$, and $a^5D - y^5D^0$ are similar

[8] C. E. Wynn-Williams, Phil. Mag. **6**, 324 (1928).
[9] C. E. Hesthal and G. R. Harrison, Phys. Rev. **34**, 543 (1929).
[10] G. R. Harrison, J. O. S. A. **18**, 492 (1929).
[11] Landsberg, Zeits. f. Physik **46**, 106 (1927).
[12] H. E. White, *Introduction to Atomic Spectra*, p. 205 *et seq.*
[13] R. F. Bacher and S. Goudsmit, *Atomic Energy States*, McGraw-Hill, 1932.

TABLE I. *Chromium I.* $I_{obs.}$, observed intensities after applying corrections for background, self-reversal, ν^4, and variation in sensitivity. I^*, intensity measurements by C. E. Hesthal.

Wavelength	Transition	$I_{theor.}$	$I_{obs.}$	I^*
Multiplet	$a^5D-y^5D^0$			
3005.1	4−3	359	522	490
3000.9	3−2	478	593	578
2996.6	2−1	419	502[1]	480
2992.0	1−0	240	274[1]	269
2986.5	4−4	1790	821	1600
2986.1	1−1	900	803	1060
2986.0	3−3			
2985.9	2−2	299	296	
2980.8	0−1	240	242	222
2975.5	1−2	419	362	337
2971.1	2−3	478	409	423
2967.6	3−4	359	359	365
Multiplet	$a^5D-x^5D^0$			
2911.1	4−3	115	118	
2910.9	3−2	154	175	
2909.1	2−1	134	160	
2905.5	1−0	77.0	87.6	
2899.2	1−1	19.2	29.9	
2896.8	2−2	96.2	130	
2894.2	0−1	77.0	74.1	
2893.2	3−3	269	269	
2889.3	4−4	577	581[2]	
2887.0	1−2	134	99.3	
2879.3	2−3	154	91.5	
2871.6	3−4	115	55.8	
Multiplet	$a^5D-w^5P^0$			
2780.7	4−3	237	237	
2769.9	3−2	123	125	
2764.3	3−3	61.4	71.0[1]	
2761.7	2−1	46.0	48.2	
2757.1	2−2	76.8	81.5	
2752.9	1−1	59.2	57.7	
2751.6	2−3	8.76	9.24	
2748.3	0−1	46.0	43.9	
2748.2	1−2			
Multiplet	$a^5S-w^5P^0$			
2736.5	2−1	45.2	45.0	
2731.9	2−2	75.3	74.5	
2726.5	2−3	105	105	

[1] Superimposed ghost.

[2] Two coincident lines—intensity arbitrarily divided.

because all three multiplets have the same lower term, a^5D. The terms a^7D, x^7P^0, and z^5G^0 overlap x^5D^0; and there are other terms lying close enough to x^5D^0 to cause anomalous intensities.

Multiplet $a^5D-w^5P^0$ $(3d^4\,4s^2-?)$. The agreement between the observed and calculated intensities is good throughout the entire range of intensities from 10 to 250, with one exception which is explained by a superimposed ghost. The self-reversal curve of this multiplet resembles that of $a^5D-x^5D^0$ and $a^5D-y^5D^0$ because the three multiplets have the same lower term.

Multiplet $a^5S-w^5P^0$ $(3d^5(^6S)4s-?)$. The observed intensities agree very well with the theoretical intensities in this multiplet, which would indicate that the type of coupling is Russell-Saunders, and that the energy levels involved are quite free from perturbations although w^5P^0 is only 40 cm^{-1} from y^5G^0 and 407 cm^{-1} from v^5P^0. Russell-Saunders coupling seems to hold completely although the separations in the levels of w^5P^0 are in the ratio of 3 : 2.5 instead of 3 : 2 as predicted by the Landé interval rule for Russell-Saunders coupling. Both Frerichs and Harrison have failed to find a correlation between deviations from the intensity rules and deviations from Landé's rule in the iron group.

Chromium II

Multiplet $a^4D-z^4F^0$ $(3d^4(^5D)4s-3d^4(^5D)4p)$. The first-order ghost of the comparatively strong line 3147.2A falls upon 3145.1A causing an abnormally high reading for the latter line intensity. The nearest energy level to z^4F^0 is $y^4P^0_{5/2}$ (separation, 1878 cm^{-1}). Appreciable perturbations may exist between the energy levels of these two terms. However, the observed intensities of this multiplet agree with the theoretical values much better than in the case of the multiplet $a^4F-z^4G^0$, in which a perturbing term y^4D^0 is only 231.8 cm^{-1} removed from z^4G^0. The self-reversal curve of the above multiplet is quite similar to the curve for $a^4D-z^4D^0$, since both have the same lower term.

Multiplet $a^4P-y^4D^0$. Intensities of two lines are missing from this multiplet because they were too weak to measure accurately. The observed intensities in this multiplet show good agreement with the calculated values.

Multiplet $a^4F-z^4G^0$ $(3d^4(^3F)4s-3d^4(^3F)4p?)$. The transition $a^4F_{9/2}-z^4G^0_{11/2}$ is not listed because the level $z^4G^0_{11/2}$ has not been identified. The energy levels $z^4G^0_{7/2}$ and $y^4D^0_{7/2}$ are only 332 cm^{-1} apart. According to Harrison and Johnson,[14]

[14] G. R. Harrison and M. H. Johnson, Jr., Phys. Rev. **38**, 757 (1931).

TABLE II. *Chromium II.* $I_{obs.}$, observed intensities after applying corrections for background, self-reversal, ν^4, and variation in sensitivity. I^*, intensity measurements by C. E. Hesthal.

Wavelength	Transition	$I_{theor.}$	$I_{obs.}$	I^*
Multiplet	$a^4D-z^4F^0$			
3159.1	7/2− 5/2	4.83	3.6	
3147.2	7/2− 7/2	100	102	
3145.1	5/2− 3/2	6.89	10.8[1]	
3136.7	5/2− 5/2	128	123	
3132.0	7/2− 9/2	861	855	
3128.7	3/2− 3/2	96.5	108	
3125.0	5/2− 7/2	589	589	
3120.4	3/2− 5/2	386	404	
3118.7	1/2− 3/2	241	264	
Multiplet	$a^4P-y^4D^0$			
3011.4	5/2− 3/2	1.37	—[4]	
2984.7	3/2− 1/2	2.28	—[4]	
2976.7	5/2− 5/2	12.4	8.95	
2961.7	3/2− 3/2	14.6	15.4	
2953.4	1/2− 1/2	11.4	11.5	
2935.1	5/2− 7/2	54.7	54.7	
2930.9	1/2− 3/2	11.4	11.7	
2928.2	3/2− 5/2	28.7	27.4[6]	
Multiplet	$a^4F-z^4G^0$ [5]			
2941.4	7/2− 5/2	2.41	9.99	
2937.1	9/2− 7/2	72.1	107	
2937.0	5/2− 5/2			
2934.0	3/2− 5/2	436	318	
2932.7	7/2− 7/2	92.0	83.0	
2928.3	5/2− 7/2	583	693[6]	
2926.2	9/2− 9/2	70.2	72.4	
2921.8	7/2− 9/2	777	311	
Multiplet	$a^4D-z^4D^0$			
2889.2	7/2− 5/2	36.9	38.8[2]	
2880.9	5/2− 3/2	46.5	49.7	
2876.0	7/2− 7/2	225	227	
2873.8	3/2− 1/2	32.8	32.0	
2870.4	5/2− 5/2	113	114	
2867.1	3/2− 3/2	52.0	68.9[1]	
2865.3	1/2− 1/2	32.8	35.6	
2858.7	1/2− 3/2	32.8	31.0	
2857.4	5/2− 7/2	36.9	14.3[3]	
2856.8	3/2− 5/2	46.5	10.4[3]	

Wavelength	Transition	$I_{theor.}$	$I_{obs.}$	I^*
Multiplet	$a^6D-z^6F^0$			
2878.5	9/2− 7/2	14.4	32.1	<89.6
2878.0	7/2− 5/2	33.2	82.9	<89.6
2876.3	5/2− 3/2	47.1	136	<89.6
2873.5	3/2− 1/2	43.8	95.5	<89.6
2867.6	1/2− 1/2	347	328	347
2866.8	3/2− 3/2	536	471	496
2865.1	5/2− 5/2	621	610	568
2862.6	7/2− 7/2	582	582	533
2860.9	1/2− 3/2	203	269	275
2858.9	9/2− 9/2	379	417	424
2855.7	3/2− 5/2	517	555	525
2849.8	5/2− 7/2	967	924	741
2843.2	7/2− 9/2	1580	1240	930
2835.6	9/2−11/2	2350	2050	1100
Multiplet	$b^4G-y^4H^0$			
2838.1	9/2− 7/2	.039	2.05	
2832.2	11/2− 9/2	.028	—[4]	
2830.3	7/2− 7/2	1.61	—[4]	
2826.2	9/2− 9/2	2.45	2.45	
2822.0	5/2− 7/2	18.3	18.1	
2818.4	7/2− 9/2	22.8	22.6	
2818.0	11/2−11/2	1.61	1.7	
2812.0	9/2−11/2	28.3	29.0	
2800.8	11/2−13/2	35.0	29.1	
Multiplet	$a^6D-z^6P^0$			
2766.5	9/2− 7/2	703	694	523
2762.6	7/2− 5/2	361	402[1]	353
2757.7	5/2− 3/2	131	164	171
2751.9	7/2− 7/2	201	208	209
2750.7	5/2− 5/2	256	256	236
2749.0	3/2− 3/2	199	199	199
2743.6	1/2− 3/2	140	122[1]	133
2742.0	3/2− 5/2	83.8	100[1, 6]	133
2740.1	5/2− 7/2	33.4	33.0	36.6
Multiplet	$a^6D-z^6D^0$ [5]			
2691.1	9/2− 7/2	119	108	
2677.2	9/2− 9/2	827	687	
2677.2	7/2− 7/2			
2677.2	5/2− 5/2			
2666.0	5/2− 7/2	167	167	
2663.4	7/2− 9/2	119	128[1]	

[1] Superimposed ghost.
[2] Two coincident lines—intensity arbitrarily divided.
[3] Uncertain because of strong neighboring line.
[4] Very weak line.
[5] Incomplete multiplet because of unknown term values.
[6] Overlapping line.

appreciable perturbations may exist between levels in Ti I that are separated by as much as 2000 cm^{-1}, and weaker lines will show a greater percentage deviation from their normal intensities, when there is a weak spin-orbit interaction such as exists in the chromium atom. The first line in the above multiplet illustrates this case.

Multiplet $a^4D-z^4D^0$ $(3d^4(^5D)4s-3d^4(^3D)4p)$. Line 2889.2A of this multiplet is coincident with 2889.3A of $a^5D-x^5D^0$. The intensity reading was arbitrarily divided so as to make the former line approximately normal. The observed intensities of the lines 2857.4A and 2856.8A in this multiplet are not dependable because strong adjacent lines interfered with the densitometer readings. The remaining line intensities are in fair agreement with the theoretical values. This indicates a lack of perturbations which is to be expected since the nearest known energy level to z^4D^0 is z^4F^0; and the separation is 2475 cm^{-1}. The self-reversal curves of $a^4D-z^4D^0$ and $a^4D-z^4F^0$ are quite similar. This is to be expected, since both multiplets have the same lower term.

Multiplet $a^6D-z^6F^0$ $(3d^4(^5D)4s-3d^4(^5D)4p)$.

As in multiplet $a^4F-z^4G^0$ the observed intensities of the weak lines differ greatly from the calculated values. The correlation between Hesthal's observed intensities and those of the present observers is especially poor for both the weaker and stronger lines. No explanation of this discrepancy was found.

Multiplet $b^4G-y^4H^0$ $(3d^4(^3G)4s-3d^4(^3G)4p)$. Two indicated lines of this multiplet are too weak to be measured on the densitometer. There is practically no self-reversal in this multiplet because b^4G is the highest term value of all known even terms; and, hence, it should be poorly populated with electrons. Consequently, there are fewer absorption transitions upward from b^4G to y^4H^0. As in the multiplets $a^4F-z^4G^0$ and $a^6D-z^6F^0$, we find an anomalous intensity for the weak line.

Multiplet $a^6D-z^6P^0$ $(3d^4(^5D)4s-3d^4(^5D)4p)$. There are three cases of superimposed ghosts and one case of an overlapping line which help to explain some of the anomalous intensities in this multiplet.

Multiplet $a^6D-z^6D^0$ $(3d^4(^5D)4s-3d^4(^5D)4p)$. Five of the seven lines missing from this multiplet involve the levels of z^6D^0 for which J equals $1/2$ and $3/2$. The term values of these two levels were not known, and so the wavelengths could not be calculated. The observed intensity of the three superimposed lines is much less than the sum of the three corresponding theoretical intensities. The explanation of this may be that the three lines are not exactly superimposed.

Sextet supermultiplet $a^6D-z^6F^0$, $a^6D-z^6D^0$, $a^6D-z^6P^0$. The multiplets forming this sextet supermultiplet have already been considered but the intensity data of such a supermultiplet may be used to compute the theoretical temperature T of the arc by means of the formula,[15] $T=0.625\Delta\sigma/\log_{10} R$, where T is the absolute temperature of the arc, $\Delta\sigma$ is the wave-number separation of the levels of the upper term, and R is the excitation factor. R is the factor by which the sum of the observed intensities of all lines originating in the same upper level is multiplied to make it equal to the sum of the corresponding theoretical intensities. The higher the level, the greater will be the value of R, because of the decreasing electronic population of the higher levels. When the values of $\log_{10} R$ are plotted against the corresponding wave-number separations $\Delta\sigma$ of the upper levels, the points[16] fall along a straight line (Fig. 1) which demonstrates

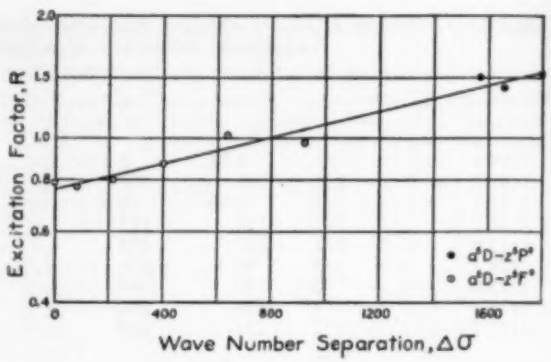

FIG. 1. Excitation curve for the sextet supermultiplet.

TABLE III. *Excitation corrections in the sextet supermultiplet.* $I_{obs.}$, observed intensities after applying corrections for background, self-reversal, ν^4, and variation in sensitivity. R, excitation factor. I_e, observed intensities corrected for excitation.

Wavelength	Transition	$I_{obs.}$	R	I_e	$I_{theor.}$
Multiplet	$a^6D-z^6F^0$				
2878.5	9/2– 7/2	32.1	0.872	28.0	12.5
2878.0	7/2– 5/2	82.9	.816	67.6	29.2
2876.3	5/2– 3/2	136	.778	106	41.1
2873.5	3/2– 1/2	95.5	.757	72.3	38.2
2867.6	1/2– 1/2	382	.757	248	303
2866.8	3/2– 3/2	471	.778	366	367
2865.1	5/2– 5/2	610	.816	498	542
2862.6	7/2– 7/2	582	.872	507	507
2860.9	1/2– 3/2	269	.778	209	177
2858.9	9/2– 9/2	417	.947	395	331
2855.7	3/2– 5/2	555	.816	453	450
2849.8	5/2– 7/2	924	.872	805	850
2843.2	7/2– 9/2	1240	.947	1170	1380
2835.6	9/2–11/2	2050	1.05	2150	2050
			Sum	7075	
Multiplet	$a^6D-z^6P^0$				
2766.5	9/2– 7/2	694	1.43	993	1040
2762.6	7/2– 5/2	402	1.37	551	536
2757.7	5/2– 3/2	164	1.32	217	194
2751.9	7/2– 7/2	208	1.43	298	298
2750.7	5/2– 5/2	256	1.37	351	379
2749.0	3/2– 3/2	199	1.32	263	295
2743.6	1/2– 3/2	122	1.32	161	208
2742.0	3/2– 5/2	100	1.37	137	124
2740.1	5/2– 7/2	33.0	1.43	47.2	49.6
			Sum	3018	

[15] G. R. Harrison, J. O. S. A. **19**, 109 (1929).

[16] Seven of the thirteen lines of multiplet $a^6D-z^6D^0$ are missing, and the remaining meager data are not used in the calculation of the arc temperature.

the existence of an excitation function. The slope of this line determines the calculated temperature of the chromium arc, which was 4060°K, with a current of 2.4 amperes and a pressure of 7 to 15 cm of mercury.

By multiplying the intensities by the proper values of the excitation factor R, as determined from the excitation curve, we obtain the intensities that would have been observed if the temperature of the arc had been infinite. This excitation correction is applied only to this supermultiplet; and the results are reported in Table III. Since this correction applies only to multiplets having the lowest term a^6D, it cannot be applied to the data on other multiplets here reported.

Grateful acknowledgment is made by one of us (J. S. V. A.) to the Ohio State University and the Charles A. Coffin Foundation for fellowships which made this research possible.

JUNE 15, 1935 PHYSICAL REVIEW VOLUME 47

Note on the Relative Transition Probabilities for Almost Closed Shells

C. W. UFFORD, *Allegheny College*

(Received February 27, 1935)

Three simplifications are given for calculating the relative transition probabilities of different multiplets from spectroscopic stability. They apply to configurations involving almost closed shells in Russell-Saunders coupling.

THE calculation of the relative transition probabilities of different multiplets in Russell-Saunders coupling from spectroscopic stability[1] can be simplified for electron configurations involving almost closed shells, so that transition probabilities for these configurations may be calculated as easily as those for the configurations containing the electrons missing from the almost closed shells. This simplification for transition probabilities is of the same type as that given by Shortley[2] for the energies. The simplifications apply to calculating the matrix elements of the electric moment in the zero order scheme. The first simplification is to represent the almost closed shells present in the zero order state by the quantum numbers of the electrons missing from these shells. This means that the representations for the states containing almost closed shells are obtained simply by changing the signs of m_l and m_s in the states of the electrons required to complete the shells.

In the second place, it is necessary to write the zero order states of but one of the two electron configurations[3] between which a single electron jumps. For simplicity, one chooses from the LSM_LM_S scheme the configuration with the fewer terms. It is possible to simplify the calculation further by writing only one zero order state for each set of values of m_l. The group of states with this set of values of m_l, obtained for different sets of values of m_s, will give multiples, constant throughout the matrix, of the matrix elements of a single state of the group. Once these numbers are found by inspection of a single group of states with a given set of values of m_l, they may be used as factors for each subsequent set of m_l values, having the same number of sets of m_s values associated with it. These simplifications enable one to alter the states already used previously for partially filled shells, so that the relative transition probabilities for the multiplets of the corresponding almost closed shells may be calculated from them.

[1] E. U. Condon and C. W. Ufford, Phys. Rev. **44**, 740 (1933); C. W. Ufford and F. M. Miller, Phys. Rev. **46**, 283 (1934).

[2] G. H. Shortley, Phys. Rev. **40**, 185 (1932).

[3] L. Goldberg found that this was sufficient for the case where a closed shell was represented by all its electrons. It is also sufficient for the representation considered here.

The Band Spectra of the Hydrides of Lithium

F. H. CRAWFORD AND T. JORGENSEN, JR., *Physics Research Laboratory, Harvard University*

(Received April 5, 1935)

About 1000 lines, comprising 26 bands, of Li^7H have been remeasured and given quantum assignments. The experimental arrangements are similar to those given in Part I on Li^7D. The corresponding $\Delta_2F_v(J)$ values have been represented as polynomials of the usual form in $J(J+1)$, where the ground state data are represented to within ± 0.018 and the upper state data to within ± 0.021 cm^{-1} (i.e., to within roughly ± 0.0024A for the whole spectrum). **Constants.** Important constants for the ground state are $B_e''=7.5131$, $D_e''=-8.617\times10^{-4}$, $H_e''=11.4\times10^{-8}$, $\omega_e''=1405.65$, $x_e''\omega_e''=+23.20$ and $y_e''\omega_e''=+0.1633$; corresponding constants for the upper state although less certain because of the errors of extrapolation (which are greater than for LiD) are in order 2.8186, 15.8×10^{-4}, $100(\pm30)\times10^{-8}$, 234.41, -28.95 and -4.185. The constants for the ground state show a small discrepancy between ρ and ω_e^i/ω_e, and ρ^2 and B_e^i/B_e. In fact from these two ratios we find $\Delta\rho=+0.000143$ (±0.00003) and $\Delta\rho=+0.00020$ (±0.00006), where the plus sign indicates the fact that the observed ρ's are these amounts *greater* than the atomic mass ρ values. Consideration of Dunham's higher order calculation of the interaction of vibration and rotation accounts for about 1/3 of the discrepancy in the ρ from the ratio of the B_e's. The vibrational numbering adopted here agrees with Nakamura's and is such that the maxima in the B_v' and $\Delta G'(v+1)$ curves occur at energies which are approximately the same for the LiH and the LiD molecule. We find *no evidence* of l-uncoupling and feel that the anomaly of the upper state is to be ascribed to an anomalous potential curve. The *electronic origin isotope shift* of this $(^1\Sigma\rightarrow{}^1\Sigma)$ system of LiH is $0.0(\pm0.5)$ cm^{-1}.

INTRODUCTION

IN a previous paper of the same title as the present (Part I[1]) the authors have presented the results of observations on the absorption spectrum of Li^7D. The corresponding spectrum of Li^7H having been reexamined in similar detail, the numerical results and intercomparisons will form the subject matter of the present paper. A more detailed examination of the potential curves of the two molecules is reserved for Part III.

The *absorption* photographs were made with the same apparatus as previously employed and under similar conditions, where, however, because of the more open nature of both the vibrational and rotational structure of the Li^7H bands a somewhat greater range of temperatures was employed. The higher temperatures and the lighter mass of the molecule both rendered the lines somewhat broader and therefore increased the difficulty of precise measurement. This was in part compensated for by measuring each lower state progression of bands on plates taken at temperatures just adequate for developing the lines in question. In any event the maximum J, v' and v'' values observed for Li^7H were in order, 18, 14 and 3 as against 25, 18 and 4 for Li^7D. The smaller number of rotational lines observable in a branch of course renders the higher coefficients in the rotational energy expression more uncertain in the present than the former case. On the other hand it was possible to obtain several well developed bands involving the $v'=1$ state and one rather faint band involving the $v'=0$ state. Furthermore, since the upper $^1\Sigma$ state involves a larger molecular radius than the lower $^1\Sigma$ state it is apparent that $(0,v'')$ bands should be more strongly developed in *emission* than absorption. Accordingly several emission photographs were made with a metallic lithium arc burning in hydrogen. These were quite difficult to obtain because of the general faintness and the frequent delays for replenishing the evaporated lithium. One 24-hour and one 6-hour exposure, however, gave the (0,5) and (0,6) bands with satisfactory intensity. Comparison of measurements on the two plates showed unfortunately a shift of about 0.10 cm^{-1}. Since this shift was quite small and fairly uniform

[1] Crawford and Jorgensen, Phys. Rev. **47**, 358 (1935). In this connection the following corrections should be made in Part I (as the result of subsequent remeasurement). In Table IV for $v''=3$, $H_v''\times10^{+8}$ should be 1.6 instead of 1.85 and the average deviation ±0.20 instead of ±0.027. This then requires that Eq. (14) now read:

$$H_v''\times10^8=2.006-0.090(v''+\tfrac{1}{2})-0.005(v''+\tfrac{1}{2})^2(\pm0.01).$$

Also the horizontal scale readings for the insert in Fig. 3, except for the value $v''=-\frac{1}{2}$, should be *lowered* by unity.

TABLE I. *Vacuum frequencies of* $^1\Sigma - {}^1\Sigma$ *bands of* Li^7H.

J	(2–2) Band 22,000 cm^{-1} R(J)	P(J)	(4–2) Band 22,000 cm^{-1} R(J)	P(J)	(5–1) Band 24,000 cm^{-1} R(J)	P(J)	(6–1) Band 25,000 cm^{-1} R(J)	P(J)	(10–0) Band 27,000 cm^{-1} R(J)	P(J)	(11–0) Band 28,000 cm^{-1} R(J)	P(J)	(13–0) Band 28,000 cm^{-1} R(J)	P(J)
0	1868.26	—	2556.74	—	—	—	1612.99	—	2524.75	—	1915.76	—	2690.73	—
1	—	1848.52	554.43	—	2234.62	2217.31	610.12	—	521.02	2504.44*	911.86	1895.48	686.51	2670.60
2	855.33	826.38	543.83	2514.92	223.15	194.32	598.57	1569.85	508.02	480.35	898.61	871.34	672.66	646.27
3	836.56	796.12	525.16	484.66	—	162.83	578.52	538.28	485.70	447.07	876.00	837.94	649.35	612.48
4	809.61	757.81	498.28	446.36	174.56	122.71	549.69	498.20	454.18	404.60	844.06	795.26	616.54	569.25
5	774.47	711.46	465.21	400.03	137.37	074.35	512.25	449.62	413.41	352.98	802.85	743.30	574.26	516.69
6	—	657.07	420.38	345.70	091.69	2017.43	466.48	392.56	363.56	292.39	752.40	682.29	522.57	454.75
7	679.70	594.71	368.91	283.44*	2037.46	1952.17	412.05	327.16	304.43	222.72	692.77	612.20	461.50	384.07?
8	620.08	524.40	309.65	213.43*	1974.83	878.64	349.20	253.49	236.34	144.14	624.04	533.21	391.14	303.30
9	552.32	446.20	242.42	135.44	903.76?	796.97	277.93	171.59	159.24	2056.74	546.20	445.12	311.58	213.83
10	476.48	360.19	167.24	2049.80	824.43	707.12	198.41	1081.51	2073.27	1960.72	459.39	348.26	222.83	—
11	392.56	266.41	2084.19	1956.76	736.83	609.61	110.53*	0983.53	1978.52	855.93	363.56*	242.95	125.02	2008.21
12	300.67	164.93	1993.34	855.72	641.05	503.50	1014.59	877.39	876.39	742.87*	259.30	128.83	2018.36	1892.27
13		1055.80	894.74	747.42	537.22	389.86	0910.43	763.58	762.97	621.19	146.15	1006.38	1902.82	767.74
14	1093.05	0939.11	788.46	631.78	425.38	268.57	798.48	642.03	642.39	—	1024.52	0874.99?	778.56	634.71
15	0977.42	815.00	674.67	508.87	305.68	140.05	—	513.29	513.47	353.05	0894.44	—	645.75	493.27
16	854.04	683.40*	552.82	378.81	178.15	1003.26	551.00	376.33	376.34	207.59	756.02	—	504.44*	343.67
17	722.98	544.50	424.68	—	1042.90	0859.45	415.65		231.06	1053.84			354.81	186.02
18	584.34		288.71	1097.64	0900.22	708.48			1077.87	0892.44			197.03	1020.56
19			1145.59	0946.50*	750.03	550.42			0916.94	723.59			1031.23	0847.28
20			0995.44	789.33	592.54	385.41			747.87*				0858.90*	666.54
21			838.42	625.24	427.64*	213.43*							676.27	
22			674.59		256.26									

it was not thought that it could affect the accuracy of the $\Delta_2F(J)$ values appreciably. Accordingly the $\Delta_2F(J)$ values accepted for final computation of the rotational constants of the $v'=0$ state were averages of the absorption and emission results. The emission spectra being less sharp and involving much more superposition (both due to the higher temperatures involved), the emission data were not employed elsewhere.

All told the vacuum frequencies of about 1000 lines were determined including 13 bands of the $(v',0)$, 6 of the $(v',1)$, 5 of the $(v',2)$, 2 of the $(v',3)$ progressions and one faint band each of the $(v',5)$ and $(v',6)$ progressions. In general the results agree with those of Nakamura[2] made at a much lower dispersion, but individual assignments of lines differ considerably and vacuum frequencies often by several cm^{-1}. In some cases indeed we have been forced to conclude that certain of Nakamura's bands (notably the (0,2) band) were merely accidental sequences of lines, many being unresolved superpositions, which on our plates are resolved and obviously members of entirely different bands. The result of course is to involve considerable differences in the molecular constants and computed origins (see Table VIII. Also compare column 2 of Table XI with Tables VII and VIII of Part I). In general, however, the differences are only such as the higher dispersion and the constant use of densitometer results would cause. Actually the densitometer records made on plates taken at a series of temperatures were, as in the case of LiD, of the very greatest aid in the analysis of the plates, enabling correct rotational assignments in a majority of cases to be made *de novo* from the records before any actual vacuum frequencies had been determined.

In Table I are recorded vacuum frequencies of some of the stronger bands of Li^7H (corresponding to the data in Table I, Part I for Li^7D), where as before the number at the head

TABLE II. *Values of* $\Delta_2F_0''(J)$.

J	(10,0) Band	(13,0) Band	Average of all (v',0) Bands	Ave. Obs.
1	44.40	44.46	44.43	−0.022
2	73.93	—	73.94	+ .005
3	103.42	103.41	103.39	− .008
4	132.72	132.66	132.66	− .014
5	161.78	161.79	161.78	+ .004
6	190.69	—	190.68	− .004
7	—	219.27	219.27	+ .039
8	247.69	247.67	247.65	− .009
9	275.62	—	275.64	+ .005
10	303.31	303.37	303.28	± .000
11	—	330.56	330.56	− .043
12	357.30	357.28	357.34	− .014
13	—	383.65	383.67	+ .001
14	—	409.55	409.54	− .010
15	434.80	434.89	434.86	+ .011
16	459.63	459.73	459.69	− .005
17	483.90	—	483.91	+ .029
				Ave. ±0.013

[2] Nakamura, Zeits. f. Physik **59**, 218 (1930).

of each pair of columns is to be *added* to the figures below to give the vacuum frequencies of the desired branch lines. This includes about one-fourth of the measured lines.

Rotational Constants

As in Part I the corresponding $\Delta_2F_v(J)$ values were computed and expressed as

$$\Delta_2F_v(J)=[B_v-3/2D_v+\cdots]4(J+\tfrac{1}{2})$$
$$-[2D_v-17/2H_v]4(J+\tfrac{1}{2})^3+12H_v(J+\tfrac{1}{2})^5+\cdots \quad (1)$$

or more simply

$$\frac{\Delta_2F_v(J)}{4(J+\frac{1}{2})}=a_v^0-a_v^1(J+\tfrac{1}{2})^2+a_v^2(J+\tfrac{1}{2})^4, \quad (2)$$

where the intercept of the curve of experimental $\Delta_2F/4(J+\frac{1}{2})$ values against $(J+\frac{1}{2})^2$ with the $(J+\frac{1}{2})^2=0$ axis gave a_v^0. Here, however, because of the larger numerical values obtained for LiH it was not feasible to determine a_v^1 and a_v^2 from the same graph. Actually it was just as rapid and rather easier to plot a second curve with

$$[\Delta_2F_v(J)/4(J+\tfrac{1}{2})-a_v^0]/(J+\tfrac{1}{2})^2$$

as ordinates and $(J+\frac{1}{2})^2$ as abscissae. The intercept of this second curve at $(J+\frac{1}{2})^2=0$ then of course gave a_v^1 and its slope a_v^2. When the coefficient a_v^2 was large it was then often desirable to replot

$$[\Delta_2F_v(J)-4a_v^2(J+\tfrac{1}{2})^5]/4(J+\tfrac{1}{2})$$

and obtain a more trustworthy value of a_v^0 and hence better a_v^1 and a_v^2 values by the second step. From these constants "theoretical" Δ_2F_v values were computed and the differences between these and the observed Δ_2F_v values determined. Occasionally where small systematic deviations seemed to be present a better representation was then obtained by slight empirical adjustments of the constants. This at times indicated that too much graphical "weight" had been given to values of $\Delta_2F(J)$ (for low J values usually) which were computed from very faint and uncertain lines. In any case the amount of adjustment possible without perceptible alteration of the accuracy of representation of the data, gave a rough indication of the reliability of the constants themselves. Here again as an illustration of the accuracy of the representations two typical sets of measured Δ_2F values are given in Tables II and III with deviations from the computed values in the last column. The values of B_v, D_v and H_v for the ground $^1\Sigma$ state and the upper $^1\Sigma$ state of Li^7H are given in Tables IV and V. Here the average deviations of observed and calculated Δ_2F values are recorded in the last column of each table. The average deviations are for the ground state ±0.018 cm^{-1}

Table III. *Values of* $\Delta_2F_3'(J)$.

J	Obs. $\Delta_2F_3'(J)$	Obs. −Calc.
1	(16.95)	+0.036
2	28.26	+ .015
3	39.52	− .003
4	50.71	− .025
5	61.80	+ .018
6	72.75	− .008
7	83.57	+ .007
8	—	—
9	104.80	+ .018
10	115.20	− .030
11	125.36	− .033
12	135.28	− .014
13	145.03	− .003
14	—	—
15	—	—
16	172.50	+ .030
		Ave. ±0.019

Table IV. *Rotational constants for lower* $^1\Sigma$ *state of* Li^7H.

v''	B_v''	$-D_v''\times10^4$	$H_v''\times10^8$	(Ave. Δ_2F_v'' calc. $-\Delta_2F_v''$ obs.)
$(-\frac{1}{2})$	(7.5131)	(8.617)	(11.4)	
0	7.4067	8.537	11.08	±0.012
1	7.1950	8.377	10.25	± .015
2	6.9848	8.216	9.17	± .014
3	6.7782	7.95	7.8	± .029
			Ave.	±0.018

Table V.

v'	B_v'	$-D_v'\times10^4$	$H_v'\times10^8$	Ave. Δ_2F' calc. $-\Delta_2F'$ obs.
$(-\frac{1}{2})$	(2.8186)	(15.8)*	(100±30)	
0	2.8536	11.87	93.	±0.019
1	2.8897	7.837	23.6	.012
2	2.9044	6.295	10.9	.017
3	2.9083	5.477	7.47	.012
4	2.9057	5.039	6.23	.017
5	2.8959	4.73	5.42	.020
6	2.8804	4.51_3	5.05	.026
7	2.8589	4.30_8	4.04	.015
8	2.8333	4.19	4.08	.019
9	2.8022	4.05	3.4	.032
10	2.7707	4.10	4.87	.027
11	2.7322	4.07	5.2	.022
12	2.6895	4.07	6.3	.016
13	2.6442	4.17	7.2	.031
14	2.5942	4.12	6.67	.023
				Ave. ±0.021

* or 16.3×10^{-4} (see text).

and for the excited state ± 0.021 cm^{-1}, indicating an uncertainty substantially that of the data in Part I.

The rotational constants of Table IV are represented by the following expressions (where $u=v+\frac{1}{2}$):

$$B_v''=7.5131-0.2132u+0.00075u^2, \quad (3)$$

$$-10^4\times D_v''=+8.617-0.1590u-0.0005u^2, \quad (4)$$

$$10^8\times H_v''=11.40-0.58u-0.125u^2. \quad (5)$$

The uncertainties in the values of B_v'', D_v'' and H_v'' are estimated as roughly ± 0.0003, $\pm 0.01\times 10^{-4}$ and $\pm 0.1\times 10^{-8}$, respectively.

To test Kratzer's relation,

$$-D_e=4(B_e)^3/\omega_e^2 \quad (6)$$

values of $4B_v^3/\omega_v^2$ were plotted against v and extrapolated to $v=-\frac{1}{2}$, and a similar procedure was used for testing Birge's approximate relation,[3]

$$H_e=(D_e/B_e)(2-\alpha\omega_e/6B_e^2). \quad (7)$$

The results are given in Table VI (where similar results for Li^{7}D are included). In Table VI are also included computed values of α_1 (the coefficient of u in Eq. (3)), from Kratzer's approximate relation[4]

$$\alpha_1=2B_ex_e \quad (8)$$

as well as from a more recent expression given by Pekeris,[5]

$$\alpha_1=2x_eB_e[3(B_e/x_e\omega_e)^{\frac{1}{2}}-3(B_e/x_e\omega_e)] \quad (9)$$

and in addition values of β_1 (the coefficient of u in Eq. (4)) from the approximate relation given by Birge.[3]

TABLE VI. *Theoretical relations among ground state constants of Li^{7}H and Li^{7}D.*

Theor. Eq.	Const.	Li^{7}H Obs.	Li^{7}H Comp.	Li^{7}D Obs.	Li^{7}D Comp.
(6)	$-D_e''\times 10^4$	8.617	8.586	2.756	2.728
(7)	$H_e''\times 10^8$	11.4	11.0	2.07	1.97
(8)	$-\alpha_1$	0.2132	0.2478	0.09198	0.1062
(9)	$-\alpha_1$	0.2132	0.1823	0.09198	0.0782
(10)	$\beta_1\times 10^4$	0.159	0.139	0.066	0.034

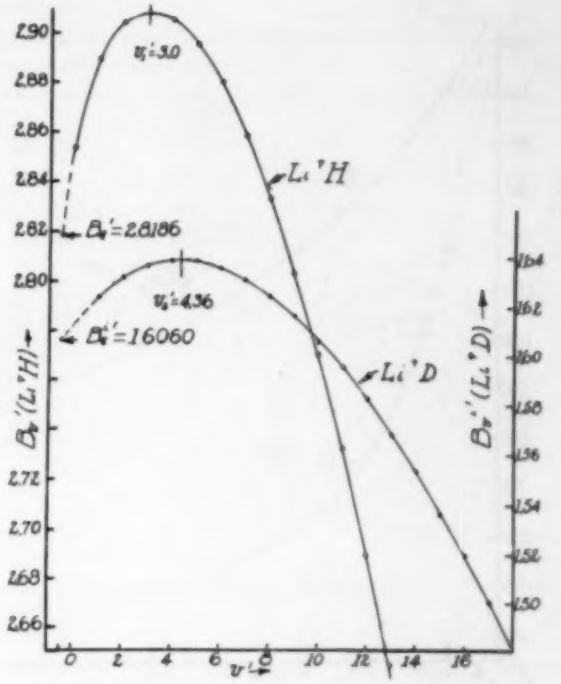

FIG. 1. Curves of B_v'' for Li^{7}H and Li^{7}D. The extraordinarily rapid rise and fall of the first curve is particularly noteworthy. The maxima of the two curves occur at approximately the same energy as we should expect if the anomalous B_v behavior is to be ascribed entirely to peculiarities in the potential energy curve. Here $(v_1'+\frac{1}{2})\approx\rho(v_2'+\frac{1}{2})$.

$$\beta_1=D_e[\omega_e\alpha_1^2/24B_e^3+5\alpha_1/B_e-8x_e]. \quad (10)$$

It is to be noted that Eq. (6) is satisfied to within almost the experimental uncertainty and that the agreement of results with Eqs. (7) and (10) is probably as good as the approximations underlying their theoretical deduction and the experimental uncertainty would warrant. On the other hand Eq. (8) gives values as much above the observed ones as Eq. (9) does below. This fact will be considered later.

The rotational constants of the upper $^1\Sigma$ state of Li^{7}H vary even more radically with vibration than do those of Li^{7}D, in fact so rapid is the change for low values of u that least-squares expressions computed for the observed range of vibration are of very little theoretical value. In order, however, to obtain approximate values for B_e', D_e' it was necessary to obtain such expressions for a small range of v' values near the origin. Actually the constant terms so determined depend rather strongly on the precise

[3] Bull. Nat. Res. Counc. (Ed. by E. C. Kemble, 1926), p. 237; Birge, Nature **116**, 783 (1925).
[4] Kratzer, Zeits. f. Physik **3**, 289 (1920).
[5] Pekeris, Phys. Rev. **45**, 98 (1934).

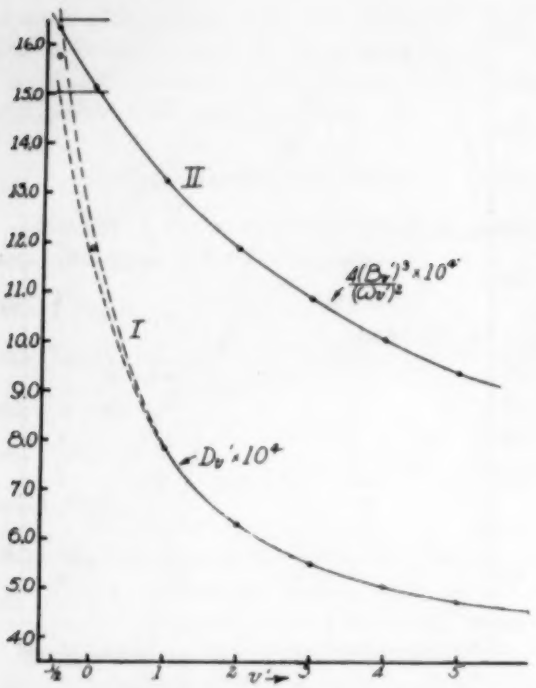

FIG. 2. Test of Kratzer's Eq. (6) for Li^7H. Here the dotted curves are drawn from least-squares curves computed from the first $7D_v'$ values with $D_0'=(11.87+0.3)\times10^{-4}$ and $(11.87-0.3)10^{-4}$, respectively. Since the extrapolation is so uncertain we can only infer that Kratzer's relation is approximately true.

number of observations used and are in consequence much more in doubt than the general precision of the data would suggest.

The expression for B_v' for LiH (with the first 6 values) is

$$B_v'(\text{LiH})=2.8186+0.078305u$$
$$-0.026271u^2+0.0041648u^3-0.000275u^4 \quad (11)$$

where the uncertainty in B_e' may be as high as ±0.005. (See Fig. 1 where B_v' for LiH and LiD are shown for comparison.)

The same difficulty arises in a more aggravated way in attempting to test Kratzer's Eq. (6). We have, however, proceeded as in the case of Li^7D, estimating the uncertainty of D_1' as $\pm0.5\times10^{-4}$ and drawing the dotted extrapolations in Fig. 2 curve I of the experimental results (with the first 7 points only). It is seen that at $v=-\frac{1}{2}$ curve II falls well within the dotted branches of I. Despite the irreducible uncertainty involved in such a process we feel justified in assuming that there is no experimental evidence of the failure of Eq. (6) and hence of the presence of l-uncoupling. We may therefore presume to take as the most likely value of D_e', the intercept of curve II, giving $D_e'=16.3\times10^{-4}(\pm0.1)$.[6]

The values of H_v' (for LiH) exhibit an even more marked variation with v' than do those of D_v', and because of the much greater uncertainty of H_1' (say $\pm20\times10^{-8}$) least-squares curves are meaningless. Here the actual numerical intercepts at $v'=-\frac{1}{2}$ (for LiD) of Eq. (7) with subscript v replacing e certainly agree to within the error of the extrapolation with the extrapolation of the H_v' values and fall within the same range for LiH. This may be taken as further evidence of the mechanical significance of H_e' and hence of the absence of l-uncoupling.

VIBRATIONAL CONSTANTS

From the rotational constants the band origins were computed as before and the frequencies given in the usual square array. These origins are given in Table VII (and for comparison in Table VIII the differences between origins as observed by us and as reported by Nakamura) where the *vertical* and *horizontal* differences are in italics and are, respectively, $\Delta G''(v+\frac{1}{2})$ and $\Delta G'(v+\frac{1}{2})$. The former are given precisely by

$$\Delta G''(v+\tfrac{1}{2})=1405.649-2\times23.200(u+\tfrac{1}{2})$$
$$+3\times0.1633(u^2-u+\tfrac{1}{3}), \quad (12)$$

where

$$\Delta G=\omega_e-2x_e\omega_e(u+\tfrac{1}{2})+3y_e\omega_e(u^2-u+\tfrac{1}{3}). \quad (13)$$

The values of $\Delta G'(v+\frac{1}{2})$ in contrast, increase very rapidly with v', attain a maximum at about $v'=10$ and thereafter decrease. Fig. 3 shows the curves for LiH and LiD, where maxima occur at approximately the same energy values. The fact that this curve rises so rapidly at the start (especially for LiH) makes the meaning of the constants of a polynomial representation in u even less significant than in the case of B_v curves. If we use the least-squares method for expressing the results in the form

$$\Delta G'(v+\tfrac{1}{2})=\omega_e-2x_1(u+\tfrac{1}{2})$$
$$+3x_2(u^2-u+\tfrac{1}{3})+\cdots \quad (14)$$

[6] The same procedure in Part I gives $D_e'(\text{LiD})=5.0\times10^{-4}(\pm0.1)$ as against the rougher value $4.8\times10^{-4}(\pm0.3)$ given there.

TABLE VII.

v'	V''' 0		1		2		3
	ORIGINS OF $^1\Sigma \rightarrow {}^1\Sigma$ BANDS OF Li^7H						
0					23268.52		
					280.96		
1			24864.32	*1314.84*	23549.48		
			312.97		*318.96*		
2	26537.02	*1359.73*	25177.29	*1314.86*	23862.44	*1270.89*	22591.55
	335.76		*335.73*		*335.71*		*335.69*
3	26872.78	*1359.76*	25513.02	*1314.87*	24198.15	*1270.91*	22927.24
	352.80		*352.78*		*352.80*		
4	27225.58	*1359.78*	25865.80	*1314.85*	24550.95		
	365.83		*365.87*				
5	27591.41	*1359.74*	26231.67				
	375.84		*375.56*				
6	27967.05	*1359.82*	26607.23				
	382.68						
7	28349.73						
	387.55						
8	28737.28						
	390.37						
9	29127.65						
	391.59						
10	29519.24						
	391.05						
11	29910.29						
	389.19						
12	30299.48						
	385.94						
13	30685.42						
	381.32						
14	31066.74						

then the values of ω_e, x_1, x_2, etc., depend unfortunately very largely on how much data are used (and on the number of the terms in the expansion—which from practical consideration of labor is limited to the term in x_3). Below (Table IX) are given the results for LiH and LiD when the values of $\Delta G'$ for the first 5 and 7 available values are used[7] (and in the latter case when all the data are used). The differences indicate clearly to what extent the molecular constants for the upper state must remain in doubt—at least until some theoretical expression better suited to this state than a power series, is available. We have, therefore, provisionally taken the constants based on the first $7\Delta G'$ values as the most probable ones. On this basis the system origin for LiH is 26,516.24 cm^{-1} and for LiD 26,513.70 where, however, the values themselves are uncertain to several cm^{-1} and hence even the *sign* of the difference is in doubt. [It should be emphasized at this point that this

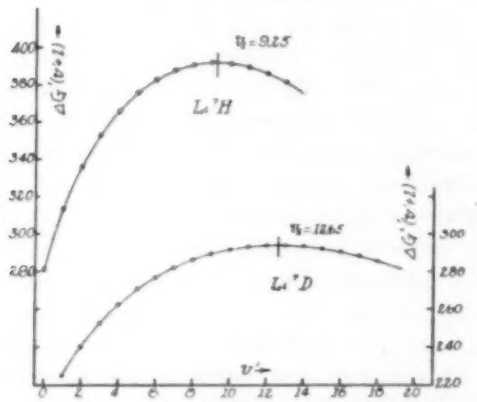

FIG. 3. $\Delta G'(v'+1) = G'(v+3/2) - G'(v+\frac{1}{2})$ for Li^7H and Li^7D. The large slope of the first curve near the origin renders the actual value of the upper state vibrational constants considerably in doubt. As in the case of the B_v' curves, the maxima occur at almost exactly the same energy values, i.e., $G'(v+\frac{1}{2}) = G''[\rho(v+\frac{1}{2})]$ and approximately $\Delta G'(v+1) = (1/\rho)\Delta G''[\rho(v+1)]$. Hence we expect to find $(v_1+1) = \rho(v_2+1)$ and actually v_2 calculated is 12.7 compared with 12.65 from the curve. (The maximum is obtained in each case quite precisely by plotting the first-difference curve.)

TABLE VIII. *Comparison of band origin as measured by us (C and J) and as measured by Nakamura (N).*

BAND	$(C+J)-N$ cm^{-1}	BAND	$(C+J)-N$ cm^{-1}	BAND	$(C+J)-N$ cm^{-1}	BAND	$(C+J)-N$ cm^{-1}
(2–0)	−1.29	(1–1)	+0.02	(8–0)	−1.52	(0–2)*	+5.92
(3–0)	−2.02	(2–1)	−0.51	(9–0)	−0.15	(1–2)	+0.18
(4–0)	−0.22	(3–1)	−0.28	(10–0)	—	(2–2)	+0.18
(5–0)	−0.79	(4–1)	+1.00	(11–0)	+1.09	(3–2)	+0.35
(6–0)	−0.15	(5–1)	−1.13	(12–0)	+0.38	(4–2)	+1.05
(7–0)	−1.27	(6–1)	—	(13–0)	+0.32		
				(14–0)	+1.74		

* Reported as uncertain by Nakamura.

[7] Fifth power least-squares calculations, in an attempt to represent the LiH data from $v'=0$ to $v'=14$, gave values differing in a regular oscillatory fashion from the observations—as they did when the same process was carried out for the *first differences* of the $\Delta G'$ values.

TABLE IX. *Vibrational constants for LiH and LiD (upper state).*

ΔG VALUES USED		ω_e	x_1	x_2	x_3	x_4	x_5
LiH	5	235.16	−28.0093	−3.64188	+0.347292	−0.01592	—
	7	234.413	−28.9474	−4.18486	+0.506467	−0.038833	+0.0012847
LiD	5	182.776	−12.6764	−0.782500	+0.20417	− .00033333	—
	7	180.711	−13.9871	−1.17839	+ .079316	− .0035303	+ .00006940
	16	183.1246	−12.74161	−0.8778501	+ .04261680	-1.332244×10^{-3}	$+1.808235\times10^{-5}$

The constants in the *second* and *fourth* row are taken as being the most likely values.

effect is not assignable to experimental uncertainties since curves of the 1st, 2nd, 3rd and 4th differences of the observed $\Delta G'$ values are quite smooth and regular. In addition the bands involving $\Delta G'(1)$ as well as those involving $\Delta G'(12)$, $\Delta G'(13)$ and $\Delta G'(14)$ were remeasured on new plates with results coincident to ± 0.02 cm^{-1} with those obtained earlier.]

ISOTOPE EFFECT IN THE GROUND STATE

As Kemble and Van Vleck have shown,[8] as long as the potential curves of a molecule (LiH) and its isotope (LiD) can be regarded as identical, the general molecular constants in the complete energy expression in frequency units written as

$$E/hc=\sum_{l=0,\,1}\ \sum_{j=0,\,1\cdots} Y_{lj}(v+\tfrac{1}{2})^l[J(J+1)]^j \quad (15)$$

can be related for the two molecules, in the simple form:

$$Y_{lj}^i/Y_{lj}=(\mu/\mu^i)^{(l+2j)/2}=\rho^{(l+2j)}, \quad (16)$$

where μ and μ^i are the respective reduced masses of the normal molecule and the isotope and $\rho=(\mu/\mu^i)^{\frac{1}{2}}$ and where further l and j are simply the powers of $(v+\frac{1}{2})$ and $J(J+1)$ in the particular term of Eq. (15) which is under consideration.[9] Thus Y_{10} corresponds to ω_e, Y_{01} to B_e, Y_{20} to $x_e\omega_e$, Y_{02} to α_1, etc. Hence Eq. (16) expresses simply the powers of ρ required for, in our case, converting the constants of LiH to those of LiD. We shall say that any case for which Eq. (16) holds is covered by the "simple isotope theory."

On this basis Table X was constructed where column 1 gives the constant involved, column 2 the power of ρ and column 3 its numerical value, column 4 the observed constant for Li^7H, column 5 this multiplied by the number in the preceding column (3) and column 6 the observed constant for Li^7D. Finally column 7 gives the amount by which the theoretical value of ρ would have to be *increased* to cause coincidence of the numbers in columns 5 and 6. Since this quantity, say $\Delta\rho$, is small, it can only be ascertained with precision actually from the ω_e's and the B_e's. It is, however, to be noted that in all save three cases (H_e'', β_2'' and γ_2'', β_2'') the numbers in column 5 are *too small*. In the three exceptions the differences are well within the experimental error.

This failure in the simple isotope theory has been noted by a number of observers,[10–13] where the corresponding values (for the ground states) of $\Delta\rho$ as obtained from B_e^i/B_e are: For AlH ($^1\Sigma$) $\Delta\rho=+0.00034$, for CaH ($^2\Sigma$) $\Delta\rho=0.00061$, for NaH ($^1\Sigma$) $\Delta\rho=+0.00023$ and for BeH ($^2\Sigma$) $\Delta\rho=+0.00025$. The corresponding values from the ratio ω_e^i/ω_e are only available for AlH and NaH and are, respectively, +0.00041 and +0.00013. The values of $+0.00020\pm0.00006$ and $+0.00014\pm0.00003$ from the B_e and ω_e ratios, respectively, for LiH are thus of the same general order of magnitude.

Now in the first place it was thought that part of the discrepancy might be due to the use of an inaccurate value of the atomic mass of H, since according to a recent announcement of Oliphant and Kempton[14] this value should be raised from 1.0778 to 1.00810. This would cause the ρ computed from $(\mu/\mu^i)^{\frac{1}{2}}$ to increase by +0.00013 provided the accepted value of $D=2.01363$ were retained. Actually, however, this

[8] E. C. Kemble and J. H. Van Vleck, Phys. Rev. **21**, 653 (1923).

[9] See Dunham, Phys. Rev. **41**, 721 (1932) for more details of this compact and useful notation.

[10] Hulthén and Holst, Zeits. f. Physik **90**, 712 (1934); (AlH).

[11] Watson, Phys. Rev. **46**, 319, 939 (1934); (CaH).

[12] E. Olsson, Zeits. f. Physik **93**, 206 (1934); (NaH).

[13] Koontz, Bull. Am. Phys. Soc. **10**, 14 (1935); (BeH).

[14] Oliphant and Kempton, Proc. Roy. Soc. (current issue) reported in Science **81**, No. 2099, Supplement p. 6.

TABLE X. *Molecular constants of ground state.*

MOLECULAR CONSTANT	CONVERSION FACTOR ρ^n	NUMERICAL VALUE	LiH Obs.	LiH $\times\rho^n$	LiD Obs.	$\Delta\rho$
ω_e''	ρ	0.750486	1405.649	1054.919	1055.12	0.00014 ±.00003
x_1''	ρ^2	.563227	+23.20	13.067	13.23	
x_2''	ρ^3	.422694	+0.16333	0.0690	0.13	
B_e''	ρ^2	.563227	7.5131	4.2316	4.23384	.00020 ±.00006
α_1''	ρ^3	.422694	−.2132	−.09012	−.09198	
α_2''	ρ^4	.317225	+.00075	.00024	.00067	
$D_e''\times10^4$	ρ^4	.317225	−8.617	−2.7335	−2.756	
$\beta_1''\times10^4$	ρ^5	.238073	+0.159	+.03785	.066	
$\beta_2''\times10^4$	ρ^6	.178670	+.0005	+.000089	−.006	
$H_e''\times10^8$	ρ^6	.178670	+11.4	+2.037	2.006	
$\gamma_1''\times10^8$	ρ^7	.134089	−.58	−.078	−.090	
$\gamma_2''\times10^8$	ρ^8	.100632	−.125	−.0126	−.005	

change produces no effect on the ratio H : D since the masses of H and D were both measured by comparison with He and hence raising H to 1.00810 raises D to 2.01423.[15] Thus the change introduced in ρ is a second order quantity. Quite recently and independently Bethe[16] has proposed a revision of the ratio of He^4 to O^{16}. He therefore determines a new set of atomic masses which includes H = 1.00807, D = 2.01423 and $Li^7 = 7.01694$. These values actually influence our ρ slightly since Li^7 was referred to O^{16}.[15] These new values give $\rho = 0.750481$ as against 0.750486, a difference which is almost inappreciable in this connection. We therefore conclude that the discrepancies in ρ of +0.00020 and +0.00014 are real. It should further be emphasized that although these values of the discrepancy, $\rho^* - \rho$, differ by no more than the experimental error involved (in the former, which is the less accurate of the two) they are not necessarily measures of the same thing.

In general for the simple isotope theory to hold (and hence for Eq. (16) to be rigorously valid) it is necessary that three classes of effects (which to a first order may be treated independently) shall be negligible. These are

(1) The perturbation of one electronic level by another, as in ordinary *l*-uncoupling, etc.[17]

(2) The interactions between nuclear and electronic motions (which are neglected when an average potential function of the usual Kratzer form is used).[18]

(3) The higher order terms in the interaction of rotation and vibration (which are neglected when the usual approximate form of Eq. (15) is derived).[9]

[15] K. T. Bainbridge, Phys. Rev. **42**, 1 (1932); **43**, 103 (1933); **44**, 56 (1933).

[16] H. Bethe on *The Masses of Light Atoms from Disintegration*, which was made available to us in manuscript form as a letter to this Journal, through the kindness of Professor Bainbridge.

In the case of the ground state of most molecules the first effect will probably be insignificant. We may, therefore, attribute the failure of Eq. (16) to the presence of small modifications in the energy expression, Eq. (15), arising from interactions of the second and third types. Now consideration of these effects has the result of modifying the simple classical interpretation of all of the empirically determined molecular constants. The experimentally determined "ω_e," which we may write ω_e^* ($\equiv Y_{10}$), is not accurately the frequency of vibration for infinitesimal vibrations around the equilibrium position nor is the empirical "B_e," which we may similarly write B_e^* ($\equiv Y_{01}$), $h/8\pi^2\mu r_e^2 c$. We must rather write

$$\omega_e^* = \omega_e(1 + b_1 + b_2 + \cdots) \tag{17}$$

and

$$B_e^* = B_e(1 + c_1 + c_2 + \cdots), \tag{18}$$

where b_1, c_1, etc., are small terms of very complicated form (as yet not definitely evaluated). They depend, among other things, on ω_e and B_e, m/M, the ratio of electronic to protonic mass, and on the coefficients of the various powers in a Kratzer potential function of the form

$$\mu(\zeta) = (\omega_e^2/4B_e)\cdot\zeta^2[1 + a_1\zeta + a_2\zeta^2 + a_3\zeta^3 + a_4\zeta^4 + \cdots], \tag{19}$$

where $\zeta = (r - r_e)/r_e$, where μ is in frequency units and ω_e and B_e have their classical meanings.

Kronig[18] has given a qualitative account of the dependence of b_1 and c_1 on the second interaction mentioned above, while Dunham[9] has deter-

[17] R. de L. Kronig, Zeits. f. Physik **50**, 347 (1928); J. H. Van Vleck, Phys. Rev. **33**, 467 (1929).

[18] R. de L. Kronig, Physica **1**, 617 (1934).

mined approximately by the Wenzel-Brillouin-Kramer method their dependence on the third interaction, and incomplete papers which he left show that a detailed discussion of the second interaction was only interrupted by his untimely death.

Since both of the interactions considered here will usually be small we may consider them approximately additive and express ρ_{lj}^*, the empirically determined value of "rho" from band constants, as:

$$\rho_{lj}^* = (Y_{lj}^i / Y_{lj})^{1/(l+2j)} = \rho + \Delta_2\rho_{lj} + \Delta_3\rho_{lj}, \quad (20)$$

where the subscripts 2 and 3 refer to the theoretical interactions (2) and (3) and (lj) identifies the band constant involved.

Using the explicit equations which Dunham gives for the first 15 Y_{lj} coefficients in Eq. (15) and the data on Li^7H of Table X, we have evaluated approximately the first four a's of Eq. (19). The results are

$$a_1 = -1.86, \quad a_2 = +2.30, \quad a_3 \approx -4, \quad a_4 \approx 13,$$

from which we find for Li^7H $B_e^* = B_e(1-0.00035)$ and (assuming the same potential curve for each molecule) for Li^7D

$$B_e^{i*} = B_e^i(1-0.00020).$$

Hence

$$B_e^{i*}/B_e^* = (B_e^i/B_e)[1+0.000157]$$
$$= \rho^2[1+0.000157] \approx (\rho+\Delta_2\rho_{01})^2,$$

where $\Delta_2\rho_{01} = +0.00006$ a value which though uncertain is about a third of the value $\rho_{01}^* - \rho = +0.00020$ which was observed. Unfortunately for computing the effect on ω_e we need very reliable values of a_4 since a small change in its value is enough to alter even the *sign* of the correction term. This is a rather laborious process and the value of a_4 depends largely on the accuracy of small constants like α_1, α_2, β_1, β_2, etc., of Table III. This calculation is in the process of being completed and will be considered again in Part III.[19]

In view of the above we may therefore say, (1) the discrepancy between the simple isotope theory and the band constant ratios, $\rho_{lj}^* - \rho$, will in general *vary* with (lj) and hence be different for ω_e^* and B_e^* ratios (the only ones which in practice are susceptible of very precise measurement) and (2) the failure of the simple isotope theory may be quite as much due to neglecting the higher interaction terms of rotation and vibration as to the effect of nuclear "wobbling." This latter possibility seems not to have been given due prominence in the literature.

Isotope Effect in the Upper State

The first point to be considered in this connection is the choice of a proper vibrational assignment, which from the results of Table IX we should expect to be somewhat ambiguous. Actually three sets of quantum assignments were considered for both LiH and LiD. If the numbering used in this paper is called (a), that with an increase of $+1$ (b) and that with an increase of $+2$ (c) (with (a^i), (b^i) and (c^i) having the same significance for the LiD numbering of Part I) then the values of ω_e, x_1, x_2, etc., for LiH (observed), for LiD (computed from LiH by the simple isotope theory) with numberings (a), (b) and (c) and for LiD (observed) with numberings (a^i), (b^i) and (c^i) may be determined.

On carrying this out it was apparent that in no case was very close agreement obtained except in combinations (aa^i) and (bc^i).[20] Of these the second looks better than the first—though actually the *first* assignment alone is possible since on this assignment alone can one obtain satisfactory agreement between the $\Delta G'$ values observed for LiD and those computed from the constants for LiH. (See Table XI where the differences in the third column are probably significant only of the unsuitability of polynomials for representing the data.) There are fortunately three other facts reconcilable only

[19] It is interesting to note in this connection that similar calculations for $D_e^*(=Y_{01})$ show that Kratzer's relation for the ground state should be in error by roughly one percent, i.e., that $|D_e^*|$ should be about one percent *greater* than $|4(B_e)^3/\omega_e^2|$. As was indicated in Part I we found for the former 2.756×10^{-4} and for the latter 2.728×10^{-4}, a difference in the same direction of almost exactly one percent ($\pm.3$ of course). For the LiH molecule we found similarly $D_e'^* = 8.62$ whereas the extrapolation of Kratzer's relation gives 8.586, a difference of about 0.35 percent.

[20] These are, however, both seen to be very much more concordant than with Nakamura's observations. Thus the difference between the ω_e-values observed and calculated is about 12 percent and between the $x_e\omega_e$ values about 150 percent (see Part I Table VIII), and the remaining constants are of an entirely different order of magnitude.

TABLE XI. $\Delta G'(v)$ *values for LiD as observed and computed from LiH.*

$\Delta G'$ Obs.	$\Delta G'$ Calc. (aa^5)	Obs. −Calc.	$\Delta G'$ Calc. (bc^5)	Obs. −Calc.
—	203.518	—	—	—
224.62	224.153	+0.47	233.165	−8.54
239.92	239.791	.13	247.718	−7.79
252.18	252.058	.12	258.966	−6.78
262.03	261.965	.07	267.995	−5.96
270.14	270.08	.06		
276.69	276.68	.01		

with difficulty with any other numbering scheme. These are the approximate satisfaction of Kratzer's Eq. (6), which would be radically untrue with a change of numbering (especially for LiH), and the equality of the energy values in the two molecules at the maxima of their B_v' curves (see Fig. 1) and of their $\Delta G'$ curves (see Fig. 3). These three facts demand that the molecular constants have approximately their classical mechanical meaning and that any peculiarities of their variation with vibration shall be deducible from peculiarities in the potential curve. If now $B_v = B_e + \alpha_1 u + \alpha_2 u^2 + \cdots$, then approximately $B_v{}^i = \rho^2 B_e{}^i + \alpha_1 \rho^3 u + \alpha_2 \rho^4 \rho^2 \cdots$ and hence $B_v{}^i/\rho^2 = B_e + \alpha_1(\rho u) + \alpha_2(\rho u)^2 + \cdots$, therefore if the B_v curve has its maximum at u_1, the $B_v{}^i$ curve should have its at u_2 where $\rho u_2 = u_1$. We find $u_1 = 3.1$ and therefore $u_2 = 4.14$ whereas actually the isotope curve has its maximum at 4.36 (± 0.2). But we know[8] also that if $G = f(v+\frac{1}{2})$, whatever the form of the function f, then $G^i = f[\rho(v+\frac{1}{2})]$. Consequently it can readily be shown that, provided the higher coefficients in the expansion of G in powers of $(v+\frac{1}{2})$ are small, we have $\Delta G(v+1) \approx \Delta G^i[\rho(v+1)]/\rho$. Hence, roughly, a maximum at v_1 in the ΔG curve should correspond to a maximum at v_2 in the isotope curve, where $(v_1+1) = \rho(v_2+1)$. Actually we find $v_1 = 10.25$ whence $v_2 = 12.7$, whereas 12.65 is found experimentally. The question of the relation of the maxima of the B_v curves to those of the ΔG curves will be considered in more detail in Part III.[21]

On the basis of the numbering thus arrived at we have computed where the LiD origins should be compared with their observed positions, i.e., determined $(\nu_0{}^i)$ obs. $-$ $(\nu_0{}^i)$ calc. where any constant difference would be taken as giving the approximate electronic isotope shift. The result of this calculation is to give discrepancies which are always *positive* and vary from $+0.71$ cm^{-1} for the (1–3) band to $+1.84$ for the (7–3) band. It is, however, not legitimate to average these to obtain a value of the electronic isotope shift for the system origin since the differences vary smoothly in both *initial* and *final* progressions. Actually by extrapolating final progression curves to $v'' = -\frac{1}{2}$ and this extrapolated curve to $v' = -\frac{1}{2}$ a value for this electronic origin shift is obtained. We have put it provisionally at 0.0 (± 0.5) cm^{-1} which is of course more reliable than the value $+2.5$ obtained above by extrapolation of the $G'(v+\frac{1}{2})$ and $G''(v+\frac{1}{2})$ curves. This behavior will be considered in more detail in Part III.

We wish to take this opportunity of expressing our gratitude to the Milton Fund of Harvard University for a grant covering part of the expenses of this investigation and to the Monroe Calculating Machine Company, Inc. for the generous loan of a machine which has greatly facilitated the large amount of numerical reckoning involved.

[21] Both Almy and Hause (Phys. Rev. **42**, 242 (1932)) and Olsson (reference 12) agree in attributing the anomalous behavior of the B_v and ΔG curves in the case of KH and NaH, respectively, to a common cause, i.e., the possession of a potential curve on the part of the excited $^1\Sigma$ state which is anomalous in particular in that the coefficient a_1 of Eq. (19) is abnormally *small* while a_2 is abnormally *large*.

A Nuclear Model

WILLIAM V. HOUSTON, *California Institute of Technology*

(Received April 4, 1935)

The problem of a number of bodies which attract each other with forces proportional to the distance can be solved completely in terms of normal vibrations, and the expressions for the frequencies can be written down. From these the quantum mechanical energy levels can be written down directly. This makes a good model for the representation of a nucleus insofar as it can be considered as composed of alpha-particles, protons and neutrons, and can be treated by ordinary quantum mechanics. The assumption of constants of a reasonable order of magnitude makes possible the computation of binding energies which show the observed general trends. The instability of Be^8 composed of two alpha-particles is attributed to the high "zero point" energy of the system, although the system of three alpha-particles, C^{12}, is stable. The Pauli exclusion principle applied to the neutrons gives a reason for the limited number of observed isotopes.

THE discovery of the neutron as a nuclear constituent suggested the possibility of ignoring altogether the difficulties connected with the presence of electrons in nuclei. Thus Heisenberg has regarded nuclei as built up of protons and neutrons. Among these, alpha-particles may be regarded as particularly stable combinations, which may exist in nuclei in a way somewhat similar to that in which atoms exist in molecules. The great advantage of this point of view is that these particles can be treated by quantum mechanics even in the small volume attributed to the nucleus. Heisenberg[1] treated the energy of such a nucleus by a statistical method and was able to show some general properties of such assemblies. However, there is some advantage in having a nuclear model whose properties can be more precisely determined. Such a model can be constructed by assuming that the various nuclear particles attract each other with forces proportional to their separation.[2] This is probably a very crude representation of the true forces but because it is susceptible of exact treatment it can be used as a zero approximation to which modifications can be applied by perturbation methods.

1. Classical Treatment of the Problem

For simplicity the treatment will be given for three different kinds of particles, and because of the application to nuclei these will be designated as alpha-particles, protons and neutrons. The extension to more different kinds of particles is immediate and obvious.

Consider a system composed of a alpha-particles, p protons and n neutrons. Let the coordinates of the alpha-particles be ξ_r, η_r, ζ_r, where $0 \leqslant r \leqslant a$, of the protons be x_r, y_r, z_r, where $0 \leqslant r \leqslant p$, and of the neutrons be u_r, v_r, w_r, where $0 \leqslant r \leqslant n$. Let the mutual potential energy of two particles be as follows:

$$
\begin{aligned}
&\text{Two alpha-particles} && V_{aa} = C_{aa}\{(\xi_r-\xi_s)^2+(\eta_r-\eta_s)^2+(\zeta_r-\zeta_s)^2\} - D_{aa}\\
&\text{Alpha-particle and proton} && V_{ap} = C_{ap}\{(\xi_r-x_s)^2+(\eta_r-y_s)^2+(\zeta_r-z_s)^2\} - D_{ap}\\
&\text{Alpha-particle and neutron} && V_{an} = C_{an}\{(\xi_r-u_s)^2+(\eta_r-v_s)^2+(\zeta_r-w_s)^2\} - D_{pn}\\
&\text{Two protons} && V_{pp} = C_{pp}\{(x_r-x_s)^2+(y_r-y_s)^2+(z_r-z_s)^2\} - D_{pp}\\
&\text{Proton and neutron} && V_{pn} = C_{pn}\{(x_r-u_s)^2+(y_r-v_s)^2+(z_r-w_s)^2\} - D_{pn}\\
&\text{Two neutrons} && V_{nn} = C_{nn}\{(u_r-u_s)^2+(v_r-v_s)^2+(w_r-w_s)^2\} - D_{nn}.
\end{aligned}
\tag{1}
$$

Let μ be the mass of the alpha-particle, M that of the proton and m that of the neutron.

[1] W. Heisenberg, Zeits. f. Physik **80**, 587 (1933).
[2] This model was mentioned by Fowler, Nature **128**, 453 (1931) but he seems not to have worked it out in any detail.

The problem is already separated along the three coordinate axes so it is only necessary to consider one axis. The differential equations of motion then have the form

$$\begin{aligned}
\mu\ddot{\xi}_r &= -2C_{aa}\sum_{s=1}^{a}(\xi_r-\xi_s)-2C_{ap}\sum_{s=1}^{p}(\xi_r-x_s)-2C_{an}\sum_{s=1}^{r}(\xi_r-u_s),\\
M\ddot{x}_r &= -2C_{ap}\sum_{s=1}^{a}(x_r-\xi_s)-2C_{pp}\sum_{s=1}^{p}(x_r-x_s)-2C_{pn}\sum_{s=1}^{n}(x_r-u_s),\\
m\ddot{u}_r &= -2C_{an}\sum_{s=1}^{a}(u_r-\xi_s)-2C_{np}\sum_{s=1}^{p}(u_r-x_s)-2C_{nn}\sum_{s=1}^{n}(u_r-u_s).
\end{aligned} \tag{2}$$

To find the normal vibrations make the usual substitutions, $\xi_r=E_re^{i\omega t}$, $x_r=F_re^{i\omega t}$, $u_r=G_re^{i\omega t}$. This leads to N simultaneous algebraic equations for E, F and G. The condition for their compatibility is that the determinant of the coefficients be equal to zero, which gives an equation of the Nth degree in ω^2. This equation can be handled by adding and subtracting rows and columns of the determinant. The first two rows are

$$\begin{matrix}
\{2(a-1)C_{aa}+2pC_{ap}+2nC_{an}-\mu\omega^2\} & -2C_{aa} & \cdots -2C_{ap}\cdots -2C_{an}\\
-2C_{aa} & \{2(a-1)C_{aa}+2pC_{ap}+2nC_{an}-\mu\omega^2\} & \cdots -2C_{ap}\cdots -2C_{an}.
\end{matrix}$$

If the second row is subtracted from the first and then the first column is added to the second, one factor of the determinant is isolated in the upper left-hand corner. This gives as one root of the equation

$$\omega^2=(1/\mu)\{2aC_{aa}+2pC_{ap}+2nC_{an}\}. \tag{3}$$

This process can be carried out $(a-1)$ times to give $(a-1)$ roots identical with (3). There then comes a transition between the rows referring to alpha-particles and those referring to protons. If this row is skipped the above process of subtracting rows and adding columns can be continued to give $(p-1)$ roots of the equation whose values are

$$\omega^2=(1/M)\{2aC_{ap}+2pC_{pp}+2nC_{pn}\}. \tag{3a}$$

By skipping the next transition there can be obtained $(n-1)$ roots,

$$\omega^2=(1/m)\{2aC_{an}+2pC_{pn}+2nC_{nn}\}. \tag{3b}$$

After this process has been carried as far as possible there remains a determinant with as many rows and columns as there are different kinds of particles. One root of this is always $\omega^2=0$, and the rest must be obtained by solving the equation. For the special case considered here

$$\begin{vmatrix}
(2pC_{ap}+2nC_{an}-\mu\omega^2) & -2pC_{ap} & -2nC_{an}\\
-2aC_{ap} & (2aC_{ap}+2nC_{pn}-M\omega^2) & -2nC_{pn}\\
-2aC_{an} & -2pC_{pn} & (2aC_{an}+2pC_{pn}-m\omega^2)
\end{vmatrix}=0. \tag{3c}$$

By adding all three columns together the root $\omega^2=0$ can be isolated and the result is a quadratic equation whose solutions are

$$\begin{aligned}
\omega^2=&\left(\frac{a}{M}+\frac{p}{\mu}\right)C_{ap}+\left(\frac{a}{m}+\frac{n}{\mu}\right)C_{an}+\left(\frac{p}{m}+\frac{n}{M}\right)C_{pn}\pm\Bigg\{\left(\frac{a}{M}+\frac{p}{\mu}\right)^2C_{ap}^2\\
&+\left(\frac{a}{m}+\frac{n}{\mu}\right)^2C_{an}^2+\left(\frac{p}{m}+\frac{n}{M}\right)C_{pn}^2-2\left[\left(\frac{a}{M}+\frac{p}{\mu}\right)\left(\frac{a}{m}+\frac{n}{\mu}\right)-2\frac{np}{\mu^2}\right]C_{ap}C_{an}\\
&-2\left[\left(\frac{a}{M}+\frac{p}{\mu}\right)\left(\frac{p}{m}+\frac{n}{M}\right)-2\frac{an}{M^2}\right]C_{ap}C_{pn}-2\left[\left(\frac{a}{m}+\frac{n}{\mu}\right)\left(\frac{p}{m}+\frac{n}{M}\right)-2\frac{ap}{m^2}\right]C_{an}C_{pn}\Bigg\}^{\frac{1}{2}}.
\end{aligned} \tag{3d}$$

These roots give the frequencies with which the various normal coordinates vibrate. The expressions for the normal coordinates in terms of the position coordinates can be readily obtained but since they are not necessary in the determination of the quantum-mechanical energy levels, they need not be given here. The coordinate corresponding to the frequency given by $\omega^2=0$ is just the center of mass of the system.

2. Quantum-Mechanical Energy Levels

Since each of the normal vibrations exists along each of the three coordinate axes, the state of minimum energy will be obtained by multiplying each frequency by $3h/2$. If any of the vibrations are excited the energy can be expressed in terms of a quantum number for each different frequency. Hence the energy for a system of three kinds of particles is

$$E=(a-1+2m_1/3)(3h/4\pi)\{(2aC_{aa}+2pC_{ap}+2nC_{an})/\mu\}^{\frac{1}{2}}+(p-1+2m_2/3)(3h/4\pi)$$
$$\times\{(2aC_{ap}+2pC_{pp}+2nC_{pn})/M\}^{\frac{1}{2}}+(n-1+2m_3/3)(3h/4\pi)\{(2aC_{an}+2pC_{pn}+2nC_{nn})/m\}^{\frac{1}{2}}$$
$$+(1+2m_4/3)(3h\omega_1/4\pi)+(1+2m_5/3)(3h\omega_2/4\pi)-a(a-1)D_{aa}/2-apD_{ap}-anD_{an}$$
$$-p(p-1)D_{pp}/2-pnD_{pn}-n(n-1)D_{nn}/2. \quad (4)$$

ω_1 and ω_2 are from Eq. (3d). The ground state is obtained by putting all the quantum numbers, $m_1\cdots m_5$ equal to zero. There is clearly a great deal of degeneracy to this problem since each m_i, except m_4 and m_5, is the sum of the quantum numbers belonging to all the normal vibrations with the given frequency. Some of this would be removed by the application of perturbations correcting the law of force between the particles and many of the finer details of nuclear behavior are perhaps to be understood in this way.

3. Application to Nuclei

It is certain from the fact of the stability of nuclei that there are effectively attractive forces between some of the nuclear constituents. Attractive forces given by potential energies of the form treated above are certainly very crude approximations but it still seems that they can be used to describe some of the characteristic features of nuclear behavior.

Nuclei containing alpha-particles only

It has often been assumed that nuclei of even atomic number contain all of their protons combined in the form of alpha-particles. This point of view has recently been emphasized by Landé.[3] Some information on the force between two alpha-particles is available from scattering experiments. The analysis of these by Taylor[4] indicates that the force is repulsive and coulomb at distances greater than about 3×10^{-13} cm; below this the force is attractive and such that at $r=0$ the potential energy has a large negative value. In accord with these results we may assume that the energy is given by (1) from $r=0$ to such a point that it becomes equal to the coulomb repulsive potential. From there on it may be considered as coulomb. The values of C_{aa} and D_{aa} can then be chosen so as to fit the known energies as well as possible. If the coulomb part of the field is entirely neglected, the energy can be written down at once.

For a system containing alpha-particles only Eq. (4) becomes

$$E=(a-1+2m_1/3)(3h/4\pi)(2aC_{aa}/\mu)^{\frac{1}{2}}$$
$$-a(a-1)D_{aa}/2. \quad (4a)$$

When a becomes large this energy decreases with a^2. This is faster than the observed decrease but it is possible to select the constants so that the general trend is represented. In order to give attention to the light nuclei we may use C^{12} to determine these constants. The binding energy is known, and if the excited level at about 8.0 $\times10^{-6}$ erg is taken as due to $m_1=1$, the constants

[3] A. Landé, Phys. Rev. **43**, 620 (1933).
[4] H. M. Taylor, Proc. Roy. Soc. **A136**, 605 (1932).

can be determined. In round numbers these are

$$C_{\alpha\alpha}=64\times10^{18}\ \text{erg/cm}, \qquad D_{\alpha\alpha}=9\times10^{-6}\ \text{erg}.$$

The binding energies computed on this basis, together with the observed values, are given in Table I.

According to this model the observed instability of Be^8 is due to the large "zero point" energy in the ground state. The lifetime in this state, estimated according to Gamow's formula, is very small, $\sim10^{-19}$ sec. The observed energies of carbon and oxygen are given very nicely, and the calculated value of the first excited level in O^{16} is $2/(3)^{\frac{1}{2}}$ as high above the ground level as in C^{12}. For the heavier atoms it is clear that the kinetic energy of the model does not increase as rapidly as necessary to overcome the rapid decrease of the potential energy. It is possible to select the constants so as to give better agreement for the heavier nuclei, but this disturbs the fit with the lighter. The first effect of including the outer part of the field would be to decrease the total energy, but it would certainly be small in the case of the stable systems.

According to Eq. (4a) the capture of an alpha-particle always represents a decrease in energy. This is in agreement with the observed fact that, in the nuclei containing alpha-particles only, the mass defect increases steadily with the atomic number.

Nuclei containing alpha-particles and neutrons

In applying the model to these cases it is simplest to include the assumption that the neutrons do not influence each other. Thus $C_{nn}=D_{nn}=0$. The energy for this case is given by

$$\begin{aligned}E=&(a-1+2m_1/3)(3h/4\pi)\{(2aC_{\alpha\alpha}+2nC_{\alpha n})/\mu\}^{\frac{1}{2}}\\&+(n-1+2m_3/3)(3h/4\pi)(2aC_{\alpha n}/m)^{\frac{1}{2}}\\&+(1+2m_4/3)(3h/4\pi)\{(a/m+n/\mu)2C_{pn}\}^{\frac{1}{2}}\\&-a(a-1)D_{\alpha\alpha}/2-anD_{\alpha n}. \qquad (4b)\end{aligned}$$

The values of $C_{\alpha n}$ and $D_{\alpha n}$ can then be chosen to approximate the observed nuclear energies. The values

$$C_{\alpha n}=64\times10^{18}\ \text{ergs/cm}^2 \text{ and } D_{\alpha n}=11.8\times10^{-6}\ \text{erg}$$

serve fairly well. They give He^5 composed of one alpha-particle and one neutron a positive energy of 3.6×10^{-6} erg. It would thus be nonexistent since there is probably almost no barrier against the escape of a neutron if there is sufficient energy. The energies of some other cases are shown in Table I. Be^9 has just about zero energy while Be^{10} is more stable than Be^9 but less so than B^{10}. Eq. (4b) shows that the energy will in general decrease with an increase in the number of neutrons and that the rate of this decrease will increase with the number of alpha-particles. It is also necessary, however, to take account of the exclusion principle for neutrons. If it is assumed that the wave functions must be antisymmetrical in the coordinates of the neutrons, the quantum number m_3 cannot be equal to zero except for the cases of one or two neutrons. For three or four it has the minimum value one, etc. This effect is shown in the energy of C^{15} which is much less stable than C^{14}, and O^{19} which is less stable than

TABLE I. *Computed and observed nuclear energies.* The energies are expressed in units of 10^{-6} ergs, and the numbers in parentheses are the observed nuclear energies.

Nuclei of even atomic number composed of alpha-particles and neutrons

He^4	0.00	He^5	+3.6				
Be^8	+0.73	Be^9	−0.04 (0.0)	Be^{10}	−1.23	Be^{11}	+6.8
C^{12}	−3.16 (−4.3)	C^{13}	−10.2 (−17.3)	C^{14}	−17.4	C^{15}	−9.3
O^{16}	−12.8 (−12.9)	O^{17}	−26.7 (−24.8)	O^{18}	−41.5 (−36.7)	O^{19}	−37.9
Ne^{20}	−28.5 (−21.0)	Ne^{21}	−50.0	Ne^{22}	−72.2 (−47.8)	Ne^{23}	−74.1
Mg^{24}	−50.7	Mg^{25}	−80.4	Mg^{26}	−110.5	Mg^{27}	−118.6
Si^{28}	−79.8 (−49.6)	Si^{29}	−117.8	Si^{30}	−156.5	Si^{31}	−170.9

Nuclei composed of protons and neutrons

H^2	−3.34 (−3.17)	H^3	−7.8 (−8.1)	H^4	−4.0
He^3	−7.8 (−6.8)	He^4	−32.4 (−43.5)	He^5	−22.8

Nuclei of odd atomic number composed of alpha-particles, one proton and neutrons

Li^6	−5.6 (−5.1)	Li^7	−17.0 (−16.7)	Li^8	−13.2
B^{10}	−15.9 (−9.8)	B^{11}	−32.4 (−25.3)	B^{12}	−33.5
N^{14}	−33.2 (−21.1)	N^{15}	−57.1 (−40.8)	N^{16}	−63.0
F^{18}	−57.6	F^{19}	−83.5 (−48.0)	F^{20}	−97.4
Na^{22}	−89.2	Na^{23}	−128.9	Na^{24}	−146.6
Al^{26}	−128.3	Al^{27}	−176.2	Al^{28}	−200.

Values of the constants used in compiling this table

$C_{\alpha\alpha}=64\times10^{18}$	$C_{\alpha n}=64\times10^{18}$	$C_{\alpha p}=64\times10^{18}$	$C_{pn}=64\times10^{18}$
$D_{\alpha\alpha}=9\times10^{-6}$	$D_{\alpha n}=11.8\times10^{-6}$	$D_{\alpha p}=11.8\times10^{-6}$	$D_{pn}=22.7\times10^{-6}$
$C_{nn}=0$	$C_{pp}=0$	$D_{nn}=0$	$D_{pp}=0$

O^{18}. For the heavier nuclei the constants used do not actually show a definite instability but this property of the model does show why the number of isotopes is not unlimited, and indicates why the maximum number of neutrons is dependent on the number of alpha-particles.

Nuclei containing alpha-particles, protons and neutrons

For the nuclei of odd atomic number the whole Eq. (4) must be used. The constants listed in Table I seem to give the general trend correctly. According to these a proton and a neutron act in the same way with an alpha-particle. Also H^2 and He^3 show the same binding energy. This is, of course, not correct but it is not a bad approximation. For these odd elements the number of neutrons is limited by their turning into protons and forming alpha-particles. Thus B^{12} is less stable than C^{12}, when the energy of the alpha-particle is considered.

4. Discussion of the Results

It is to be emphasized that no great significance is to be attached to the exact numerical results nor to the exact values of the constants used. It is surely not correct to use the same force constant between all kinds of particles, but the determination of the differences would hardly be justified by the accuracy of the model. The constants are of a reasonable order of magnitude and the results show the correct general trends, although the actual values of the energy deviate widely for the higher atomic numbers because the constants have been selected to fit the lighter nuclei, as well as because of the crudeness of the model.

The assumption of a strong force between protons and neutrons and no force between protons gives, as indicated by Wigner,[5] the right general trend in H^2, H^3, He^3, He^4. Together with the exclusion principle it also makes He^5 less stable than He^4. The amount is different from that obtained by treating He^5 as an alpha-particle and a neutron, but this difference is not surprising in view of the rough determination of the constants. The increase in mass defect with the increase in the number of alpha-particles and with the increase in the number of neutrons is in accord with the observations. The application of the exclusion principle to the neutrons leads to a limitation on the number of neutrons which can be added with a decrease in total energy.

Two outstanding characteristics of nuclei which are not apparent in the model are the alpha-particle radioactivity of some heavy nuclei, and the large number of close-lying excited energy levels which are observed. Heisenberg attributes the radioactivity to the repulsive force between protons. This exists also between alpha-particles. Since this has not been included here it is not surprising that the instability does not appear. On the other hand the excited levels of the model are required to be rather far apart because of the values of the constants, and it seems difficult to reduce sufficiently the constants and at the same time preserve the necessary binding energy relationships. Nevertheless a relatively small change in the form of the force might remove enough of the degeneracy to provide the necessary number of close excited levels.

In spite of the extreme simplification this model is free from the objections to the consideration of one nuclear particle moving in an average field due to all the rest, and gives a description of the trends of the binding energies

[5] E. Wigner, Phys. Rev. **43**, 252 (1933).

Theory of the Photoelastic Effect of Cubic Crystals

HANS MUELLER, *The George Eastman Laboratory, Massachusetts Institute of Technology*

(Received March 8, 1935)

The theory of Ewald and Born of the double refraction of crystals is applied to the calculation of the photoelastic properties of D lattices. Only in special cases, as for instance in KCl for pressure parallel [111], is the effect determined by the anisotropy of the Lorentz and Coulomb forces. In these cases the photoelastic data determine the ratio R_{Cl}/R_K of the ionic refractions. Satisfactory agreement with all observations can be reached by assuming that the elastic deformations produce optical anisotropy of the atoms. Introducing this assumption in the Ewald-Born theory leads to an explanation of the change of the index of refraction with the density, and of the different photoelastic properties of NaCl, KCl, CaF_2 and diamond. The photoelastic constants of other crystals are predicted. It is shown that the "cavity" method of Lorentz and Bragg gives the same Lorentz force as the theory of Born and Ewald. The calculations of the photoelastic effect by Herzfeld and Banerjee are incorrect and incomplete.

IF a cubic crystal is subjected to a pressure normal to a cube face, it becomes tetragonal, and hence doubly refracting. According to Ewald[1] and Born[2] the birefringence of crystals is due to the anisotropy of the Lorentz-Lorenz force. In ionic crystals the anisotropy of the Coulomb forces is an additional cause of birefringence. Taking into account both effects, Hylleraas[3] calculated the optical properties of calomel, rutile, anatas and quartz. For carbonates and nitrates, W. L. Bragg[4] developed a somewhat different theory in which the birefringence is primarily due to the optical anisotropy of the CO_3 or NO_3 groups.

The success of these theories gives reason to anticipate that they could also explain the accidental double refraction of cubic crystals. We shall show that, in general, this expectation is not justified. Neither Ewald-Born's nor Bragg's theory can explain the photoelastic behavior of cubic crystals, except in some special cases. This conclusion has been reached previously by Herzfeld,[5] Herzfeld and Lee, and Banerjee.[6] It will, however, be demonstrated here that Herzfeld's papers contain a numerical error and that Banerjee's method is wrong. Hence their results are not conclusive.

In a previous paper the writer[7] has shown that a third cause of the photoelastic effect must be considered. A deformation of the lattice changes the energy levels and transition probabilities of the optical electrons, and hence alters the refraction of the atoms. This effect is a generalization of the results of Fajans and Joos[8] who showed that in crystals the refraction of the ions are usually smaller than in solutions. We assume that a decrease of the lattice constant reduces the refractions still further. But, contrary to Fajans and Joos, we do not believe that this effect is due to the Coulomb forces between the ions. The effect exists also in homopolar crystals. It is caused by a change of the charge distribution or the binding of the optical electrons. It can be considered as produced by the repulsive forces between the atoms[9] and depends primarily on the arrangement of, and the distances between nearest neighboring atoms.

In photoelastic experiments the lattice distances parallel to the pressure are decreased, and the distances normal to the stress are increased. This gives rise to an anisotropy of the atomic refractions.

By taking into account all three effects we are able to give a satisfactory explanation of the observed photoelasticity of simple cubic lattices.

[1] P. Ewald, Thesis, Munich, 1912; Ann. d. Physik **49**, 1, 117 (1916).
[2] M. Born, *Handbuch der Physik* Vol. 24, p. 770.
[3] E. Hylleraas, Zeits. f. Physik **36**, 859 (1926); Zeits. f. Krist. **65**, 469 (1927).
[4] W. L. Bragg, Proc. Roy. Soc. **A105**, 307 (1924); **A106**, 346 (1924).
[5] K. F. Herzfeld, J. Opt. Soc. Am. **17**, 26 (1928); Herzfeld and Lee, Phys. Rev. **44**, 625 (1933).
[6] K. Banerjee, Ind. J. Phys. **2**, 195 (1927).
[7] H. Mueller, Physics **6**, 179 (1935).
[8] Fajans and Joos, Zeits. f. Physik **23**, 1 (1924).
[9] The possibility that the repulsive forces may deform and even polarize an atom, giving rise to negative polarizabilities, was discussed by Heckmann, Zeits. f. Krist. **61**, 250 (1925).

Classical Theory of Photoelasticity

The phenomenological theory of photoelasticity of crystals was developed by F. Pockels.[10] The theory assumes that the elastic deformations, and not the stresses, are primarily responsible for the birefringence. The behavior of cubic crystals is characterized by three elasto-optical constants p_{11}, p_{12}, p_{44}, which for the purpose of our calculation are best defined as follows:

A simple strain z_z in the direction [001] produces uniaxial birefringence and we have

$$\begin{aligned} n-n_z&=\tfrac{1}{2}n^3p_{11}z_z,\\ n-n_x&=\tfrac{1}{2}n^3p_{12}z_z,\\ n_x-n_z&=\tfrac{1}{2}n^3(p_{11}-p_{12})z_z; \end{aligned} \tag{1}$$

n is the index of refraction of the undeformed crystal, and n_z and n_x are the indices for light whose electric vector oscillates in the direction parallel and perpendicular to the strain.

The combination of a strain x_x' in the direction [110] and a strain $y_y'=-x_x'$ in the direction $[1\bar{1}0]$ represents a shear $x_y=2x_x'$ and produces biaxial birefringence with the axis of the index ellipsoid in the directions $x'=[110]$, $y'=[1\bar{1}0]$, $z'=[001]$. Then

$$n_{x'}=n+\Delta n,\ n_{y'}=n-\Delta n,\quad n_z=n,\quad \text{and}$$
$$\Delta n=-n^3p_{44}x_x'. \tag{2}$$

The "Cauchy relation" $p_{44}=\frac{1}{2}(p_{11}-p_{12})$ holds only for amorphous solids. For hydrostatic pressure, for which $x_x=y_y=z_z=dV/3V=-d\rho/3\rho$, where ρ is the density, the index of refraction changes by

$$\begin{aligned} dn&=-\tfrac{1}{2}n^3[p_{11}z_z+p_{12}(x_x+y_y)]\\ &=(p_{11}+2p_{12})n^3d\rho/6\rho. \end{aligned} \tag{3}$$

If $p_{11}-p_{12}>0$ a pressure normal to a cube face produces positive birefringence. This is the case[11] for KCl, KBr, KI and NH_4I. $p_{11}-p_{12}$ is negative for NaCl, CaF_2, NaF, ZnS, diamond, Al- and NH_4-alum. If p_{44} is negative, the crystal shows negative uniaxial birefringence for pressure normal to an octahedral face. This is the case for NaCl, KCl and the alums; but, for CaF_2, p_{44} is positive. A satisfactory theory must be able to account for these reversals of sign.

The comparison between theory and observation is simplified by introducing

$$\begin{aligned} p_z&=n^4p_{12}(n^2-1)^{-2}=-2n(n^2-1)^{-2}dn_z/dz_z,\\ p_z&=n^4p_{11}(n^2-1)^{-2}=-2n(n^2-1)^{-2}dn_z/dz_z,\\ p'=p_{z'}&=2n^4p_{44}(n^2-1)^{-2}\\ &=-2n(n^2-1)^{-2}dn_{x'}/dx_x',\\ p=p_z-p_z&=n^4(p_{11}-p_{12})(n^2-1)^{-2}. \end{aligned} \tag{4}$$

The Ewald-Born Theory of the Lorentz-Lorenz Force

We consider a lattice with only one atom at the corners of the elementary cells. Each atom carries a charge $e=1$, and a continuous charge distribution of constant density $\rho=-1/\Delta$ compensates for the discrete charges. Δ is the volume of the elementary cell, which is determined by the three vectors a_1, a_2, a_3. The position of the atoms is given by the vectors $r^l=l_1a_1+l_2a_2+l_3a_3$. Except at the points r^l the electric potential ψ satisfies everywhere Poisson's equation

$$\Delta\psi=4\pi/\Delta \tag{5}$$

and has the value[2]

$$\psi=\psi_1+\psi_2,$$

where

$$\begin{aligned} \psi_1&=\frac{4\pi}{\Delta}\sum{}'\exp\left[-\frac{1}{4\epsilon^2}|q^l|^2+j(q^lr)\right]\Big/|q^l|^2,\\ \psi_2&=\sum G(\epsilon|r^l-r|)/|r^l-r|-\pi/\epsilon^2\Delta; \end{aligned} \tag{6}$$

$j=\sqrt{(-1)}$, ϵ is an arbitrary parameter; $q^l=2\pi(l_1b_1+l_2b_2+l_3b_3)$, where $b_1=[a_2\times a_3]/\Delta$, etc., are the vectors of the reciprocal lattice; $G(x)=1-2\pi^{-1}\int_0^x e^{-\alpha^2}d\alpha$; and the summations are to be taken over all combinations (l_1, l_2, l_3), excepting $(0, 0, 0)$ in the summations Σ'.

Let us now consider a second lattice, geometrically identical with the first, but each lattice point carrying a charge $e=-1$ and displaced by a vector dr with respect to the atoms

[10] F. Pockels, Wied. Ann. **37**, 151 (1889); *Lehrbuch der Kristallphysik*, Leipzig and Berlin, 1906.

[11] Johnson, *Neues Jahrbuch für Mineralogie*, 1902, Vol. II, p. 146.

of the first lattice. At the point r the second lattice produces a potential $\psi^* = -\psi + (dr \operatorname{grad} \psi)$. Since the continuous charges cancel each other, the two lattices together represent a lattice of dipoles with the moments $\mu = -dr$. Their potential is $\phi = \psi + \psi^* = -(\mu \operatorname{grad} \psi)$. In order to find the field due to all other dipoles acting on the dipole at the origin, one subtracts the field of this dipole and gets the potential $\bar{\phi} = -(\mu \cdot \operatorname{grad} \bar{\psi})$, $\bar{\psi} = \psi - 1/r$. We consider now the simple case, where all dipoles are parallel to the applied field E_x. The total field acting on any dipole is the Lorentz-Lorenz force

$$F_x = E_x - (d\bar{\phi}/dx)_0 = E_x + \mu_x (\partial^2 \bar{\psi}/\partial x^2)_0 = E_x + 4\pi L_x P_x, \quad (7)$$

where $P_x = \mu_x/\Delta$ is the polarization, and where we have introduced the "Lorentz factor"

$$L_x = (\Delta/4\pi)(\partial^2 \bar{\psi}/\partial x^2)_0. \quad (8)$$

From (5) it follows that $L_x + L_y + L_z = 1$, and hence for a simple cubic lattice[12] $L_x = L_y = L_z = 1/3$.

For a simple tetragonal lattice, where $a_1 = a_2 \neq a_3$, we have $L_x = L_y$, $L_z = 1 - 2L_x$. The numerical calculation is conveniently carried out for $L_x - L_z$. Choosing $\epsilon = \pi^{-1}\Delta^{-1}$ we get

$$L_x - L_z = -\sum{}'(Q_x - Q_z)Q^{-1} \exp(-Q) + \sum{}'(R_x - R_z)(3/2R + 1)R^{-1} \exp(-R) + (3\pi^{\frac{1}{2}}/4)\sum(R_x - R_z)R^{-5/2}G(R^{\frac{1}{2}}), \quad (9)$$

where

$$Q = Q_x + Q_y + Q_z = \pi\Delta^{\frac{1}{2}}(l_1^2/a_1^2 + l_2^2/a_2^2 + l_3^2/a_3^2),$$

$$R = R_x + R_y + R_z = \pi\Delta^{-1}(l_1^2 a_1^2 + l_2^2 a_2^2 + l_3^2 a_3^2).$$

All the series in (9) converge very rapidly. The values of L_x and L_z depend only on the ratio a_3/a_1.

The results in Fig. 1 show that for $a_3/a_1 > 2$ they can be represented by the approximation $L_z = 1 - 2L_x = 1 - 0.72\, a_3/a_1$. For $a_3/a_1 > 1.4$ and for $a_3/a_1 < 0.6$ one Lorentz factor becomes negative. Hence in many crystals the interaction

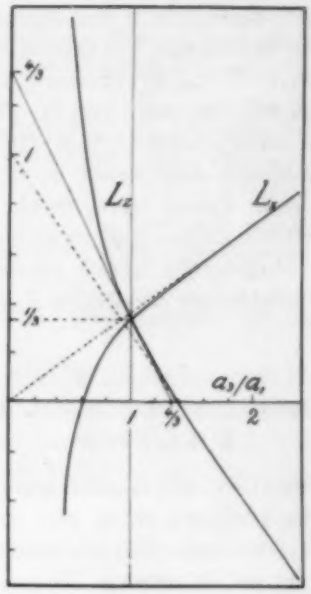

FIG. 1. The Lorentz factor for simple tetragonal lattices.

between the dipoles does not increase, but decreases the polarization.[13]

If $a_3/a_1 < 1$ the crystal is a chain lattice. For light oscillating parallel to the chains the L factor is larger than for light oscillating normal to the chains. Hence chain lattices show positive birefringence. On the other hand, for layer lattices, where $a_3/a_1 > 1$, the L factor is small for light oscillating normal to the layers and the birefringence is negative. The observations verify these rules for arbitrary layer and chain lattices.[14]

In the problem of photoelasticity of cubic crystals we are interested in the values of L_x and L_z for a lattice which differs only slightly from a cubic lattice. A strain z_z produces an axial ratio $a_1 : a_2 : a_3 = 1 : 1 : (1 + z_z)$ and the L factors differ from ⅓ by small amounts; hence

$$L_x = L_y = \tfrac{1}{3} + s_x z_z; \quad L_z = \tfrac{1}{3} + s_z z_z \quad (10)$$

and we must have $2s_x + s_z = 0$. (11)

The differentiation $s_x = dL_x/dz_z$ leads to com-

[12] The same derivation of the factor ⅓ can also be used for a random distribution of atoms. Another derivation by Darwin, Proc. Roy. Soc. **A146**, 17 (1934).

[13] In these cases Havelock's assumption (Proc. Roy. Soc. **A80**, 31 (1908)), which replaces Lorentz's spherical cavity by an ellipsoid, cannot hold. Negative Lorentz factors can be used to explain the fact that the anomalous dielectric properties of Rochelle salt occur only for fields in direction of the a axis (H. Mueller, Phys. Rev. **47**, 175 (1935)).

[14] W. A. Wooster, Zeits. f. Krist. **80**, 495 (1931).

plicated expressions. Much less numerical work is involved in calculating the difference quotient $s_x=\{L_x(1+z_x)-\frac{1}{3}\}/z_x$. By choosing $z_x=0.01$ we obtain sufficiently accurate values. Thus we get for simple cubic lattices $L_x(1.01)=0.33832$, $L_z(1.01)=0.32333$, and hence $s_x=0.499$, $s_z=-1.000$. These values agree with Herzfeld's results $s_x=0.501$, $s_z=-1.01$, which are calculated from Madelung's lattice potential. From Banerjee's calculation we derive $s_x=0.5045$, $s_z=-1.0090$.

The Lorentz-Lorenz Force in Strained D Lattices*

If the elementary cells contain several different atoms at the positions r_i, r_k, etc., carrying the moments μ_{kx}, one must find the field of all other dipoles acting on an atom i. This leads to the Lorentz factors L_{ikx} and the Lorentz force[15]

$$F_{ix}=E_x+4\pi\sum_k L_{ikx}P_{kx};\quad P_{kx}=\mu_{kx}/\Delta. \tag{12}$$

If the elementary cell is orthorhombic, one finds by choosing again $\epsilon=\pi^{-\frac{1}{2}}\Delta^{-\frac{1}{3}}$

$$\begin{aligned}L_{iix}&=(\Delta/4\pi)(\partial^2\bar{\psi}/\partial x^2)_0\\&=\tfrac{1}{3}-\sum{}'Q_xQ^{-1}\exp(-Q)\\&\quad+\sum{}'R_xR^{-1}\exp(-R)\\&\quad+\tfrac{1}{2}\sum{}'(3R_xR^{-1}-1)R^{-1}\exp(-R)\\&\quad+(\pi^{\frac{1}{2}}/4)\sum{}'(3R_xR^{-1}-1)R^{-\frac{1}{2}}G(R^{+\frac{1}{2}}),\end{aligned}\tag{13}$$

$$\begin{aligned}L_{ikx}&=(\Delta/4\pi)(\partial^2\psi/\partial x^2)_{r_{ik}}\\&=-\sum{}'Q_xQ^{-1}\exp[-Q+j(q'r_{ik})]\\&\quad+\sum R_{ikx}R_{ik}^{-1}\exp(-R_{ik})\\&\quad+\tfrac{1}{2}\sum(3R_{ikx}R_{ik}^{-1}-1)R_{ik}^{-1}\exp(-R_{ik})\\&\quad+(\pi^{\frac{1}{2}}/4)\sum(3R_{ikx}R_{ik}^{-1}-1)R_{ik}^{-\frac{1}{2}}G(R_{ik}^{+\frac{1}{2}}),\end{aligned}\tag{14}$$

and analogous equations for L_{iky} and L_{ikz}. Q and R are defined by (10) and $R_{ik}=R_{ikx}+R_{iky}+R_{ikz}=\pi\Delta^{-\frac{1}{3}}[(l_1a_1-x_{ik})^2+(l_2a_2-y_{ik})^2+(l_3a_3-z_{ik})^2]$ where x_{ik}, y_{ik}, z_{ik} are the components of the vector $r_{ik}=r_i-r_k$. From (5) it follows that for all indices ik

$$L_{ikx}+L_{iky}+L_{ikz}=1. \tag{15}$$

These equations serve to calculate the Lorentz factors for elastically deformed diagonal lattices. For undeformed D lattices (15) leads to $\Sigma L_{ikx}P_{kx}=\frac{1}{3}P_x$, and the Lorentz-Lorenz equation is valid. To determine the L factors for any D lattice which is deformed by a strain $z_x=0.01$ or a shear $x_y/2=x_x'=-y_y'=0.01$, it is only necessary to carry out the calculations for the three orthorhombic cells shown in Fig. 2. The symmetry of these cells requires that for fields parallel to the edges of the cells all dipole moments be parallel to the electric field. Hence $L_{ikxy}=0$, excepting $L_{ikxz}=L_{ikx}$. For reasons of symmetry $L_{ikx}=L_{kix}$ and there are a large number of relations between the 48 L factors given below.[16]

Since for an undeformed D lattice $F=E+4\pi P/3$, we write for a lattice deformed by a strain z_x

$$F_{ix}=E_x+(4\pi/\Delta)\sum n_k\mu_{kx}(\tfrac{1}{3}+s_{ikx}z_x). \tag{16}$$

For a shear $x_x'=-y_y'=x_y/2$ we write

$$F_{ix'}=E_x+(4\pi/\Delta)\sum n_k\mu_{kx'}(\tfrac{1}{3}+s_{ikx'}x_x'). \tag{17}$$

* In Born's diagonal or D lattices the atoms of the elementary cell are located on the body diagonal of the elementary cube. The face- and body-centered cubic lattice, and the lattices of diamond, NaCl, CsCl, CaF_2 and ZnS are D lattices.

[15] In the general case, the dipole moments μ_k are not all parallel to the applied field and the Lorentz force is $F_{ix}=E_x+4\pi\Sigma_i\Sigma_y L_{ikxy}P_{ky}$. We consider here only such cases where the symmetry of the crystal requires that $L_{ikxy}=0$ for $x\neq y$.

[16] There are 16 relations due to Eq. (15). For cell A there exist 10 obvious equalities $L_{ikx}=L_{iky}$, 3 relations $\Sigma_k L_{1kx}=8L_{1x}$, and 4 relations with the results in Fig. 1, as, for instance $\frac{1}{4}(L_{11x}+L_{12x}+L_{13x}+L_{14x})=L_x(2.02)$. Similar relations exist for cell B and C, and there are 8 relations connecting the results for different cells. In the calculation we have not made use of any of these relations. The fact that all are satisfied shows that the errors cannot be larger than 0.0001. In the summations terms smaller than 0.00002 were neglected. All series converge very rapidly. We find the "Lorentz factors" given in Table I.

Table I. *Lorentz factors.* In cell A we have $a_1:a_2:a_3=1:1:1.01$, in cell B $a_1:a_2:a_3=1.01:0.99:2^{\frac{1}{3}}$, and in cell C $a_1:a_2:a_3=1.01:0.99:2^{-\frac{1}{3}}$.

	Cell A				Cell B		
ik	L_{ikx}	L_{iky}	L_{ikz}	ik	L_{ikx}	L_{iky}	L_{ikz}
11	0.3383	0.3383	0.3233	11	0.4858	0.5258	−0.0116
12	2.7528	−.8710	−.8818	12	.1689	.1530	.6781
13	−.8710	2.7528	−.8818	13	−.2716	−.2584	1.5300
14	−.8340	−.8384	2.6768	14	.9637	.8996	−.8633
15	.3286$_5$	.3286$_5$	−.3427			Cell C	
16	−.3509	.6634	.6875	11	0.1077	0.1337	0.7586
17	.6634	−.3509	.6875	12	.5664	.5262	−.0926
18	.6837$_3$	.6837$_3$	−.3675	13	−.5359	1.1866	.3494
				14	1.1706	−.4882	.3176

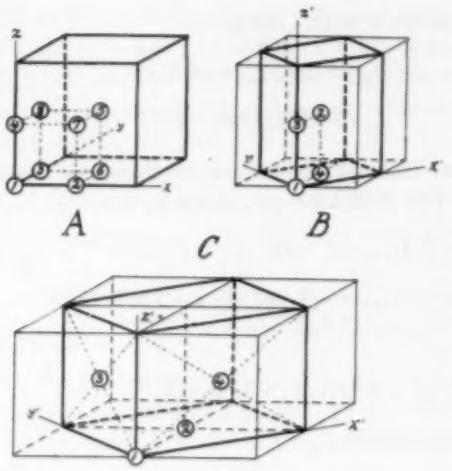

FIG. 2. Orthorhombic cells.

n_k is the number of atoms of the kind k within an elementary cell. Replacing again the derivative by the difference quotient, we can now calculate the factors s_{ikx}, s_{iky}, $s_{ikz'}$, etc. The cell A gives the factors s_{ikx} for the simple cubic (SC), body centered (BC), and face centered (FC) cubic lattices, and for the lattice types of NaCl, CsCl, ZnS, CaF_2 and diamond (DI). The cell B furnishes the factors $s_{ikz'}$ for (SC), (FC) and NaCl, and cell C gives these factors for (BC), CsCl, ZnS, CaF_2 and DI. For instance we get for the NaCl lattice

$$s_{11x}=s_{11y}=100\{\tfrac{1}{4}(L_{11x}+L_{16x}+L_{17x}+L_{18x})_A-\tfrac{1}{3}\},$$

$$s_{12x}=s_{21z}=100\{\tfrac{1}{4}(L_{12x}+L_{13x}+L_{14x}+L_{15x})_A-\tfrac{1}{3}\},$$

$$s_{11x'}=s_{22x'}=-s_{11y'}=100\{\tfrac{1}{2}(L_{11x}+L_{12x})_B-\tfrac{1}{3}\},$$

$$s_{12x'}=-s_{12y'}=s_{21x'}=100\{\tfrac{1}{2}(L_{13x}+L_{14x})_B-\tfrac{1}{3}\}.$$

Similar expressions give the s_{ikx} for the other lattice types. The symmetry of all lattices requires $s_{ikx}=s_{iky}$ and $s_{ikz'}=-s_{iky'}$ and from (15) it follows that $s_{ikx}=-2s_{ikz}$ and $s_{ikz'}=0$. For NaCl, CsCl, and ZnS we have evidently $s_{11x}=s_{22x}$, but for CaF_2 this is not true.[17]

The factors s_{ikx} and $s_{ikz'}$ in Table II determine the change of the Lorentz-Lorenz force produced by a uniform strain or shear. Our calculation does not,[18] however, take into account the "inner displacements" which occur for shear in ZnS and CaF_2.

TABLE II. *Change of Lorentz-factor with deformation.*

CRYSTAL TYPE	*SC*	*FC*	*BC*	NaCl	CsCl	ZnS	CaF_2		DI
$s_{11x}=s_{11y}$	0.50	0.03	0.01₅	0.03	0.50	0.03	0.03	0.50	−0.22
s_{11z}	−1.00	−.06	−.03	−.06	−1.00	−.06	−.06	−1.00	.44
$s_{12x}=s_{21y}$				.97	−.47	−.47	−.47	−.47	
s_{12z}				−1.94	.94	.94	.94	.94	
$s_{11x'}=-s_{11y'}$	.33	−.60	−.62	−.60	.33	−.60	−.60	.33	−1.09
$s_{12x'}$				1.26	−1.58	−1.58	−1.58	−1.58	

These values agree neither with Herzfeld's nor with Banerjee's results. Comparison with Herzfeld's notation shows (his Eq. (12)) that his values α and β give for the NaCl lattice

$$s_{11x}= 0.585-\tfrac{2}{3}=-0.082$$
$$s_{12x}=-1.248-\tfrac{2}{3}=-1.915$$
$$s_{11z}= 0.081-\tfrac{2}{3}=-0.586$$
$$s_{12z}= 2.255-\tfrac{2}{3}= 1.588.$$

s_{11x} and s_{12x} are in fair agreement with our values, but s_{11z} and s_{12z} are not. Since Poisson's equation requires $s_{11x}=-2s_{11z}$ and $s_{12x}=-2s_{12z}$, Herzfeld's values of s_{11z} and s_{12z} must be wrong.[19] Herzfeld's calculation is marred only by a numerical error, whereas Banerjee's method contains a fundamental error which is discussed in the next section.

BRAGG'S THEORY OF THE LORENTZ-LORENZ FORCE

Bragg's method is based on the classical procedure of H. A. Lorentz. One considers a spherical or cubical boundary around the chosen atom. The solid outside the boundary is considered

[17] For CaF_2 the first column in Table II refers to Ca, the second to F.

[18] These displacements, which give rise to the piezoelectric effect and invalidate the Cauchy relation for the elastic constants, complicate our problem considerably. They lead to $L_{ikx}\neq 0$. We neglect this effect, because the magnitude of the displacements is not known.

[19] The relation between s_{ik} and α, β was communicated to the writer by Professor Herzfeld. Professor Herzfeld agrees that his values, −0.081 and 2.255, are incorrect. He has asked me to call attention to the following corrections to his paper (J. Opt. Soc. Am. **17**, 26 (1928)): The first formula on p. 31 has the wrong sign and is incomplete. (The corresponding equation in the appendix is almost correct.) The factor 3 in the next formula should be omitted. In the second equation in the appendix, (3+1) should be replaced by (3+⅓) and, in the first formula on p. 36 some coefficients are wrong. A recalculation, carried out by Dr. M. Goeppert-Mayer, gives, for stress parallel to the field, $\alpha=-0.590$ and $\beta=1.276$. Using Poisson's equation, this gives for stress normal to the field $\alpha=-.706$, $\beta=-1.638$. These new values give $s_{11x}=0.039$, $s_{12x}=0.971$, $s_{11z}=-0.077$, $s_{12z}=-1.943$. They are in good agreement with our values, which have an accuracy of ±0.01.

continuous matter, and one adds to the field of this polarized continuum the field of the dipoles within the boundary. Banerjee[6] applies this method in the following manner. He considers a cubical boundary. The field of the continuum is then $4\pi P/3$ and the field of the dipoles within the cube is $F_x'=3\sum\mu_{ix}x_i^2/r_i^5-\sum\mu_{ix}/r_i^3$. In the undeformed state the latter vanishes for D lattices. Deformation due to a strain z_x changes the coordinates of each dipole from x_i, y_i, z_i to x_i, y_i, $z_i(1+z_x)$ and the field of the dipoles within the boundary can be developed in powers of z_x. In first approximation

$$F_x'=z_x[3\sum\mu_{ix}z_i^2/r_i^5-15\sum\mu_{ix}x_i^2z_i^2/r_i^7],$$
$$F_y'=z_x[3\sum\mu_{iy}z_i^2/r_i^5-15\sum\mu_{iy}y_i^2z_i^2/r_i^7],$$
$$F_z'=z_x[9\sum\mu_{iz}z_i^2/r_i^5-15\sum\mu_{iz}z_i^4/r_i^7].$$

Banerjee calculates these sums for the NaCl and CaF_2 lattice. His results can be written $F_{1x}'=8z_x\Delta^{-1}[B_{11x}\mu_{1x}+B_{12x}\mu_{2x}]$, where the B_{ikx} are the numerical values of the finite lattice sums. Since these sums contain only the coordinates of the atoms in the undeformed state, Banerjee extends the summations over a cube. But this is wrong. The atoms which are within a cube in the deformed state, are not within a cube in the original state. In other words, Banerjee does not calculate the field of the atoms contained in a cube of the deformed crystal, but of the atoms within a rectangular box with the dimensions $A_x:A_y:A_z=1:1:(1+z_z)$. Hence the field of the continuum is not $F''=4\pi P/3$ but

$$F_z''=4P_z\sin^{-1}\{2A_xA_yA_z(A_x^2+A_y^2+A_z^2)^{\frac{1}{2}}/(A_x^2+A_y^2)\cdot(A_x^2+A_z^2)\}.$$

This gives, in first approximation

$$F_x''=4\pi P_x/3+4P_x3^{-\frac{1}{2}}z_z,$$
$$F_z''=4\pi P_z/3-8P_z3^{-\frac{1}{2}}z_z$$

and the Lorentz-Lorenz forces are therefore

$$F_{ix}=E_x+F_{ix}'+F_x''$$
$$=E_x+4\pi\Delta^{-1}\sum n_k\mu_{kx}\times[\tfrac{1}{3}+z_z(2B_{ikx}\pi^{-1}n_k^{-1}+\pi^{-1}3^{-\frac{1}{2}})],$$
$$F_{iz}=E_z+F_{iz}'+F_z''$$
$$=E_z+4\pi\Delta^{-1}\sum n_k\mu_{kz}\times[\tfrac{1}{3}+z_z(2B_{ikz}\pi^{-1}n_k^{-1}-2\times3^{-\frac{1}{2}}\pi^{-1})].$$

Comparison with (16) gives

$$s_{ikx}=2B_{ikx}/\pi n_k+3^{-\frac{1}{2}}\pi^{-1},$$
$$s_{ikz}=2B_{ikz}/\pi n_k-2\times3^{-\frac{1}{2}}\pi^{-1}$$

and we can calculate s_{ikx} from Banerjee's value of B_{ikx}. For NaCl we get, since $n_1=n_2=4$

$$s_{11x}=-2s_{11z}=1.9005/2\pi-2\times3^{-\frac{1}{2}}\pi^{-1}=-0.0651,$$
$$s_{12z}=-2s_{12x}=-9.9613/2\pi-2\times3^{-\frac{1}{2}}\pi^{-1}=-1.9529.$$

For CaF_2, where $n_1=4$, $n_2=8$,

$$s_{11x}=-0.0651,$$
$$s_{22x}=-2s_{22z}=-8.0608/4\pi-2\times3^{-\frac{1}{2}}\pi^{-1}=-1.0090,$$
$$s_{12x}=-2s_{12z}=16.4904/4\pi-2\times3^{-\frac{1}{2}}\pi^{-1}=0.9447.$$

In Banerjee's paper the terms $2\times3^{-\frac{1}{2}}\pi^{-1}$ are neglected.[20]

The agreement between these and our previous results shows that the Ewald-Born and the Lorentz-Bragg methods are equivalent.

The Anisotropy of the Coulomb Forces

In an ionic lattice the potential of an atom i due to the charges $z_k\epsilon$ of all the other ions is $V_i=z_i\epsilon\psi(0)+\epsilon\sum'z_k\psi(r_{ik})$ ϵ is the positive value of the electronic charge and z_k is the valence of the ions k. The equilibrium condition demands $(\text{grad } V_i)_0=0$.

Under the influence of a light wave oscillating in the x direction the atom i becomes an oscillator. With Born[3] we make the assumption that the oscillator can be considered as a vibrating "electron" with the charge $-f_i\epsilon$. The forces acting on this electron are the binding force of the atom i, the Lorentz force of the light wave, and the Coulomb forces of all other ions. If the electron has a displacement u_{ix} from its rest position, the Coulomb field is

$$F_{ix}^c=-(\partial^2V_i/\partial x^2)_0\cdot u_{ix}=-\epsilon u_{ix}[z_i(\partial^2\bar{\psi}/\partial x^2)_0+\sum_{i\neq k}z_k(\partial^2\psi/\partial x^2)_{r_{ik}}].$$

[20] It is surprising that, in spite of this large error, Banerjee finds reasonable results. This is probably due to his questionable method for calculating the refractive index (Banerjee's Eq. (6) and (8)). We have not succeeded in correcting his calculations for shear.

In a D lattice it follows from (15) that $(\partial^2\bar{\psi}/\partial x^2)_0 = (\partial^2\psi/\partial x^2)_{r_{ik}} = 4\pi/3\Delta$ and hence $F_{ix}{}^c = -\epsilon u_{ix} 4\pi/3\Delta \cdot \sum z_k = 0$ because of the neutrality condition. Hence the Coulomb forces do not influence the refraction of D lattices.

In an elastically deformed D lattice, we get, using (13) and (14) $F_{ix}{}^c = -4\pi\epsilon u_{ix}\Delta^{-1}\sum z_k L_{ikx}$. Since $-u_{ix} f_i \epsilon = \mu_{ix}$, $\sum z_k = 0$, this can also be written

$$F_{ix}{}^c = 4\pi\mu_{ix} z_i (f_i\Delta)^{-1} \sum z_k n_k s_{ikx}. \tag{18}$$

Analogous equations hold for $F^c{}_{iz}$, $F^c{}_{ix'} = -F^c{}_{iy'}$. In amorphous[7] solids all $s_{ikx} = 1/15$, $s_{iks} = -2/15$ and hence, since $\sum n_k z_k = 0$, Coulomb forces have no influence.

Influence of Hydrostatic Pressure

Hydrostatic pressure does not change the symmetry of cubic crystals. Since $x_x = y_y = z_z$ it follows from (15) that the Lorentz factor is $1/3$ and the Coulomb forces have no influence. This supports our previous statement that, in cubic crystals, the change of refraction is not due to the Coulomb forces, but is caused by a change in the binding force of the optical electrons.

The Lorentz-Lorenz equation must therefore be valid for hydrostatic pressure and should determine the change of the index of refraction n with the density ρ. Pockels[10] has calculated $dn/d\rho$ from photoelastic data, using (3), and has shown that for NaCl, CaF_2, and probably also for KCl, it has practically the same value as $-1/\alpha \cdot dn/dt$, where α is the coefficient of temperature expansion. But the observed increase of n with density is considerably smaller than the value given by the Lorentz-Lorenz equation. This equation can only be reconciled with the observations if we assume that a compression reduces the polarizabilities of the atoms. We must assume that a change of volume ΔV increases all refractions $R_i' = R_i(1+\lambda_i \Delta V)$ and get then

$$\rho \cdot dn/d\rho = (n^2-1)(n^2+2)(1-\lambda_0)/6n$$
$$\lambda_0 = \sum \lambda_i n_i R_i / \sum n_i R_i. \tag{19}$$

The data in Table III show that λ_0 has, within the accuracy of the data, the same value for NaCl, KCl, and CaF_2, and differs but little from the value[7] 0.4 found for glasses.

TABLE III.

CRYSTAL	$\rho dn/d\rho$	$-(1/\alpha)dn/dt$	$(n^2-1)(n^2+2)/6n$	λ_0
NaCl	0.304	0.305	0.656	0.536
KCl		.30	.576	.48
CaF_2	.251	.22	.498	.50

Optical Anisotropy of the Atoms

It is natural to assume that in unstrained D lattices all atoms are optically isotopic. Since a hydrostatic pressure alters the refractions, a strain will produce optical anisotropy of the atoms. A distortion of the lattice produces a deformation of the atoms. We must assume a linear change of the molar refractions R_k, or the polarizabilities α_k, with the strain. If A is Avogadro's number, we have

$$R_{kz} = 4\pi A\alpha_{kz}/3 = R_{ky} = R_k(1+\lambda_{kz} z_z),$$
$$R_{kx} = 4\pi A\alpha_{kx}/3 = R_k(1+\lambda_{kz} z_z). \tag{20}$$

For a shear we must assume

$$R_{kx'} = R_k(1+\lambda_{kx'} x_x'), \quad R_{ky'} = R_k(1+\lambda_{ky'} x_x').$$

The change of the refraction due to hydrostatic pressure is determined by $\lambda_i = \frac{1}{3}(\lambda_{iz} + 2\lambda_{ix})$.

Calculation of the Photoelastic Constants

Under the influence of the Lorentz and Coulomb forces the atoms i acquire the dipole moments $\mu_{iz} = \alpha_{iz}(F_{iz} + F_{iz}{}^c)$, where α_{iz} is the polarizability for the frequency of the lightwave. Introducing the expressions from Eqs. (16), (18) and (20), we get a set of linear equations for the moments μ_{iz}

$$\mu_{iz} = 3R_i(1+\lambda_{iz} z_z) A^{-1}\left[E_z/4\pi + \Delta^{-1}\sum n_k \mu_{kz}(\tfrac{1}{3} + s_{ikz} z_z) + \mu_{iz} z_z (f_i\Delta)^{-1}\sum z_k n_k s_{ikz}\right].$$

From their solutions we determine

$$(n_z{}^2-1)/4\pi = P_z/E_z = \sum n_k \mu_{kz}/E_z. \tag{21}$$

For $z_z = 0$, one finds the Lorentz-Lorenz equation $(n^2-1)/(n^2+2) = \sum n_k R_k / A\Delta$. Differentiation of (21) gives, according to (4), p_z, and if the same

way one determines p_z and $p_{z'}$. In differentiating we must take into account the fact that a strain z_z changes the volume Δ of the elementary cell. The final result can be written

$$\begin{aligned} p_x &= p_0 + p_x^L + p_x^c + p_x^A, \\ p_z &= p_0 + p_z^L + p_z^c + p_z^A, \\ p_{z'} &= \quad p^L{}_{z'} + p^c{}_{z'} + p^A{}_{z'}. \end{aligned} \tag{22}$$

p_0 is due to the change of the density

$$p_0 = (n^2+2)/3(n^2-1). \tag{23}$$

This term is responsible for the fact that p_{11} and p_{12} always have positive values. p_x^L is due to the anisotropy of the Lorentz force

$$p_x^L = -\sum_{i,\,k} s_{ikx} n_i n_k R_i R_k / (\sum n_k R_k)^2, \tag{24}$$

p_x^c gives the effect produced by the Coulomb field of the ions

$$p_x^c = -\sum R_i^2 n_i f_i^{-1} \sum_k n_k z_k s_{ikx} / (\sum n_k R_k)^2. \tag{25}$$

If the refraction of the atoms i is represented by a set of oscillators with the refractions R_{it} and strengths f_{it}, one must substitute $R_i^2/f_i = \sum R_{it}^2/f_{it}$; $R_i = \sum R_{it}$. p_x^A is the contribution of the optical anisotropy of the atoms due to strains

$$p_x^A = -(n^2+2)\lambda_x/3(n^2-1), \tag{26}$$

where

$$\lambda_x = \sum \lambda_{ix} n_i R_i / \sum n_i R_i.$$

Equations analogous to (24), (25), (26) give p_z^L, $p^L{}_{z'}$, etc. Finally we write

$$p = p_z - p_x = p^L + p^c + p^A, \tag{27}$$

where, since for all D lattices $s_{ikz} = -2s_{ikx}$, $p^L = -3p_x^L$, $p^c = -3p_x^c$, $p^A = -\lambda(n^2+2)/3(n^2-1)$; $\lambda = \lambda_z - \lambda_x$. λ_0, which determines the change of refraction due to hydrostatic pressure, is

$$\lambda_0 = \tfrac{1}{3}(\lambda_z + 2\lambda_x). \tag{28}$$

The shear constant of photoelasticity is given by

$$p' = p'^L + p'^c + p'^A, \tag{29}$$

where

$$p'^L = p^L{}_{z'};\ p'^c = p^c{}_{z'};\ p'^A = -\lambda'(n^2+2)/3(n^2-1);$$
$$\lambda' = \sum \tfrac{1}{2}(\lambda_{ix'} - \lambda_{iy'}) n_i R_i / \sum n_i R_i.$$

Eqs. (27) and (29) represent our final result. They give p and p', which, according to (4), are proportional to the elasto-optical constants.

Comparison With Experimental Results

In the experiments the accidental birefringence is measured as a function of the applied pressure. If C is the difference in optical path of the ordinary and extraordinary ray produced by a pressure of 1 dyne/cm² directed normal to the light path of 1 cm length, then

$$p_{11} - p_{12} = 2\lambda C_1 / n^3 (s_{11} - s_{12});$$
$$p_{44} = 2\lambda C_2 / n^3 s_{44}.$$

Here λ is the wavelength of the light, s_{ik} are Voigt's elastic moduli, and C_1 and C_2 refer to pressure normal to the cube and octahedral faces, respectively. If the pressure is normal to a dodecahedral face, one gets[21] $C_3 = C_2$, $C_4 = \tfrac{1}{2}(C_1 + C_2)$, where C_3 and C_4 are for light normal to dodecahedral and cubic faces, respectively. Only determinations of C for small pressures have a physical significance. Large pressures produce translation gliding and lead to irreversible effects.[22]

Reliable determinations of all the quantities C_i, s_{ik} and n are available only for NaCl, KCl and CaF_2.[23] They refer to sodium light and give for NaCl $p = -0.124$, $p' = -0.065$; for KCl $p = 0.179$, $p' = -0.182$ and for CaF_2 $p = -0.653$ $p' = 0.179$.

For crystals of the type NaCl the theory gives

$$p = (R_1+R_2)^{-2}[0.09(R_1^2+R_2^2) + 5.82R_1R_2 + 2.82z(R_1^2/f_1 - R_2^2/f_2)] - \lambda(n^2+2)/3(n^2-1), \tag{30}$$

$$p' = (R_1+R_2)^{-2}[0.60(R_1^2+R_2^2) - 2.52R_1R_2 - 1.86z(R_1^2/f_1 - R_2^2/f_2)] - \lambda'(n^2+2)/3(n^2-1). \tag{31}$$

[21] Pockels' data verify these relations, but Banerjee's data give slightly different results. According to our theory we must expect deviations from Pockels' theory, because the λ_{ix} are not components of a simple tensor.

[22] The results of Maris, J. Opt. Soc. Am. **15**, 194 (1927) are probably due to this effect. This is shown by Ritzel, Zeits. f. Krist. **52**, 275 (1912).

[23] The values for NaCl are averages calculated from the

The index 1 refers to the negative ion, and z is the valence of both ions.

Under a pressure normal to a cube face the NaCl lattice approaches the structure of a chain lattice. Consequently the influence of the Lorentz force given by the first two terms of (30) produces positive birefringence. The next terms are due to the Coulomb forces. The negative ions give a positive contribution because they are surrounded by positive ions which attract the optical electron. A pressure increases this attraction in the direction of the stress, and hence this gives rise to positive birefringence. For the positive ions this effect is reversed, but, since in most cases $R_1 > R_2$, the net effect of the Coulomb forces is a positive double refraction. Hence in every case the Born-Ewald theory gives positive birefringence for any NaCl lattice compressed normal to a cube face. The fact that sodium chloride shows negative birefringence shows clearly the importance of the optical anisotropy of the atoms due to pressure. We conclude that p is the difference between two large terms of equal magnitude, and this explains why it is always small for NaCl lattices, and why it can be positive or negative.

For pressure normal to an octahedral face the Lorentz force gives either a small positive or a negative effect. But the Coulomb forces and the anisotropy produce negative birefringence, and hence p' is always negative for NaCl lattices.

A quantitative test of the theory requires the values of R and f. The ionic refractions are known with a satisfactory degree of accuracy. However, very little is known concerning the strengths f_i of the oscillators. Herzfeld and Wolf[24] have shown that for ions f probably has the same values as for the corresponding inert gases. We shall base our calculation on this assumption, but we are aware that this may be incorrect. From the point of view of the quantum theory of dispersion there is even some doubt whether our f values are identical with the strength of the oscillators.[25]

If we use for NaCl and KCl the values given by Herzfeld and Wolf, we get

$$\text{for NaCl } p = 0.401 + 0.597 - 1.055\lambda;\ p' = 0.392 - 0.394 - 1.055\lambda';$$

$$\text{for KCl } p = 1.008 + 0.426 - 1.152\lambda;\ p' = 0.005 - 0.282 - 1.152\lambda'.$$

To get agreement with the experimental results, we must have for NaCl, $\lambda = 1.06$, $\lambda' = 0.06$; for KCl, $\lambda = 1.08$, $\lambda' = -0.09$.

These results are very satisfactory for the following three reasons:

(1) The order of magnitude of the values of λ is the same as for glasses. For glasses[7] we calculated $L^* \sim 0.6$, and this represents an average value between λ and λ'. From (28) and the data in Table II we get for NaCl, $\lambda_s = 1.24$, $\lambda_z = 0.18$; for KCl, $\lambda_s = 1.20$, $\lambda_z = 0.11$. This leads to the same conclusions as in our first paper. A strain of 1 percent increases the refractions parallel to the strain by about 1.2 percent. Moreover, it increases slightly the refractions perpendicular to the strain.

(2) Although they have different photoelastic properties, both crystals lead to almost identical values of all factors λ. This agrees with the fact that the refraction of NaCl and KCl is largely due to the Cl ions.

(3) In both crystals the anisotropy produced by a strain z_z is much larger than the anisotropy produced by a shear. A strain alters the distance between nearest neighboring atoms. For a shear, however, the NaCl distance remains unchanged. Hence $\lambda > \lambda'$. The optical anisotropy due to a shear is caused by the change of the Cl-Cl distance. In NaCl the Cl ions are in contact with each other because the Na ions are smaller than the Cl ions. In KCl the Cl-Cl distance is larger; hence $\lambda'_{NaCl} > \lambda'_{KCl}$. A negative value of λ' is improbable and can be avoided by choosing slightly different values of R_i and f_i.

If, as in KCl, the anion and cation are almost equal in size and structure, it is reasonable to assume $\lambda' = 0$ and $f_1 = f_2$. The shear constant of photoelasticity is then determined by the Ewald-Born theory, and this offers a unique method

data of F. Pockels, Ann. d. Physik **39**, 440 (1890), and of K. Banerjee, Ind. J. Phys. **2**, 195 (1927). Their results differ by about 8 percent. Pockels' results for KCl are corrected by using Försterling's values of the elastic constants (Zeits. f. Physik **2**, 172 (1920)). CaF_2 was measured by Pockels, Ann. d. Physik **37**, 372 (1889). Many other investigators have verified the signs and order of magnitude of the six constants.

[24] Herzfeld and Wolf, Ann. d. Physik **78**, 35 (1925).

[25] Herzfeld and Lee, Phys. Rev. **44**, 623 (1933) conclude that f is probably larger than the strength of the oscillator.

for the determination of the ratio $r=R_1/R_2$ of the ionic refractions. Namely, it follows then from (31)

$$(1+r)^2p'=0.60(1+r^2)-2.52r-1.86(r^2-1)/f.$$

Assuming $f_K=f_{Cl}=f_{A^r}=4.58$ leads to $r=5.12$, and since $R_K+R_{Cl}=R_{KCl}=10.85$ we get $R_{Cl}=9.07$, $R_K=1.78$. R_{Cl} is in very good agreement with the value given by Born and Heisenberg.[26] R_K is somewhat smaller than the accepted value for the free ion, $R_K=2.23$. Agreement with the values of Fajans and Joos[8] and Pauling[27] can be reached by choosing $f=5.9$, or by assuming a 30 percent larger experimental value. The latter alternative is not excluded because Pockels and Voigt report that their KCl crystals were optically and elastically imperfect.

For CaF_2 the theory gives, if we introduce $R_F=2.5$, $R_{Ca}=1.35$, $f_F=2.37$, $f_{Ca}=4.58$, $p=0.46-0.73-1.28\lambda$; $p'=0.35+0.48-1.28\lambda'$. For a pressure normal to a cube face the Lorentz force again produces positive birefringence, but this is compensated by the negative contribution of the Coulomb forces. Hence CaF_2 becomes negatively birefringent. For a pressure normal to an octahedral face the Lorentz and Coulomb forces produce positive birefringence which cannot be compensated by the relatively small anisotropy due to shear. Qualitatively the theory explains the photoelastic properties of fluorite. Quantitatively, however, we find $\lambda=0.3$, which is certainly too small, and $\lambda'=0.5$, which is too large. By choosing $f_F=5$, much more sensible values, $\lambda=0.61$, $\lambda'=0.06$, are obtained. An investigation of the dispersion of the photoelastic effect should determine the proper choice of the f values. It is doubtful whether the inner displacements would change the result.

For diamond Wertheim[28] observed a negative stress optical constant, but he does not state the direction of pressure. The fact that the photoelastic effect can be observed even in small crystals in spite of the large elastic constants of diamond, indicates that either p or p' must have an unusually large negative value. The theory confirms that $p=-0.66-\lambda(n^2+2)/3(n^2-1)$ is negative and at least ten to twenty times larger than for NaCl. Since the index of refraction of diamond increases with temperature,[29] λ is probably also unusually large.

[26] Born and Heisenberg, Zeits. f. Physik **23**, 388 (1924).
[27] L. Pauling, Proc. Roy. Soc. **A114**, 181 (1927).
[28] Wertheim, Pogg. Ann. **86**, 321 (1852).

Photoelasticity and Crystal Structure

Pockels[10] has classified the cubic crystals in four groups according to the signs of $(p_{11}-p_{12})$ and p_{44}, or, what is equivalent, of p and p'.

Group	p	p'	*Example*
I	+	+	none
II	−	−	NaCl
III	−	+	CaF_2
IV	+	−	KCl

Observations with crossed nicols of the interference colors produced by pressure decide to which group a crystal belongs.

In general the theory is not able to predict the sign of p and p'. Negative values are assured if the Lorentz and Coulomb forces produce negative birefringence, because the anisotropy will always give a negative effect. If p^L and p^c together give a positive value, the result depends on whether or not (p^L+p^c) is large enough to compensate the effect of the anisotropy of the atoms. Since the magnitude of the latter cannot be predicted, no definite answer can be given. Our results on glasses, NaCl and KCl indicate that p^A has for most substances nearly the same value. Hence we expect a positive value of p if $(p^L+p^c)>1$. For shear the anisotropy produces a smaller effect and hence p' will be positive if $(p'^L+p'^c)>0.3$. The choice of these limits is somewhat arbitrary, and in border cases our conclusions will not always be justified.

Using these critical values we are now able to predict certain correlations between Pockels' groups and the various cubic lattice types. For monoatomic crystals we have $p^c=0$, $p^L=3s_{11x}$, and $p'^L=-s_{11x'}$. From the values in Table II we conclude that simple cubic lattices belong to group IV, face- and body-centered and diamond lattices to group III or eventually to group II. Experimental verification is only possible for diamond.

For the diatomic ionic lattice types, NaCl, CsCl and ZnS, the results depend on the ratio

[29] A. Sella, Rend. Acc. Lincei **7**, 300 (1891).

$r=R_-/R_+$, the values of f_-, f_+ and the valency z. For all three types we have

$$p^L+p^c=3s_{11z}+3(s_{12z}-s_{11z})\times(1+r)^{-2}\cdot[2r+(r^2-f_-/f_+)z/f_-],$$

$$p'^L+p'^c=-s_{11z'}+(s_{11z'}-s_{12z'})\times(1+r)^{-2}\cdot[2r+(r^2-f_-/f_+)z/f_-].$$

Fig. 3 shows the variation of p^L+p^c and $p'^L+p'^c$ with r. The dotted curves give p^L and p'^L. We have assumed[30] $f_-/f_+=1$, and have used the values $z/f_-=0.2$ and $z/f_-=0.4$. For most crystals z/f_- will be between these limits. For lattices of the type CaF_2 we get two sets of curves, one corresponding to CaF_2, BaF_2, etc., the other to Li_2O, Na_2O, etc. The curves in Fig. 3 are calculated for $f_-=3$ and $f_-=6$, $f_-/f_+=1$.

Fig. 3 shows that, whenever p^L+p^c is large, $p'^L+p'^c$ is small or negative, and *vice versa*. Consequently, none of the lattice types considered corresponds to Pockels' group I. No crystal belonging to this group has ever been found.

For the lattice type NaCl p' is always negative; hence these crystals belong either to group II or IV. They belong to group IV if $r<10$ or if z/f_- is large. This is the case for all K-, Rb-, Cs- and NH_4-halides, and for the bivalent salts, BaO, CaO, etc. The Na- and Li-halides, however, belong to group II. According to Fig. 3 no other lattice type belongs to group IV. This fact can therefore be used for the determination or verification of crystal structures.

The CsCl structures can belong to group II or III, but, since group II requires $r>10$, all the Cs- and NH_4-halides will have the photoelastic properties of group III. No observations on these crystals have been made. Measurements

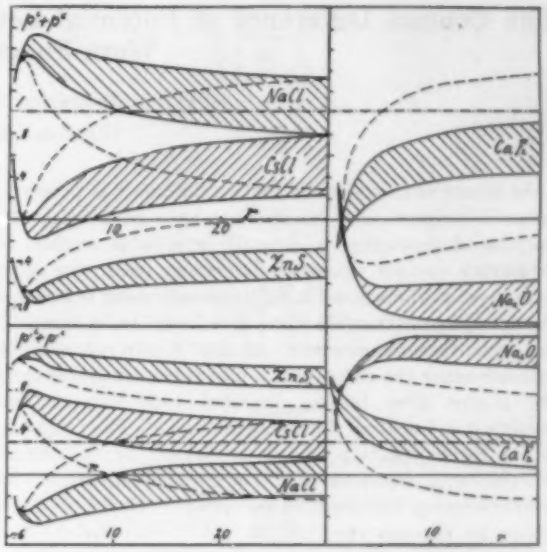

FIG. 3. Variation of photoelastic constants with ionic refraction ($r=R_-/R_+$).

on the ammonium-halides would furnish an interesting test of the theory because the two modifications of these crystals should show different photoelastic properties.

Crystals of the type CaF_2 behave like CsCl and all known crystals belong to group III.

All crystals of the types ZnS and Na_2O should belong to group III irrespective of whether the binding is homopolar or ionic. For ionic crystals an unusually large effect would have to be expected.

All these conclusions agree with the known facts. The number of reliable[31] observations is very limited, and we hope to present soon further verification of the theory. An extension of the theory to more complicated lattices requires the calculation of intricate lattice sums.

[30] In all cases where f_-/f_+ differs much from unity the ratio r is so large that the value of f_-/f_+ is immaterial.

[31] Many observers do not realize that in cubic crystals the photoelastic effect depends on the direction of pressure and observation, and their results cannot be used since they neglect to state these directions.

The Contact Difference of Potential Between Tungsten and Barium. The External Work Function of Barium

PAUL A. ANDERSON, *State College of Washington*

(Received January 26, 1935)

An intensive study of the contact difference of potential between tungsten and barium has been made with the purpose of developing a generally applicable method of measuring contact potential differences under the most rigorous conditions possible. Extreme outgassing of surfaces in the highest attainable vacuum is found to be essential but when these requirements are met highly reproducible measurements can be obtained. The tubes are sealed from the pumps after baking, gettered with barium, and immersed in liquid air during measurement. The tungsten, in the form of a thin ribbon, is cleaned by flashing at 2800°K until its work function remains unaltered by further heating. Barium films are deposited on the tungsten ribbon by thermal vaporization and their reproducibility checked by measuring a succession of films formed in a fractional distillation of the metal. The measuring technique is designed to detect any changes in work function which may occur immediately after the preparation of a clean surface and to prevent accidental contamination of those parts of the tube which must be maintained at constant work function. Sharp localization of the surface areas for which electron current-potential characteristics are taken and an increased sensitivity of measurement are secured by using a narrow and intense beam of electrons and determining displacements of the characteristics in the retarding potential region. Measurements with three types of tubes and with samples of tungsten and barium from several different sources give the value 2.13 ± 0.05 volts for the contact difference of potential between tungsten and barium; 2.39 ± 0.05 equivalent volts for the external work function of barium. The method can, presumably, be quite generally applied to the measurement of the contact potential difference between a tungsten reference surface and any other metal and is adapted, also, to the study of dilute films of any metal on tungsten.

IT is a consequence of the Sommerfeld theory that the contact difference of potential between two metal surfaces is equal to the difference between their external work functions:[1]

$$V_{ab}=\phi_a-\phi_b.$$

Contact potential measurements should be capable (1) of determining work function values for a far wider range of surfaces than can be studied by either thermionic or photoelectric methods, and (2) of furnishing a powerful means of attack upon adsorption problems, in which studies of highly dilute adsorbed films may be expected to be especially significant.

The fact that these rather attractive possibilities have not been more fully realized in practice probably can be attributed to the lack of a generally applicable technique of measurement providing for adequate vacuum conditions and sufficiently thorough outgassing of surfaces. This lack, evident even in much of the recently published work, is reflected in the discordant results which have characterized contact potential measurements generally. It was the purpose of the present work to make a careful study of contact potential in a single system of intrinsic importance with a view to determining the vacuum and outgassing conditions required for reproducible measurements, and to developing a method of measurement applicable to a wide variety of metals.

The main features of the method as it has been worked out are: (1) After thorough outgassing the tube is sealed from the pumping system, gettered by the vaporization of barium, and immersed in liquid air during measurement. (2) Clean tungsten is chosen as a reference surface to which the contact potential difference of the pair of metals is referred. For the purpose of systematizing the results of different investigations the selection of a standard reference surface has manifest advantages. Since tungsten is one of the few metals which can be heated to temperatures necessary for the removal of all gaseous and solid surface impurities and since its work function is known so accurately that a reliable determination of the contact potential between it and any "unknown" surface establishes the work function of the latter, it is well suited to the purpose. (3) The metal surface to be measured against tungsten is formed by thermally vaporizing the metal and the purity of the film

[1] Eckart, Zeits. f. Physik **47**, 38 (1928).

finally measured checked by measuring the contact potential of each of a succession of films formed in a fractional distillation of the metal. The attainment of a contact potential unaltered by further distillation is taken as the criterion of a clean film. It is likely that the metals which melt or vaporize at temperatures below the vaporizing temperatures of the common oxides and salts, i.e., most of the common metals, can be freed of solid surface impurities as well as adsorbed gases only by such a distillation in high vacuum. The extension of the technique to the general case in which barium is not one of the metal pair undergoing measurement involves merely the addition of a separate barium gettering chamber to the tube. (4) A method of measurement is used which makes it possible to follow closely any changes in work function which may be experienced by the tungsten immediately after it is flashed, or by the freshly distilled metal film immediately after it is formed. It was found early in the course of this work that in an unsatisfactory vacuum the work function of a fresh surface changes very rapidly and may then attain a constant value which, without provision for immediate measurement, might be accepted as characteristic of the clean surface.

Method

Contact differences of potential have been measured in the past by the well-known Kelvin method[2] and by determining the displacement along the potential axis between the parallel electron current-potential characteristics given by surfaces of different work function. The latter method has been employed in various modifications by Mönch,[3] Langmuir and Kingdon,[4] and Kösters,[5] and Mönch[6] has published some results which seem to indicate that the Kelvin and electron methods when applied to a given surface yield values which agree within the experimental error.[7]

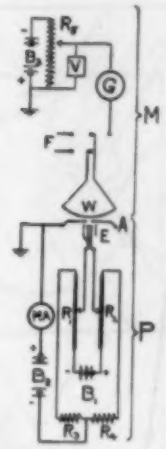

FIG. 1. The circuits: P for producing electron beam and M for determining electron current-potential characteristics of the surface W. $R_1=R_2=1.2$ ohms. $R_3=R_4=300$ ohms. F = flashing current leads.

In the present work the electron method as previously employed has been modified by using, instead of a diffuse stream or space-charge cloud of electrons spread over a relatively large area of the receiving surface, an intense and narrow beam of slow electrons projected against a small and sharply defined section of the surface. This area, while large with respect to the small-scale structural variations which characterize the surface, is small enough to eliminate uncertainties due to accidental large-scale variations over the surface. The sensitivity of measurement, as determined by the slope of the electron current-potential characteristic, is also materially increased. By using the characteristic curve displacement in the region of retarding potential it has been possible to obtain with a short period galvanometer of only moderate sensitivity (10^{-8} amp.) a precision of measurement of the order of 10^{-3}–10^{-4} volt, or from ten to one hundred times the best reproducibility which can be expected. Fig. 1 is a self-explanatory diagram of the electrical circuits with a schematic indication of the tube.

The method of measurement may be outlined as follows. A beam of 4 to 8 volt electrons is directed by the electron gun EA against a small area near the center of the strip of tungsten foil W and the current to the foil plotted as a func-

[2] An interesting modification of the Kelvin method has been described by Zisman, Rev. Sci. Inst. **3**, 367 (1932).
[3] Mönch, Zeits. f. Physik **47**, 522 (1928).
[4] Langmuir and Kingdon, Phys. Rev. **34**, 129 (1929).
[5] Kösters, Zeits. f. Physik **66**, 807 (1930).
[6] Mönch, Zeits. f. Physik **65**, 233 (1930).
[7] It should be pointed out that it is only in the work of Langmuir and Kingdon that the outgassing methods employed have been adequate. Their technique is adapted only to the study of surface films of substances which have an appreciable vapor pressure at room or slightly elevated temperatures.

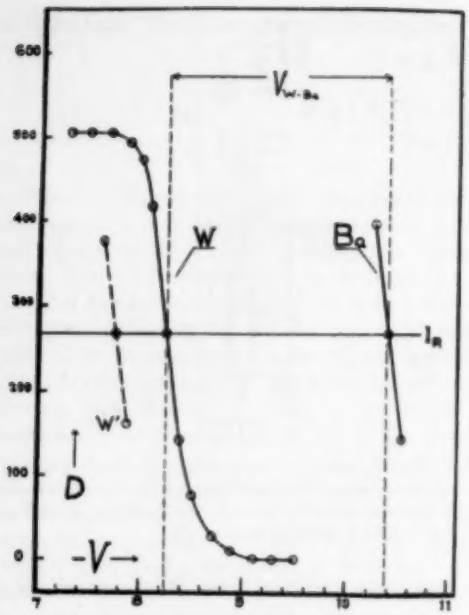

FIG. 2. Typical current-potential characteristics for clean tungsten *W*, barium *Ba*, and incompletely cleaned tungsten *W'* surfaces. Current in mm galvanometer deflection *D* Retarding potential $-V$ in volts. 7 volt electrons.

tion of the retarding potential applied to the strip. A typical curve is reproduced in Fig. 2. Any change in the work function of the surface, whether due to a readsorption of gas or to the deposition of another metal, produces a shift of the straight-line portion of the curve by an amount equal to the contact difference of potential between the initial and final states of the surface. The shifts produced by a barium coating and by a slight gas contamination are indicated in the figure. In practice the shift is determined by first plotting the curve for the clean tungsten reference surface, choosing a reference current I_R near the middle of the straight-line part of the curve, and then determining the change in applied potential necessary to reestablish this reference current. Rapid changes in work function such as occur immediately after flashing tungsten in an unsatisfactory vacuum are followed by observing the drift in the galvanometer deflection for a fixed applied potential. In an adequate vacuum this drift becomes negligible during the time required for a set of measurements.

In the early stages of the work an ionization manometer was used for measurement of residual gas pressures in the tube but it became clear that the testing procedure just outlined, referred to hereafter as the "vacuum test," was more reliable than measurements with the ionization gauge, which itself usually evolves or cleans up gas during operation. Such ionization gauge measurements as were made showed the pressure to be 10^{-8} mm or less when the vacuum test was satisfactory.

Photoelectric emission from *W* under the stimulus of light from the electron emitter was a possible source of error which had to be considered. An inverse electron current large enough to introduce such an error would, however, produce a detectable overrunning of the galvanometer zero at high retarding potentials. Since no overrunning could be detected either with tungsten or with barium surfaces the inverse currents if present must have been negligibly small.

THE TUBE

Tubes of three different types, only one of which will be described in detail, have been studied during the course of this work. The first tubes to be tried out, designated Type 1, were of very simple design. The tungsten strip was mounted opposite the mouth of an electron gun of the Farnsworth pattern[8] and barium vaporized from a molybdenum foil oven mounted at the side of the tube between gun and strip. After outgassing, sealing off, gettering, and prolonged immersion of the tube under liquid air or liquid hydrogen[9] the vacuum was such that the galvanometer deflection read a few seconds after flashing the tungsten at 2800°K remained unchanged to within 1 mm when the tungsten was allowed to stand cold for periods as long as 20 minutes; i.e., the work function remained constant to within 0.001 volt during this period. The behavior of a freshly deposited barium film was similar, but upon removing the barium by flashing and repeating the measurements, or carrying through measurements on successively deposited films, erratic variations in the contact potential differences amounting to several decivolts were found.

[8] Farnsworth, J. O. S. A. and Rev. Sci. Inst. **15**, 290 (1927).

[9] This part of the work was carried out at the Kältelaboratorium of the P. T. R., Berlin, during the tenure of a National Research Fellowship.

These variations were attributed, correctly as later work showed, to contamination of the electron gun with barium, which apparently migrated over the outside of the oven and was vaporized from its bottom. As would be expected, the variations between successive measurements decreased as repeated contaminations brought the gun surfaces nearer to an equilibrium state, and in fact the contact potential value finally obtained with this type of tube agrees to within 0.1 volt with our latest value.

It was clearly desirable, however, to devise a tube in which all possibility of contamination of parts which must remain at constant work function is eliminated. The later tubes were, therefore, designed to meet the following specific requirements. (1) During deposition of barium or other metal on the tungsten surface it must be impossible for the vapor to come into contact with any part of the electron gun. (2) It must be possible to fuse and vaporize the metal in the oven while access of vapor to the tungsten is prevented and then, without cooling the oven, to form the film which is to be measured. (3) It must be possible to remove the metal film from the tungsten without permitting the vapor to strike the gun. (4) The tungsten receiving strip must be close enough to the mouth of the electron gun during the measurements to insure the localization of the beam at a small spot near the middle of the strip. Of these requirements the first is essential in any measurement, the second is added to eliminate the possibility of forming the film while the vaporizing metal is emitting gas which it has absorbed while standing cold, the third to allow of repeating the measurements under constant conditions, and the fourth to eliminate errors due to electrons picked up by lead wires or the less thoroughly outgassed ends of the receiving strip. Other necessary features of a satisfactory design are the elimination of large metal parts which cannot be thoroughly outgassed and sufficient compactness to permit of immersing the tube under liquid air.

The tube used in our latest measurements is sketched in plan and elevation in Fig. 3. The requirements noted above are met by placing the tungsten ribbon W on a simple rotating spindle S and by suitable geometric arrangement of the electron gun EA, vaporizing oven B, and mica

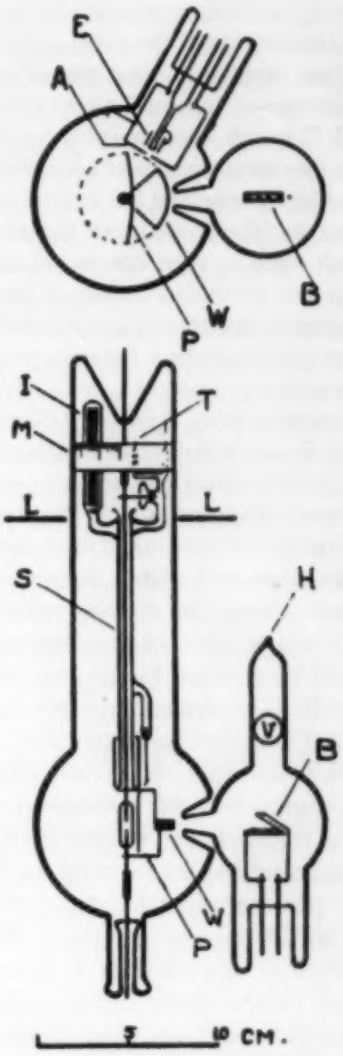

FIG. 3. The tube. W = tungsten ribbon. B = barium oven. EA = electron gun. S = rotating spindle.

shield P.[10] The spindle was built of two lengths of 1.5 mm tungsten wire connected by a Pyrex bead as shown, and a length of close-fitting Pyrex capillary which carried the shield, glass-enclosed armature I, and glass sights T. The spindle was mounted on small nickel sockets pressed on the 1.5 mm tungsten leads which supplied the flashing current to the strip, and driven by the action of a small electromagnet on I. Any desired setting of the spindle could be easily obtained to

[10] A glass or quartz shield would be preferable. The mica was badly blistered by the heat radiated from the tungsten ribbon during flashing.

±0.25 mm by sighting across the paper scale M, pasted on the outside of the tube, and the sharp-pointed glass sights. During measurement the tube was immersed in liquid air to the level LL. The shield P, which became coated with barium during the measurements, was grounded through a whisker which connected the light molybdenum wire supporting the shield with the walls of the tube, which were in turn connected by another whisker to the grounded anode of the electron gun. The spindle sheath was petticoated as shown to preserve the insulation between the leads to W and ground.

The vaporizing oven B was of 0.01 mm molybdenum foil 5 mm wide, bent to form a shallow trough in its horizontal section and carried up to form a heated deflector, which directed an adequate quantity of barium vapor toward the orifice. The oven and orifice defined the vapor beam which entered the main chamber and it is clear that all of the requirements mentioned above could be satisfied by appropriate settings of the spindle. The electron gun consisted of the emitter E of tungsten foil $0.02\times2\times8$ mm bent into a narrow stirrup with effective emitting surface 2×2 mm, a focusing cylinder made of foil of the same thickness and welded to the negative emitter lead, and the accelerating diaphragm A, a strip of pure tungsten foil $0.01\times10\times30$ mm mounted on 1.5 mm current leads. The hole at the center of A was 1.2 mm in diameter. The field set up by the anode and focusing cylinder concentrated the electrons from the emitter upon the center of the anode near the orifice, increased the electron beam intensity and the slope of the current-potential curves, and prevented the straying of electrons around the edges of the anode. The construction of the anode allowed it to be cleaned by flashing not only during the outgassing period but at any time during the course of the measurements.

The tungsten ribbon W, $0.025\times4\times30$ mm, was cut from foil which was stated by the makers, the P. R. Mallory Company, to be the purest available. It, as well as the emitter, anode, and oven, was attached to its molybdenum support wires with small molybdenum rivets to prevent contamination of the surfaces by migrating welding flux.

Procedure

During outgassing the tube was connected at V with a conventional pumping system which consisted of, numbering from the tube, two liquid air traps in series, CO_2 trap, McLeod gauge, and Gaede two-stage mercury diffusion pump. There were, of course, no waxed or greased joints between pump and tube. The liquid air trap nearest the tube showed no trace of condensed mercury at any time. Before the barium was put into the oven the tube was baked at 500°C for at least 48 hours and the metal parts given a preliminary heating. The tube was then opened at H, about 1.5 grams of barium placed in the oven, and the tube quickly sealed off and evacuated. Barium from two sources was used in the measurements, a sample prepared originally by Dr. A. J. King and furnished to me by Professor P. W. Bridgman with an analysis showing a trace of strontium as the only impurity, and a sample obtained from Osram which was stated to contain traces of strontium and iron as the only impurities. No differences between the samples were detected in the measurements.

After re-evacuation the oven was glowed and the barium melted down thoroughly. The tube was then baked again for at least 60 hours at 350°C (a slow distillation of barium which destroys the insulation in the tube seems to occur at 500°) and all of the tungsten strips flashed intermittently, A at about 1600°K, E at 2200, and W at 2200 with occasional short flashes at 2800. The glowing temperatures were determined to sufficiently close approximation by making an initial rough calibration of the readings of an optical pyrometer against heating currents for each of the strips. During these treatments the molybdenum support wires became white hot and the tungsten leads themselves probably were heated sufficiently to effect a superficial outgassing of their surfaces. The tube was sealed from the pumps while still hot and a fresh coat of barium immediately deposited on the walls of the oven chamber.

The final cleaning of the tungsten ribbon W was accomplished after sealing off and immersing the tube in liquid air, and the progress of this cleaning followed by taking the current-potential characteristics for the strip after successive flash-

ings. A new heating current-temperature calibration was made for W through an uncoated section of the Dewar cylinder. The strip was given repeated flashings at 2800°K and accepted as clean only after the potential setting for a given reference current remained unchanged by each of several successive flashings. During this cleaning process fresh barium coatings were periodically deposited on the oven chamber walls and the vacuum test applied to check the vacuum conditions in the tube.

The general features of the measuring procedure have been described above. After obtaining the potential setting for the clean tungsten surface, W was turned into the barium vapor jet and immediately after a film had been deposited swung in front of the electron gun. The setting of the sights was such that the electron beam was centered on the deposit; it was also the same as in the preceding measurement on clean tungsten to insure an equivalent geometric arrangement in the two measurements. After the applied potential had been altered to reestablish the reference deflection this deflection was watched for drift, which would indicate a progressive change in the work function of the fresh film. We were surprised to find that these barium films were actually more stable than the freshly cleaned tungsten surfaces. In practically all cases the work function of a fresh barium film remained constant to within a few millivolts for periods of at least 20 or 30 minutes and continuation of the observations on a single film for an hour or more has failed to discover variations greater than this. Since these variations were fluctuations rather than progressive drifts they probably originated in the measuring circuit or emitter rather than in the film. After determining the correct setting for the first film a succession of fresh films was formed and each measured immediately after being deposited. Presumably due to the fact that the barium had been melted repeatedly during the gettering and a considerable fraction of it vaporized no progressive change in work function was found even in the first sequence of films to be formed and the measurements on these films were highly reproducible throughout a complete set of determinations in which as many as 22 different films were measured. Repeated checks to within a few millivolts could be obtained and the appearance of larger variations could be accepted as a reliable indication of a change in electron emission from the gun. After establishing the potential setting for barium and thus completing one determination of contact potential difference the barium film was removed by flashing the strip and the whole measuring procedure repeated. As many as eight such determinations could be made before the tungsten strip burned out.

Great care was taken to hold the total electron emission of the gun constant during a series of determinations. The filament battery was made up of six 100 ampere hour accumulators of similar discharge history in parallel, the sliding contacts of the rough-adjustment 1.2 ohm rheostats (Fig. 1) were replaced by screw clamps, and fine regulation of the emitter heating current accomplished by a heavy alloy rod moving in a mercury well. The total electron current was checked frequently and adjusted if necessary.

Results

Table I is a resumé of the measurements made with the final tube, Type 3, together with the value obtained with the Type 1 tube (which as mentioned above was not regarded as entirely reliable at the time it was made) and two measurements made with the Type 2 tube, which was somewhat similar in design to the Type 3. Only the two measurements recorded were made with the Type 2 tube before the tungsten ribbon, which had been given an excessive heat treatment, burned out. The measurements, with the exception of the two differentiated with aster-

TABLE I. *Measurements of the contact difference of potential between tungsten and barium.* Accepted value: 2.13 volts.

Cell type	$(-V)$ W	$(-V)$ Ba	Contact potential
3	7.70	10.30	2.60*
3	7.90	10.30	2.40*
3	8.16	10.30	2.14
3	8.15	10.30	2.15
3	8.15	10.30	2.15
3	8.17	10.30	2.13
3	8.19	10.30	2.11
3	8.18	10.30	2.12
1	2.30	4.52	2.22
2	7.99	10.10	2.11
2	8.09	10.17	2.08

isks, group closely about the value 2.13 volts. Examination of the potential settings shows that the two high values originate in abnormally high work function states of the tungsten surface. Since the adsorption of any of the gases which are likely to be present in a tube raises the work function of clean tungsten[11] these high values have been disregarded and 2.13 ± 0.05 volts chosen as the value to be considered representative of these measurements. If the work function of clean tungsten is taken as 4.52 equivalent volts[12] the external work function of barium obtained by application of the Sommerfeld relation is 2.39 ± 0.05 equivalent volts.

The photoelectric measurements of Pohl and Pringsheim[13] made on barium which was not outgassed indicated a "threshold" between 1.7 and 2.3 volts. Since the presence of gas generally lowers the work functions of the electropositive metals and correction of an apparent threshold to its true value at 0°K leads to a higher work function value, the true value for barium would be expected to be near or above Pohl and Pringsheim's upper limit of 2.3 volts. Nelson[14] has measured the contact difference of potential between tungsten and barium-coated tungsten emitters incidentally to a study of their thermionic properties. He reports a value of 2.8–2.9 volts, which corresponds in order of magnitude to measurements taken in the present work between barium and tungsten surfaces which had not been completely cleaned. Nelson gives few details of the outgassing treatment to which he subjected the metal parts of his tube. Since these parts were very closely spaced, heating of the anode, oxide-coated filaments, and collector by radiation from the emitter might have caused them to give up gas during the measurements. The barium was supplied by evaporation from oxide-coated filaments and there is the additional possibility that the electrolysis of the oxide may have been accompanied by a slight evolution of oxygen. In view of the tendency of impurities to decrease the work functions of the electropositive metals and, especially, of the difficulty of freeing a tungsten surface from the oxygen coating which raises its work function, it seems probable that the true value of the contact difference of potential W-Ba is at least as low as the value found in the present work.

By adjusting the temperature of the barium oven to give a low rate of vaporization and limiting the time of exposure of the tungsten ribbon to the vapor jet we have found it possible to prepare and measure dilute films of barium on tungsten (covering factor θ of the order of unity and less). As would be expected from the results of thermionic measurements[15] the work function of the composite surface decreases with increasing coverage to a minimum and then increases to the value characteristic of pure barium. The results of these measurements will be reported in detail in a later communication, together with results for barium films on silver and gold. The interpretation of such measurements is a problem quite distinct from that involved in contact potential measurements on pure metals and it is desirable that considerably more data which can be compared with existing photoelectric and thermionic measurements be obtained before an interpretation is attempted.

I should like to thank Dr. W. Meissner and Former President Paschen of the Reichsanstalt for their kindness in granting me the facilities of their laboratories, where the first part of this work was carried out.

[11] Langmuir, J. Am. Chem. Soc. **38**, 2221 (1916); Warner, Proc. Nat. Acad. Sci. **13**, 56 (1927).
[12] Dushman, Rowe, Ewald and Kidner, Phys. Rev. **25**, 338 (1925).
[13] Pohl and Pringsheim, Verh. d. Deutsch. Phys. Ges. **13**, 474 (1911); Hughes and DuBridge, *Photoelectric Phenomena*, p. 75.
[14] Nelson, Physics **1**, 84 (1931).
[15] Langmuir and Kingdon, Phys. Rev. **24**, 510 (1924); J. A. Becker, Phys. Rev. **28**, 341 (1926).

Simplified Theory of the Michelson-Morley Experiment

ROY J. KENNEDY, *University of Washington*

(Received March 22, 1935)

It is shown that a correct application of Huygens' principle in the theory of the experiment leads to the same expression for the expected result as is derived in the simple classical theory. The effect due to path difference is shown to be the same as the effect derivable from the relative rotation of the interfering beams. Critics of the classical theory have mistakenly regarded the latter value as a compensating factor almost exactly offsetting the first.

THE usually accepted theory of the Michelson-Morley experiment has been adversely criticized in a number of papers, the first of which apparently was that of Hicks.[1] Since then Righi[2] and Hedrick[3] have concluded that the effect is not the accepted one, at least not for the so-called "ideal" adjustment of the mirrors, while Woempner[4] and Cartmel[5] derive a third-order expression for the fringe-shift. (By the order of the effect is meant the degree of the ratio β of the velocity of the system through the ether to the velocity of light.) The formulas derived by all these writers involve factors which depend on the adjustment of the apparatus. Righi, Hedrick and Woempner suppose that the fringe-shift to be expected in view of the difference in the times required to traverse the two paths in the interferometer is compensated for by the relative rotation of the two recombining beams, at least in special cases. Their procedure seems to be essentially that of computing the same quantity approximately in two different ways, and then mistakenly subtracting one result from the other. They find that the position of the central fringe is practically unaffected by rotation of the apparatus, but wrongly infer from this fact a null (or very small) effect for the experiment. Oddly enough the third-order effects derived by Woempner and by Cartmel seem to be in good agreement with Miller's experimental data if the linear velocity of the solar system due to rotation of the galaxy is used in evaluating the ratio β.

It was long ago demonstrated by Lorentz[6] that a rotation of the interfering beams of the magnitude actually occurring could not offset the phase difference produced by the relative lengthening of one path as compared to the other. Contrary results have been reached by so many other investigators, however, that it has seemed worth while to attack the problem by a variation of their detailed method with a view to reconciling it with Lorentz's beautifully simple treatment. The present discussion is based almost entirely on the careful application of Huygens' principle to the reflection from the moving mirrors. By this means the directions of the rays in a reference system supposed fixed in the ether are computed; from these directions it is a simple matter to infer the courses of the two beams with respect to the apparatus, and the fringe-shift (or relative phase change) which would result from rotation of the apparatus. It turns out to be unnecessary to compute the lengths of the actual paths in the ether.

In the first place a simple demonstration will be given of the relation of the angle of reflection ϕ to the angle of incidence θ (glancing angles) of a beam of light falling on a mirror moving with velocity v in a direction at an angle α with the normal to the back of the mirror. In Fig. 1 is represented an element of the mirror of length $\delta s(=\overline{op})$. During the time δt between the arrival of the wave front at o and its arrival at p the point p of the mirror will have moved a distance $v\delta t=\overline{pp'}$ to the position p'. Hence by the usual argument it is evident that the reflected wave front will be along $\overline{gp'}$, which is tangent to the

[1] Hicks, Phil. Mag. **6**, 3, 32, 555 (1902).

[2] Righi, Comptes rendus, 1917, several papers. These are summarized in English by Stein, Memori della Societa Astronomica Italiana **1**, 283 (1920).

[3] Hedrick, Conference on the Michelson-Morley Expt., Astrophys. J. **68** (1928).

[4] Woempner, unpublished manuscript.

[5] Cartmel, paper presented at the Pittsburgh Meeting of the Am. Phys. Soc., Dec. 27–29, 1934. Phys. Rev. **47**, 333A (1935).

[6] Lorentz, demonstration restated at Conference, reference 3.

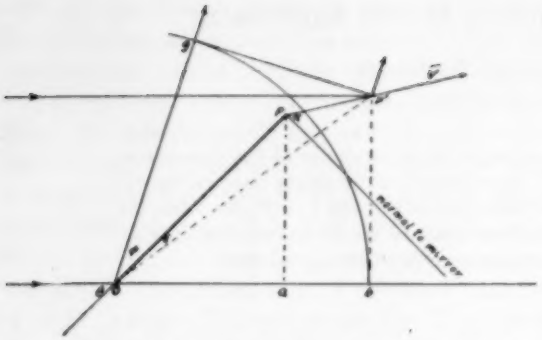

FIG. 1. Mirror OP moving with velocity $\bar{v}$. Incident ray at a glancing angle θ.

elementary wavelet centered at o. The point b, which is the projection of p' on the direction of the incident light is at a distance $c\delta t$ from o, c being the velocity of light. Hence from symmetry $\phi=\theta-2\epsilon$. Also

$$\sin\epsilon=(\overline{pp'}/\overline{po})\sin\angle pp'o=v(\delta t/\delta s)\cos(\alpha+\epsilon);$$

$$\therefore\qquad \tan\epsilon=\frac{(v\delta t\cos\alpha)/\delta s}{1+(v\delta t/\delta s)\sin\alpha}.$$

Now $c\delta t=\overline{ob}=\overline{oa}+\overline{ab}$

$$=\delta s\cos\theta+v\delta t\cos(\pi/2-\theta-\alpha)$$

$$\therefore\qquad \delta t=(1/c)\delta s\cos\theta/[1-\beta\sin(\theta+\alpha)].$$

Substituting in above expression we get

$$\tan\epsilon=(\beta\cos\alpha\cos\theta)/(1-\beta\sin\theta\cos\alpha);$$

$$\therefore\quad \varphi=\theta-2\beta\cos\alpha\cos\theta-\beta^2\cos^2\alpha\sin 2\theta. \qquad (1)$$

Here and throughout the discussion terms involving higher powers than the second in β are disregarded, as are also terms such as $\omega^3\beta$, $\gamma_0^3\beta$, $\gamma_0^2\omega\beta$ and $\gamma_0\omega^2\beta$; γ_0 and ω are defined hereafter.

Following the plan of others, we consider the position of interference bands formed on a screen S due to a plane-parallel beam incident from the left on the diagonal mirror M_1 (Fig. 2). This of course is an idealization of the actual experiment, but it will be shown that similar effects are to be expected. Hence the angle of incidence on M_1 of a ray inclined at a small angle γ to the x axis (fixed in the apparatus as in the figure) will be

$$\theta_1=\pi/4-\gamma=\pi/4-[\gamma_0-\beta\sin(\gamma_0-\psi)],$$

$$\text{where}\quad \psi=\alpha-\pi/4.$$

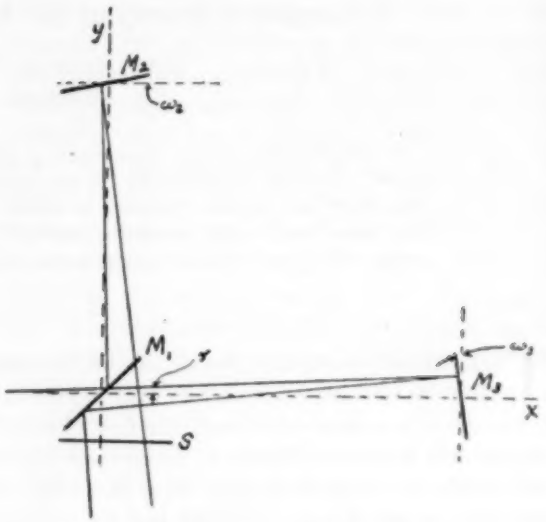

FIG. 2. Arrangement of mirrors.

This expression is got by adding the aberration, $-\beta\sin(\gamma_0-\psi)$, to the angle of incidence that would exist if the system were at rest. This angle is taken as slightly different from $\pi/4$ for the sake of generality.

Applying Eq. (1) to the beam B initially reflected from M_1 and then from M_2 (which is inclined at a small angle ω_2) and to the beam B' initially traversing M_1, then reflected from M_3 (inclined at angle ω_3) and again from M_1 we obtain, after correcting for the aberration, the inclinations of the emergent beams to the y axis fixed in the apparatus as, respectively

$$\rho=2\omega_2+\gamma_0+\beta^2\gamma_0+(\beta^2/2)\sin 2\psi+\beta^2/2\cos 2\psi$$

and

$$\rho'=2\omega_3+\gamma_0-\beta^2\gamma_0+(\beta^2/2)\sin 2\psi-\beta^2/2\cos 2\psi.$$

The computation is long and tedious and will not be given here. The list below contains a few details, the subscripts referring to the particular mirror involved; the primed values are for reflection of the beam B' from M_1.

$$\theta_1=\pi/4-[\gamma_0-\beta\sin(\gamma_0-\psi)],\quad \alpha_1=\psi+\pi/4,$$

$$\theta_2=\varphi_1+\pi/4-\omega_2,\qquad \alpha_2=\tfrac{3}{2}\pi+\psi-\omega_2,$$

$$\theta_3=\pi/2-\omega_3-[\gamma_0-\beta\sin(\gamma_0-\psi)],\quad \alpha_3=\psi+\omega_3,$$

$$\theta_1'=-\varphi_3+\tfrac{3}{4}\pi+\omega_3,\qquad \alpha_1'=\psi+\tfrac{3}{4}\pi.$$

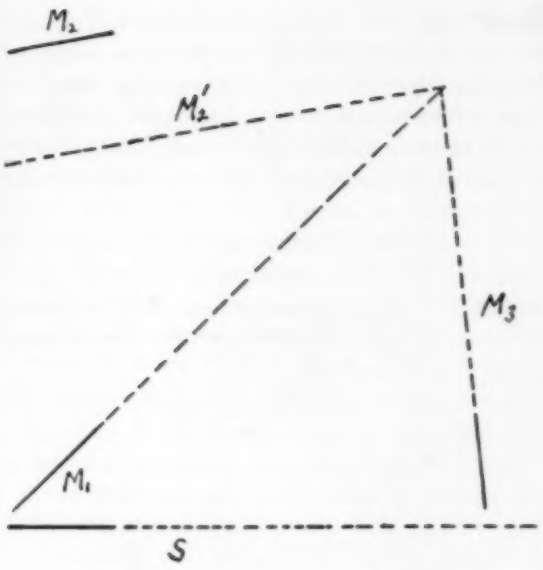

FIG. 3. Positions of mirrors extended.

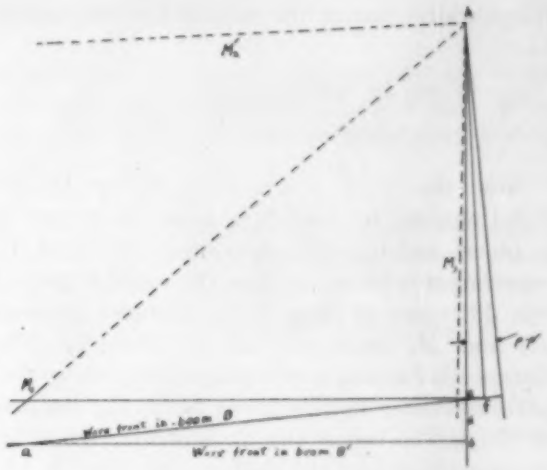

FIG. 4. Positions of interfering wave fronts.

The angle between the wave fronts, then, is simply

$$\rho-\rho'=2(\omega_2-\omega_3)+\beta^2\cos 2\psi.$$

We resort now to a simple device. Let us imagine the mirror M_3, say, extended as indicated by the dotted lines in Fig. 3 to intersect M_1, also extended. From the intersection we imagine a mirror M_2' drawn parallel to M_2. In such an arrangement the angles characterizing the rays would be the same as in the actual case. Now the central fringe, defined as that resulting from the interference of rays having a difference in path in space equal to zero, would evidently be produced by rays incident on the diagonal mirror in the neighborhood of the intersection of the mirrors. Hence this fringe would be formed on the extended screen in the neighborhood of M_3. Furthermore, the expressions for ρ and ρ' indicate that the fringe is practically stationary since, but for the effect of the terms $(\beta^2/2)\sin 2\psi$, the wavefronts oscillate symmetrically about a line (hf, Fig. 4) fixed in the moving system; i.e., they are at equal angles on opposite sides of hf which vary with the orientation of the apparatus.

Now the fringe of interest is not the central fringe defined above, but rather the fringe in the neighborhood of the y axis, in this case a distance from the central fringe approximately equal to the separation l of M_3 and M_1. By referring to Fig. 4 it is seen that a wave front (af) in the beam B, instantaneously passing through the fringe f, produces a fringe at a (in the neighborhood of the y axis) by interfering with a wavefront (ab) in B' with respect to which it is retarded by a constant number n of waves, such that

$$n\lambda=d=l\tan 2(\omega_2-\omega_3).$$

As the apparatus rotates, the fringe formed at this intersection will move about the y axis, its x coordinate being (except for a small constant) evidently

$$x=l-d\cot\left[2(\omega_2-\omega_3)+\beta^2\cos 2\psi\right]$$

$$=l\left[1-\frac{\tan 2(\omega_2-\omega_3)}{\tan 2(\omega_2-\omega_3)+\beta^2\cos 2\psi}\right]$$

$$=\frac{l\beta^2\cos 2\psi}{\tan 2(\omega_2-\omega_3)}\text{ approximately.}\quad(2)$$

The approximation is justified, since in the usual performance of the experiment $\omega_2-\omega_3$ is of the order 10^{-4} while β^2 is 10^{-8} for the earth's orbital velocity and 10^{-6} for its velocity due to galactic rotation.

Since the mean width of the fringes is $\lambda/\tan 2(\omega_2-\omega_3)$ where λ is the wavelength of the light employed, we find for the shift expressed in

fringe-widths simply the ratio of x to this width, i.e.,

$$\frac{l\beta^2 \cos 2\psi/\tan 2(\omega_2-\omega_3)}{\lambda/\tan 2(\omega_2-\omega_3)}=\frac{l}{\lambda}(-\beta^2 \cos 2\psi). \quad (3)$$

Now the wave fronts from mirror M_2 are indistinguishable from those from M_2' except as to phase, and from the elementary theory of the experiment it turns out that the variable part of this difference of phase is the distance between M_2 and M_2' multiplied by $(\beta^2/\lambda)\cos 2\psi$. The distance is $l \tan \omega_2$ so the fringe-shift due to this path-difference is $(l/\lambda)\beta^2 \cos 2\psi \tan \omega_2$; because of the factor $\tan \omega_2$ this is evidently ignorable in comparison with the shift expressed in Eq. (3).

The errors of the writers referred to are of two kinds: they either confuse the central fringe defined above with the axial fringe, and so infer a null effect from the fact that the former is practically stationary, or else regard the effect computed above from the angular deviations of the rays as but one component of the whole effect, the other being the shift due to the difference in the lengths of the two paths. By computing the latter approximately (to the second order) and the former to the third order, one erroneously derives a third-order effect. It is readily shown, however, that the *total* effect is expressed in Eq. (3) which we have derived. For the wavefronts in each beam are parallel planes at fixed distances apart, two of which intersect in a line (the central fringe established by a hypothetical case) which is practically fixed in the axes moving with the apparatus. Hence their intersections, and the fringes formed at them, are completely determined in position by the angles between the wave fronts.

Hence the total effect to be expected in the experiment is expressed in Eq. (3), which is the same as results from the simple approximate theory.

The same variation in phase exists in the "ideal" case, i.e., that in which the end-mirrors are exactly perpendicular to the axes, although then the approximate expression in terms of fringe-width would not be valid and the fringes would become indefinitely broad. Nevertheless the method employed, by the writer[7] and Illingworth,[8] in which the phase-shift would exhibit itself by unbalancing a split photometric field, would still be applicable. In other words the "ideal" case is special only in that the fringes produced are too broad to permit direct visual estimation of their positions.

The actual experiment, of course, deals with cones of rays brought finally to a focus in a telescope, instead of plane waves interfering on a screen. The latter have been considered here only because they have given rise to the whole confusion. It is much simpler, paraphrasing Lorentz, to treat the general case. The phase-differences may be computed by the elementary method in which the second-order differences in direction discussed above are ignored for the reason that such directional differences can only produce errors of order higher than the second in the result. For, if the approximate value for the length of either path be l_0 while the actual length is a function $l(\epsilon_1, \epsilon_2, \epsilon_3)$ where the arguments are the small angles (of the order of β^2) between corresponding segments of the actual and approximate paths, then on expansion of the function we find for the error

$$l(\epsilon_1, \epsilon_2, \epsilon_3)-l_0=\epsilon_1\frac{\partial l}{\partial \epsilon_1}+\epsilon_2\frac{\partial l}{\partial \epsilon_2}+\epsilon_3\frac{\partial l}{\partial \epsilon_3}$$

$+$terms involving higher powers of the ϵ's.

But Fermat's principle requires that the path be a minimum; hence the first derivatives vanish, showing that the error involves only powers of β higher than the third, and therefore ignorable.

[7] Kennedy, Proc. Nat. Acad. Sci. **12**, 621 (1926).
[8] Illingworth, Phys. Rev. **30**, 692 (1927).

LETTERS TO THE EDITOR

Prompt publication of brief reports of important discoveries in physics may be secured by addressing them to this department. Closing dates for this department are, for the first issue of the month, the twentieth of the preceding month; for the second issue, the fifth of the month. The Board of Editors does not hold itself responsible for the opinions expressed by the correspondents.

The Helium Content of Beryls

The late Lord Rayleigh showed in 1908 that many beryls contained large quantities of helium. If this had accumulated in the minerals as a result of atomic disintegrations of beryllium we should expect high helium content only in the older beryls. If, however, the helium was trapped in the mineral when it was formed, (which is unlikely since other siliceous minerals do not absorb helium), or if it is due to a short lived radioactive material initially present, we should expect large helium content in the younger beryls since opportunities for its escape would have been less. Lord Rayleigh's[1] results decidedly support the former alternative. Beryls from the younger rocks have not in any case been found to contain much helium; beryls from the older formations usually contain a relatively large amount. These measurements, which have been confirmed by Paneth and Peters,[2] suggest that the helium found in beryls is due to the disintegration of beryllium.

There is, as yet, no definite evidence of the terrestrial existence of ${}_4Be^8$. It is noteworthy that by extrapolating Aston's mass defect curve it is found that the nuclear binding energy of ${}_4Be^8$ is very small and may indeed be little greater than zero. R. d'E. Atkinson[3] supposed that this isotope has a negative mass defect so that ${}_4Be^8$ is spontaneously radioactive, breaking up into two α-particles. It has, therefore, been suggested that the helium found in beryls may be the disintegration product of ${}_4Be^8$ which was trapped in the minerals when they crystallized out. On general grounds (and by analogy with the other light elements) it would appear more probable that ${}_4Be^8$ is stable, i.e., that it has a positive, though small, mass defect. It is likely, therefore, that ${}_4Be^8$ is not spontaneously radioactive.

In a later communication Lord Rayleigh[4] considered the possibility that ${}_4Be^9$ might be radioactive as suggested by Langer and Raitt;[5] but he has shown that on this assumption the calculated time necessary for the accumulation of the helium is much greater than can be allowed and concludes that the helium in beryls cannot be brought into line with any "existing emission of α-particles," this conclusion being independent of whether beryllium or some other constituent is thought to be the parent element. More recently, moreover, Evans and Henderson,[6] Gans, Harkins and Newson,[7] and Libby[8] have proved conclusively that ${}_4Be^9$ is not radioactive.

In this connection the recent work of Szilard and Chalmers[9] and Gentner[10] is of significance. These investigators have shown that γ-radiation is capable of ejecting neutrons from ${}_4Be^9$, the results of Gentner indicating that ${}_4Be^9$ is stable with a mass defect energy of 0.45×10^6 e.v. It is thus apparent that γ-radiation is capable of disintegrating ${}_4Be^9$ according to one or other of the reactions

$${}_4Be^9+\gamma\rightarrow{}_4Be^8+n;\ {}_4Be^9+\gamma\rightarrow{}_2He^4+{}_2He^4+n.$$

In addition, if ${}_4Be^8$ has a small but positive nuclear binding energy it will not be spontaneously radioactive, though it will probably be easily disintegrated into two α-particles by the nuclear absorption of γ-radiation thus:

$${}_4Be^8+\gamma\rightarrow{}_2He^4+{}_2He^4.$$

Hence, since there are widely disseminated radioactive substances in the earth's crust, and since the atmosphere is continually bombarded by the shower producing secondary γ-radiation due to cosmic rays, it is apparent that any stable ${}_4Be^8$ atoms originally present in beryls (or produced from ${}_4Be^9$ as above) may be broken down to form helium as may ${}_4Be^9$ atoms also. In consequence, the helium content of beryls may be due to the disintegration of "stable" (i.e., nonradioactive) beryllium isotopes. Thus ${}_4Be^9$, though stable, may have disappeared from the earth owing to disruption by cosmic radiation. It is to be noted that if the ${}_4Be^8$ mass defect energy is very low the α-particles produced will have such short ranges that no perceptible ionization due to them will be observed, since the nuclear processes discussed above are not sufficiently energetic to give rise to α-particles which could be detected by the normal methods.

In a similar way it would, therefore, appear probable that the just stable ${}_2He^5$ has disappeared from the earth's atmosphere, since this isotope, consisting of an α-particle and a loosely bound neutron, could also be disintegrated into an α-particle and a neutron by the secondary γ-radiation of cosmic rays. Thus both ${}_4Be^9$ and ${}_2He^5$, though stable (in that they have small positive nuclear binding energies), may have disappeared from the earth in the form of helium, i.e., may have died out as if they were "radioactive."

H. J. WALKE.

Department of Physics,
Washington Singer Laboratories,
University College, Exeter, England.
March 25, 1935.

[1] Rayleigh, Nature **123**, 607 (1929).
[2] Paneth and Peters, Zeits. f. physik. Chemie **B1**, 187 (1925).
[3] R. d'E. Atkinson, Astrophys. J. **73**, 250 (1931).
[4] Rayleigh, Nature **131**, 724 (1933).
[5] Langer and Raitt, Phys. Rev. **43**, 585 (1933).
[6] Evans and Henderson, Phys. Rev. **44**, 59 (1933).
[7] Gans, Harkins and Newson, Phys. Rev. **44**, 512 (1933).
[8] Libby, Phys. Rev. **44**, 512 (1933).
[9] Szilard and Chalmers, Nature **134**, 437 (1934).
[10] Gentner, Comptes rendus **199**, 1211 (1934).

Slow Neutrons

Following our earlier experiments[1] we have investigated further the production of slow neutrons from fast neutrons through collisions with H nuclei. A 500 mc Rn-Be neutron source bulb, with about 0.75 mm lead foil around it, was suspended about 65 cm from a Li lined ionization chamber connected to an amplifier-thyratron recording system. The source was then successively surrounded by paraffin spheres from 0 to 23 cm radius, and the number of slow neutrons which were capable of disintegrating Li, and being anomalously absorbed by Cd, was observed by taking readings with and without Cd interposed, in order to separate out the slow and fast neutrons. Cd shields protected the chamber from slow neutrons scattered back from the room.

In Fig. 1, the upper solid curve shows the readings without Cd, and the lower solid curve the readings with Cd interposed (neutrons outside the Cd absorption region), the dashed intermediate curve being the difference between the two, or the slow neutron component only. The lowest dotted curve shows the decrease in fast neutrons detected through projected protons from previous data[2] for comparison. The number of slow neutrons present in the original source is apparently zero, but since the mean free path of fast neutrons in paraffin is of the order of 4–5 cm, in order to account for the production of some slow neutrons with near thermal velocities with only about 3 cm of paraffin, it seems necessary to conclude that there are a large number of neutrons in the original source which are already below the ordinary fast neutron limits, i.e., probably below 100,000 e.v., where the M.F.P. is already smaller. This is consistent with other evidence.[3] The decrease observed after the maximum may be due to some absorption process, such as with H to form deuterium, or possibly with C. Since the slow neutron M.F.P. in paraffin is of the order of 2 mm, the actual number of collisions in the large spheres is enormous, so the probability of capture per collision does not need to be large. The behavior of water was practically the same as paraffin at the points tested.[4] The slight rise in the lower solid curve with Cd interposed implies that Li detects some neutrons above the Cd absorption region, in the intermediate range between fast and slow.

Measurements of slow neutron-nucleus collision cross sections have now been made over a wider range of elements, and under more refined conditions. The slow neutron-proton cross section is revised upward to about 31×10^{-24} cm², and that of the neutron-deuteron is about 5.3×10^{-24} cm², compared to about 1.6×10^{-24} cm² for both with fast neutrons. Al and S cross sections with slow neutrons are probably less than for fast neutrons. Samarium and terbium, from some rare earth samples kindly supplied by Dr. A. F. Daggett, show the highest absorption coefficients yet measured, even larger than Cd, with cross sections of about 5000×10^{-24} cm², when measured with a reasonably parallel beam of slow neutrons. It does not seem likely that the presence of impurities of unknown cross section could cause any large part of the effect. Cd shows a nearly exponential absorption curve for an approximately parallel slow neutron beam, and gives a neutron-nucleus cross section of about 3300×10^{-24} cm².

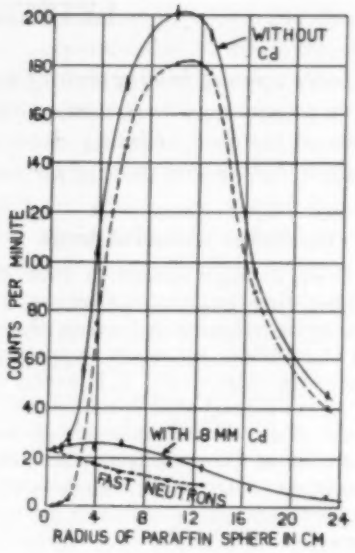

FIG. 1.

Previous attempts to measure elastic scattering of slow neutrons from Cd have shown it to be so small that introduction of a Cd scattering cylinder actually decreased the observed number of neutrons, since it shielded the chamber from neutrons scattered back from the room somewhat, although such materials as Cu, MgO or $CaCO_3$ showed large scattering. A new experiment to eliminate room scattering, was performed by placing the source (paraffin sphere) and Li chamber at opposite ends of a tight cylindrical enclosure made of Cd. The direct beam of slow neutrons was eliminated by interposing a Cd disk between the source and chamber. The presence of any slow neutrons scattered from the walls of the Cd cylinder was tested by measuring the effect of placing a Cd sheet before the ionization chamber. Less than one neutron per minute was scattered from the Cd (which might be due to the air rather than Cd), whereas with Cu or Mg under similar conditions more than 100 per minute would be observed. The large stopping power of Cd for slow neutrons (0.005 cm is sufficient to absorb about one-half) is then due almost entirely to capture and absorption, and not to elastic scattering. Rough experiments indicate that this is also true for the other highly absorbing elements.

J. R. DUNNING
G. B. PEGRAM
G. A. FINK
D. P. MITCHELL

Pupin Physics Laboratories,
Columbia University,
June 3, 1935.

[1] J. R. Dunning and G. B. Pegram, Phys. Rev. **47**, 640 (1935).
[2] J. R. Dunning, G. B. Pegram and G. A. Fink, Phys. Rev. **47**, 325 (1935).
[3] J. R. Dunning, Phys. Rev. **45**, 586 (1934).
[4] Westcott and Bjerge, Proc. Camb. Phil. Soc. 145 (1935).

The Emission of Negative Electrons from Lithium and Fluorine Bombarded with Deuterons

In the last issue of *The Physical Review* we published the energy spectrum of beta-rays from boron bombarded with deuterons, which we were able to obtain by bombarding a target inside the cloud chamber. Continuing with the same experimental set-up we have obtained the beta-ray spectra from two other substances, which we suppose are Li^8 and F^{20}, and which also have short half-lives. In both cases an automatic switching device was used which shut off the bombarding ion beam before the chamber expansion, so that only delayed effects were observed.

Lithium Bombarded with Deuterons

The points in Fig. 1 show the distribution in energy of 1646 electrons obtained from 1000 cloud chamber photographs, taken about $\frac{1}{2}$ second after bombardment, with $\frac{1}{2}$ microampere deuteron current at 0.8 M.E.V. The tracks were curved in a magnetic field of 1500 gauss to determine their energy. 0.3 M.E.V. has been added to all points to compensate for the stopping power of the foil surrounding the target, so that they give directly the energy of the electrons. The reaction is probably

$$Li^7+H^2\rightarrow Li^8+H^1\rightarrow Be^8+\epsilon^-+H^1\rightarrow He^4+He^4+\epsilon^-+H^1.$$

If the first part of the reaction is correct, the second disintegration, in which Be^8 splits into two alpha-particles probably follows, since several pieces of information indicate that Be^8 is unstable. There is no assurance, however, that the two disintegrations do not take place in the reverse order, that is,

$$Li^7+H^2\rightarrow Li^8+H^1\rightarrow He^4+H^4+H^1\rightarrow He^4+He^4+\epsilon^-+H^1.$$

The protons emitted during bombardment may be expected to have an energy in the neighborhood of 4 M.E.V.

To determine the half-life of the active constituent, we adjusted the timing device so that the ion beam was shut off at $\frac{1}{4}$, $\frac{1}{2}$, $\frac{3}{4}$ and 1 second before the chamber expansion. 50 photographs were taken at each of these settings, and the average numbers of tracks per photograph were found to be 7.08, 4.84, 3.70 and 2.45, respectively. These, plotted on a log scale lie quite closely on a straight line, and indicate a half-life of 0.5 ± 0.1 second.

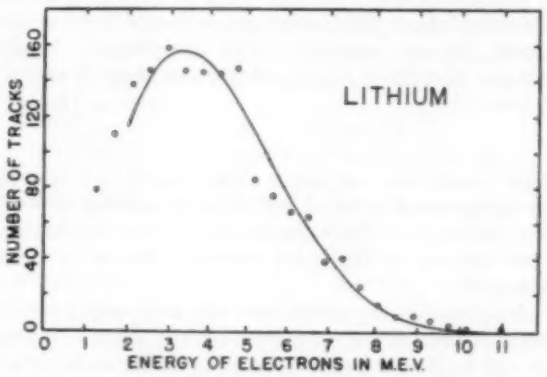

FIG. 1. Energy distribution of negative electrons emitted from a lithium chloride target after bombardment with deuterons.

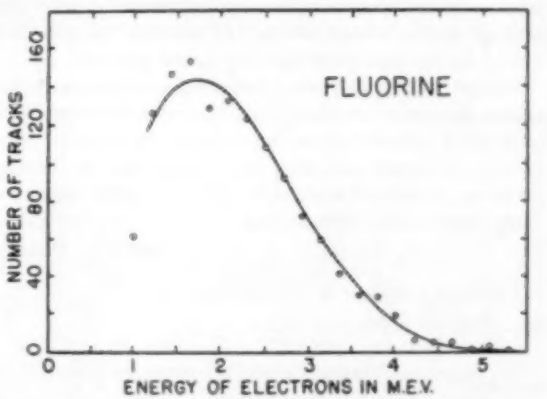

FIG. 2. Energy distribution of negative electrons emitted from a calcium fluoride target after bombardment with deuterons.

Fluorine Bombarded with Deuterons

The points in Fig. 2 show the energy distribution of 1363 electron tracks obtained from 800 cloud chamber photographs taken with $\frac{1}{2}$ microampere deuteron current, at 0.8 M.E.V., and 1500 gauss magnetic field. These points have also been corrected for the stopping power of the foil. The electrons probably arise from the reaction

$$F^{19}+H^2\rightarrow F^{20}+H^1\rightarrow Ne^{20}+\epsilon^-+H^1.$$

We have measured the half-life of the radio-fluorine by means of an ionization chamber and found it to be 12 ± 2 seconds.

Comparison with Theory

The energy distributions of the electrons in Figs. 1 and 2 do not fit at all with those derived from Fermi's theory in its original form, according to which we should expect the maxima of the curves, for such high energy spectra, to lie at points only slightly less than half the upper limit of energy. It should be kept in mind, however, that the experimentally obtained energy distributions are somewhat influenced by instrumental conditions, which tend, in general, to make unreliable the relative numbers of low energy tracks measured, but we feel that this distortion is important only below 1 or 1.5 M.E.V. It is not probable, therefore, that this can account for the large difference between the observed positions of the maxima and those predicted by Fermi's theory. Professor Oppenheimer has pointed out to us that the data are in very much better agreement with a formula of the form:

$$N(E)=\text{const.}\ E^2(E_0-E)^4.$$

Such a formula would follow if the coupling energy between the neutron-proton and the electron-neutrino field were taken proportional to the first derivative of the neutrino function, and this possibility has been advanced by Uhlenbeck and Konopinski on empirical grounds. The

curves in Figs. 1 and 2 have been drawn according to this formula, fitting the data as well as possible, which necessitated taking as upper limits E_0, 10.5 and 5.25 M.E.V., respectively. It is seen that these fit the experimental points well within the probable statistical fluctuations, although, from the standpoint of the data alone, one might be inclined to place the upper limits slightly lower than 10.5 and 5.25 in consideration of the possibility of a little straggling. The lifetimes of these substances, on the other hand, lie too near those to be expected on the basis of Fermi's original formulation to permit the inclusion of higher derivatives in the interaction energy.

H. R. Crane
L. A. Delsasso
W. A. Fowler
C. C. Lauritsen

Kellogg Radiation Laboratory,
California Institute of Technology,
May 31, 1935.

Interaction of Nuclear Particles

Heisenberg,[1] in an important set of papers, attributed nuclear binding entirely to proton-neutron attractions. Supposing these to be of a classical nature it is easy to show (if the proton-neutron potential energy is a simple monotonic function of the inter-particle distance) that the nuclear binding energy is

$$W \sim -Z(A-Z). \tag{1}$$

This is essentially what is obtained if the Coulomb repulsion between protons is neglected. Inclusion of Coulomb forces would, however, still give a binding energy varying quadratically with the number of nuclear particles. If this were right we could not understand natural radioactivity and the ending of the periodic system of elements. The failure of a classical interaction law is not apparent for the lightest nuclei and Wigner[2] was able to show that the mass defects of the deuteron and the α-particle were compatible with classical forces. From the experimental law that mass defects are roughly proportional to the number of nuclear particles we see that our theory must give instead of Eq. (1)

$$W \sim -A. \tag{2}$$

Now $Z(A-Z)$ is just the number of interactions of Z protons with $A-Z$ neutrons. Heisenberg, and later Majorana,[3] saw that the simplest way of obtaining something like Eq. (2) instead of Eq. (1) was the introduction of interactions of such a nature that a given proton or neutron feels only those neutrons or protons in the same quantum state. They introduced such an interaction and obtained instead of Eq. (2)

$$W \sim -Z. \tag{3}$$

Heisenberg's proposed interaction gave saturation with one-proton-one-neutron, but the proposal of Majorana allowed two-protons-two-neutrons to interact in an effective way. The latter is much more satisfactory.

These were steps in the right direction but, for heavy nuclei, Eqs. (2) and (3) are not equivalent and experiment favors Eq. (2). To improve the theory we must depart from the original Heisenberg hypothesis that only neutron-proton bonds are important. With neutron-neutron and proton-proton bonds of the type suggested by Majorana for the proton-neutron bond, it is possible to develop a theory giving binding energies $\sim -A$ and nuclear radii $\sim A^{\frac{1}{3}}$. These bonds are taken to be the same without regard to the kind of interacting particles. To make this statement more definite we will give, for comparison, expressions for the nuclear potential energy in the theories discussed in this letter.

$$\begin{aligned}
&\text{(Classical)} \quad V = -\int \rho_\pi(\mathbf{r}_1) I(r_{12}) \rho_\nu(\mathbf{r}_2) d\tau_1 d\tau_2, \\
&\text{(Majorana)} \quad V = -\int \rho_\pi(\mathbf{r}_1, \mathbf{r}_2) I(r_{12}) \rho_\nu(\mathbf{r}_2, \mathbf{r}_1) d\tau_1 d\tau_2, \\
&\text{(Proposed)} \quad V = -\int \rho(\mathbf{r}_1, \mathbf{r}_2) I(r_{12}) \rho(\mathbf{r}_2, \mathbf{r}_1) d\tau_1 d\tau_2 + S.
\end{aligned}$$

In these expressions ρ_π and ρ_ν are the density functions for protons and neutrons, respectively. Where one argument is written, these are just the usual functions but if two arguments are indicated the density matrices of Dirac are to be used. In the last equation $\rho = \rho_\pi + \rho_\nu$ and S is such a function that this expression does not include the interaction of any particle with itself.

The assumption that $I(r)$ has the form of a simple potential hole of depth αmc^2 and radius $\beta e^2/mc^2$ has been made. To get agreement with experimental binding energies of nuclei it was found that the parameters α and β must be

$$\alpha \sim 40, \qquad \beta \sim 1.00.$$

The calculations on which these results rest are not accurate enough to allow one to decide whether or not all the bonds are of the same strength. It is probable that they are not, so the above numbers must be a sort of average.

Independent arguments for the existence of strong neutron-neutron and proton-proton binding can be found in the number theory properties of stable nuclei. For Z odd and $A > 2Z$ the number of neutrons $A-Z$ is always even. The most simple and unforced explanation of this seems to be that strong attractive interactions exist between paired neutrons. In order that the balance between protons and neutrons, within the nucleus, be preserved, similar forces must exist between paired protons.

White[4] has just published preliminary results on proton-proton scattering which indicate just such large deviations from the Coulomb law at distances of the order 10^{-13} cm. It is to be hoped that such experiments and furthermore accurate theoretical work will teach us a great deal about these fundamental interactions.

Lloyd A. Young

Carnegie Institute of Technology,
May 27, 1935.

[1] W. Heisenberg, Zeits. f. Physik **77**, 1 (1932); **78**, 156 (1933); **80**, 587 (1933).
[2] E. Wigner, Phys. Rev. **43**, 252 (1933).
[3] E. Majorana, Zeits. f. Physik **82**, 137 (1933).
[4] M. G. White, Phys. Rev. **47**, 573 (1935).

Evidence for the Formation of $_4Be^8$ in the Disintegration of Lithium by Deuterons

From the determination of the range of the alpha-particles produced by the reaction

$$_1H^2+{}_3Li^7\rightarrow 2{}_2He^4+{}_0n^1.$$

Oliphant, Kempton and Rutherford[1] found the energy released in the disintegration to be 14.6±0.25 MEV. By measuring the ranges of the recoil protons which had sufficient energy to penetrate a mica sheet (stopping power 114 cm) which was placed in the center of a high pressure cloud chamber, we have investigated the energy distribution of the neutrons in this reaction which were emitted with energies over 11 MEV. The chamber was operated at expanded pressures of 11.9 and 14.7 atmospheres. Otherwise, the experimental procedure was identical to that described in our article which appears in this issue. We have taken over 9000 pictures in which 86 tracks penetrated the mica and satisfied our requirement of being projected in the forward direction.[2]

Fig. 1 shows the energy distribution of these measured tracks. The points on the lower curve represent the actual number of tracks observed in an energy interval of 0.4 MEV, while the points on the upper curve have been corrected according to the varying probability, due to the geometry of the apparatus, of observing tracks of different lengths. Both curves show a pronounced maximum near 13 MEV. We believe that this increase is due to neutrons from the reaction

$$_1H^2+{}_3Li^7\rightarrow {}_4Be^8+{}_0n^1.$$

Evidence that $_4Be^8$ is formed in other nuclear reactions has been presented by Kirchner and Neuert,[3] and by Crane, Delsasso, Fowler and Lauritsen.[4] A preliminary investigation of the number of neutrons emitted with energies lower than 10 MEV shows that there is a much larger number with energies in the neighborhood of 2 or 3 MEV.

The maximum energy of the neutrons emitted at 90° appears to be 13.4 MEV. The calculated value of the energy of disintegration is 14.3±0.5 MEV. From the value 14.6± 0.25 MEV obtained by Oliphant, Kempton and Rutherford, we have calculated that the mass of $_4Be^8$ is 0.3±0.75 MEV greater than that of two alpha-particles. A recalculation of Kirchner's mass of $_4Be^8$ with Bethe's[5] new values gives a mass just equal to that of two alpha-particles; Crane and Lauritsen's mass of $_4Be^8$ is 1.5±0.5 MEV greater that that of two alpha-particles. These agree with our results within the rather large limits of error.

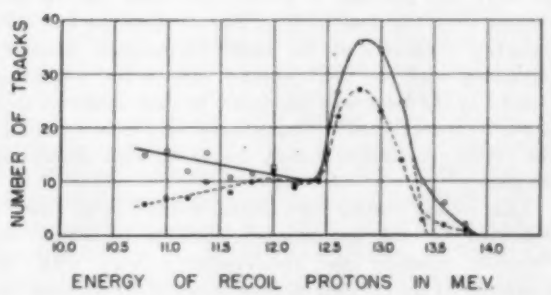

FIG. 1. Energy distribution curve of recoil-protons projected in forward direction.

Such a mass of $_4Be^8$ gives evidence for a resonance level in the interaction of two alpha-particles. This may be an important factor in the anomalous scattering, as pointed out by Beck and Horsley.[6]

Thanks are due Professor C. C. Lauritsen and Dr. H. R. Crane for the use of the high potential apparatus, and for valuable suggestions. We are indebted to the Seeley W. Mudd fund for the financial support of this work.

T. W. BONNER*
W. M. BRUBAKER

Kellogg Radiation Laboratory,
California Institute of Technology,
May 4, 1935.

[1] Oliphant, Kempton and Rutherford, Proc. Roy. Soc. **A149**, 406 (1935).
[2] See article by Bonner and Brubaker in this same issue.
[3] Kirchner and Neuert, Physik. Zeits. **35**, 293 (1934).
[4] Crane and Lauritsen, Phys. Rev. **47**, 420 (1935); Crane, Delsasso, Fowler and Lauritsen, Phys. Rev. **47**, 887 (1935).
[5] H. Bethe, Phys. Rev. **47**, 633 (1935).
[6] G. Beck and L. H. Horsley, Nature **135**, 430 (1935).
* National Research Fellow.

The Correlation of Wave Functions with the States of Physical Systems

In their recent article, *Can Quantum-Mechanical Description of Physical Reality be Considered Complete?*[1] Einstein, Podolsky and Rosen arrive at the conclusion that the question put by the title of their paper must be answered in the negative. In the writer's opinion their argument is not sound.

The essential feature of their reasoning is the purported demonstration by means of an example that "*it is possible to assign two different wave functions . . . to the same reality.*" If this were true, it would mean that quantum-mechanical description is erroneous as well as incomplete, for each different wave function involves a different prediction regarding the future behavior of the system described and the authors of the above paper clearly intend the phrase "the same reality" to refer to the same system in the same physical state. Actually, however, the demonstration cited is incorrect.

The special problem discussed by Einstein, Podolsky and Rosen is that of a compound system whose two component systems α and β are assumed to interact during a limited time interval $0<t<T$. (We may suppose that the interaction is a collision between an atom and a free electron which takes place during this time interval.) After the interaction it is possible to measure any physical property of the system α without disturbing β. According to the usual quantum-mechanical procedure the wave function to be assigned to the system β after the observation of α depends on the type of observation made and on

its result. But since β has not been disturbed by the observation of α, Einstein, Podolsky and Rosen argue that it cannot be affected by that observation and must in all cases constitute "the same physical reality." In other words, they assume it to be in the same "state" in all cases. Here lies a fallacy, however, for whenever two systems interact for a short time there is a correlation between the subsequent behavior of one system and that of the other. Thus in the case of a pair of systems with a definite total energy or definite total linear momentum we can infer from the measured value of the energy or momentum of one system after a collision what the value of the corresponding quantity for the other system must be. In the Compton effect each photon scattered at a definite angle from a unidirectional monochromatic primary beam is correlated with a recoil electron driven off at a definite corresponding angle. The process of reducing the wave packet[2] is the orthodox procedure for taking this correlation into account and, *of course*, it yields a different wave function for the recoil electrons correlated with photons scattered at one angle from that for recoil electrons whose photons have been scattered at another angle. If our mathematics did not work out that way we should have to revise it.

It is quite true, as pointed out by E., P. and R., that the act of observing the system α can hardly be supposed to change the state of a system β which may be widely separated from it in space, but it can and does reveal something about the state of β which could not have been deduced from the initial wave function of the combination system without such an observation. Thus each possible wave function for system β gives a correct description of the corresponding state of that system.

These remarks would hardly clear up the whole question if no specific mention were made of the interpretation of quantum mechanics as a statistical mechanics of assemblages of like systems. This point of view most clearly formulated by Slater[3] seems the only way of solving the paradoxes of the average presentation of elementary quantum theory. It asserts that the wave functions of the Schrödinger theory have meaning primarily as descriptions of the behavior of (infinite) assemblages of identical systems similarly prepared. When we say that the "state" of an electron in motion is described by $\psi(x, t)$ we mean that an assemblage of a very large number of similarly prepared electrons would have statistical properties described by this function, and that we cannot know more about an individual electron than the fact that it belongs to a suitably chosen potential assemblage of this character. Every analysis of a wave function into a linear combination of orthogonal functions can be interpreted as a resolution of the complete assemblage into a collection of sub-assemblages. The expansion set up by E., P. and R. of the complete wave function $\Psi(x_\alpha, x_\beta)$ for the combination system into eigenfunctions of a dynamical variable A of the system α shows that in each sub-assemblage we have a correlation between a particular pure state of the variable A and a corresponding state of the system β. The act of measuring the variable A is the physical counterpart of this mathematical expansion and when successful[4] shows which sub-assemblage a particular pair of systems α, β belongs to. The "reduction of the wave packet" is the process of substituting the wave function of the sub-assemblage for that of the original complete assemblage which must accompany the transfer of one's attention from an arbitrary member or members of the original assemblage to systems known to belong to said sub-assemblage.

There seems no reason to doubt the completeness of the quantum-mechanical description of atomic systems within the frame of our present experimental knowledge.

EDWIN C. KEMBLE

The Physical Laboratories,
Harvard University,
May 25, 1935.

[1] A. Einstein, B. Podolsky and N. Rosen, Phys. Rev. **47**, 777 (1935).
[2] Reference 1, p. 779.
[3] J. C. Slater, J. Frank. Inst. **207**, 449 (1929).
[4] In most measurements of the properties of atomic systems we do not get a definite result for every system in the group under investigation.

The Dielectric Constant and Resistance of Colloidal Solutions

It has been noticed by various investigators[1–6] that the dielectric constant of aqueous colloidal solutions is often considerably higher than that of water. It has usually been assumed that this increase results from the colloidal particles acting as dipoles, but there is evidence[3, 4] that this is not the essential principle involved, and the following experiments throw further light on the situation.

Over a range of frequencies from 0.25 to 2000 kilocycles/sec. measurements were made with a Wheatstone bridge by a substitution method, comparison being made with potassium chloride solutions taken to have a dielectric constant equal to that of water and resistances independent of the frequency. Electrode polarization is a difficulty at low frequencies, but can be eliminated by measuring at different electrode distances.

Coarse suspensions are particularly suitable for study and we have used Nujol, sulfur, ferric oxide and kaolin, in sodium oleate and gelatin; cream (natural and homogenized); and cellulose in water, with mean particle size ranging from 10μ down to 0.5μ. For all these, we find high dielectric constants at the lower frequencies, generally increasing with the total internal surface and increasing rapidly as the frequency decreases, so that values as high as 40,000 are obtained in certain cases. As is to be expected,[7] the resistance simultaneously increases with decreasing frequency.

That we are dealing with the same effect in all cases is indicated by the characteristic fashion in which the dielectric constant and the resistance vary with the frequency (Fig. 1). Over a wide range of frequencies the values of $(D - D_\infty)$, where D_∞ is the constant value of the dielectric constant obtained at high frequencies, vary as

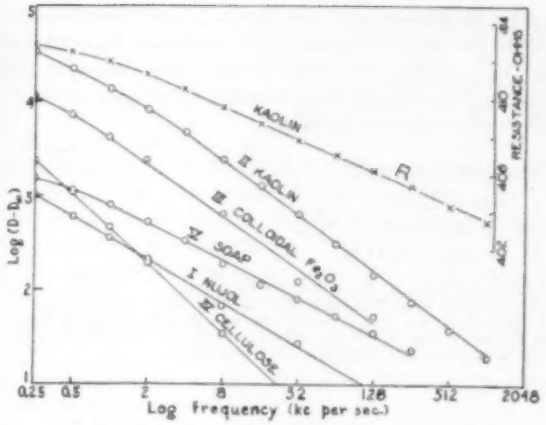

FIG. 1. Dielectric constant as a function of frequency for (I) 60 percent Nujol in 1.5 percent sodium oleate (mean diam. 5μ); (II) 45 percent kaolin in 1.5 percent sodium oleate (diam. 0.5μ); (III) 1.5 percent colloidal ferric oxide (submicroscopic); (IV) 2 percent cellulose in water; (V) 1.5 percent soap. The resistance-frequency curve is shown for 45 percent kaolin in 1.5 percent sodium oleate.

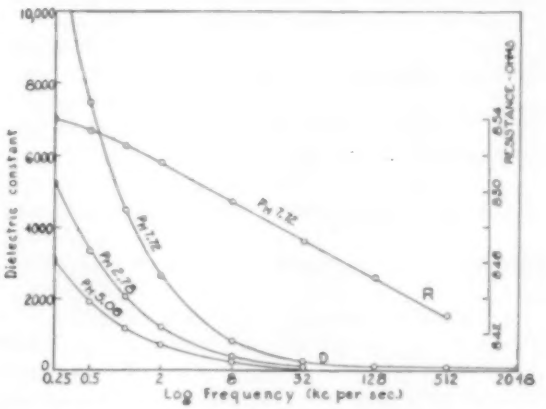

FIG. 2. The dielectric constant as a function of frequency for suspensions of kaolin in 1.5 percent gelatin at different pH values. The resistance-frequency curve is shown for one of the suspensions. Volume concentration of kaolin is 23 percent.

an inverse power of the frequency, with an exponent which is always near unity, and exactly this value in a great number of cases.

As a possible explanation of these results, it may be observed that since part of the current (representing the surface conductance) passes through the highly charged regions which are generally present at and near the surfaces of the colloidal particles, an increased dielectric constant and resistance would result at the lower frequencies if the current, in passing into such regions, were polarized as one would expect it to be. From the point of view of this interpretation it should be remarked that the polarization (represented by the polarization capacity and the polarization resistance), which is observed at interfaces such as metal electrodes or membranes (collodion or biological membranes) is also characterized by its being a power function of the frequency, although with widely varying values of the exponent from system to system.[7, 8]

The experiments represented in Fig. 2 were made to test the relation of the increased dielectric constant to the charge on the colloidal particles. Suspensions of kaolin in gelatin were measured at three different pH values. At $pH = 5.0$, which is close to the isoelectric point of gelatin, the electrophoretic velocity of the kaolin particles is nearly zero and the dielectric constant smallest. That the value is still high may be explained on the grounds that the zero charge on a kaolin particle, at the isoelectric point, results from a time or space average of equal positive and negative charges.

Other systems studied include colloidal ferric oxide,[9] soap (commercial), sodium oleate, gum arabic and gelatin. For ferric oxide and soap (1.5 percent) the frequency curves for resistance and dielectric constant present the same general forms as those obtained for coarser suspensions (Fig. 1). For sodium oleate (1.5 percent) as well as for gum arabic (10 percent) and gelatin (1.5 percent), the resistance and dielectric constant are independent of the frequency.

HUGO FRICKE
HOWARD J. CURTIS
Walter B. James Laboratory for Biophysics,
The Biological Laboratory,
Cold Spring Harbor, New York,
May 27, 1935.

[1] R. Fürth, Ann. d. Phys. **70**, 64 (1923).
[2] J. Errera, J. de phys. et rad. **4**, 225 (1923); J. chim. phys. **29**, 577 (1932).
[3] R. Fricke and L. Havestadt, Zeits. f. anorg. Chemie **188**, 357 (1930); **196**, 120 (1931).
[4] R. Fricke, Kolloid Zeits. **56**, 166 (1931).
[5] T. Nanty and M. Valet, Comptes rendus **194**, 883 (1932).
[6] A. and B. Piekera, Comptes rendus **198**, 803 (1934).
[7] H. Fricke, Phil. Mag. **14**, 310 (1932).
[8] H. Fricke, Physics **1**, 106 (1932).
[9] Maffia, Kolloidchem. Beiheft. **3**, 93 (1912).

Welding Arcs in Argon

The purpose of this note is to give an interpretation to some experiments with arcs in argon recently reported in these columns by G. E. Doan and W. C. Schulte.[1] They found that in pure argon gas there is "a complete absence of crater formation in the base metal or previous weld deposit, and a resulting complete lack of penetration into, and fusion of the parts being welded." This was observed at values of total arc wattage equal to or greater than that required to produce satisfactory welds in air.

The relatively poor heat transfer due to the lack of a dissociation-diffusion-recombination process in the monatomic argon is probably responsible for these results. By a variation of the velocity of sound method previously reported,[2] we have measured the gas column temperature in a welding arc between an iron plate and a 3/16" commercial coated iron welding rod (type W-20) at 125 amperes d.c. and find a mean value of 6000°K. From recently determined[3] equilibrium constants for the dissociation processes $O_2 \rightleftarrows 2O$, $N_2 \rightleftarrows 2N$, the arc atmosphere is calculated to be 81 percent atomic gas at the observed temperature. The effectiveness of dissociated gas in heating metallic surfaces, which act as catalysts for the recombination process, is well known. Langmuir[4] has shown that for

the H_2 arc the alternative process, direct thermal conduction through the gas, is relatively unimportant. The high percentage of atomic gas which we have observed in welding arcs suggests that these arcs depend to a large extent upon the diffusion-recombination process for heat transfer. The experimental results of Doan and Schulte support this view.

The relative effectiveness of the diffusion of H through H_2 and N through N_2 in heat transfer may be calculated from

$$h_H/h_N = aD_H V_H/aD_N V_N = \lambda_H C_H V_H/\lambda_N C_N V_N,$$

where h is the quantity of heat, a is a constant, D is the diffusion coefficient, V is the dissociation potential, C is the mean molecular velocity, λ is the m.f.p., and the subscripts refer to the respective gases. With the values $V_H = 4.4$ and $V_N = 11.7$, $h_H/h_N = 2.6$. Thus for the same degree of dissociation the diffusion heat transfer in nitrogen is nearly half as effective as in hydrogen.

C. G. SUITS

Research Laboratory,
General Electric Co.,
Schenectady, N. Y.,
May 24, 1935.

[1] Doan and Schulte, Phys. Rev. **47**, 785 (1935).
[2] C. G. Suits, Proc. Nat. Acad. Sci. **21**, 48 (1935).
[3] Giauque and Clayton, J. Am. Chem. Soc. **55**, 4887 (1933); Johnston and Walker, J. Am. Chem. Soc. **55**, 191 (1933); **55**, 179 (1933).
[4] I. Langmuir, Gen. Elec. Rev. **29**, 153 (1926).

Author Index to Volume 47

References with (A) are to abstracts of papers presented at meetings of the Physical Society. References with (L) are to Letters to the Editor.

Adel, Arthur and V. M. Slipher. Difference bands in the spectra of the major planets—651

——— **and V. M. Slipher.** Methane content of the giant planet atmospheres—787(A)

——— **and V. M. Slipher.** Principal limit of the transmission of solar radiation by the earth's atmosphere in the far infrared—251(L)

———, **V. M. Slipher and E. F. Barker.** Absorption of sunlight by the earth's atmosphere in the remote infrared region of the spectrum—580

Agruss, M. S. (see Grosse, A. V.)—91(L), 93(L)

Albers, V. M. (see Knorr, H. V.)—329(A)

———, **H. V. Knorr and Paul Rothemund.** Fluorescence of the chlorophyll series: The reversible reduction of chlorophyll *a* and *b*—198(A)

Albertson, Walter. Arc spectrum of samarium and gadolinium. Normal electron configurations of the rare earths—370

Allen, J. S. V. and C. E. Hesthall. Intensity relations in chromium spectra—926

Allis, W. P. (see Morse, Philip M.)—806(A)

Almy, G. M. and G. D. Kinzer. Emission spectrum of diatomic arsenic—199(A), 721

Altar, Wm. Intramolecular forces between bound atoms—804(A)

Alvarez, Luis W. Artificial radioactivity induced by cosmic rays—320(L)

——— Energies of x-ray photoelectrons—636(L)

Anderson, J. A. Astronomical seeing—637(A) (Title only)

Anderson, L. C. (see Bates, John R.)—332(A) (Title only)

Anderson, O. E. (see Ballard, S. S.)—256(A) (Title only)

Anderson, Paul A. Contact difference of potential between tungsten and barium. The external work function of barium—958

Appleton, E. V. Recent measurements of upper-atmospheric ionization—89(L)

——— Seasonal variation of ionization in region F_2 of the ionosphere—704(L)

Armstrong, A. H. (see Hudson, J. C.)—809(A)

Armstrong, J. E. Magnetoresistance of liquid sodium-potassium alloy—391

——— (see Heaps, C. W.)—336(A)

Arthur, John M. (see Way, Katharine)—198(A)

Atkinson, R. d'E. Energy and angular momentum in certain optical problems—623, 639(A)

Bacher, R. F. Prediction of atomic energy states—699(A) (Title only)

——— **and R. A. Sawyer.** Isotope shift in Mg I—587

Badger, Richard M. and Charles M. Blair, Jr. Note on the band spectrum of silicon fluoride—881(L)

Balinkin, Isay A. Transverse vibrations of long rods—340(A)

Ball, T. R. Observations on the Allison magnetic-optic apparatus—548

Ballard, James W. and E. D. Wilson. On the nature of the barrier plane in the cuprous-oxide photovoltaic cell—794(A)

Ballard, S. S., O. E. Anderson and H. E. White. Fine structure and hyperfine structure of doubly ionized beryllium—256(A)

Barker, E. F. (see Adel, Arthur)—580

——— (see Bartunek, Paul F.)—330(A)

——— (see Ginsburg, Nathan)—641(A)

——— (see Migeotte, M. V.)—812(A)

——— **and Marcel Migeotte.** Low frequency double vibrations of the deutero-ammonias—702(L)

Barnes, R. Bowling. Pure rotation spectra of NH_3 and ND_3—658

——— (see Brattain, R. Robert)—793(A)

———, **W. S. Benedict and C. M. Lewis.** Far infrared absorption of benzene—129

———, **W. S. Benedict and C. M. Lewis.** Far infrared spectrum of H_2O—918

——— **and R. Robert Brattain.** Near infrared spectrum of MgO—416(L)

———, **R. Robert Brattain and R. S. Firestone.** Powder filfers for the infrared—792(A)

Barr, E. S. (see Plyler, E. K.)—793(A)

Barrett, Charles S. Slip, twinning and cleavage in silicon ferrite (4.17 percent Si)—809(A)

——— X-ray diffraction and the fatigue of metals—333(A)

——— X-ray measurement of depth of cold work—338(A)

Barrows, W. M., Jr. (see Green, J. B.)—131

Bartberger, C. L. Energy levels of the rare gas configurations—803(A)

Bartlett, J. H., Jr. (see Gibbons, J. J., Jr.)—340(A), 692

——— (see Shoupp, W. E.)—705(L)

———, **J. J. Gibbons, Jr. and C. G. Dunn.** Normal helium atom—679, 804(A)

Bartlett, William W. (see Harrison, George R.)—799(A)

Barton, Henry A. (see Mueller, Donald W.)—796(A)

Bartunek, Paul F. (see Roth, Frank L.)—526

——— **and E. F. Barker.** Fundamental band of H^3CN at 17.5μ—330(A)

Bates, John R., J. O. Halford, L. C. Anderson and R. D. Swisher. Study of the deuterium exchange reaction involving acetone—332(A) (Title only)

Bazzoni, Charles B. (see McCorkle, Paul)—804(A)

Beach, J. Y. (see Pauling, Linus)—686

Beams, J. W. (see Pickels, E. G.)—336(A)

——— (see Trotter, Herbert, Jr.)—641(A)

Bearden, J. A. Refraction of the copper $K\beta$ line by a diamond prism—811(A)

——— Ruled grating measurements of x-ray wavelengths—804(A)

——— Scale of x-ray wavelengths—883(L)

Bearden, J. A. X-ray wavelengths and the electronic charge—645(A)
——— (see Shaw, C. H.)—332(A)
——— **and W. R. Kanne.** On the emission of protons by samarium—639(A)
Beasley, I. E. (see Glasser, Otto)—570(L), 789(A)
Beck, F. J., Jr. (see Clash, R. F., Jr.)—158
Beck, Guido. Energy levels of light nuclei—809(A)
——— Present state of the neutrino hypothesis—202(A)
——— **and L. H. Horsley.** Nonelastic collision cross sections for slow neutrons—510(L)
Beckwith, M. M. (see Clark, G. L.)—200(A)
Bell, M. E. (see Johnson, R. P.)—426(A)
Bell, Raymond M. (see Jeppesen, Myron A.)—546
Benade, J. M. and R. L. Doan. Apparatus for transmitting cosmic-ray data from stratosphere—198(A)
Bender, David. Raman effect of water vapor—252(L)
Benedict, W. S. Isotope effect in polyatomic molecules—699(A) (Title only)
——— Ultraviolet absorption spectra of the deutero-ammonias—641(A)
——— (see Barnes, R. Bowling)—129, 918
Bennett, Clarence E. Molar polarization of nitrogen and argon by displacement interferometry—790(A)
Bennett, Ralph D., Gordon S. Brown and Henry A. Rahmel. Frequency and magnitude of cosmic-ray bursts as a function of elevation—339(A), 437
Bennett, Willard H. Electrostatic generator with small vertical clearance—791(A)
Bethe, H. A. Atomic weights derived from nuclear transmutations—795(A)
——— Capture and scattering of neutrons—640(A)
——— Masses of light atoms from transmutation data—633(L)
——— Theory of disintegration of nuclei by neutrons—747
Beuschlein, W. L. (see McNabney, Ralph)—695
Bhagavantam, S. and A. Veerabhadra Rao. Vibrational Raman scattering in liquids—921
Bien, R. P. Study of the crystal structure of heat-treated filaments—806(A)
Bingham, Eugene C. and Charles E. Coombs. Fluidity and molecular complexity—645(A)
Birge, Raymond T. and Edwin McMillen. Value of the electronic charge—320(L)
Bitter, Francis. Relationship between the elastic and magnetic properties of metals—428(A) (Title only)
Blair, Charles M., Jr. (see Badger, Richard M.)—881(L)
Bleakney, Walker (see Hipple, J. A., Jr.)—802(A)
——— (see Smyth, H. D.)—800(A)
——— **and J. A. Hipple, Jr.** Study of oxygen isotopes—800(A)
Bloch, F. and P. A. Ross. Radiative auger effect—884(L)
Bonner, T. W. (see Brubaker, W. M.)—255(A)
——— **and W. M. Brubaker.** Energy of the neutrons from the disintegration of beryllium by deutons—254(A)
——— **and W. M. Brubaker.** Energy spectrum of the neutrons from the disintegration of beryllium by deuterons—910
——— **and W. M. Brubaker.** Evidence for the formation of $_4Be^8$ in the disintegration of lithium by deuterons—973(L)
Bouckaert, L. (see Lemaitre, G.)—434
Bowen, I. S. Low terms in the Mn V and Fe VI—924
Boyce, J. C. Spectra of argon and krypton in the extreme ultraviolet—799(A)
——— Spectra of krypton in the extreme ultraviolet—718
——— **and C. A. Rieke.** Provisional wavelength standards for the extreme ultraviolet—653
Boynton, W. P. Equations of state and thermodynamic functions for substances with variable specific heat—258(A)
Bozler, Emil (see Cole, Kenneth S.)—644(A)
Bradley, Charles A., Jr. (see McKellar, Andrew)—787(A)
——— **and Andrew McKellar.** Absorption of the acetylenes in the photographic infrared—793(A)
——— **and Andrew McKellar.** On the absorption of acetylene and di-deutero-acetylene in the photographic infrared—914
Bradley, Charles D. Cloud chamber study of the initiation of ionization in spark discharge—802(A)
——— **and L. B. Snoddy.** Ion distribution during the initial stages of spark discharge in nonuniform fields—541
Brady, James J. Formation of a potassium film on silver—197(A)
Bramley, Arthur. Validity of the applications of electrodynamics—321(L)
Brandt, W. H. (see Loomis, F. W.)—199(A)
Brattain, R. Robert (see Barnes, R. Bowling)—416(L), 792(A)
———, **R. Bowling Barnes and Frederick Seitz.** Infrared absorption spectrum of MgO—793(A)
Braun, Milton L. Coefficient of linear expansion for stretched rubber bands at room temperatures—798(A)
——— Rubber deformations caused by uniformly repeated stresses—336(A)
Breazeale, William M. Electro-optical Kerr effect in NH_3, N_2 and O_2—789(A)
Breit, G. Some applications of group theory to Dirac's relativistic theory—338(A) (Title only)
——— (see Wills, L. A.)—704(L)
——— **and F. L. Yost.** Radiative capture of protons by carbon—508(L)
Brewer, A. Keith. Abundance ratio of the isotopes of lithium—571(L)
Brice, R. T. and John Strong. Optical properties of magnesium oxide—255(A)
Brickwedde, F. G. Ortho- and para-deuterium—332(A) (Title only)
——— (see Scott, R. B.)—794(A)
——— (see Silsbee, F. B.)—794(A)
Bridgman, P. W. High pressure transitions of bismuth—427(A)
——— On the effect of slight impurities on the elastic constants, particularly the compressibility of zinc—393
Brown, Gordon S. (see Bennett, Ralph D.)—339(A), 437
Brown, Joseph G. Analysis of the diurnal variation of the Earth's potential gradient—259(A)
Brubaker, W. M. (see Bonner, T. W.)—254(A), 910, 973(L)
——— **and T. W. Bonner.** Automatic high pressure Wilson cloud chamber—255(A)

Bryan, A. L. (see Knauss, H. P.)—842
Burwell, J. T. (see Warren, B. E.)—330(A)

Cairns, J. E. I. Production of induced radioactivity by the cosmic radiation—194(L), 631(L)
Cardwell, Alvin B. Thermionic properties of tantalum—628
Carl, Howard (see Petersen, Max)—803(A)
Carman, Everett F. (see Harkins, William D.)—797(A)
Cartmel, W. B. Theoretical discussion of Professor Miller's paper on the ether drift experiments—333(A)
Challacombe, C. N. (see Kruger, P. Gerald)—509(L)
——— **and P. Gerald Kruger.** Hyperfine structure of Y II lines—798(A)
Christy, Andrew. On the band spectrum of sulfur—251(L)
Chu, T. C. (see Woo, Sho-Chow—886(L)
Clark, C. H. Douglas. Periodicity of Morse's function—238
Clark, G. L. and M. M. Beckwith. Mathematical modulus derived from x-ray data for evaluation of residual distortion in crystals—200(A)
Clash, R. F., Jr. and F. J. Beck, Jr. Directions of discontinuous changes in magnetization in monocrystal bars and disks of silicon-iron—158
Clements, J. H. On the absorption spectrum of sulphur dioxide—224
——— Temperature variation method to assist in vibrational analyses of complex molecular spectra—220
Colby, Walter F. Isotope effect in acetylene—388
Cole, Kenneth S. and Emil Bozler. Electric impedance of muscle—644(A)
Colwell, R. C. and N. I. Hall. High speed electrical motors —337(A)
Compton, Arthur H. Incoherent scattering and the concept of discrete electrons—203(A), 367
——— **and I. A. Getting.** Apparent effect of galactic rotation on the intensity of cosmic rays—817
Constant, F. Woodbridge. Variation of thermal e.m.f. with magnetization and temperature—794(A)
Cookson, John W. Theory of the piezo-resistive effect—194(L)
——— (see Osterberg, Harold)—781(L)
Coolidge, Albert Sprague (see James, Hubert M.)—700(L)
Coombs, Charles E. (see Bingham, Eugene C.)—645(A)
Coon, Edith M. and E. R. Laird. Raman effect in solutions of magnesium sulphate of varying concentrations—889(L)
Cowie, D. B. (see Swann, W. F. G.)—811(A)
Crane, H. R., L. A. Delsasso, W. A. Fowler and C. C. Lauritsen. Emission of negative electrons from boron bombarded by deuterons—887(L)
———, **L. A. Delsasso, W. A. Fowler and C. C. Lauritsen.** Gamma-rays from boron bombarded with deutons—253(A)
———, **L. A. Delsasso, W. A. Fowler and C. C. Lauritsen.** Gamma-rays from the disintegration of beryllium by deuterons and protons—782(L)
———, **L. A. Delsasso, W. A. Fowler and C. C. Lauritsen.** Emission of negative electrons from lithium and fluorine bombarded with deuterons—971(L)
——— **and C. C. Lauritsen.** Masses of Be^8, Be^9 and B^{11} as determined from transmutation data—420(L)
Crary, A. P. (see Ewing, Maurice)—797(A)
———, **Maurice Ewing and E. B. Douglas.** Propagation of elastic waves in lake ice—797(A)
Cravath, A. M. Photoelectric effect and spark mechanism—254(A)
——— **and L. B. Loeb.** Mechanism of the high velocity of propagation of lightning discharges—259(A)
Crawford, F. H. and T. Jorgensen, Jr. Band spectra of the hydrides of lithium. Part I: $Li^{(7)}D$—358; Part II: Li^7H—932
Crawford, M. F. Hyperfine structure formulae for the configuration of d^2s. Application to $5d^26s\ ^4F$ states of La I —768
——— **and Norman S. Grace.** Hyperfine structures in La III. Nuclear magnetic moment of lanthanum—536
Cross, Paul C. Analysis of the hydrogen sulfide band at 10,100A—7
Curtis, Howard J. (see Fricke, Hugo)—974(L)
Cuykendall, T. R. (see Jones, M. T.)—643(A)
——— **and M. T. Jones.** Two-crystal transmission spectrometer for ultra-short x-rays—643(A)

Danforth, W. E. and W. F. G. Swann. On the electrostatic deflection of cosmic radiation—421(L)
Darling, B. T. (see Kruger, P. Gerald)—790(A)
Davey, Wheeler P. (see Haring, W. J.)—337(A)
——— (see McCormick, W. E.)—330(A)
——— (see Waldo, P. G.)—338(A)
Davis, Hallowell. Electrical phenomena of the cochlea and the auditory nerve—338(A) (Title only)
Davisson, C. J. Electron optics—332(A) (Title only)
Delsasso, L. A. (see Crane, H. R.)—253(A), 782(L), 887(L), 971(L)
Delsasso, Leo P. and John H. Munier. Preliminary report on the experimental method of detecting anomalous dispersion of sound in air in the audible range as a function of frequency and humidity—259(A)
Deming, J. H. (see Jauncey, G. E. M.)—804(A)
Dempster, A. J. New ion source for mass-spectroscopy—331(A)
Dennison, David M. and Manfred Johnston. Interaction between vibration and rotation for symmetrical molecules—93(L)
Devol, Lee. Metastable nuclei produced by the hard gamma-rays from radium B+C—325(A)
DeVore, Lloyd T. Connecting link between classical electromagnetic theory and wave mechanics via a derivation of the Schrödinger equations as a boundary value problem on the atom—333(A)
——— Correlation between electromagnetic theory and wave mechanics—638(A)
Dieke, G. H. Class of perturbations of molecular levels—870
——— On isotopic shifts in the spectra of diatomic molecules—661
——— Use of deuterium in spectroscopic investigations of molecules—332(A) (Title only)
——— **and R. W. Blue.** Fulcher bands of HD and D_2—261
Doan, Gilbert E. and William C. Schulte. Arcs in inert gases—III—783(L)

Doan, R. L. (see Benade, J. M.)—198(A)
Dolecek, R. L. Discussion of Fermi's theory of the beta-decay—202(A)
Dorsey, Herbert Grove. Shoal fathometer—334(A)
Douglas, E. B. (see Crary, A. P.)—797(A)
——— (see Ewing, Maurice)—797(A)
Duffendack, O. S. (see Emeleus, K. G.)—460
——— (see Manley, J. H.)—56
——— (see Smith, R. W.)—473
Duffin, Richard J. Virial theorem and quantum statistics—421(L)
Dufford, R. T. Evidence from Raman effect for a slight asymmetry of the carbon atom—199(A)
——— (see Emberson, Richard M.)—202(A)
——— (see Skaggs, Lester S.)—201(A)
Dull, Raymond B. Note on the spectrum of boron fluoride—458
Duncan, A. B. F. Ultraviolet absorption spectrum of ammonia—822
——— Ultraviolet absorption spectrum of ND_3—886(L)
Dunn, C. G. (see Bartlett, J. H., Jr.)—679, 804(A)
——— (see Shoupp, W. E.)—705(L)
Dunning, J. R. (see Pegram, G. B.)—325(A)
——— **and G. B. Pegram.** Absorption and scattering of slow neutrons—640(A)
———, **G. B. Pegram and G. A. Fink.** Capture, stability and radioactive emission of neutrons—325(A)
———, **G. B. Pegram, G. A. Fink and D. P. Mitchell.** Absorption and velocity of slow neutrons—796(A)
———, **G. B. Pegram, G. A. Fink and D. P. Mitchell.** Interaction of low energy neutrons with atomic nuclei—416(L)
———, **G. B. Pegram, G. A. Fink and D. P. Mitchell.** Slow neutrons—970(L)
———, **G. B. Pegram, D. P. Mitchell and G. A. Fink.** Thermal equilibrium of slow neutrons—888(L)
Dunnington, Frank G. Precision magnetic field standard—257(A)
Duveneck, F. B. (see Webster, D. L.)—699
Duwez, Pol. On the plasticity of crystals—494

Earls, Lester T. and Ralph A. Sawyer. Classification of the first spark spectrum of lead: Pb II—115
Eaton, William W. Collisions of alpha-particles with neon nuclei—796(A)
——— (see Pollard, Ernest)—597
——— **and Ernest Pollard.** Proportional (Geiger-Klemperer) nuclear particle counter, and attempts to detect deuterons from two favorable reactions—640(A)
Eckart, Carl. Some studies concerning rotating axes and polyatomic molecules—552
Edwards, Hiram W. High speed oil diffusion pump—259(A)
——— Null method photoelectric photometer—258(A)
Einstein, A., B. Podolsky and N. Rosen. Can quantum-mechanical description of physical reality be considered complete?—777
Ellis, Cecil and Ralph A. Sawyer. Extension of the thallium II spectrum—799(A)
Ellis, Joseph W. and Joseph Kaplan. Polarization effects in the Hilger E1 quartz spectrograph—255(A)
Emberson, Richard M. and R. T. Dufford. Search for a photomagnetic effect—202(A)
Emeleus, K. G. and O. S. Duffendack. Spectral and impact phenomena in the Faraday dark space—460
Epstein, Paul S. Propagation of micro-radio waves—258(A)
Evans, Robley D. (see Livingston, M. Stanley)—795(A)
———, **Gladys D. Finney, Arthur F. Kip and Raymond Mugele.** New methods for the detection of minute quantities of thorium in common materials—791(A)
——— **and R. A. Mugele.** Gamma-ray sensitivity of tube-counters and the measurement of the thorium content of rocks—427(A)
Ewing, Maurice (see Crary, A. P.)—797(A)
———, **A. P. Crary and E. B. Douglas.** Dispersion in flexural waves in lake ice—797(A)

Failla, G. Simple device for producing very small unidirectional currents—805(A)
Farnsworth, H. E. Depth of penetration of electrons diffracted by single crystals—331(A)
Farwell, H. W. and J. B. Hawkes. Time lags in magneto-optics—78
Fearon, Robert E. Electrical conductance of short cold-metal gaps in air—802(A)
Feenberg, Eugene. Neutron-proton interaction. Part I. The binding energies of the hydrogen and helium isotopes—809(A), 850; Part II. The scattering of neutrons by protons—857
——— On the Born-Infeld field theory of the electron—148
Fink, G. A. (see Dunning, J. R.)—325(A), 416(L), 796(A), 888(L), 970(L)
Finney, Gladys D. (see Evans, Robley D.)—791(A)
Firestone, R. S. (see Barnes, R. Bowling)—792(A)
Flowers, J. W. Oscillographic study of overvolted discharges—801(A)
Forsythe, W. E. Color temperature scale of the Nela Laboratories—789(A)
Foster, J. S. Interpretation of anomalous Stark intensities—329(A)
——— **and A. H. Snell.** Stark effect in the hydrogen isotopes—338(A)
Fowler, W. A. (see Crane, H. R.)—253(A), 782(L), 887(L), 971(L)
Fox, Gerald W. and Walter A. Fraser. X-ray extinction in piezoelectrically oscillating crystals—200(A), 899
Fox, M. (see Millman, S.)—801(A)
———, **S. Millman and I. I. Rabi.** Nuclear spin and magnetic moment of Li^7—801(A)
Frank, N. H. Effect of pressure on the electrical conductivities of the alkalies—282
Fraser, Walter A. (see Fox, Gerald W.)—200(A), 899
Freed, Simon and Harry G. Thode. Magnetic study of the metallic state and the Fermi-Dirac statistics—335(A)
Fricke, Hugo and Howard J. Curtis. Dielectric constant and resistance of colloidal solution—974(L)
Frost, A. A. and O. Oldenberg. Spectroscopic investigation of chemical reactions of OH in the electric discharge—788(A)
Fussler, Karl H. (see Ruark, Arthur E.)—790(A)

Gagge, A. P. Annual and diurnal variations of ions in urban communities—786(A)
Galli-Shohat, N. Huygen's principle and the Lorentz contraction hypothesis—639(A)
Gamow, G. Problems of beta-disintegration—428(A) (Title only)
Gans, David M. (see Harkins, William D.)—52, 511(L)
——— **and William D. Harkins.** Nuclear chemistry and the scattering of protons in collisions with neutrons—795(A)
Getting, I. A. (see Compton, Arthur H.)—817
Giauque, W. F. and D. P. MacDougall. Thermodynamic temperature scale in the region below 1° Absolute—885(L)
Gibbons, J. J., Jr. (see Bartlett, J. H., Jr.)—679, 804(A)
——— **and J. H. Bartlett, Jr.** Magnetic moment of the K^{39} nucleus—340(A), 692
Gibbs, R. C. Interferometric studies of alpha-lines of hydrogen and deuterium—332(A) (Title only)
Gilbert, W. P. Extension of the Rh I-like isoelectronic sequence to the spectrum of Ag III—803(A)
——— Some higher terms in the spectrum of Ag II—847
Gilliland, T. R. (see Kirby, S. S.)—632(L)
Gingrich, N. S. and Ralph Hultgren. Fourier analyses of x-ray patterns of phosphorus—808(A)
Ginsburg, Nathan and E. F. Barker. Infrared absorption spectrum of methyl deuteride—641(A)
Glasser, Otto and I. E. Beasley. Effect of visible light upon the ultraviolet fluorescence of various compounds previously irradiated with Roentgen or gamma-rays—789(A)
——— **and I. E. Beasley.** Induced ultraviolet fluorescence and its release by visible light—570(L)
Glockler, George and Charles E. Morrell. Symmetric C–D bond vibration in heavy acetylene—569(L)
Goetz, Alexander. Phenomenon of supercooling—257(A)
——— (see Jacobs, Robert B.)—94(L), 257(A)
Goldberg, Leo (see Menzel, Donald H.)—424(L)
Goslin, Roy (see Hughes, Gordon)—317(L)
Goss, Wilbur H. (see Henderson, Joseph E.)—259(A)
Grace, Norman S. (see Crawford, M. F.)—536
——— (see Spedding, Frank H.)—38
Granath, L. P. Measurement of nuclear magnetic moments from hyperfine structure data—699(A) (Title only)
——— (see Stranathan, R. K.)—801(A)
Gray, J. A. and J. F. Hinds. Diffusion of radioactive atoms—813(A)
Green, J. B. and W. M. Barrows, Jr. Zeeman effect of the spectra of arsenic—131
Griggs, H. P. (see Reardon, A. J.)—199(A)
Grosse, A. V. (see Pierce, W. C.)—432
——— **and M. S. Agruss.** Fermi proton effect—91(L)
——— **and M. S. Agruss.** Gamma-ray neutrons and the Fermi proton effect—93(L)
Gunn, Ross. Electricity of rain and thunderstorms—786(A)
Gurney, R. W. Theory of electrical double layers in adsorbed films—479

Hafstad, L. R. and M. A. Tuve. Induced radioactivity using carbon targets—506(L)
——— **and M. A. Tuve.** Resonance transmutations by protons—506(L)
Haines, C. L. Characteristics of Geiger-Müller counters filled with different gases—791(A)
Halford, J. O. (see Bates, John R.)—332(A) (Title only)
Hall, Leo G. On the low temperature diffusion of solid aluminum into iron—418(L)
Hall, N. I. (see Colwell, R. C.)—337(A)
Ham, W. R. Equations for diffusion of gases through metals—645(A)
——— (see Sauter, J. D.)—645(A)
——— **and J. D. Sauter.** Diffusion of hydrogen through iron and palladium—337(A)
Hansen, W. W. New type of expansion in radiation problems—139
——— (see Webster, D. L.)—699
Hardy, J. D. and Carl Muschenheim. Diffuse infrared transmission of solids—789(A)
Haring, W. J. and Wheeler P. Davey. Expansion of copper from absolute zero to its melting point—337(A)
Harkins, William D. Nuclear reactions and their classification by atomic and isotopic numbers—702(L)
——— (see Gans, David M.)—795(A)
———, **Everett F. Carman and Herman E. Ries, Jr.** Surface pressures and potentials of monomolecular films of long molecules: Hydroxy-decanoic acid polymers—797(A)
———, **David M. Gans and Henry W. Newson.** Disintegration of the nuclei of light atoms by neutrons. II. Neon, fluorine and carbon—52
———, **David M. Gans, Martin Kamen and Henry W. Newson.** Scattering of protons in collisions with neutrons—511(L)
Harnwell, G. P. (see Smyth, H. D.)—800(A)
Harrison, George R. and William W. Bartlett. Wavelength measurements in the spectra of the neodymium arc and the standard Pfund iron arc—799(A)
Hawkes, J. B. (see Farwell, H. W.)—78
Heaps, C. W. and J. E. Armstrong. Magnetoresistance in sodium-potassium alloy—336(A)
Hector, L. G. (see Schultz, H. L.)—327(A)
——— **and H. L. Schultz.** Measurement of the dielectric constant of air at radiofrequencies—327(A)
Henderson, Joseph E., Wilbur H. Goss and John E. Rose. Comparison of the rotary voltmeter and the sphere gap up to 830 kilovolts—259(A)
Henderson, Malcolm C. (see Lawrence, Ernest O.)—254(A), 273
Henry, D. E. (see Rentschler, H. C.)—807(A)
Hesthal, C. E. (see Allen, J. S. V.)—926
Hickman, Roger W. and Frederick V. Hunt. Exact measurement of electron tube coefficients—787(A)
Hinds, J. F. (see Gray, J. A.)—813(A)
Hipple, J. A., Jr. (see Bleakney, Walker)—800(A)
——— **and Walker Bleakney.** Products of ionization in methane—802(A)
Hirsh, F. R., Jr. and F. K. Richtmyer. Comments on the Coster-Kronig theory of a new type of Auger effect—805(A)

Hoffmann, Banesh. Gravitational and electromagnetic mass in the Born-Infeld electrodynamics—804(A), 877
——— Spherically symmetric field in the Born-Infeld theory—639(A)
Holmes, R. M. and L. C. Whitman. Temperature effects on photo-voltaic current and e.m.f. of a selenium monocrystal platinum film combination—337(A)
Hopfield, John J. Extension of the absorption spectrum of the hydrogen molecule—788(A)
Horsley, L. H. (see Beck, G.)—519(L)
Houston, William V. Forces between nuclear particles—260(A)
——— Nuclear model—819(A), 942
Howe, J. D. (see Lark-Horovitz, K.)—331(A)
——— **and E. M. Purcell.** New method of making extremely thin films—329(A)
Hudson, J. C., H. G. Vogt and A. H. Armstrong. New lines in the *K* series spectrum of tungsten—809(A)
Huffman, John R. (see Vance, John E.)—215
Hughes, A. L. Physics at Washington University—197(A) (Title only)
Hughes, Gordon and Roy Goslin. Photography of minima in magneto-optic apparatus—317(L)
Hulburt, E. O. Concerning the ionosphere—422(L)
Hultgren, Ralph (see Gingrich, N. S.)—808(A)
——— **and B. E. Warren.** Crystal structure of black phosphorus—808(A)
Humphreys, C. J. Third spectrum of krypton—712, 799(A)
Hunt, Frederick V. (see Hickman, Roger W.)—787(A)
Hutchisson, E. Effect of electrostatic field upon rate of vaporization—328(A)

Ide, John. Measurement of Young's modulus in rocks by a new dynamical method—797(A)
Inglis, D. R. Magnetic moments of the deuton and other nuclei—334(A)
——— On nuclear moments—84
——— Nuclear states and moments—813(A)

Jacobs, Robert B. and Alexander Goetz. Intensities of x-ray reflection from Bi crystals between 25° and 530° Abs.—257(A)
——— **and Alexander Goetz.** Temperature function of x-ray reflection in the neighborhood of the melting point of a crystal—94(L)
Jacobson, M. G. New balanced circuit for resistance thermometers, combustible gas indicators, etc.—336(A)
James, Hubert M. and Albert Sprague Coolidge. Hylleraas method applied to lithium—700(L)
Jauncey, G. E. M. Diffuse scattering of x-rays by crystals—201(A)
——— **and J. H. Deming.** Extra negative term in the incoherent part of the diffuse scattering from neon-like crystals—804(A)
Jenkins, F. A. Alternating intensities in the spectrum of P_2—783(L)
——— **and L. A. Strait.** Spectrum of AsO—136, 257(A)
Jeppesen, Myron A. and Raymond M. Bell. Objective study of the Allison magneto-optic method of analysis—546
Johnson, R. P., M. E. Bell and W. B. Nottingham. Vacuum tube amplifier for thermocouple e.m.f.—426(A)
Johnson, Thomas H. Evidence for a positron-negatron component of the primary cosmic radiation—318(L), 642(A)
——— North-south asymmetry of the cosmic radiation—326(A)
——— North-south asymmetry of the cosmic radiation in Mexico—91(L)
——— (see Stevenson, E. C.)—578
Johnston, H. L. Chemical separation of the isotopes of hydrogen—332(A) (Title only)
Johnston, Manfred (see Dennison, David M.)—93(L)
Jones, M. T. (see Cuykendall, T. R.)—643(A)
——— **and T. R. Cuykendall.** Absorption of x-rays in the wavelength range 50 X.U. to 200 X.U.—643(A)
Jordan, Edward B. Probability of collision for slow H^+, $(H^1H^1)^+$, $(H^1H^2)^+$, $(H^2H^2)^+$, $(H^2)^+$ and He^+ ions in argon—467
Jorgensen, T., Jr. (see Crawford, F. H.)—358, 932
Judson, E. B. Ionosphere studies—509(L)
——— (see Kirby, S. S.)—632(L)

Kamen, Martin (see Harkins, William D.)—511(L)
Kanne, W. R. (see Bearden, J. A.)—639(A)
Kaplan, Joseph. Light of the night sky—193(L)
——— New band systems in nitrogen—255(A)
——— New system of nitrogen bands—259(A)
——— (see Ellis, Joseph W.)—255(A)
Kemble, E. C. Contribution to the theory of the W.B.K. method—426(A)
——— Correlation of wave functions with the states of physical systems—973(L)
Kennedy, Roy J. Constancy of the velocity of light—533
——— Simplified theory of the Michelson-Morley experiment—965
Kernaghan, Marie. Surface tension of mercury in the presence of gases. I. Dry air—202(A)
Kimball, George E. Electronic structure of diamond—810(A)
King, Aruthur S. Experimental features of the spectrum of samarium—256(A)
King, Paul B., Jr. and Harry Rowe Mimno. Recording of ionosphere echoes at non-vertical incidence—786(A)
King, Ronold. New type radio transmitter for short waves—787(A)
Kinzer, G. D. (see Almy, G. M.)—199(A), 721
Kip, Arthur F. (see Evans, Robley D.)—791(A)
Kirby, S. S., T. R. Gilliland and E. B. Judson. Ionosphere studies during partial solar eclipse—632(L)
Knauss, H. P. (see Strong, Herbert M.)—642(A)
——— **and A. L. Bryan.** Spectral characteristics of electrically exploded mercury—842
Knipp, Charles T. Liquefaction of gases—a demonstration—200(A)
Knipp, Julian K. On the Zeeman effect in diatomic molecular states having *L*-uncoupling—672, 803(A)
——— Wave mechanical treatment of the LiH molecule—339(A)
Knorr, H. V. (see Albers, V. M.)—198(A)

Knorr, H. V. and V. M. Albers. Fluorescence of the chlorophyll series: Fluorescence and photodecomposition in solutions of pheophorbide *b* and methyl pheophorbide *b* —329(A)
Knudsen, Vern O. Absorption of sound in gases—338(A) (Title only)
——— **and Leonard Obert.** Transfer of translational and vibrational energy in oxygen as influenced by small impurities of water or ammonia vapor—256(A)
Koch, W. R. Electrical method for the non-destructive testing of sodium-filled valves—326(A)
Kock, Winston E. Inductive glow discharge oscillator—339(A)
——— On the principle of uncertainty in sound—339(A)
Koller, L. R. Sputtering of thorium and barium from tungsten—806(A)
Kolthoff, I. M. and Charles Rosenblum. Mechanism of the aging of freshly prepared lead sulfate crystals—631(L)
Konopinsky, E. J. and G. E. Uhlenbeck. On the comparison with experiment of the Fermi theory of beta-ray disintegration—202(A)
Koontz, Philip G. Band spectra of beryllium deuteride—641(A)
Kruger, P. Gerald. Nuclear shells: Angular and magnetic momenta of nuclei—605
——— (see Challacombe, C. N.)—798(A)
——— (see Weissberg, S. G.)—798(A)
——— **and C. N. Challacombe.** Hyperfine structure of Y II lines—509(L)
——— **and B. T. Darling.** Hollow cathode as an ion source —790(A)
Krutter, Harry M. Electronic structure of copper—810(A)
——— Thomas-Fermi method in metals—426(A)
——— (see Slater, J. C.)—559
Kuper, J. B. H. (see Turner, Louis A.)—813(A)
Kurie, Franz N. D. Disintegration of nitrogen by neutrons —97, 253(A)
——— (see Richardson, J. R.)—253(A)
———, **J. R. Richardson and H. C. Paxton.** Energies of the beta-rays and positrons emitted by various artificially produced radioactive substances—796(A)

Ladenburg, R. Distribution of atmospheric ozone—637(A) (Title only)
Laird, E. R. (see Coon, Edith M.)—889(L)
Lamar, E. S. (see Morse, Philip M.)—806(A)
——— **and E. W. Samson.** High current ion source—791(A)
Lane, C. T. Size and arrangement of bismuth microcrystals formed from vapor—644(A)
Langer, R. M. Foucault pendulum with constant amplitude —258(A)
Langmuir, David B. Contact potential of thoriated tungsten —328(A)
——— Temperature variation of contact potential—813(A)
Langseth, A. and J. Rud Nielsen. Raman spectra of N_3^-, NCS^- and CO_2—198(A)
Lark-Horovitz, K. and E. P. Miller. X-ray diffraction pattern of liquid and solid glycerine films—813(A)
———, **H. J. Yearian and J. D. Howe.** Intensity distribution in electron diffraction patterns—331(A)
Larking, Chas. R. Use of thermionic vacuum tubes for voltage control—793(A)
Latimer, W. M. (see Libby, W. F.)—193(L), 424(L)
Lauritsen, C. C. (see Crane, H. R.)—253(A), 420(L), 782(L), 887(L), 971(L)
Lawrence, Ernest O. Transmutations of sodium by deutons —17
——— (see McMillan, Edwin)—254(A), 343
———, **Edwin McMillan and Malcolm C. Henderson.** Transmutations of nitrogen by deutons—254(A), 273
LeGalley, Donald P. X-ray intensity measurements with a Geiger-Müller counter, and the determination of the structure factor for KCl—333(A)
Lemaitre, G., M. S. Vallarta and L. Bouckaert. On the north-south asymmetry of cosmic radiation—434
Letner, H. R. and G. W. Stewart. Comparison by x-ray diffraction of *p*-azoxyanisol in liquid and liquid crystalline phases—332(A)
Lewis, C. M. (see Barnes, R. Bowling)—129, 918
Libby, W. F. and W. M. Latimer. Absorption and scattering of neutrons—193(L)
———, **E. A. Long and W. M. Latimer.** Action of neutrons on heavy water—424(L)
Lindsay, R. B. (see Wilson, W. S.)—638(A), 681
Linford, Leo H. Emission of electrons by swiftly moving mercury ions—279
Lipson, Harry C. and Allan C. G. Mitchell. Quenching of cadmium resonance radiation (3261) by hydrogen—638(A)
——— **and Allan C. G. Mitchell.** Quenching of cadmium resonance radiation (3261) by N_2, CO and CH_4—807(A)
Livingston, M. Stanley (see McMillan, Edwin)—452
——— **and Robley D. Evans.** Correlation of nuclear disintegration processes—795(A)
Locher, G. L. Construction and use of Geiger-Müller counters—326(A)
——— (see Swann, W. F. G.)—326(A)
Loeb, L. B. (see Cravath, A. M.)—259(A)
Long, E. A. (see Libby, W. F.)—424(L)
Loomis, F. W. and W. H. Brandt. Band spectrum of OH^+—199(A)
Loughridge, Donald H. Theories of ion condensation—792(A)
——— (see Young, R. W.)—258(A)
Lozier, W. W. (see Smyth, H. D.)—800(A)
Luhr, Overton. Triatomic ions in mixtures of the hydrogen isotopes—331(A)
Lyons, W. James. Behavior of the absorption band of uranine solution under high pressure—198(A)

MacDougall, D. P. (see Giauque, W. F.)—885(L)
Mack, J. E. (see Whitelaw, N. G.)—677
MacPherson, H. G. Investigation of the magneto-optic method of chemical analysis—254(A), 310
Manley, J. H. and O. S. Duffendack. Collisions of the second kind between magnesium and neon—56
Margenau, Henry. Natural width of the *Kα*-lines—89(L)
——— (see Pollard, E.)—571(L), 795(A), 833
——— **and Ernest Pollard.** Alpha-particle scattering by deuterons and protons—640(A)

Marvin, H. H. Deep configurations of cobalt—521
Mason, R. C. Accommodation coefficient of mercury ions on a mercury surface—241
Maxfield, Frederick A. (see Ruark, Arthur Edward)—107
Maxwell, Louis R. and V. M. Mosley. Electron diffraction by transmission through thin silica glass films—330(A)
McAlister, E. D. Christiansen light filters—328(A)
McCorkle, Paul and Charles B. Bazzoni. Effect of target temperature on the wavelengths of soft x-rays from metals—804(A)
McCormick, W. E. and Wheeler P. Davey. Glassy state of arsenic—330(A)
McKellar, Andrew (see Bradley, Charles A., Jr.)—793(A), 914
——— **and Charles A. Bradley, Jr.** Spectrum of carbon deuteride—787(A)
McMillan, Edwin M. Production of x-radiation by very fast electrons—801(A)
——— (see Birge, Raymond T.)—320(L)
——— (see Lawrence, Ernest O.)—254(A), 273
——— **and Ernest O. Lawrence.** Transmutations of aluminum by deutons—254(A), 343
——— **and M. Stanley Livingston.** Artificial radioactivity produced by the deuteron bombardment of nitrogen—452
McNabney, Ralph, Wells Moulton and W. L. Beuschlein. Dielectric constants of air and hydrogen at high pressures —695
McNish, A. G. and G. R. Wait. Variation of small-ion production near the earth's surface—785(A)
Menzel, Donald H. and Leo Goldberg. New method for calculating relative multiplet strengths in a transition array—424(L)
Michels, Walter C. and Barbara Raines. Rotating coil alternating-current potentiometer—793(A)
——— **and Gladys White.** Heat losses from a tungsten wire in helium—197(A)
Migeotte, Marcel V. (see Barker, E. F.)—702(L)
——— **and E. F. Barker.** Resolution of the ND_3 bands at 13.5μ—812(A)
Miller, E. P. (see Lark-Horovitz, K.)—813(A)
Miller, Franklin, Jr. Simplification of Prins' formula for diffraction of x-rays by a perfect crystal—201(A), 209
Millikan, Robert A. and H. Victor Neher. Equatorial longitude effect in cosmic rays—205
Millman, J. Electronic energy bands in metallic lithium —286
Millman, Sidney. On the nuclear spins and magnetic moments of the principle isotopes of potassium—739
——— (see Fox, M.)—801(A)
———, **M. Fox and I. I. Rabi.** On the nuclear spin and magnetic moment of K^{41}—801(A)
Mimno, Harry Rowe (see King, Paul B., Jr.)—786(A)
——— (see Selvidge, H.)—786(A)
Mitchell, Allan C. G. (see Lipson, Harry C.)—638(A), 807(A)
——— **and Edgar J. Murphy.** Scattering of neutrons—881(L)
——— **and Edgar J. Murphy.** Qualitative experiment on scattering of neutrons—812(A)
Mitchell, D. P. (see Dunning, J. R.)—416(L), 796(A), 888(L), 970(L)
Mohler, Fred L. (see Taylor, Lauriston S.)—805(A)
Montgomery, C. G. (see Montgomery, D. D.)—339(A)
——— **and D. D. Montgomery.** Variation with altitude of the production of bursts of cosmic-ray ionization—429
———, **D. D. Montgomery and W. F. G. Swann.** Enhancement of cosmic-ray nuclear bursts by the presence of subsidiary material—512(L), 642(A)
Montgomery, D. D. (see Montgomery, C. G.)—429, 512(L), 642(A)
——— **and C. G. Montgomery.** Production of cosmic-ray showers by lead at different elevations—339(A)
Mooney, R. C. L. Crystal structure of ammonium chlorobromoiodide—807(A)
More, Kenneth R. Nuclear magnetic moment of cobalt—256(A)
Morgan, Frank (see Shawhan, E. N.)—199(A), 377
——— **and E. N. Shawhan.** Band spectrum of arsenic oxide (AsO)—192(L)
Morningstar, O. (see Warren, B. E.)—808(A)
Morrell, Charles E. (see Glockler, George)—569(L)
Morse, Philip M., W. P. Allis and E. S. Lamar. Velocity distribution of electrons in gas discharge problems—806(A)
Mosley, V. M. (see Maxwell, Louis R.)—330(A)
Moulton, Wells (see McNabney, Ralph)—695
Mouzon, J. C. and Newell H. Smith. Ionization of neon and argon by singly charged magnesium ions—802(A)
Mueller, Donald W. and Henry A. Barton. Neutron effects in a photographic emulsion—796(A)
Mueller, George J. Production of very small electric currents—793(A)
Mueller, Hans. Properties of Rochelle salt—175
——— Theory of photoelasticity—790(A)
——— Theory of the photoelastic effect of cubic crystals —947
Mugele, R. A. (see Evans, Robley D.)—427(A), 791(A)
Mulliken, Robert S. Structure, ionization and ultraviolet spectra of methyl iodide and other molecules—413
Munier, John H. (see Delsasso, Leo P.)—259(A)
Murphy, Edgar J. (see Mitchell, Allan C. G.)—812(A); 881(L)
Muschenheim, Carl (see Hardy, J. D.)—789(A)

Nathanson, J. B. and H. S. Seifert. Optical properties of sputtered metal films—328(A)
Neher, H. Victor. East-west and longitude effects—417(L)
——— (see Millikan, Robert A.)—205
von Neumann, J. Representations and ray representations in quantum mechanics—338(A) (Title only)
Newson, Henry W. (see Harkins, William D.)—52, 511(L)
Nickerson, J. L. Some bands in the extreme ultraviolet spectrum of helium—707
Nielsen, Alvin H. and Harald H. Nielsen. Infrared spectrum and molecular constants of hydrogen iodide—585
Nielsen, Harald H. (see Nielsen, Alvin H.)—585
——— (see Steward, Wendell B.)—792(A), 828
Nielsen, J. Rud (see Langseth, A.)—198(A)

Nix, Foster C. Loss and restoration of photoconductivity in red mercuric iodide—72, 337(A)
Nordheim, Gertrud. Orbital valency according to an extended Heitler-London method—803(A)
Nordheim, L. W. Free path and thermoelectric effects—794(A)
——— Production of pairs by collisions of particles—646(A)
Nottingham, W. B. Thermionic emission from tungsten with weak accelerating fields—806(A)
——— (see Johnson, R. P.)—426(A)
Null, F. E. Mean kinetic energy and mean energy spent in excitation by electrons drifting through dense gases—301

Obert, Leonard (see Knudsen, Vern O.)—256(A)
O'Brien, Brian. Introduction—637(A) (Title only)
Oldenberg, O. (see Frost, A. A.)—788(A)
Oppenheimer, J. R. Are the formulae for the absorption of high energy radiations valid?—44
——— Disintegration of the deuteron by impact—845
——— Note on charge and field fluctuations—144
——— Note on the production of pairs by charged particles—146
Osterberg, Harold and John W. Cookson. Electrocoupling of vibrating quartz plates—781(L)

Parker, Alice H. (see Parker, Allan E.)—812(A)
Parker, Allan E. Band systems of MgCl, CaCl and SrCl—349, 642(A)
——— **and Alice H. Parker.** Band system of TiCl—812(A)
Parratt, Lyman G. Precision x-ray wavelength measurements—882(L)
——— **and Lloyd P. Smith.** X-ray line widths: Correction for finite resolving power of crystals—805(A)
Paton, R. F. Proton emission resulting from alpha-ray bombardment of boron and phosphorus—197(A)
Patterson, A. L. Determination of the components of interatomic distances in crystals—330(A)
Paul, Fred W. Atomic absorption spectra of the rare earths—799(A)
Pauling, Linus and J. Y. Beach. Van der Waals interaction of hydrogen atoms—686
Paxton, H. C. (see Kurie, Franz N. D.)—796(A)
Pearson, G. L. Shot effect and thermal agitation in an electron current limited by space charge—327(A)
Pegram, G. B. (see Dunning, J. R.)—325(A), 416(L), 640(A), 796(A), 888(L), 970(L)
——— **and J. R. Dunning.** Electrolytic separation of polonium and Ra D—325(A)
Petersen, Max and Howard Carl. Spectra of helium by high frequency excitation—803(A)
Pfund, A. H. and J. A. Sanderson. Diffraction gratings for use in the far infrared—792(A)
Phillips, C. J. Raman spectra and the latent heat of fusion of nonassociated substances—792(A)
Pickels, E. G. Vacuum centrifuge—797(A)
——— **and J. W. Beams.** High rotational speeds in vacuum—336(A)
Pickering, W. H. Note on the production of cosmic-ray showers—423(L)
Pierce, W. C. and A. V. Grosse. *M* series of element 91—protactinium—532
Pietenpol, W. B. Proposed mass spectrograph—331(A)
——— (see Westerfield, E. C.)—325(A)
Pike, Eugene W. New measurements on the lifetimes of excited states in neon—802(A)
——— Observations on the Townsend discharge in neon—811(A)
Plyler, E. K. and E. S. Barr. Infrared absorption spectra of acetic acid and acetic anhydride—793(A)
Podolsky, B. (see Einstein, A.)—777
Poindexter, Franklin E. Effect of pressure on the refractive index of carbon disulfide—202(A)
Pollard, Ernest. Heights of nuclear potential barriers—640(A)
——— Nuclear potential barriers: Experiment and theory—611
——— (see Eaton, William W.)—640(A)
——— (see Margenau, Henry)—640(A)
——— **and William W. Eaton.** Disintegration of nitrogen and boron and possible emission of deuterons—597
——— **and Henry Margenau.** Collisions of alpha-particles in deuterium—833
——— **and Henry Margenau.** Interaction between deuterons and alpha-particles—795(A)
——— **and Henry Margenau.** Resonance interaction between deuterons and alpha-particles—571(L)
Pool, M. L. (see Whitmer, C. A.)—795(A)
Poritsky, H. and C. G. Suits. Sound velocity in gas mixtures at high temperatures—335(A)
Posin, D. Q. Townsend coefficients in nitrogen—258(A)
Posnov, M. V. (see Schulwas-Sorokin, R. D.)—166
Present, R. D. and J. H. Van Vleck. On the intensity formulas for $^3\Sigma^+ - ^3\Sigma^-$ transitions in band spectra—788(A)
Price, W. C. Absorption spectra of acetylene, ethylene and ethane in the far ultraviolet—444
——— Far ultraviolet absorption spectra and ionization potentials of H_2S, CS_2 and SO_2—788(A)
——— Far ultraviolet absorption spectra and ionization potentials of methyl bromide and chloride—510(L)
——— Far ultraviolet absorption spectrum of methyl iodide—419(L)
Purcell, E. M. (see Howe, J. D.)—329(A)

Quarles, L. R. Relation between field emission and work function of liquid mercury—328(A)

Rabi, I. I. Determination of the sign of nuclear magnetic moments by the method of atomic beams—338(A)
——— Nuclear moments from molecular beams—699(A) (Title only)
——— Nuclear spin in isotopic mixtures—334(A)
——— (see Fox, M.)—801(A)
——— (see Millman, S.)—801(A)
——— (see Rosin, S.)—645(A)
Rahmel, Henry A. (see Bennett, Ralph D.)—339(A), 437
Raines, Barbara (see Michels, Walter C.)—793(A)
Ramberg, E. and F. K. Richtmyer. Auger effect for Au (79) and the origin of certain *L*-satellites in x-ray spectra—805(A)

Ramberg, E. and F. K. Richtmyer. Calculation of the x-ray energy level widths of Au (79)—644(A)
Randall, R. H. and Harold W. Webb. Electron temperatures in mercury vapor afterglow—638(A)
Rank, D. H. (see Wood, R. W.)—792(A)
Rao, A. Veerabhadra (see Bhagavantam, S.)—921
Rayton, W. (see Wilkins, T. R.)—812(A)
Read, G. E. (see Sears, J. F.)—197(A)
Reardon, A. J. and H. P. Griggs. Solarization at low intensity—199(A)
Rentschler, H. C. and D. E. Henry. Photoelectric threshold of uranium, calcium and thorium treated with limited amounts of oxygen—807(A)
Rice, O. K. On the Stokes phenomenon for the differential equations which arise in the problem of inelastic atomic collisions—426(A)
Richardson, J. R. (see Kurie, Franz N. D.)—796(A)
——— **and Franz N. D. Kurie.** Energy of the neutrons emitted from beryllium when bombarded by deutons—253(A)
Richtmyer, F. K. (see Hirsh, F. R., Jr.)—805(A)
——— (see Ramberg, E.)—644(A), 105(A)
Ridenour, Louis N., K. Shinohara and Don M. Yost. Disintegration of beryllium by photons and its possible bearing on the mass of Be^9—318(L)
———, **D. M. Yost and K. Shinohara.** Chemical identification of the radioactive element produced from carbon by deuton bombardment—253(A)
Rieke, C. A. (see Boyce, J. C.)—653
Rieke, Foster F. Transfer of rotational energy—788(A)
Ries, Herman E., Jr. (see Harkins, William D.)—797(A)
Risser, J. H. (see Turner, Louis A.)—813(A)
Robinson, Howard A. Spectra of phosphorus, P II, P III, P IV—799(A)
Rodebush, W. H. Liquid state—513(L)
Roller, Duane (see Townes, Edith)—197(A)
Rose, Albert. Dependence on applied field of thermionic constants for thoriated tungsten—806(A)
——— Temperature coefficient of the work function for composite surfaces—889(L)
Rose, John E. (see Henderson, Joseph E.)—259(A)
Rose, John L. Hyperfine structure of singly ionized lead—122
Rose, Morris E. (see Roy, Angus S.)—335(A)
——— **and George E. Uhlenbeck.** Formation of electron pairs by internal conversion of gamma-radiation—811(A)
Rosen, N. (see Einstein, A.)—777
Rosenblum, Charles (see Kolthoff, I. M.)—631(L)
Rosenthal, Jenny E. Vibrations of symmetrical tetratomic molecules—235
Rosin, S. Scattering of alkali atoms in various gases—798(A)
——— **and I. I. Rabi.** Scattering of potassium and sodium atoms in various gases—645(A)
Ross, P. A. (see Bloch, F.)—884(L)
Roth, Frank L. and Paul F. Bartunek. Zeeman effect in the arc spectrum of cobalt—526
Rothemund, Paul (see Albers, V. M.)—198(A)
Roy, Angus S. and Morris E. Rose. Rotational dispersion of sound in hydrogen—335(A)
Ruark, Arthur Edward. X-ray wavelength scales—316(L), 644(A)
——— (see Warfield, Calvin N.)—700(L)
——— **and Karl H. Fussler.** Half-lives of potassium, rubidium, neodymium and samarium—790(A)
——— **and Frederick A. Maxfield.** X-ray levels of radioactive elements with applications to beta and gamma-ray spectra—107

St. Helens, H. (see Wilkins, T. R.)—812(A)
Samson, E. W. (see Lamar, E. S.)—791(A)
Sanderson, J. A. (see Pfund, A. H.)—792(A)
Sauter, J. D. (see Ham, W. R.)—337(A)
——— **and W. R. Ham.** Diffusion of hydrogen through highly degassed palladium—645(A)
Sawyer, J. H., Jr. Secondary and tertiary particles produced by cosmic rays—515
——— Shower producing cosmic-ray primaries—635(L)
Sawyer, Ralph A. (see Bacher, R. F.)—587
——— (see Earls, Lester T.)—115
——— (see Ellis, Cecil)—799(A)
Schiff, L. I. and L. H. Thomas. Quantum theory of metallic reflection—790(A), 860
Schneider, Edwin G. Optical properties of lithium fluoride in the Schumann region—789(A)
Schoepfle, G. K. Spectra of lead IV and bismuth V—232, 330(A)
Schriever, William. Space charge in a conducting electrolyte—327(A)
Schulte, William C. (see Doan, Gilbert E.)—783(L)
Schultz, H. L. (see Hector, L. G.)—327(A)
——— **and L. G. Hector.** On the use of radio broadcast carriers for constant high frequency currents—327(A)
Schulwas-Sorokin, R. D. and M. V. Posnov. Time of relaxation in crystals of Rochelle salt—166
Scott, R. B. (see Silsbee, F. B.)—794(A)
———, **F. B. Silsbee and F. G. Brickwedde.** Establishment and destruction of superconductivity at radiofrequency—794(A)
Sears, J. F. and G. E. Read. Study of the electrical characteristics of Geiger-Müller tubes using a cathode-ray oscillograph—197(A)
Seifert, H. S. (see Nathanson, J. B.)—328(A)
Seitz, Frederick. On the reduction of space groups—810(A)
——— Theoretical binding properties of metallic lithium—344(A)
——— Theoretical constitution of metallic lithium—400
——— (see Brattain, R. Robert)—793(A)
Selvidge, H. and Harry Rowe Mimno. Mobile radio research laboratory—786(A)
Shane, C. D. (see Spedding, Frank H.)—38
——— **and Frank H. Spedding.** Spectroscopic determination of e/m—33
Shaw, C. H. and J. A. Bearden. Shapes and wavelengths of K series x-ray lines—332(A)
Shawhan, E. N. (see Morgan, Frank)—192(L)
——— **and Frank Morgan.** Absorption spectrum of lead oxide—377

Shawhan, E. N. and Frank Morgan. Band spectrum of arsenic oxide and lead oxide—199(A)
Shenstone, A. G. Hyperfine structure of the cadmium resonance line—317(L)
Shinohara, Ken'ichi. Note on the diffraction of cathode rays by single crystals—730
——— (see Ridenour, L. N.)—253(A), 318(L)
Shnidman, L. S. (see Wilkins, T. R.)—251(L)
Shortley, George H. Line strengths in intermediate coupling—295; addition—419(L)
Shoupp, W. E., J. H. Bartlett, Jr. and C. G. Dunn. Magnetic moment of the Na^{23} nucleus—705(L)
Silsbee, F. B. (see Scott, R. B.)—794(A)
———, **F. G. Brickwedde and R. B. Scott.** New phenomenon in the superconducting transition of tin and tantalum—794(A)
Simard, G. L. and B. E. Warren. X-ray analysis of amorphous rubber—808(A)
Skaggs, Lester S. and R. T. Dufford. Index of refraction of water and paraffin at high frequencies—201(A)
Skinner, Selby M. Efficiency of the tuber counter—791(A)
Slater, J. C. and H. M. Krutter. Thomas-Fermi method for metals—559
Slipher, V. M. (see Adel, Arthur)—251(L), 580, 651, 787(A)
Sloan, David H. Radiofrequency high voltage generator—62
Smith, Lloyd P. On x-ray line shapes and the double crystal spectrometer—333(A)
——— (see Parratt, Lyman G.)—805(A)
Smith, Newbern. Diffraction of electrons by thin films of iron oxides and hydrates—803(A)
Smith, Newell H. (see Mouzon, J. C.)—802(A)
Smith, R. W. and O. S. Duffendack. Conductivity produced in neon and helium by irradiation with their own resonance radiations and the effect of foreign gases on this conductivity—473
Smith, Sinclair. F 1 quartz spectrograph—257(A)
Smyth, H. D., G. P. Harnwell, W. Bleakney and W. W. Lozier. Production of helium of mass three?—800(A)
Snell, A. H. (see Foster, J. S.)—338(A)
Snoddy, L. B. (see Bradley, Charles D.)—541
Soller, Walter and A. J. Thompson. Crystal structure of cuprous ferrite—644(A)
Solomon, Arthur K. On the nuclear radius—249(L)
Spedding, Frank H. (see Shane, C. D.)—33
———, **C. D. Shane and Norman S. Grace.** Fine structure of $H\alpha$—38
Stephens, W. E. Elastic scattering of fast electrons in mercury and agreement with Mott's theory—255(A)
Stern, Otto. Magnetic moment of the deuton—332(A) (Title only)
Stevenson, E. C. (see Street, J. C.)—891
——— **and Thomas H. Johnson.** Coincidence counter studies of the variation of intensities of cosmic-ray showers and vertical rays with barometric pressure—578
——— **and J. C. Street.** Nature of the penetrating cosmic radiation at sea level—643(A)
Steward, Wendell B. and Harald H. Nielsen. Infrared absorption spectrum of silane—792(A), 828
Stewart, G. W. Study of the nature of liquids by means of x-ray diffraction—201(A)
——— (see Letner, H. R.)—332(A)
Strait, L. A. (see Jenkins, F. A.)—136, 257(A)
Stranathan, J. D. On the peculiarities of dielectric constant *versus* pressure curves for vapors—794(A)
Stranathan, R. K. and L. P. Granath. Hyperfine structure and nuclear magnetic moment of caesium—801(A)
Street, J. C. (see Stevenson, E. C.)—643(A)
——— (see Woodward, R. H.)—643(A), 800(A)
———, **R. H. Woodward and E. C. Stevenson.** Absorption of cosmic-ray electrons—891
——— **and R. T. Young.** Shower groups in the cosmic radiation—572(L)
Strong, Herbert M. and H. P. Knauss. Bands of BF excited by the electrodeless discharge—642(A)
Strong, John and E. Gaviola. Spectrum of aluminum vapor emitted by a tungsten coil in vacuum—256(A)
——— (see Brice, R. T.)—255(A)
Studer, F. J. and W. D. Williams. Hall effect in sodium, potassium and caesium—291, 336(A)
Suits, C. G. Optical observations of sound waves in arcs—335(A)
——— Welding arcs in argon—975(L)
——— (see Poritsky, H.)—335(A)
Swann, W. F. G. Corpuscular theory of the cosmic rays—800(A)
——— Nature of the cosmic radiation—575
——— Origin of the hardening of cosmic rays in passing through matter—250(L)
——— (see Danforth, W. E.)—421(L)
——— (see Montgomery, C. G.)—512(L), 642(A)
——— **and D. B. Cowie.** Effect of cosmic-ray energy upon Stoss production—811(A)
——— **and G. L. Locher.** Measurements of the angular distribution of cosmic-ray intensities in the stratosphere with Geiger-Müller counters—326(A)
Swisher, R. J. (see Bates, John R.)—332(A) (Title only)
Synge, J. L. Angular momentum, mass-center and the inverse square law in special relativity—760

Taylor, D. D. Modified Aston-type mass spectrometer and some preliminary results—666
Taylor, H. S. Deuterium and reaction kinetics—332(A) (Title only)
Taylor, Lauriston S. and Fred L. Mohler. Ionization of liquids by x-rays—805(A)
Thatcher, Everett W. Multiple space charge in double and triple grid tubes—327(A)
Thode, Harry G. (see Freed, Simon)—335(A)
Thomas, L. H. Interaction between a neutron and a proton and the structure of H^3—810(A), 903
——— (see Schiff, L. I.)—790(A), 860
Thompson, A. J. (see Soller, Walter)—644(A)
Thompson, L. Propagation of explosion condensation through air—811(A)
Throop, Charlotte G. (see Wick, Frances G.)—329(A)
Throop, George R. Wayman Crow, Founder of Washington University—197(A) (Title only)
Tonks, Lewi. Anchored mercury pool cathode spot—638(A)

Tonks, Lewi. Force at the anchored cathode spot—807(A)
——— Momentum of ions leaving a region of ionization—621
Torrey, H. C. Viscosity of deuterium—644(A)
Townes, Edith and Duane Roller. Electrical resistance of cadmium films—197(A)
Townsend, Agnes. Change in thermal energy which accompanies a change in magnetization of nickel—306, 335(A)
Trotter, Herbert, Jr. and J. W. Beams. Acceleration of electrons to high energies—641(A)
Turner, Louis A. Stepwise fluorescence in mercury vapor; the 3650 line—807(A)
———, **J. B. H. Kuper and J. H. Risser.** Simple circuit for counting pulses at high speed—813(A)
Tuve, M. A. Nuclear reactions produced by high-speed deutons—332(A) (Title only)
——— (see Hafstad, L. R.)—506(L)
Tyndall, E. P. T. Note on the probable values of the elastic constants of the zinc crystal—398

Ufford, C. W. Relative transition probabilities for almost closed shells—330(A), 931
Uhlenbeck, George E. (see Konopinski, E. J.)—202(A)
——— (see Rose, Morris E.)—811(A)
Underwood, Newton. Photoelectric properties of the (100) and (111) faces of a single copper crystal—502
Urey, H. C. Methods of separation of isotopes—699(A) (Title only)

Valasek, Joseph. Effect of chemical combination on the $K\beta_1$ lines of sulphur, chlorine and potassium—896
——— X-ray spectra and chemical combination—332(A)
Vallarta, M. S. On the longitude effect of cosmic radiation—647, 800(A)
——— (see Lemaitre, G.)—434
Vance, John E. and John R. Huffman. Ultraviolet absorption band of Li_2—215
Van den Akker, J. A. Electrostatic pendulum—199(A)
Van Vleck, J. H. Rotational energy of polyatomic molecules—487
——— Some applications of group theory to nonrelativistic problems—338(A) (Title only)
——— (see Present, R. D.)—788(A)
Varney, Robert N. Ionization of inert gases by positive alkali ions—255(A), 483
Vinti, J. P. (see Witmer, E. E.)—538
Vogt, H. G. (see Hudson, J. C.)—809(A)

Wait, G. R. Distinction between Langevin ions and dust-particles in the atmosphere—786(A)
——— Ionization balance of the atmosphere near the earth's surface—810(A)
——— (see McNish, A. G.)—785(A)
Waldo, P. G. and Wheeler P. Davey. Technique for making sound ingots for density determination—338(A)
Walke, H. J. Helium content of beryls—969(L)
Warfield, Calvin N. Analysis of the data on radioactivity induced by neutron bombardment—796(A)
——— **and Arthur E. Ruark.** Analysis of data on radioactivity induced by neutron bombardment—700(L)
Warren, B. E. (see Hultgren, Ralph)—808(A)
——— (see Simard, G. L.)—808(A)
——— **and J. T. Burwell.** Structure of rhombic sulphur—330(A)
——— **and O. Morningstar.** X-ray analysis of vitreous B_2O_3—808(A)
Warren, Dana T. Ultraviolet absorption of iodine vapor—1
——— Ultraviolet I_2 fluorescence—642(A)
Wataghin, Gleb. Thermal equilibrium of elementary particles—423(L)
Watson, William W. Band spectra of barium hydride at 10,000A—213
——— Comparison of the spectra of CaH and CaD—27
Way Katherine and John M. Arthur. Spectrographic determination of calcium in plant ashes—198(A)
Webb, Glenn M. Elastic scattering of electrons in argon and krypton—379
——— Elastic scattering of electrons in argon, krypton and hydrogen—200(A)
——— Elastic scattering of electrons in molecular hydrogen—384
Webb, Harold W. (see Randall, R. H.)—638(A)
Weber, Ernst. Failure of Ohm's law at high current densities—327(A)
Webster, D. L., W. W. Hansen and F. B. Duveneck. Errata: Ionization area of He and Bethe's theory—699
Weissberg, S. G. and P. Gerald Kruger. Deep terms in ions of the isoelectronic sequence Cl I to Mn IX—798(A)
Wells, D. A. Longitudinal motion of a long coil spring suspended vertically from a rigid support—339(A)
Wells, W. H. Scattering of protons on protons—591
Wente, E. C. Some new instruments of acoustical research—338(A) (Title only)
Westerfield, E. C. and W. B. Pietenpol. Nuclear structure and the negative proton—325(A)
White, Gladys (see Michels, Walter C.)—197(A)
White, H. E. (see Ballard, S. S.)—256(A)
White, Milton G. Collisions of high energy protons in hydrogen—573(L)
White, W. P. Heat-flow calorimetric method—797(A)
Whitelaw, N. G. and J. E. Mack. On perturbed series, especially in C III, B I and O IV—677
Whitman, L. C. (see Holmes, R. M.)—337(A)
Whitmer, C. A. and M. L. Pool. Low voltage disintegration of lithium with lithium—795(A)
Wick, Frances G. and Charlotte G. Throop. Luminescence of frozen solutions of certain dyes—329(A)
Wigner, E. Symmetry relations in various physical problems—338(A) (Title only)
Wilhelmy, Ernst. Width of the $K\alpha$-lines from gaseous krypton—322(L)
Wilkins, T. R., W. Rayton and H. St. Helens. High frequency parallel rod method for the determination of alpha-ray speeds—812(A)
———, **W. Rayton and H. St. Helens.** Some alpha-ray and proton tracks in photographic emulsions—812(A)
——— **and L. S. Shnidman.** Isotopes in induced radioactivity—251(L)

Williams, Clarke. Erratum: Thermal expansion and the ferromagnetic change in volume of nickel—88
Williams, E. J. High energy formulae—569(L)
Williams, S. R. Need of physicists to study the problem of hardness and its measurements—427(A)
Williams, W. D. (see Studer, F. J.)—291, 336(A)
Wills, L. A. and G. Breit. Nuclear magnetic moment of Na^{22}—704(L)
Wilson, E. D. (see Ballard, James W.)—794(A)
Wilson, Thomas A. Crystal structure of beta-manganese—332(A)
Wilson, W. S. and R. B. Lindsay. Approximate atomic wave functions for some excited states of helium—638(A)
———**and R. B. Lindsay.** Atomic wave functions for some excited states of helium—681
Witmer, Enos E. Energy levels of the asymmetrical rotator in the new quantum theory—340(A)
——— **and J. P. Vinti.** Symmetry properties and the identity of similar particles—538
Wold, P. I. Equation of a wave in a medium with velocity a function of time—333(A), 735
——— On the redward shift of spectral lines of nebulae—217
Wollan, E. O. Scattering of x-rays by gases—201(A)
Woo, Sho-Chow and T. C. Chu. Ultraviolet absorption bands of diacetylene—886(L)
Wood, Lawrence A. Current-voltage relations in blocking layer photo-cells—337(A)
Wood, R. W. Anomalous intensity distribution in spectra given by certain ruled diffraction gratings—642(A)
——— Some unusual optical problems—332(A) (Title only)
——— **and D. H. Rank.** Complete Raman spectrum of heavy chloroform—792(A)
Woodward, R. H. (see Street, J. C.)—891
——— **and J. C. Street.** Absorption of cosmic-ray electrons in lead—643(A)
——— **and J. C. Street.** Production and absorption of cosmic-ray showers—800(A)
Woolard, Edgar W. Geometrical theory of halos—637(A) (Title only)
Wulf, Oliver R. Light absorption in the atmosphere and its photochemistry—638(A) (Title only)
Wylie, C. C. Rate of fall of meteoric material on the earth—192(L)

Yearian, H. J. Intensity distribution in electron diffraction patterns of ZnO and atom factor—200(A)
——— (see Lark-Horovitz, K.)—331(A)
Yost, D. M. (see Ridenour, L. N.)—253(A), 318(L)
Yost, F. L. (see Breit, G.)—508(L)
Young, Lloyd A. Interaction of nuclear particles—809(A), 972(L)
Young, R. T. (see Street, J. C.)—572(L)
Young, R. W. and D. H. Loughridge. Relative measurement of the standing wave system in a mechanically blown flute tube—258(A)

Zachariasen, W. H. Note on the scattering of x-rays from fluids containing polyatomic molecules—277
——— Structure of liquid methyl alcohol—201(A)
——— Structure of radicals in crystals—201(A)
Zeleny, John. Role of surface instability in electrical discharges from drops of alcohol and water in air at atmospheric pressure—638(A)
Zener, Clarence. Hall coefficients of alkali metals—636(L)
——— Modification of the Heitler and London method—334(A)
——— Theories of the spectral selective photoelectric effect—15

Analytic Subject Index to Volume 47

References with (A) are to abstracts of papers presented at meetings of the Physical Society. References with (L) are to Letters to the Editor.

Absorption coefficient (see also **X-ray, absorption; Collision diameter**)
Of high energy radiation, A. Bramley—321(L); J. R. Oppenheimer—44; E. J. Williams—569(L)

Absorption of light (see also **Spectra, absorption**)
Absorption of sunlight by earth's atmosphere in infrared, A. Adel, V. M. Slipher, E. F. Barker—251(L), 580
Infrared transmission of solids, J. D. Hardy, C. Muschenheim—789(A)

Accommodation coefficient
Force at cathode spot, L. Tonks—807(A), 638(A)
Geometry of electrode as a factor, L. Tonks—621
Of He and W wire, W. C. Michels, G. White—197(A)
Of Hg ions on Hg surface, R. C. Mason—241

Acoustics
Dispersion of sound in air, L. P. Delsasso, J. H. Munier—259(A)
Dispersion of sound in H_2, A. S. Roy, M. E. Rose—335(A)
Standing wave system in a flute, R. W. Young, D. H. Loughridge—258(A)
Transfer of translational and vibrational energy in O_2, V. O. Knudsen, L. Obert—256(A)
Uncertainty principle in sound, W. E. Kock—339(A)
Velocity in gas mixtures at high temperatures, H. Poritsky, C. G. Suits—335(A)
Velocity of sound waves in arcs, C. G. Suits—335(A)
Waves in lake ice, A. P. Crary, M. Ewing, E. B. Douglas—797(A)

Afterglow
Electron temperatures in Hg vapor, R. H. Randall, H. W. Webb—638(A)

Arcs (see **Discharge of electricity in gases**)

Astrophysics
Absorption of sunlight by earth's atmosphere in infrared, A. Adel, V. M. Slipher, E. F. Barker—251(L), 580
Constancy of the velocity of light, R. J. Kennedy—533
Difference bands in spectra of major planets, temperature of planets, A. Adel, V. M. Slipher—651
Diurnal variation of the earth's potential gradient, J. G. Brown—259(A)
Galactic rotation and intensity of cosmic rays, A. H. Compton, I. A. Getting—817
Light of the night sky, J. Kaplan—193(L)
Methane content of giant planet atmospheres, A. Adel, V. M. Slipher—787(A)
Rate of fall of meteoric material, C. C. Wylie—192(L)
Redward shift of nebulae lines, P. I. Wold—217

Atmospheric electricity (see **Meteorology**)

Atomic and molecular beams
Scattering of alkali atoms, S. Rosin—798(A); S. Rosin, I. I. Rabi—645(A)
Sign of nuclear magnetic moments, I. I. Rabi—338(A)

Atomic structure (see **Spectra, atomic**)

Barkhausen effect (see **Magnetic properties**)

Biophysics
Electric impedance of muscle, K. S. Cole, E. Bozler—644(A)
Fluorescence of pheophorbide *b* and methyl pheophorbide *b*, H. V. Knorr, V. M. Albers—329(A)
Infrared transmission of solids, J. D. Hardy, C. Muschenheim—789(A)
Reduction of chlorophyll *a* and *b*, V. M. Albers, H. V. Knorr, P. Rothemund—198(A)
Spectrographic determination of Ca in plant ashes, K. Way, J. M. Arthur—198(A)

Cold emission (see **Field currents**)

Collision diameter (see also **Scattering of electrons; Disintegration of nucleus**)
High energy protons in H_2, M. G. White—573(L)
Scattering of alkali atoms in gases, S. Rosin, I. I. Rabi—645(A); S. Rosin—798(A)
Scattering of α-particles in D_2O, E. Pollard, H. Margenau—833
Scattering of protons on protons, W. H. Wells—591

Collisions of second kind
Between Mg and Ne, J. H. Manley, O. S. Duffendack—56

Conductivity, electrical (see **Electrical conductivity; Discharge of electricity in gases**)

Constants, physical, standards
Electronic charge, R. T. Birge, E. McMillan—320(L)
Electronic charge and x-ray wavelengths, L. Alvarez—636(L); J. A. Bearden—645(A), 804(A); A. E. Ruark—316(L), 644(A)

Contact potential
Between W and Ba, P. A. Anderson—958
Temperature variation of, D. B. Langmuir—813(A)
Of thoriated W, D. B. Langmuir—328(A)

Cosmic radiation
Absorption of electrons, J. C. Street, R. H. Woodward, E. C. Stevenson—643(A), 891
Absorption of high energy radiation, A. Bramley—321(L); J. R. Oppenheimer—44; E. J. Williams—569(L)
Angular distribution in stratosphere, W. F. G. Swann, G. L. Locher—326(A)
Apparatus for transmitting data from stratosphere, J. M. Benade, R. L. Doan—198(A)
East-west and longitude effects, H. V. Neher—417(L)
Electrostatic deflection, W. E. Danforth, Jr., W. F. G. Swann—421(L)
Energy, and Stoss production, W. F. G. Swann, D. B. Cowie—811(A)
Enhancement of nuclear bursts, secondary, tertiary, C. G. Montgomery, D. D. Montgomery, W. F. G. Swann—512(L), 642(A)

Hardening of rays in passing through matter, W. F. G. Swann—250(L)
Intensity and galactic rotation, A. H. Compton, I. A. Getting—817
Longitude effect, R. A. Millikan, H. V. Neher—205; M. S. Vallarta—647, 800(A)
Nature of radiation, W. F. G. Swann—575, 800(A)
Nature of radiation at sea level, E. C. Stevenson, J. C. Street—643(A)
North-south asymmetry, T. H. Johnson—91(L), 326(A); G. Lemaitre, M. S. Vallarta, L. Bouckaert—434
Pairs produced by collisions of particles, L. Nordheim—646(A)
Positron-negatron component in primary radiation, T. H. Johnson—318(L), 642(A)
Secondary and tertiary particles, J. H. Sawyer, Jr.—515
Shower groups, J. C. Street, R. T. Young—572(L); R. H. Woodward, J. C. Street—800(A)
Shower producing primaries, J. H. Sawyer, Jr.—635(L)
Showers as a function of altitude, R. D. Bennett, G. S. Brown, H. A. Rahmel—339(A), 437; D. D. Montgomery, C. G. Montgomery—339(A), 429
Showers produced under water, W. H. Pickering—423(L)
Variation of showers and vertical rays with barometric pressure, E. C. Stevenson, T. H. Johnson—578

Crystalline state
Aging of freshly prepared $PbSO_4$ crystals, I. M. Kolthoff, C. Rosenblum—631(L)
Bi microcrystals formed from vapor, C. T. Lane—644(A)
Cd films on glass, E. Townes, D. Roller—197(A)
Cleavage in silicon ferrite, C. S. Barrett—809(A)
Constitution of metallic Li, F. Seitz—334(A), 400
Depth of cold work, C. S. Barrett—338(A)
Diffraction of x-rays by a perfect crystal, F. Miller, Jr.—201(A), 209
Diffuse scattering of x-rays, G. E. M. Jauncey—201(A)
Diffusion of gases through metals, W. R. Ham—645(A); J. D. Sauter, W. R. Ham—337(A), 645(A)
Diffusion of solid Al into Fe, L. G. Hall—418(L)
Elastic constants of the Zn crystal, E. P. T. Tyndall—398
Electron diffraction by thin silica glass films, L. R. Maxwell, V. M. Mosley—330(A)
Electronic structure of Cu, H. M. Krutter—810(A)
Electronic structure of diamond, G. E. Kimball—810(A)
Expansion of Cu from 0°K to melting, W. J. Haring, W. P. Davey—337(A)
Glassy state of As, W. E. McCormick, W. P. Davey—330(A)
Hardness and its measurements, S. R. Williams—427(A)
Heat-treated W filaments, R. P. Bien—806(A)
High pressure transitions of Bi, P. W. Bridgman—427(A)
Penetration of diffracted electrons, H. E. Farnsworth—331(A)
Photoelastic effect of cubic crystals, H. Mueller—642(A), 947
Photoelectric properties of a Cu single crystal, N. Underwood—502
Piezo-resistive effect, J. W. Cookson—194(L)
Plasticity of crystals, P. Duwez—494
K films on Ag, J. J. Brady—197(A)
Rochelle salt, correlation of various properties, H. Mueller—175
Rochelle salt under constant electric field and mechanical stress; relaxation time, R. D. Schulwas-Sorokin, M. V. Posnov—166
Slight impurities and elastic constants, P. W. Bridgman—393
Sound ingots, technique for making, P. G. Waldo, W. P. Davey—338(A)
Structure of radicals in crystals, W. H. Zachariasen—201(A)
Supercooling; paracrystalline mesophase, A. Goetz—257(A)
Thomas-Fermi method applied to metals, H. M. Krutter—426(A); J. C. Slater, H. M. Krutter—559
X-ray data and distortion in crystals, G. L. Clark, M. M. Beckwith—200(A)
X-ray diffraction and fatigue of metals, C. S. Barrett—333(A)
X-ray extinction in oscillating crystals, G. W. Fox, W. A. Fraser—899
X-ray extinction in piezoelectric crystals, G. W. Fox, W. A. Fraser—200(A)
X-ray reflection from Bi crystals 25° to 530°Abs., R. B. Jacobs, A. Goetz—94(L), 257(A)

Crystals, structure
Of ammonium chlorobromoiodide, R. C. L. Mooney—807(A)
Analysis of amorphous rubber, G. L. Simard, B. E. Warren—808(A)
Analysis of vitreous B_2O_3, B. E. Warren, O. Morningstar—808(A)
Of β-manganese, T. A. Wilson—332(A)
Of black P, R. Hultgren, B. E. Warren—808(A)
Of cuprous ferrite, W. Soller, A. J. Thompson—644(A)
Determination of interatomic distances, A. L. Patterson—330(A)
Fourier analyses of P pattern, N. S. Gingrich, R. Hultgren—808(A)
Heat-treated W filaments, R. P. Bien—806(A)
P-azoxyanisol in liquid and liquid crystalline phases, H. R. Letner, G. W. Stewart—332(A)
Reduction of space groups, F. Seitz—810(A)
Of rhombic S, B. E. Warren, J. T. Burwell—330(A)

Dielectrics and dielectric properties
Of air and H_2 at high pressures, R. McNabney, W. Moulton, W. L. Beuschlein—695
Of colloidal solutions, H. Fricke, H. J. Curtis—974(L)
Dielectric constant of air at radiofrequencies, L. G. Hector, H. L. Schultz—327(A)
Dielectric constant *versus* pressure curves for vapors, J. D. Stranathan—794(A)

Diffraction of electrons (see **Electron diffraction**)

Diffusion
Of gases through metals, equations, W. R. Ham—645(A); J. D. Sauter, W. R. Ham—337(A), 645(A)
Of solid Al into Fe, L. G. Hall—418(L)

Discharge of electricity in gases (see also **Electrons in gases; Spark discharge**)
Anchored Hg pool cathode spot, L. Tonks—638(A), 807(A)
Arcs in inert gases, G. E. Doan, W. C. Schulte—783(L); C. G. Suits—975(L)
Chemical reactions of OH in discharge, A. A. Frost, O. Oldenberg—788(A)
Conductivity produced in Ne and He by resonance radiations, R. W. Smith, O. S. Duffendack—473
Ion distribution during initial stages of spark, C. D. Bradley, L. B. Snoddy—541; C. D. Bradley—802(A)
Kinetic energy of electrons,—energy of excitation, F. E. Null—301
Lifetimes of excited states in Ne, E. W. Pike—802(A)
Hg vapor afterglow, R. H. Randall, H. W. Webb—638(A)
Momentum of ions, L. Tonks—621
Phenomena in Faraday dark space, K. G. Emeleus, O. S. Duffendack—460
Surface instability; discharge from drops, J. Zeleny—638(A)
Townsend coefficients in N_2, D. Q. Posin—258(A)
Townsend discharge in Ne, E. W. Pike—811(A)
Velocity distribution of electrons, P. M. Morse, W. P. Allis, E. S. Lamar—806(A)
Velocity of sound waves in arcs, C. G. Suits—335(A)

Discharge of electricity in high vacuum (see also **Thermionic emission; High voltage tubes and machines**)
Shot effect and thermal agitation, in space charge limited current, G. L. Pearson—327(A)
Space charge in double and triple grid tubes, E. W. Thatcher—327(A)

Disintegration of nucleus (see also **Nucleus; Radioactivity**)
Of Al by deuterons, E. McMillan, E. O. Lawrence—254(A), 343
Of Be, γ-rays, H. R. Crane, L. A. Delsasso, W. A. Fowler, C. C. Lauritsen—782(L)
Of Be by photons, L. N. Ridenour, K. Shinohara, D. M. Yost—318(L)
Of Be by deuterons, emission of electrons, H. R. Crane, L. A. Delsasso, W. A. Fowler, C. C. Lauritsen—887(L)
Of C, Ne and F by neutrons, W. D. Harkins, D. M. Gans, H. W. Newson—52
Correlation of disintegration processes, M. S. Livingston, R. D. Evans—795(A)
Disintegration of deuterons by impact, J. R. Oppenheimer—845
Emission of neutrons, J. R. Dunning, G. B. Pegram, G. A. Fink—325(A)
Energy distribution of neutrons from Be, T. W. Bonner, W. M. Brubaker—910
Fermi proton effect, A. V. Grosse, M. S. Agruss—91(L), 93(L)
He in beryls, H. J. Walke—969(L)
Of Li and Cd by slow neutrons, J. R. Dunning, G. B. Pegram, D. P. Mitchell, G. A. Fink—970(L)
Of Li and formation of $_4Be^8$, T. W. Bonner, W. M. Brubaker—973(L)
Of Li and LiOH; low voltage, C. A. Whitmer, M. L. Pool—795(A)
Of Ne, with α-particles, W. W. Eaton—796(A)
By neutrons, theory of, H. A. Bethe—640(A), 747
Of N and B, E. Pollard, W. W. Eaton—597
Of N by deuterons, F. N. D. Kurie—97, 253(A); E. O. Lawrence, E. McMillan, M. C. Henderson—254(A), 273; E. McMillan, M. S. Livingston—452
Proton emission from α-ray bombardment of B and P, R. F. Paton—197(A)
Radiative capture of protons, G. Breit, F. L. Yost—508(L); L. R. Hafstad, M. A. Tuve—507(L)
Resonance interaction deuterons, α-particles and protons, E. Pollard, H. Margenau—571(L), 640(A), 795(A), 833
Of Na by deuteron bombardment, E. O. Lawrence—17

Dissociation, heat of (see also **Molecular structure and constants**)
Of AsO, F. A. Jenkins, L. A. Strait—136, 257(A); F. Morgan, E. N. Shawhan—192(L), 199(A)

Dynamics
Deduction of inverse square law, J. L. Synge—760
Longitudinal motion of a long coil spring, D. A. Wells—339(A)
Transverse vibrations of long rods, I. A. Balinkin—340(A)

Elasticity
Dispersion in flexural waves in lake ice, M. Ewing, A. P. Crary, E. B. Douglas—797(A)
Elastic constants of the Zn crystal, E. P. T. Tyndall—398
Electrocoupling of vibrating quartz plates, H. Osterberg, J. W. Cookson—781(L)
Linear expansion for stretched rubber bands, M. L. Braun—798(A)
Longitudinal motion of a long coil spring, D. A. Wells—339(A)
Plasticity of crystals, P. Duwez—494
Rubber under uniformly repeated stresses, M. L. Braun—336(A)
Slight impurities and elastic constants of Zn crystals, P. W. Bridgman—393
Transverse vibrations of long rods, I. A. Balinkin—340(A)
Waves in lake ice, A. P. Crary, M. Ewing, E. B. Douglas—797(A)
Young's modulus in rocks by dynamical method, J. Ide—797(A)

Electrical circuits (see **Methods and instruments**)

Electrical conductivity and resistance
Of Bi microcrystals, C. T. Lane—644(A)
Of colloidal solutions, H. Fricke, H. J. Curtis—974(L)
Effect of pressure on the alkalies, N. H. Frank—282
Impedance of muscle, K. S. Cole, E. Bozler—644(A)
Magnetoresistance in Na-K alloy, C. W. Heaps, J. E. Armstrong—336(A); J. E. Armstrong—391
New phenomenon in supraconducting transition of Sn and Ta, F. B. Silsbee, F. G. Brickwedde, R. B. Scott—794(A)

Ohm's law at high current densities, E. Weber—327(A)
Short cold-metal gaps in air, R. E. Fearon—802(A)
Space-charge in electrolytes, W. Schriever—327(A)
Supraconductivity at radiofrequency, R. B. Scott, F. B. Silsbee, F. G. Brickwedde—794(A)

Electromagnetic theory
Application of electrodynamics, J. R. Oppenheimer—44; A. Bramley—321(L)
Born-Infeld theory, E. Feenberg—148; B. Hoffmann—639(A), 804(A), 877
Charge and field fluctuations, J. R. Oppenheimer—144
Classical electromagnetic theory and wave mechanics, L. T. DeVore—333(A), 638(A)
Constancy of the velocity of light, R. J. Kennedy—533
New expansion in radiation problems, W. W. Hansen—139

Electromagnetic waves
Propagation of 50 cm radio waves, P. S. Epstein—258(A)

Electron diffraction (see also **Scattering of electrons**)
Depth of penetration of electrons, H. E. Farnsworth—331(A)
Envelope of Kikuchi lines, K. Shinohara—730
Films of Fe oxides and hydrates, N. Smith—803(A)
Intensity distribution, K. Lark-Horovitz, H. J. Yearian, J. D. Howe—331(A)
Patterns of ZnO and atom factor, H. J. Yearian—200(A)
By thin silica glass films, L. R. Maxwell, V. M. Mosley—330(A)

Electrons (see also **Positive electron**)
Born-Infeld field theory, E. Feenberg—148; B. Hoffmann—639(A), 804(A), 877

Electrons in gases (see also **Discharge of electricity in gases**)
Elastic scattering of electrons in A, Kr and H_2, G. M. Webb—200(A), 379, 384
Velocity distribution of electrons, P. M. Morse, W. P. Allis, E. S. Lamar—806(A)

Electrons in metals
Effect of pressure on electrical conductivities, N. H. Frank—282
Energy bands in metallic Li, J. Millman—286
Free path and thermoelectric effects, L. W. Nordheim—794(A)
Magnetic properties and Fermi-Dirac statistics, S. Freed, H. G. Thode—335(A)
Magnetoresistance in Na-K alloy, C. W. Heaps, J. E. Armstrong—336(A); J. E. Armstrong—391
Thomas-Fermi method applied, J. C. Slater, H. M. Krutter—559; H. M. Krutter—426(A)

Electrons, scattering of (see **Electrons in gases**)

Electrons, secondary
Produced by swiftly moving Hg ions, L. H. Linford—279

Electro-optical effects (see also **Photoelectric effect and properties**)
Kerr effect in NH_3, N_2 and O_2, W. M. Breazeale—789(A)

e/m
Spectroscopic determination, $H^1\alpha$ and $H^2\alpha$ lines, C. D. Shane, F. H. Spedding—33
Triatomic ions of H isotopes, O. Luhr—331(A)

Energy states of atoms (see **Spectra, atomic**)

Equations of state
Liquid state, W. H. Rodebush—513(L)

Errata
Ionization area of He and Bethe's theory, D. L. Webster, W. W. Hansen, F. B. Duveneck—699
Latitude and azimuthal effects, G. Lemaitre, M. S. Vallarta, L. Bouckaert—434
Thermal expansion and the ferromagnetic change in volume of Ni, C. Williams—88

Evaporation
Effect of electrostatic field, E. Hutchisson—328(A)

Excitation of atoms and molecules
Lifetimes in Ne, E. W. Pike—802(A)

Field currents
Overvolted discharges, J. W. Flowers—801(A)
Short cold-metal gaps in air, R. E. Fearon—802(A)

Fine structure (see **Spectra**, etc.; **Hyperfine structure**)

Fluorescence
Induced by x-rays and γ-rays, O. Glasser, I. E. Beasley—570(L), 789(A)
Of I_2, ultraviolet, D. T. Warren—642(A)
Reduction of chlorophyll *a* and *b*, V. M. Albers, H. V. Knorr, P. Rothemund—198(A)
Stepwise fluorescence in Hg, L. A. Turner—807(A)

Hall effect
In Na, K and Cs, F. J. Studer, W. D. Williams—291, 336(A); C. Zener—636(L)

Heat conduction (see also **Thermal conductivity**)
Heat losses from a W wire in He, W. C. Michels, G. White—197(A)
Precision of calorimetric method, W. P. White—797(A)

High voltage tubes and machines
Electrons of high energies, transmission line method, H. Trotter, Jr., J. W. Beams—641(A)
Electrostatic generator with small vertical clearance, W. H. Bennett—791(A)
Radiofrequency high-voltage generator, D. H. Sloan—62
Rotary voltmeter and sphere gap, J. E. Henderson, W. H. Goss, J. E. Rose—259(A)

Hyperfine structure (see also **Nuclear spin**)
Of Be III, S. S. Ballard, O. E. Anderson, H. E. White—256(A)
Of Cd λ2288, A. G. Shenstone—317(L)
Of Cs, R. K. Stranathan, L. P. Granath—801(A)
Formulae for the configuration d^2s, M. F. Crawford—768
In La III, M. F. Crawford, N. S. Grace—536
Of Pb II, J. L. Rose—122
In Na^{23}, L. A. Wills, G. Breit—704(L); W. E. Shoupp, J. H. Bartlett, Jr., C. G. Dunn—705(L)
Of $^2S_{\frac{1}{2}}$ state in K, S. Millman—739
Of Y II lines, P. G. Kruger, C. N. Challacombe—509(L), 798(A)

Instruments (see **Methods and instruments**)

Intensities in spectra (see also **Spectra,** etc.)
In Cr I and Cr II, J. S. V. Allen, C. E. Hesthal—926
Line strengths in intermediate coupling, G. H. Shortley—295, 419(L)
Relative multiplet strengths in a transition array, D. H. Menzel, L. Goldberg—424(L)
Transition probabilities of almost closed shells, C. W. Ufford—330(A), 931
Ionization by electrons
Errata, ionization area of He, D. L. Webster, W. W. Hansen, F. B. Duveneck—699
Ionization by positive ions
Of inert gases, R. N. Varney—255(A), 483
Of Ne and As by Mg^+, J. C. Mouzon, N. H. Smith—802(A)
Ionization potentials
Of H_2S, Cs_2 and SO_2, W. C. Price—788(A)
Of methyl bromide and chloride, W. C. Price—510(L)
Ionization by radiation
Of liquids by x-rays, L. S. Taylor, F. L. Mohler—805(A)
Ions in gases (see also **Electrons in gases**)
Products of ionization in methane, J. A. Hipple, Jr., W. Bleakney—802(A)
Triatomic ions of H isotopes, O. Luhr—331(A)
Isotopes (see also **Nucleus**)
In acetylene, W. F. Colby—388
He^3(?), H. D. Smyth, G. P. Harnwell, W. Bleakney, W. W. Lozier—800(A)
In induced radioactivity, T. R. Wilkins, L. S. Shnidman—251(L)
Of Li abundance ratio, A. K. Brewer—571(L)
Masses of light atoms from transmutation data, H. Bethe—633(L), 795(A)
Of N produced from C by deuteron bombardment, L. N. Ridenour, D. M. Yost, K. Shinohara—253(A)
Of O, W. Bleakney, J. A. Hipple, Jr.—800(A)
Relative abundance, I. I. Rabi—334(A)
Shift in Mg I spectra, R. F. Bacher, R. A. Sawyer—587
Shifts in spectra of diatomic molecules, G. H. Dieke—661

Liquids
Ionization by x-rays, L. S. Taylor, F. L. Mohler—805(A)
Liquid state, W. H. Rodebush—513(L)
Nature of liquids, G. W. Stewart—201(A)
Space-charge in electrolytes, W. Schriever—327(A)
Structure of methyl alcohol, W. H. Zachariasen—201(A)
Low temperature phenomena
Liquefaction of gases—a demonstration, C. T. Knipp—200(A)
Thermodynamic scale region below 1°K, W. F. Giauque, D. P. MacDougall—885(L)
Luminescence
Of frozen solutions of dyes, F. G. Wick, C. G. Throop—329(A)

Magnetic properties
Directions of discontinuous changes in Si-Fe, R. F. Clash, Jr., F. J. Beck, Jr.—158
Erratum, ferromagnetic change in volume of Ni, C. Williams—88
Of Gd and Au at low temperature, W. F. Giauque, D. P. MacDougall—885(L)
Photomagnetic effect, R. M. Emberson, R. T. Dufford—202(A)
Thermal e.m.f. and magnetization, F. W. Constant—794(A)
Thermal energy in magnetization of Ni, A. Townsend—306, 335(A)
Magneto-optical effects
Magneto-optic method of analysis, T. R. Ball—548; M. A. Jeppesen, R. M. Bell—546; H. G. McPherson—254(A), 310
Photography of minima in magneto-optic apparatus, G. Hughes, R. Goslin—317(L)
Time lags in magneto-optics, H. W. Farwell, J. B. Hawkes—78
Mass spectrograph (see also **Methods and instruments**)
Masses of light atoms from transmutation data, H. Bethe—633(L), 795(A)
Modified Aston-type mass spectrometer, preliminary results, D. D. Taylor—666
New ion source for mass-spectroscopy, A. J. Dempster—331(A)
Products of ionization in methane, J. A. Hipple, Jr., W. Bleakney—802(A)
Proposed mass-spectrograph, W. B. Pietenpol—331(A)
Triatomic ions of H isotopes, O. Luhr—331(A)
Mechanics, quantum-atomic structure and spectra
Excited states of He wave functions, W. S. Wilson, R. B. Lindsay—638(A), 681
Hylleraas method applied to Li, H. M. James, A. S. Coolidge—700(L)
Normal He atom, J. H. Bartlett, Jr., J. J. Gibbons, Jr., C. G. Dunn—679, 804(A)
Rare gas configurations, C. L. Bartberger—803(A)
Relative transition probabilities, C. W. Ufford—931
Mechanics, quantum-general
Charge and field fluctuations, J. R. Oppenheimer—144
Classical electromagnetic theory and wave mechanics, L. T. DeVore—333(A), 638(A)
Double layers in adsorbed films, R. W. Gurney—479
Energy levels of asymmetrical rotator, E. E. Witmer—340(A)
Inelastic atomic collisions, O. K. Rice—426(A)
Metallic reflection, L. I. Schiff, L. H. Thomas—790(A), 860
Quantum-mechanical description of reality, A. Einstein, B. Podolsky, N. Rosen—777, E. C. Kemble—973(L)
Reduction of space groups, F. Seitz—810(A)
Scattering by protons, E. Feenberg—857
Scattering of x-rays and discrete electrons, A. H. Compton—203(A), 367
Symmetry properties and identity of particles, E. E. Witmer, J. P. Vinti—538
Theory of the W. B. K. method, E. C. Kemble—426(A)
Mechanics, quantum-molecular structure and spectra
Binding energies of H and He isotopes, E. Feenberg—809(A), 850
Classification of perturbations, G. H. Dieke—870
Forces between bound atoms, W. Altar—804(A)

Isotopic shifts in diatomic molecules, G. H. Dieke—661
LiH molecule, J. K. Knipp—339(A)
Modification of Heitler and London method, C. Zener—334(A)
Rotating axes and polyatomic molecules, C. Eckart—552
Rotational energy of polyatomic molecules, J. H. Van Vleck—487
Van der Waals interaction of H atoms, L. Pauling, J. Y. Beach—686

Mechanics, statistical
Thermal equilibrium of elementary particles, G. Wataghin—423(L)
Virial theorem and quantum statistics, R. J. Duffin—421(L)

Metals (see **Crystalline state; Electrons in metals**)

Metastable atoms and molecules
In a gaseous discharge, R. W. Smith, O. S. Duffendack—473

Meteorology
Annual and diurnal variations of ions, A. P. Gagge—786(A)
Diurnal variation of the earth's potential gradient, J. G. Brown—259(A)
Electricity of rain and thunderstorms, R. Gunn—786(A)
Height of F region in ionosphere, E. B. Judson—509(L)
Ionization balance near earth's surface, G. R. Wait—810(A)
Ionosphere during partial solar eclipse, S. S. Kirby, T. R. Gilliland, E. B. Judson—632(L)
Langevin ions and dust particles, G. R. Wait—786(A)
Mechanism of lightning discharges, A. M. Cravath, L. B. Loeb—259(A)
Recording of ionosphere echoes, P. B. King, Jr., H. R. Mimno—786(A)
Seasonal variation of ionization in ionosphere, E. V. Appleton—704(L)
Small-ion production near earth's surface, A. G. McNish, G. R. Wait—785(A)
Upper-atmospheric ionization, E. V. Appleton—89(L); E. O. Hulburt—422(L)

Methods and instruments
Alternating-current potentiometer, W. C. Michels, B. Raines—793(A)
Amplifier for thermocouple e.m.f., R. P. Johnson, M. E. Bell, W. B. Nottingham—426(A)
Anomalous intensity distribution by diffraction gratings, R. W. Wood—642(A)
Apparatus for transmitting data from stratosphere, J. M. Benade, R. L. Doan—198(A)
Balanced circuit for resistance thermometers, M. G. Jacobson—336(A)
Broadcast carriers for constant high frequency currents, H. L. Schultz, L. G. Hector—327(A)
Characteristics of G-M tubes, J. F. Sears, G. E. Read—197(A)
Christiansen light filters, temperature effects, E. D. McAlister—328(A)
Continuous spectrum source in ultraviolet, H. P. Knauss, A. L. Bryan—842
Detection of minute quantities of Th, R. D. Evans, G. D. Finney, A. F. Kip, R. Mugele—791(A)
Determination of Ca in plant ashes, K. Way, J. M. Arthur—198(A)
Determination of interatomic distances in crystals, A. L. Patterson—330(A)
Diffraction gratings for far infrared, A. H. Pfund, J. A. Sanderson—792(A)
Foucault pendulum with constant amplitude, R. M. Langer—258(A)
γ-ray sensitivity of tube-counters, R. D. Evans, R. A. Mugele—427(A)
G-M counter for x-rays, D. P. LeGalley—333(A)
G-M counters, construction and use, G. L. Locher—326(A)
G-M counters, different gases, C. L. Haines—791(A)
Glow discharge oscillator, W. E. Kock—339(A)
Heat-flow calorimetric method, W. P. White—797(A)
High rotational speeds in vacuum, E. G. Pickels, J. W. Beams—336(A)
High speed electrical motors, R. C. Colwell, N. I. Hall—337(A)
High speed oil diffusion pump, H. W. Edwards—259(A)
Ion condensation in cloud chambers, D. H. Loughridge—792(A)
Ion source, capillary, E. S. Lamar, E. W. Samson—791(A)
Ion source, hollow cathode, P. G. Kruger, B. T. Darling—790(A)
Ion source for mass-spectroscopy, A. J. Dempster—331(A)
Liquefaction of gases—a demonstration, C. T. Knipp—200(A)
Mobile radio laboratory, H. Selvidge, H. R. Mimno—786(A)
Modified Aston-type mass spectrometer, D. D. Taylor—666
New expansion in radiation problems, W. W. Hansen—139
Null method photoelectric photometer, H. W. Edwards, 258(A)
Optical properties of MgO, R. T. Brice, J. Strong—255(A)
Pendulum driven by electrostatic forces, J. A. Van den Akker—199(A)
Polarization effects in Hilger E1 spectrograph, J. W. Ellis, J. Kaplan—255(A)
Powder filters for the infrared, R. B. Barnes, R. R. Brattain, R. S. Firestone—792(A)
Precision magnetic field standard, F. G. Dunnington—257(A)
Propagation of explosion condensation through air, L. Thompson—811(A)
Proportional counter, E. Pollard, W. W. Eaton—597, 640(A)
Proposed mass-spectrograph, W. B. Pietenpol—331(A)
Radiofrequency high-voltage generator, D. H. Sloan—62
Radio transmitter for short waves, R. King—787(A)
Recording of ionosphere echoes, P. B. King, Jr., H. R. Mimno—786(A)

Reduction of chlorophyll *a* and *b*, fluorescence spectra, V. M. Albers, H. V. Knorr, P. Rothemund—198(A)
Rotary voltmeter and sphere gap, comparison, J. E. Henderson, W. H. Goss, J. E. Rose—259(A)
Separation of Po and Ra D, G. B. Pegram, J. R. Dunning—325(A)
Shoal fathometer, H. G. Dorsey—344(A)
Small unidirectional currents, G. Failla—805(A); G. J. Mueller—793(A)
Solarization at low intensity, A. J. Reardon, H. P. Griggs—199(A)
Sound ingots, technique for making, P. G. Waldo, W. P. Davey—338(A)
Standing wave system in a flute, R. W. Young, D. H. Loughridge—258(A)
Testing of Na-filled valves, electrical method, W. R. Koch—326(A)
Thermionic tubes for voltage control, C. R. Larkin—793(A)
Thin metallic films, J. D. Howe, E. M. Purcell—329(A)
Tube coefficients, measurement of, R. W. Hickman, F. V. Hunt—787(A)
Tube counter, efficiency, S. M. Skinner—791(A)
Two-crystal spectrometer for ultra-short x-rays, T. R. Cuykendall, M. T. Jones—643(A)
Vacuum centrifuge, E. G. Pickels—797(A)
Wide aperture quartz spectrograph, S. Smith—257(A)
Wilson cloud chamber, high pressure, W. M. Brubaker, T. W. Bonner—255(A)
Wilson cloud tracks, method of measurement, W. W. Eaton—796(A)
Window to admit deuteron beam, E. McMillan, M. S. Livingston—452
X-ray diffraction and fatigue of metals, C. S. Barrett—333(A)

Molecular structure and constants (see also **Spectra, molecular and Raman spectra**)
C−D bond vibration in heavy acetylene, G. Glockler, C. E. Morrell—569(L)
Of deutero-ammonias, E. F. Barker, M. Migeotte—702(L)
Forces between bound atoms, W. Altar—804(A)
Of H I, A. H. Nielsen, H. H. Nielsen—585
Of H^2CN, P. F. Bartunek, E. F. Barker—330(A)
Of H_2S, P. C. Cross—7
Isotope effect in acetylene, W. F. Colby—388
Of the LiH molecule, J. K. Knipp—339(A)
Of MgCl, CaCl and SrCl, A. E. Parker—349, 642(A)
Of methyl iodide and other molecules, R. S. Mulliken—413
Orbital valency; extended method, G. Nordheim—803(A)
Raman spectra and latent heat of fusion, C. J. Phillips—792(A)
Rotating axes and polyatomic molecules, C. Eckart—552
Rotational energy of polyatomic molecules, J. H. Van Vleck—487
Of silane, W. B. Steward, H. H. Nielsen—792(A), 828
Transfer of translational and vibrational energy in O_2, V. O. Knudsen, L. Obert—256(A)

Neutrons (see also **Nucleus**)
Absorption of slow neutrons, G. Beck, L. H. Horsley—510(L); J. R. Dunning, G. B. Pegram—640(A); J. R. Dunning, G. B. Pegram, G. A. Fink, D. P. Mitchell—416(L), 888(L), 970(L); W. F. Libby, W. M. Latimer—193(L)
Absorption and velocity of slow neutrons, temperature effect, J. R. Dunning, G. B. Pegram, G. A. Fink, D. P. Mitchell—796(A)
Action on heavy water, W. F. Libby, E. A. Long, W. M. Latimer—424(L)
Capture and scattering, H. A. Bethe—640(A)
Effects in photographic emulsion, D. W. Mueller, H. A. Barton—796(A)
Interaction with protons, L. H. Thomas—810(A), 903
Scattering by Cu and Fe, A. C. G. Mitchell, E. J. Murphy—812(A), 881(L)
Scattering by protons, E. Feenberg—857; W. D. Harkins, D. M. Gans, M. Kamen, H. W. Newson—511(L)
Thermal equilibrium of slow neutrons, J. R. Dunning, G. B. Pegram, D. P. Mitchell, G. A. Fink—888(L)

Nuclear moments and spin (see also **Hyperfine structure**)
Calculated values, D. R. Inglis—84
Of Co, K. R. More—256(A)
Of the deuteron and other nuclei, D. R. Inglis—334(A)
In isotopic mixtures, I. I. Rabi—334(A)
Of La, M. F. Crawford, N. S. Grace—536
Of Li^7, M. Fox, S. Millman, I. I. Rabi—801(A)
Of P_2, F. A. Jenkins—783(L)
Of K, S. Millman—739
Of K^{39}, J. J. Gibbons, J. H. Bartlett—340(A), 692
Of K^{41}, S. Millman, M. Fox, I. I. Rabi—801(A)
Of Na^{23}, W. E. Shoupp, J. H. Bartlett, Jr., C. G. Dunn—705(L); L. A. Wills, G. Breit—704(L)
Sign of nuclear magnetic moments, use of atomic beams, I. I. Rabi—338(A)
States and moments, D. R. Inglis—813(A)

Nucleus (see also **Disintegration of nucleus**)
Angular and magnetic momenta of nuclei, P. G. Kruger—605
Binding energies of H and He isotopes, E. Feenberg—809(A), 850
Capture, stability and radioactive emission of neutrons, J. R. Dunning, G. B. Pegram, G. A. Fink—325(A)
Disintegration of deuterons by impact, J. R. Oppenheimer—845
Energy levels of light nuclei, G. Beck—809(A)
Formation of electron pairs by internal conversion of γ-radiation, M. E. Rose, G. E. Uhlenbeck—811(A)
γ-rays from B bombarded with deuterons, H. R. Crane, L. A. Delsasso, W. A. Fowler, C. C. Lauritsen—253(A)
He in beryls, H. J. Walke—969(L)
Interaction of nuclear particles, L. A. Young—809(A), 972(L)
Interaction between neutron and proton, L. H. Thomas—810(A), 903
Masses of Be^8, Be^9 and B^{11}, H. R. Crane, C. C. Lauritsen—420(L)

Masses of light atoms from transmutation data, H. Bethe—633(L), 795(A)
Metastable nuclei produced by the hard γ-rays, L. Devol—325(A)
Model, forces between particles, W. V. Houston—260(A), 819(A), 942
Negative proton, E. C. Westerfield, W. B. Pietenpol—325(A)
Neutrons from Be bombarded by deuterons, J. R. Richardson, F. N. D. Kurie—253(A); T. W. Bonner, W. M. Brubaker—254(A)
Nuclear chemistry, D. M. Gans, W. D. Harkins—795(A)
Potential barriers, E. Pollard—611, 640(A)
Radius, A. K. Solomon—249(L)
Reactions classified, W. D. Harkins—702(L)
Scattering of α-particles in deuterium, E. Pollard, H. Margenau—571(L), 640(A), 795(A), 833
Structure of H^3, L. H. Thomas—903
Theory of disintegration, H. A. Bethe—747

Optical constants and properties
Anomalous intensity distribution by diffraction gratings, R. W. Wood—642(A)
Index of refraction of H_2O and paraffin; 10 cm waves, L. S. Skaggs, R. T. Dufford—201(A)
Of LiF in Schumann region, E. G. Schneider—789(A)
Molar polarization of N_2 and A, C. E. Bennett—790(A)
Pressure effect on refractive index of CS_2, F. E. Poindexter—202(A)
Of sputtered metal films, J. B. Nathanson, H. S. Seifert—328(A)
Optical instruments (see **Methods and instruments**)
Optical theory
Energy and angular momentum, R. d'E. Atkinson—623, 639(A)
Huygen's principle and the Lorentz hypothesis, N. Galli-Shohat—639(A)
Quantum theory of metallic reflection, L. I. Schiff, L. H. Thomas—790(A), 860
Theory of Michelson-Morley experiment, R. J. Kennedy—965
Velocity of light a function of time, P. I. Wold—333(A), 735

Philosophy of physics
Quantum-mechanical description of reality, A. Einstein, B. Podolsky, N. Rosen—777, E. C. Kemble—973(L)
Photoconductivity
In red mercuric iodide, F. C. Nix—72, 337(A)
Photoelasticity
Theory of, H. Mueller—790(A), 947
Photoelectric effect and properties; cells
Of a Cu single crystal, N. Underwood—502
Energies of x-ray photoelectrons, L. Alvarez—636(L)
Of K films on Ag, J. J. Brady—197(A)
Selective effect, theories of, C. Zener—15
And spark mechanism, A. M. Cravath—254(A)
Threshold of Ur, Ca and Th, action of O_2, H. C. Rentschler, D. E. Henry—807(A)
Work function of Ta, A. B. Cardwell—628

Photography
Effect of neutrons, D. W. Mueller, H. A. Barton—796(A)
Solarization at low intensity, A. J. Reardon, H. P. Griggs—199(A)
Photometry
Null method photoelectric photometer, H. W. Edwards—258(A)
Photovoltaic effect
Current-voltage relations, L. A. Wood—337(A)
Nature of barrier plane, J. W. Ballard, E. D. Wilson—794(A)
And photomagnetic effect, R. M. Emberson, R. T. Dufford—202(A)
Temperature effects, Se-mono-crystal Pt film combination, R. M. Holmes, L. C. Whitman—337(A)
Piezoelectric effect
Electrocoupling of vibrating quartz plates, H. Osterberg, J. W. Cookson—781(L)
X-ray extinction in crystals, G. W. Fox, W. A. Fraser—200(A)
X-ray extinction in oscillating crystals, G. W. Fox, W. A. Fraser—899
Positive electron
Production of pairs by charged particles, J. R. Oppenheimer—146

Quantum mechanics (see **Mechanics, quantum,** etc.)
Quenching of radiation
Of Cd resonance radiation, H. C. Lipson, A. C. G. Mitchell—638(A), 807(A)

Radio
Mobile radio laboratory, H. Selvidge, H. R. Mimno—786(A)
Seasonal variation of ionization in ionosphere, E. V. Appleton—704(L)
Transmitter for short waves, R. King—787(A)
Radioactivity (see also **Disintegration of nucleus**)
Analysis of data, C. N. Warfield—796(A); C. N. Warfield, A. E. Ruark—700(L)
β-ray disintegration, Fermi theory, R. L. Dolecek—202(A); E. J. Konopinski, G. E. Uhlenbeck—202(A)
β-ray and positron energies, induced radioactivity, F. N. D. Kurie, J. R. Richardson, H. C. Paxton—796(A)
Detection of minute quantities of Th, R. D. Evans, G. D. Finney, A. F. Kip, R. Mugele—791(A)
Diffusion of radioactive atoms, J. A. Gray, W. M. Barrows, Jr.—813(A)
Element produced from C by deuteron bombardment, L. N. Ridenour, D. M. Yost, K. Shinohara—253(A)
Emission of neutrons, J. R. Dunning, G. B. Pegram, G. A. Fink—325(A)
γ-rays from B bombarded with deuterons, H. R. Crane, L. A. Delsasso, W. A. Fowler, C. C. Lauritsen—253(A)
Half-lives of K, Rb, Nd and Sm, A. E. Ruark, K. H. Fussler—790(A)
Induced in C by H^1 and D^2, L. R. Hafstad, M. A. Tuve—506(L)

Induced by cosmic radiation, L. W. Alvarez—320(L); J. E. I. Cairns—194(L), 631(L)
Induced by neutron bombardment, A. V. Grosse, M. S. Agruss—91(L), 93(L); W. F. Libby, W. M. Latimer—193(L)
Induced in N by deuteron bombardment, E. McMillan, M. S. Livingston—452
Isotopes in induced radioactivity, T. R. Wilkins, L. S. Shnidman—251(L)
Of Li and F bombarded with deuterons, H. R. Crane, L. A. Delsasso, W. A. Fowler, C. C. Lauritsen—971(L)
Metastable nuclei produced by the hard γ-rays, L. Devol—325(A)
Neutrino hypothesis, continuous β-rays, G. Beck—202(A)
Protons from Sm, J. A. Bearden, W. R. Kanne—639(A)
Radiative capture of protons, G. Breit, F. L. Yost—508(L); L. R. Hafstad, M. A. Tuve—506(L)
Of Na, induced by deuteron bombardment, E. O. Lawrence—17
Th content of rocks, R. D. Evans, R. A. Mugele—427(A)
X-ray levels, applications to β and γ-ray spectra, A. E. Ruark, F. A. Maxfield—107

Raman spectra
Asymmetry of the C atom, R. T. Dufford—199(A)
Of C_2D_2, G. Glockler, C. E. Morrell—569(L)
Of heavy chloroform, R. W. Wood, D. H. Rank—792(A)
Latent heat of fusion, C. J. Phillips—792(A)
Of $MgSO_4$, E. M. Coon, E. R. Laird—889(L)
Of N_3^-, NCS^- and CO_3, A. Langseth, J. R. Nielsen—198(A)
Vibrational scattering in liquids, S. Bhagavantam, A. V. Rao—921
Of H_2O vapor, D. Bender—252(L)

Relativity
Constancy of the velocity of light, R. J. Kennedy—533
Deduction of inverse square law, J. L. Synge—760
Discussion of the ether drift experiments, W. B. Cartmel—333(A)
Huygen's principle and the Lorentz hypothesis, N. Galli-Shohat—639(A)
Redward shift of nebulae lines, P. I. Wold—217
Theory of Michelson-Morley experiment, R. J. Kennedy—965
Velocity of light a function of time, P. I. Wold—333(A), 735

Resistance, electrical (see **Electrical conductivity and resistance**)

Scattering of electrons, ions and molecules (see also **Electrons in gases; Electron diffraction**)
Of alkali atoms in gases, S. Rosin, I. I. Rabi—645(A); S. Rosin—798(A)
In A, Kr and H_2, G. M. Webb—200(A), 379, 384
Collision of H and He ions in A, E. B. Jordain—467
Fast electrons in Hg vapor, W. E. Stephens—255(A)
Resonance interaction deuterons, α-particles and protons, E. Pollard, H. Margenau—571(L), 640(A)
Scattering of protons on protons, W. H. Wells—591

Secondary electrons (see **Electrons, secondary**)

Spark discharge
Ion distribution during initial stages, C. D. Bradley, L. B. Snoddy—541; C. D. Bradley—802(A)
Oscillographic study, J. W. Flowers—801(A)
Photoelectric effect, A. M. Cravath—254(A)

Specific heat
Equations of state for substances with variable specific heat, W. P. Boynton—258(A)

Spectra, absorption (see also **Absorption of light**)
Of acetic acid and acetic anhydride, infrared, E. K. Plyler, E. S. Barr—793(A)
Of acetylene, ethylene and ethane, far ultraviolet, W. C. Price—444
Of acetylenes, infrared, C. A. Bradley, Jr., A. McKellar—793(A)
Of NH_3, ultraviolet, A. B. F. Duncan—822
Of NH_3 and ND_3, ultraviolet, A. B. F. Duncan—822, 886(L)
Of benzene far infrared, R. B. Barnes, W. S. Benedict, C. M. Lewis—129
Of C_2H_2 and C_2D_2, infrared, C. A. Bradley, Jr., A. McKellar—914
Of deutero-ammonias, ultraviolet, W. S. Benedict—641(A)
Of diacetylene, ultraviolet, S. Woo. T. C. Chu—886(L)
Of GeH_4, infrared, W. B. Steward, H. H. Nielsen—792(A), 828
Of HI, infrared, A. H. Nielsen, H. H. Nielsen—585
Of H_2, to 738Å, J. J. Hopfield—788(A)
Of H_2S at 10,100A, P. C. Cross—7
Of H_2S, CS_2 and SO_2, ultraviolet, W. C. Price—788(A)
Of I vapor, ultraviolet, D. T. Warren—1
Of PbO and AsO, E. N. Shawhan, F. Morgan—192(L), 199(A), 377
Of LiD, F. H. Crawford, T. Jorgensen, Jr.—358
Of LiH, F. H. Crawford, T. Jorgensen, Jr.—932
Of Li_2, ultraviolet, J. E. Vance, J. R. Huffman—215
Of MgO, R. R. Brattain, R. B. Barnes, F. Seitz—793(A)
Of MgO, near infrared, R. B. Barnes, R. R. Brattain—416(L)
Methane content of giant planet atmospheres, A. Adel, V. M. Slipher—787(A)
Of methyl bromide and chloride; ionization potentials, W. C. Price—510(L)
Of methyl deuteride, N. Ginsburg, E. F. Barker—641(A)
Of methyl iodide, W. C. Price—419(L)
Of OH, A. A. Frost, O. Oldenberg—788(A)
Of rare earths, F. W. Paul—799(A)
Of silane, W. B. Steward, H. H. Nielsen—828
Of SO_2, temperature variation, J. H. Clements—224
Sunlight absorbed by atmosphere, A. Adel, V. M. Slipher, E. F. Barker—251(L), 580
Of uranine solution under high pressure, W. J. Lyons—198(A)

Spectra, atomic
Of Al vapor in high vacuum, J. Strong, E. Gaviola—256(A)
Of A and Kr extreme ultraviolet, J. C. Boyce—799(A)
Of C III, B I and O IV perturbed series, N. G. Whitelaw, J. E. Mack—677

Of Co, deep configuration, H. H. Marvin—521
In Cr I and Cr II, intensity relations, J. S. V. Allen, C. E. Hesthal—926
Excited states of He, W. S. Wilson, R. B. Lindsay—638(A), 681
Fine and hyperfine structure of Be III, S. S. Ballard, O. E. Anderson, H. E. White—256(A)
Fine structure of *Hα*, F. H. Spedding, C. D. Shane, N. S. Grace—38
Of He, band at 600A, J. L. Nickerson—707
Of He, high frequency excitation, M. Peterson, H. Carl—803(A)
Hyperfine structure formulae, M. F. Crawford—768
Isoelectronic sequence Cl I to Mn IX, S. G. Weissberg, P. G. Kruger—798(A)
Of Kr, extreme ultraviolet, J. C. Boyce—718
Of Kr III, C. J. Humphreys—712, 799(A)
Of Pb II, L. T. Earls, R. A. Sawyer—115
Of Pb IV and Bi V, G. K. Schoepfle—232, 330(A)
Line strengths in intermediate coupling, G. H. Shortley—295, 419(L)
Of Mg I, isotope shift, R. F. Bacher, R. A. Sawyer—587
Of Mn V and Fe VI, low terms, I. S. Bowen—924
Of P II, P III, P IV, H. A. Robinson—799(A)
Rare gas configurations, calculations, C. L. Bartberger—803(A)
Relative transition probabilities, C. W. Ufford—330(A), 931
Of Sm, A. S. King—256(A)
Of Sm I and Gd I. Configuration of rare earths, W. Albertson—370
Of Ag II, higher terms, W. P. Gilbert—847
Of Ag III, W. P. Gilbert—803(A)
Of Tl II, C. Ellis, R. A. Sawyer—799(A)

Spectra, general
Difference bands in spectra of major planets, temperature of planets, A. Adel, V. M. Slipher—651
Exploded Hg stream, H. P. Knauss, A. L. Bryan—842

Spectra, molecular (see also **Molecular structure and constants**)
Alternating intensities in P_2, F. A. Jenkins—783(L)
Of NH_3 and ND_3; pure rotation, R. B. Barnes—658
Difference bands in spectra of major planets, temperature of planets, A. Adel, V. M. Slipher—651
Of AsO, F. A. Jenkins, L. A. Strait—136, 257(A); F. Morgan, E. N. Shawhan—192(L), 199(A)
Of As_2, G. M. Almy, G. D. Kinzer—199(A)
Of As_2, emission, G. M. Almy, G. D. Kinzer—721
Band system of TiCl, A. E. Parker, A. H. Parker—812(A)
Band systems in N_2, J. Kaplan—255(A), 259(A)
Of BaH at 10,000A, W. W. Watson—213
Of BF, R. B. Dull—458
Of BF, H. M. Strong, H. P. Knauss—642(A)
Of BeD^+, P. G. Koontz—641(A)
Of CaH and CaD, W. W. Watson—27
Of CD, A. McKellar, C. A. Bradley, Jr.—787(A)
Classification of perturbations, G. H. Dieke—870
Of deutero-ammonias, E. F. Barker, M. Migeotte—702(L)
Of HD and D_2, Fulcher bands, G. H. Dieke, R. W. Blue—261
Of H^2CN at 17.5μ, P. F. Bartunek, E. F. Barker—330(A)
Of H_2O for infrared, R. B. Barnes, W. S. Benedict, C. M. Lewis—918
Intensity formulas for $^2\Sigma^+-{}^2\Sigma^-$ transitions, R. D. Present, J. H. Van Vleck—788(A)
Interaction between vibration and rotation, D. M. Dennison, M. Johnston—93(L)
Isotopic shifts, G. H. Dieke—661
Light of the night sky, J. Kaplan—193(L)
Of LiH, F. H. Crawford, T. Jorgensen, Jr.—932
Of MgCl, CaCl and SrCl analysis, A. E. Parker—349, 642(A)
Of OH^+, F. W. Loomis, W. H. Brandt—199(A)
Periodicity of Morse's function, C. H. D. Clark—238
Rotational energy of polyatomic molecules, J. H. Van Vleck—487
Of SiF, high dispersion, R. M. Badger, C. M. Blair, Jr.—881(L)
Of S_2, A. Christy—251(L)
Temperature variation in molecular spectra, J. H. Clements—220
Transfer of rotational energy, F. F. Rieke—788(A)
Vibrations of symmetrical tetratomic molecules, J. E. Rosenthal—235

Spectroscopy, technique, standards
Continuous spectrum source in ultraviolet, H. P. Knauss, A. L. Bryan—842
Determination of Ca in plant ashes, K. Way, J. M. Arthur—198(A)
Fe and Nd standards, G. R. Harrison, W. W. Bartlett—799(A)
Temperature variation in molecular spectra, J. H. Clements—220
Wavelength standards for the extreme ultraviolet, J. C. Boyce, C. A. Rieke—653

Sputtering
Of Th and Ba from W, L. R. Koller—806(A)

Stark effect
Anomalous intensities; interpretation, J. S. Foster—329(A)
In H isotopes, J. S. Foster, A. H. Snell—338(A)

Supraconductivity (see **Electrical conductivity and resistance**)

Surface phenomena
Pressures and potentials of monomolecular films, hydroxy-decanoic acid polymers, W. D. Harkins, E. F. Carman, H. E. Ries, Jr.—797(A)
Surface tension of Hg, M. Kernaghan—202(A)

Thermal conductivity
Heat-flow calorimetric method, W. P. White—797(A)

Thermal expansion
Erratum, thermal expansion of Ni, C. Williams—88
Of Cu from 0°K to melting, W. J. Haring, W. P. Davey—337(A)

Thermal radiation
Color temperature scale, W. E. Forsythe—789(A)

Thermionic emission of electrons; Emitting surfaces
Applied field and thermionic constants for thoriated W. A. Rose—806(A)
Double layers in adsorbed films; Ca, Sr and Ba, R. W. Gurney—479
Field emission and work function of Hg, L. R. Quarles—328(A)
Heat-treated W filaments, R. P. Bien—806(A)
Properties of Ta, A. B. Cardwell—628
W in weak acceleration fields, W. B. Nottingham—806(A)
Work function of Ba, P. A. Anderson—958
Work function for composite surfaces, temperature coefficient, A. Rose—889(L)
Thermodynamics
Equations of state and thermodynamic functions, W. P. Boynton—258(A)
Liquid state, W. H. Rodebush—513(L)
Thermoelectric effects
Thermal e.m.f. and magnetization, F. W. Constant—794(A)
Transmutation phenomena (see **Disintegration of nucleus**)

Vacuum tubes
Space charge in double and triple grid tubes, E. W. Thatcher—327(A)
Van der Waals forces
Interaction of H atoms, L. Pauling, J. Y. Beach—686
Vaporization (see **Evaporation**)
Viscosity
Of D_2O, H. C. Torrey—644(A)
And molecular complexity, E. C. Bingham, C. E. Coombs—645(A)

Work function (see **Thermionic emission of electrons; Photoelectric effect**)

X-rays, absorption
Ionization of liquids by x-rays, L. S. Taylor, F. L. Mohler—805(A)
Ultraviolet fluorescence induced by x-rays and γ-rays, O. Glasser, I. E. Beasley—570(L), 789(A)
X-rays, diffraction, scattering, reflection, refraction and polarization
Diffraction pattern of liquid and solid glycerine films, K. Lark-Horovitz and E. P. Miller—813(A)
Diffuse scattering from crystals, G. E. M. Jauncey—201(A); G. E. M. Jauncey, J. H. Deming—804(A)
Incoherent scattering and discrete electrons, A. H. Compton—203(A), 367
Prins' formula, simplification, F. Miller, Jr.—201(A), 209
In range 50 X.U. to 200 X.U., M. T. Jones, T. R. Cuykendall—643(A)
Refraction of Cu $K\beta$ line by diamond, J. A. Bearden—811(A)
Scattering from fluids containing polyatomic molecules, W. H. Zachariasen—277
Scattering by gases, E. O. Wollan—201(A)
Structure of methyl alcohol from x-ray diffraction patterns, W. H. Zachariasen—201(A)
Temperature function of reflection from crystals, R. B. Jacobs, A. Goetz—94(L), 257(A)

X-rays, emission (see also **X-rays, spectra and spectroscopy,** etc.)
Chemical combination and spectra, J. Valasek—332(A), 896
Energy level widths of Au(79), E. Ramberg, F. K. Richtmyer—644(A)
Intensity measurements with a G–M counter, D. P. LeGalley—333(A)
Levels of radioactive elements, β and γ-ray spectra, A. E. Ruark, F. A. Maxfield—107
Line widths: finite resolving power of crystals, L. G. Parratt, L. P. Smith—805(A)
M-series of protactinium 91, W. C. Pierce, A. V. Grosse—532
New lines in *K* series of W, J. C. Hudson, H. G. Vogt—809(A)
New type of Auger effect, Coster-Kronig theory of satellites, F. R. Hirsh, Jr., F. K. Richtmyer—805(A)
Origin of *L*-satellites, E. Ramberg, F. K. Richtmyer—805(A)
Radiative Auger effect, F. Bloch, P. A. Ross—884(L)
Shapes and wavelengths of *K* series Ti to Ge, C. H. Shaw, J. A. Bearden—332(A)
Target temperature on wavelength, P. McCorkle, C. B. Bazzoni—804(A)
By very fast electrons, E. McMillan—801(A)
Width of the $K\alpha$-lines, H. Margenau—89(L)
Width of the Kr $K\alpha$-lines, E. Wilhelmy—322(L)
X-rays, spectra and spectroscopy, wavelength measurements (see also **X-rays, emission**)
Grating and crystal wavelengths, R. T. Birge, E. McMillan—320(L)
Line shapes and double crystal spectrometer, L. P. Smith—333(A)
Wavelength measurements, L. Alvarez—636(L); J. A. Bearden—645(A), 804(A), 883(L); L. G. Parratt—882(L); A. E. Ruark—316(L), 644(A)
X-rays, tubes, apparatus
Two-crystal spectrometer for ultra-short x-rays, T. R. Cuykendall, M. T. Jones—643(A)

Zeeman effect
In As I, As II and As III, J. B. Green, W. M. Barrows, Jr.—131
In Co I, F. L. Roth, P. F. Bartunek—526
Diatomic molecular states having *L*-uncoupling, J. K. Knipp—672, 803(A)

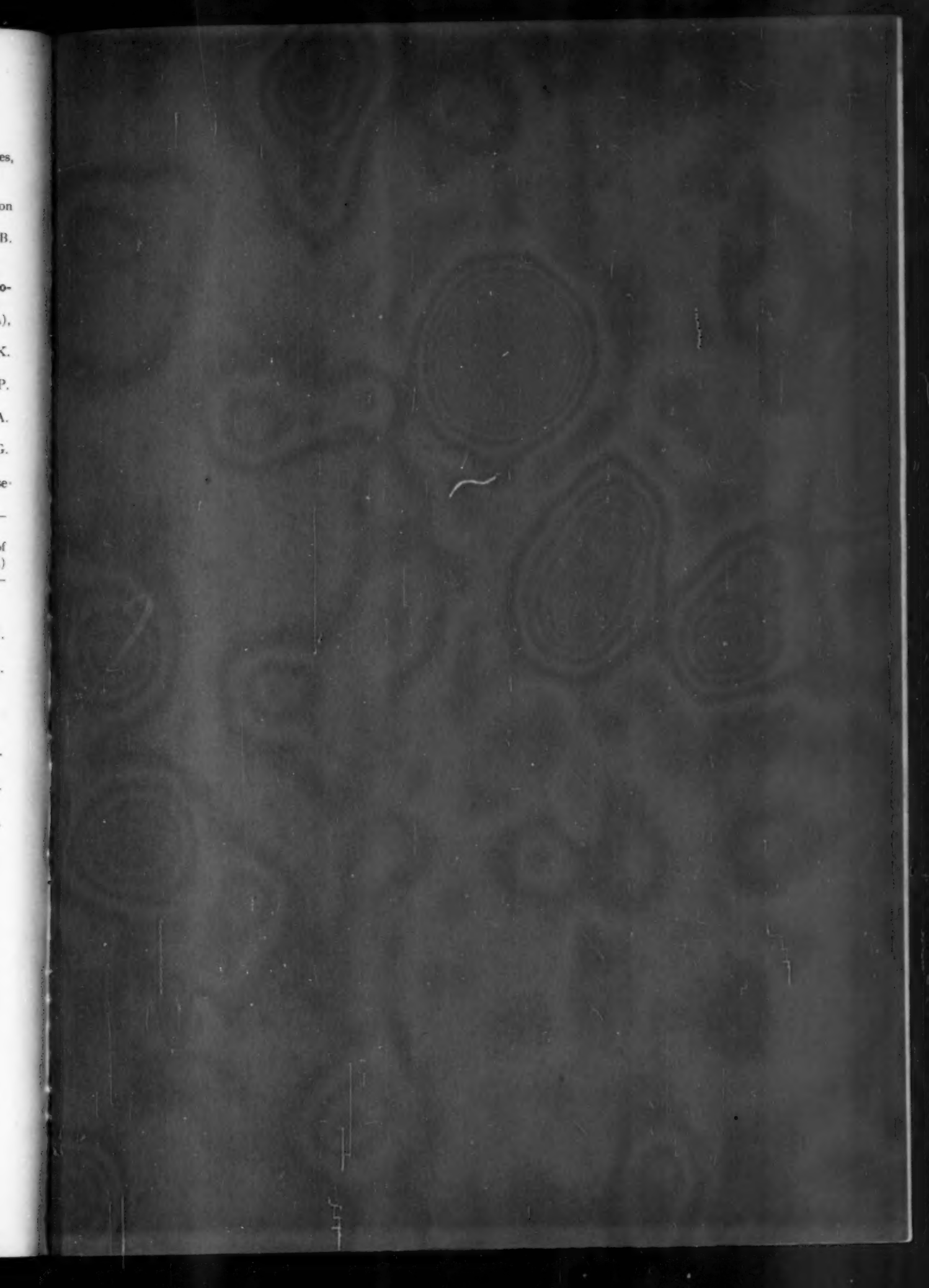

CONTENTS

PHYS. REV. 47 (1935) JUNE 15

Absorption of Cosmic-Ray Electrons . . . . . J. C. STREET, R. H. WOODWARD AND E. C. STEVENSON 891

Effect of Chemical Combination on the $K\beta_1$ Lines of Sulphur, Chlorine and Potassium . . . . . JOSEPH VALASEK 896

X-Ray Extinction in Piezoelectrically Oscillating Crystals . . . . . GERALD W. FOX AND WALTER A. FRASER 899

Interaction Between a Neutron and a Proton and the Structure of H^3 . . . . . L. H. THOMAS 903

Energy Spectrum of the Neutrons from the Disintegration of Beryllium by Deuterons . . . . . T. W. BONNER AND W. M. BRUBAKER 910

On the Absorption of Acetylene and Di-Deutero-Acetylene in the Photographic Infrared . CHARLES A. BRADLEY, JR. AND ANDREW MCKELLAR 914

Far Infrared Spectrum of H_2O . . . . . R. BOWLING BARNES, W. S. BENEDICT AND C. M. LEWIS 918

Vibrational Raman Scattering in Liquids . . . . . S. BHAGAVANTAM AND A. VEERABHADRA RAO 921

Low Terms in Mn V and Fe VI. . . . . I. S. BOWEN 924

Intensity Relations in Chromium Spectra . . . . . J. S. V. ALLEN AND C. E. HESTHAL 926

Note on the Relative Transition Probabilities for Almost Closed Shells . . . . . C. W. UFFORD 931

Band Spectra of the Hydrides of Lithium . . . . . F. H. CRAWFORD AND T. JORGENSEN, JR. 932

Nuclear Model . . . . . WILLIAM V. HOUSTON 942

Theory of the Photoelastic Effect of Cubic Crystals . . . HANS MUELLER 947

Contact Difference of Potential Between Tungsten and Barium. The External Work Function of Barium. . . . . PAUL A. ANDERSON 958

Simplified Theory of the Michelson-Morley Experiment. ROY J. KENNEDY 965

Letters to the Editor:

Helium Content of Beryls . . . . . E. J. WALKER 969

Slow Neutrons . . . . . J. R. DUNNING, G. B. PEGRAM, G. A. FINK AND D. P. MITCHELL 970

Emission of Negative Electrons from Lithium and Fluorine Bombarded with Deuterons . . . . . H. R. CRANE, L. A. DELSASSO, W. A. FOWLER AND C. C. LAURITSEN 971

Interaction of Nuclear Particles . . . . . LLOYD A. YOUNG 972

Evidence for the Formation of $_3Be^8$ in the Disintegration of Lithium by Deuterons . . . . . T. W. BONNER AND W. M. BRUBAKER 973

Correlation of Wave Functions with the States of Physical Systems . . . . EDWIN C. KEMBLE 973

Dielectric Constant and Resistance of Colloidal Solutions . HUGO FRICKE AND HOWARD J. CURTIS 974

Working Arm in Argon . . . . . C. G. SUITS 975

Author Index to Volume 47 977

Analytic Subject Index to Volume 47 990
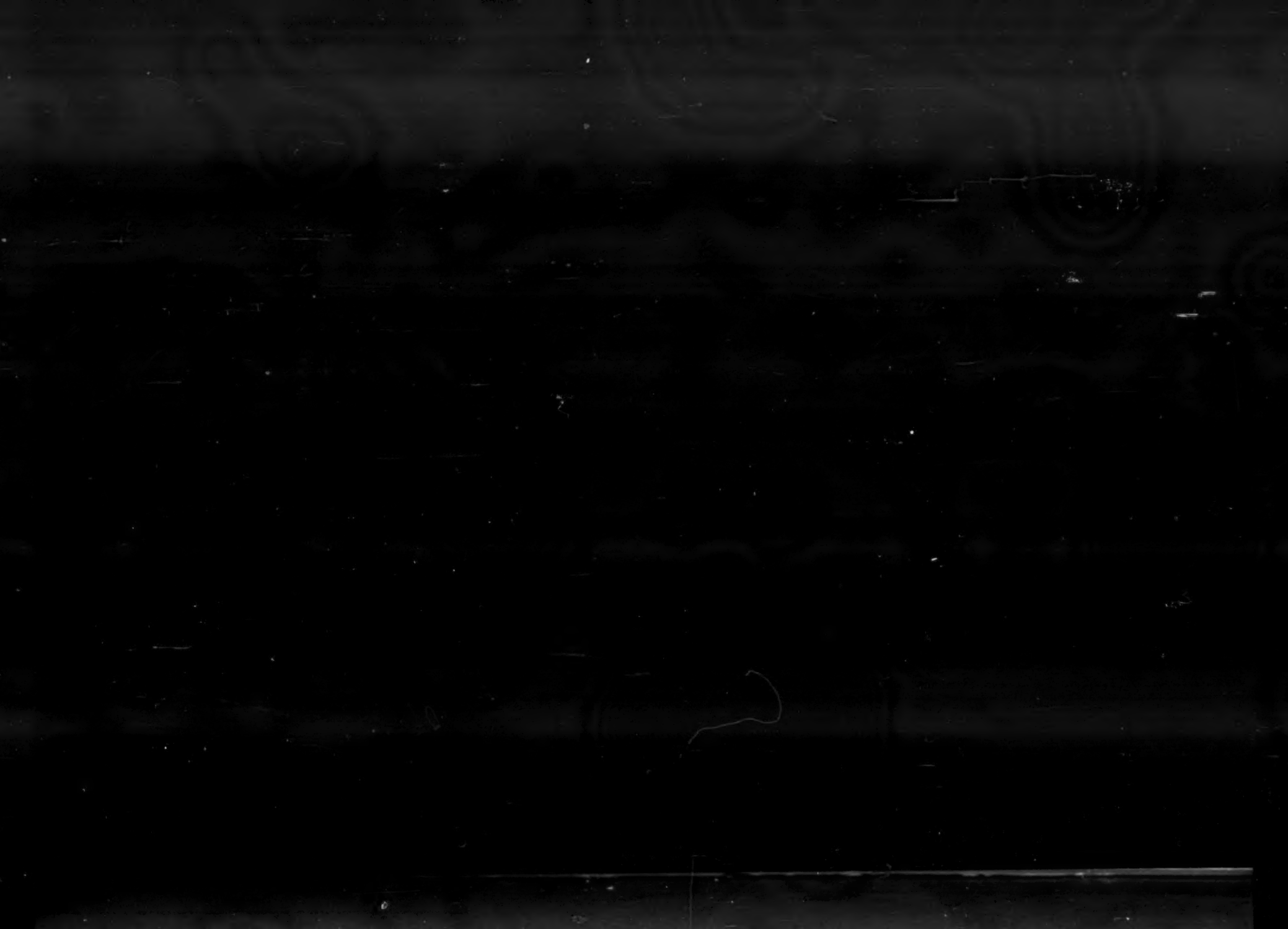
LANCASTER PRESS INC., LANCASTER, PA.